# Oxygen delivery scaffolds for tissue engineering

By Huaifa Zhang

Faculty of Dentistry

McGill University

Montreal, Quebec Canada


November 2015

A thesis submitted to McGill University in partial fulfillment of the requirements for the degree of Doctor of Philosophy

## DEDICATION

This document is dedicated to my family.

“The world as we have created it is a process of our thinking. It cannot be changed without changing our thinking.”

Albert Einstein

**Acknowledgements**

I would like to thank Dr. Jake Barralet for your hard work, guidance, and patience. Thank you so much for your encouragement, enthusiasm, and insight, from which I have learned so much. Without you, this would not have been possible.

I would like to thank Dr. Simon Tran for your encouraging, valuable suggestions and extensive support.

I would like to express my appreciation to my committee members: Dr. Jake Barralet, Dr. Svetlana Komarova, Dr. Faleh Tamimi, Dr. Reghan Hill, and Dr. Satya Prakash, for your valuable advice and guidance.

I would like to thank Dr. Mirko Gilardino, Hani Shash, Amal Al-Odaini, Dr. Steven Paraskevas, Craig Hasilo, Tomasz Jüngst, and Dr. Uwe Gbureck for their contribution to this work. It was a great pleasure to work with all of you.

I would like to thank Dr. Uwe Gbureck for inviting me to work overseas in Germany.

I would like to thank the staff in Animal Resource Division of the Research Institute of the McGill University Health Center for supporting my research work.

I would like to thank lab members in Dr. Barralet's lab and Dr. Tran's lab for your friendship and help in my studies. I also would like to thank Dr. Géraldine Merle, Alison Fraser, Mohamed

Abdulla, and Zishuai Zhang for helping me edit my thesis. Last but not the least, I would like to thank Ms. Yu Ling Zhang for her help during my study.

All of you have made my study here a memorable time of my life.

## Author contributions and statements of originality

1. Oxygen delivery from materials and bloodless life

Huaifa Zhang, Jake Barralet

- H. Zhang gathered all the information from literature and wrote the manuscript
- J. Barralet supervised the study and revised the manuscript

Originality: For the first time we reviewed all the oxygen delivery methods and strategies that utilize biomaterial materials for tissue engineering, tissue and organ preservation, and wound healing.

2. Comparison of oxygen delivery to hypoxia resistant and intolerant cells in anoxia

Huaifa Zhang, Daisuke Sato, Svetlana Komarova, Simon Tran, Jake Barralet

- H. Zhang designed the experiments, participated in all the experimental work, analyzed the data, and wrote the manuscript
- D. Sato performed the surgical procedures
- S. Tran provided cell culture facilities
- S. Komarova provided instruments, reagents, and training for q-PCR
- J. Barralet supervised the study and revised the manuscript

Originality: In this work, a novel self-oxygenating biodegradable scaffold was developed. The oxygen delivery scaffold exhibited excellent biocompatibility and oxygen-release capacities. Moreover, the effect of oxygen delivery scaffolds on cell viability *in vivo* and vascularization post transplantation was investigated.

3. Blood vessel preservation with a self-oxygenating scaffold

Huaifa Zhang, Simon Tran, Jake Barralet

- H. Zhang designed the experiments, performed all the experimental work, analyzed the data, and wrote the manuscript
- S. Tran provided cell culture facilities
- J. Barralet supervised the study and revised the manuscript

Originality: Rat blood vessels were successfully preserved for one week under anoxia at physiological temperature while maintaining the functionality of the blood vessels. This work suggested that tissues could be preserved at physiological temperature by oxygen delivery and that the prevailing rewarming injuries in tissue and organ preservation could be avoided.

4. Oxygen delivery effectively prevented tissue necrosis in ischemic wounds

Huaifa Zhang, Hani Shash, Amal Al-Odaini, Mirko Gilardino, Jake Barralet

- H. Zhang designed the material part of the experiments, prepared the materials, analyzed the data, and wrote the manuscript
- H. Shash designed the surgical part of the experiments and performed part of the surgery (convex part)
- A. Al-Odaini did pathological grading of the wounds
- M. Gilardino performed part of the surgery (concave part)
- J. Barralet supervised the study and revised the manuscript

Originality: An oxygen-release wound patch was developed that released oxygen *in situ*. The oxygen-release patch successfully preserved wounded tissues and promoted wound healing in

an ischemic rabbit ear wound model. This oxygen-release patch has a great potential for clinical applications.

5. Effect of hydrogel volume ratio on *ex vivo* adipose tissue viability in a self-oxygenating scaffold

Huaifa Zhang, Simon Tran, Jake Barralet

- H. Zhang designed the experiments, performed all the experimental work, analyzed the data and wrote the manuscript
- S. Tran provided cell culture facilities
- J. Barralet supervised the study and revised the manuscript

Originality: For the first time, large volumes of adipose tissue (0.3 mL) were preserved under anoxia by oxygen delivery. The effect of hydrogel volume ratio on cell viability in adipose tissue was investigated. This work may provide an approach to keep cells in adipose tissue alive after transplantation, and thus can have an important impact on plastic surgery.

6. Ongoing work

Originality: For the first time, preservation of various tissues and organs using a biodegradable self-oxygenating scaffold at physiological temperature, the influence of oxygen delivery on vascularization in subcutaneously implanted scaffolds, and development of a biodegradable self-oxygenating scaffold by 3D printing were explored.

## Abstract

Molecular oxygen plays an important role in the metabolic activities of aerobic cells. It is essential for oxidative phosphorylation, which produces the most energy for cell activities. Oxygen shortage, i.e. hypoxia, induces adverse cellular events, such as elevated glycolysis, cell apoptosis, and even necrosis. However, hypoxia and even anoxia (absence of oxygen) often occur during tissue engineering, organ preservation, and wound healing, due to the low solubility and limited effective diffusion distance of oxygen in water and a lack of or compromised oxygen supply by blood vessels. Various approaches and materials have been developed to deliver oxygen to tissues and cells, including hyperbaric oxygen therapy, normobaric oxygen therapy, perfluorocarbons, hemoglobin, peroxides, and tropical oxygen therapy devices or dressings. However, these approaches are either expensive, cause oxidative toxicity, have limited availability, result in serious side effects, or require toxic or extremely high concentrations of additives.

This thesis examines the use of calcium peroxide (CP) as an oxygen-generating agent and the control of its decomposition rate. The oxygen-release rate was adjusted by biodegradable hydrophobic polymers and alginate hydrogel. Hydrophobic polymers reduced the decomposition rate of CP by expelling water available to CP. Alginate hydrogel further reduced the amount of water available to CP and slowed down CP decomposition. In addition, the presence of hydrogel alleviated burst release of oxygen towards cells and inhibited the formation of gas bubbles which could kill cells. The oxygen delivery system (ODS) was found to rescue primary human fibroblasts and Madin-Darby canine kidney (MDCK) cells under anoxia. Subsequently, MDCK cell transplantation with the oxygen-release scaffolds on rats demonstrated that oxygen delivery supported cell growth and promoted vascularization in the

scaffold. Preservation of rat blood vessels under anoxia was performed to optimise the oxygen-release materials. The preserved blood vessels maintained high cell viability, normal mitochondrial membrane potentials in endothelial cells, and normal mechanical properties for up to seven days. An ischemic rabbit ear wound model was then used to assess the potential for this system to be used as a topical oxygen delivery system. The oxygen-release system protected ischemic wounds from necrosis and promoted the wound healing process. Moreover, the oxygen-release material was able to preserve large volumes of rat adipose tissue under anoxia for up to seven days. Preservation of other rodent organs or tissues, such as islets, heart slices, brain slices, liver slices, and marrow, under anoxia was attempted to determine if there was any tissue-specific cytotoxicity. Finally the effects of oxygen delivery on vascularization in a porous scaffold were investigated, and incorporation of the oxygen-release material into three dimensional (3D) printed scaffolds was explored.

In conclusion, an ODS was developed for tissue engineering, tissue and organ preservation, and wound healing. This system was biodegradable, biocompatible, and stable at room temperature, and exhibited excellent oxygen delivery capacities to cells and tissues. While full degradation of this material was not demonstrated, a significant step was made towards the development of a biodegradable oxygen-release system.

**Résumé**

L'oxygène moléculaire joue un rôle important dans les activités métaboliques des cellules aérobies, comme la réaction de phosphorylation oxydative qui produit le plus d'énergie pour les activités cellulaires. Un manque d'oxygène, i.e. hypoxie, induit des événements cellulaires indésirables, tels que l'augmentation de la glycolyse, l'apoptose des cellules, et même la nécrose. Cependant, l'hypoxie et l'anoxie (absence totale d'oxygène) se produisent souvent durant les procédés d'ingénierie tissulaire, la préservation d'organes, et la cicatrisation. Ceci est dû à la faible solubilité et à la courte distance de diffusion de l'oxygène dans l'eau, un apport en oxygène compromis dû à un manque de vaisseaux sanguins. Diverses approches et matériaux ont été développés pour fournir de l'oxygène aux tissus et aux cellules, comme l'oxygénothérapie hyperbare ou normobare, les fluorocarbones, l'hémoglobine, les peroxydes et finalement les dispositifs ou les pansements d'oxygénothérapie topiques. Toutefois, ces approches sont généralement coûteuses avec une disponibilité limitée, provoquent une toxicité oxydative, ou de graves effets secondaires, et nécessitent des concentrations toxiques ou extrêmement élevées en additif.

Cette thèse porte sur l'utilisation de peroxyde de calcium (CP) comme agent de production d'oxygène, et comment il est possible de contrôler sa vitesse de décomposition. Le taux de libération d'oxygène a été ajusté par un polymère biodégradable hydrophobe et un hydrogel d'alginate en limitant la quantité d'eau disponible. En outre, cet hydrogel permet d’atténuer un dégagement trop rapide d'oxygène vers les cellules et inhibe la formation de bulles de gaz qui pourraient tuer les cellules. Le système de délivrance en oxygène (ODS) a permis la survie de fibroblastes primaires humains, et de cellules rénales canines Madin-Darby (MDCK) dans des conditions d'anoxie. Par la suite, la transplantation dans des rats de cellules MDCK encapsulés

dans un échafaudage libérant de l'oxygène a montré que l'apport d'oxygène permettait la croissance cellulaire et stimulait la vascularisation dans l'échafaudage. Les vaisseaux sanguins de rat sous anoxie ont été préservés afin d'optimiser les matériaux libérant de l'oxygène. Les vaisseaux sanguins conservés ont maintenu une viabilité cellulaire élevée, des potentiels de membrane mitochondriale normaux dans les cellules endothéliales, et les propriétés mécaniques normales jusqu'à sept jours de culture. Un modèle de blessure ischémique sur des oreilles de lapin a ensuite été utilisé pour évaluer le potentiel en tant que système de libération en oxygène topique. Le système de libération d'oxygène a protégé les blessures de la nécrose et amélioré le processus de cicatrisation. De plus, le matériau libérant de l'oxygène a été capable de conserver de grands volumes de tissu adipeux du rat sous anoxie jusqu'à sept jours de culture. La préservation sous anoxie d'autres organes ou tissus de rongeurs, tels que des îlots pancréatiques, des tranches de cœur, des tranches de cerveau, des tranches de foie ainsi que la moelle osseuse, a été réalisée afin de déterminer si il y avait une spécificité tissulaire cytotoxique. Enfin, les effets de l'apport d'oxygène sur la vascularisation dans un support poreux ont été étudiés, et l'incorporation du matériau libérant de l'oxygène dans des échafaudages imprimés en trois dimensions (3D) a été explorée.

En conclusion, un ODS a été développé pour l'ingénierie tissulaire, la conservation de tissus et des organes, et enfin la cicatrisation. Ce système en plus d'être biodégradable, biocompatible, et stable à température ambiante, présente d'excellentes propriétés pour l'apport d'oxygène aux cellules et tissus. Bien que la dégradation complète de ce matériau n'a pas été démontrée dans cette thèse, une étape importante a été faite vers le développement d'un système de libération d'oxygène biodégradable.

## Abbreviations

| | |
|---|---|
| HBOT | Hyperbaric oxygen therapy |
| NBOT | Normobaric hyperoxia therapy |
| PFCs | Perfluorocarbons |
| PFD | Perfluorodecalin |
| FC 43 | Perfluorotributylamine |
| PLA | Polylactide |
| TET | Tissue-engineered trachea |
| RBCs | Red blood cells |
| LtEc | Lumbricus terrestric erythrocruorin |
| CDCs | Cardiosphere-derived cells |
| TLV | Total (or tidal) liquid ventilation |
| PLV | Partial liquid ventilation |
| ROS | Reactive oxygen species |
| FDA | Food and Drug Administration |
| SOS | Self-oxygenating scaffold |
| ODS | oxygen delivery system |
| $O_2$ | Oxygen |
| $H_2O_2$ | Hydrogen peroxide |
| CP | Calcium peroxide |
| $Na_2CO_3$•1.5 $H_2O_2$ | Sodium percarbonate |
| PCL | Polycaprolactone |
| PLGA | Poly(lactide-co-glycolide) |
| PVA | Polyvinyl alcohol |

| | |
|---|---|
| $Fe_3O_4$ | Iron oxide |
| TUNEL | Terminal deoxynucleotidyl transferees (TdT)-mediated dUTP nick end labeling |
| GLUT 1 | Glucose transporter 1 |
| BNIP3 | Bcl-2/adenovirus E1B 19kD-interacting protein 3 |
| B2M | Beta-2-microglobulin |
| ROS | Reactive oxygen species |
| DMPD | N,N-dimethyl-p-phenylenediamine |
| KI | Potassium iodide |
| KCl | Potassium chloride |
| CHO cells | Chinese hamster ovary cells |
| MDCK cells | Madin-Darby canine kidney cells |
| FBS | Fetal bovine serum |
| PBS | Phosphate buffer solution |
| UV | Ultraviolet light |
| $CO_2$ | Carbon dioxide |
| $N_2$ | Nitrogen |
| HBSS | Hanks' balanced salt solution |
| KH solution | Krebs Henseleit solution |
| SEM | Scanning electron microscope |
| EDX | Energy dispersive X-ray spectroscopy |
| XRD | X-ray diffraction |
| P/S | Penicillin/Streptomycin |
| DMEM | Dulbecco's Modified Eagle Medium |
| LDH assay | Lactate Dehydrogenase assay |

| | |
|---|---|
| TMRM | Tetramethylrhodamine methyl ester |
| CFSE | Carboxyfluorescein succinimidyl ester |
| H&E | Hematoxylin and eosin |
| HIF-1α | Hypoxia-inducible factor 1-alpha |
| VEGF | Vascular endothelial growth factor |

## Contents

## List of Figures

**Figure 4.2.** SEM image of CP powders (a), $MnO_2$ (b) and oxygen-release microparticles (c and d). The oxygen-release microparticles had a spherical shape and were porous. CP powders were nano particles. $MnO_2$ particles are polyhedrons with a size ranging from 20-80 μm. The prepared oxygen-release microparticles had a spherical shape and a porous structure (Figure 2d). -----131

**Figure 4.3.** Specific surface area of CP powders and CP-$MnO_2$-PCL microparticles. The specific surface area of microparticles was 50% of that of CP powders. -----132

**Figure 4.4.** Release of radicals (a) and $H_2O_2$ (b) from the materials as well as pH changes in culture medium (c) after 60 min. The presence of alginate hydrogel greatly mitigated color changes in a and b, suggesting there were less $H_2O_2$ and free radicals release when the microparticles were in hydrogel. In contrast, significant color changes around the microparticles were observed without hydrogel in a and b. For pH changes (c), however, no color change was noticed in culture medium, either with or without hydrogel, suggesting that pH did not change much in culture medium. -----133

**Figure 4.5.** Fluorescent images of the aorta tissue, preserved under various conditions for 7 d, stained by Ethidium bromide-1 and Hoechst 33258. Dead cells were stained red, and all the nuclei were stained blue. The cross section images (a, c and e) exposed both smooth muscle cells (in the ring) and endothelial cells (inner side). The lumen-side images (b, d and f) showed the layer of endothelial cells. After 7 d, most cells died in aortas preserved under either normoxia (c and d), i.e. 20% $O_2$, 37 ℃, or anoxia (e and f), i.e. 0% $O_2$, 37 ℃. -----135

**Figure 4.6.** Fluorescent images of aortas stored under hypothermia before and after rewarming. After three days, very few cells were stained dead from cold preserved aorta (a), after rewarming, however, a large amount of dead cells were found, including both endothelial cells and smooth muscle cells (b). After seven days, a majority of endothelial cells died but most of the smooth muscle cells stayed alive (c). Nevertheless, after rewarming for 150 min many smooth muscle cells were found to be dead (d). -----136

**Figure 4.7.** Cross sectional images of fluorescently stained aortas preserved by self-oxygenating scaffolds (SOS) with different concentrations of microparticles under anoxia, i.e. 0% $O_2$, 37 ℃, after 3 d. Dead cells were stained red, and all the nuclei were stained blue. a: 10 mg/mL, b: 20 mg/mL microparticles, c: 40 mg/mL microparticles. Dead cells were observed in a and c. -----138

**Figure 4.8.** Fluorescent images of tetramethylrhodamine methyl ester (TMRM) stained endothelium mitochondrial membrane potential after seven days. The aorta preserved under anoxia, i.e. 0% $O_2$, 37 ℃, in the presence of the self-oxygenating scaffold (SOS) maintained a normal endothelium mitochondrial membrane potential (a) while samples preserved under anoxia (b), normoxia (c), i.e. 20% $O_2$, 37 ℃, and hypothermia (d) lost their endothelium mitochondrial membrane potentials. -----139

**Figure 4.9.** KCl stimulated contraction force of aortic rings after seven days. The presence of self-oxygenating scaffold (SOS) under anoxia (0% $O_2$, 37 ℃), maintained normal stimulated contraction force for up to seven days, however, the other conditions, namely anoxia, normoxia (20% $O_2$, 37 ℃) and cold (20% $O_2$, 4 ℃) failed to retain the KCl stimulated contraction force. -----140

**Figure 4.5S.** Fluorescent images of tetramethylrhodamine methyl ester (TMRM) stained endothelium mitochondrial membrane potential after three days. The aorta preserved under anoxia, i.e. 0% $O_2$, 37 ℃, in the presence of self-oxygenating scaffold (SOS) maintained a normal endothelium mitochondrial membrane potential (a) while samples preserved under anoxia (b) and normoxia (c), i.e. 20% $O_2$, 37 ℃, lost their endothelium mitochondrial membrane potentials. The aorta kept at 4 ℃, 20% $O_2$ (d) retained partial of their endothelium mitochondrial membrane potentials. -----150

**Figure 4.6S.** Potassium chloride (KCl) stimulated contraction force of aorta tissue rings after three days. The presence of self-oxygenating scaffold (SOS) under anoxia (0% $O_2$, 37 ℃, 20 mg/mL microparticles in the scaffold) maintained 90% of the aortas' stimulated contraction force after three days, however, the other conditions, namely anoxia, normoxia (20% $O_2$, 37 ℃) and cold (20% $O_2$, 4 ℃) retained less than 60% of the tissue's stimulated contraction force. -----151

**Figure 4.7S.** Color changes of KI-starch solution in the presence of different concentration of $H_2O_2$. The color of the solution changed from light blue to dark blue as the concentration of $H_2O_2$ increased from 0.0001% to 0.005%. ` -----151

**Figure 5.1.** Ischemic wound on a rabbit ear. Four full thickness wounds were created with a diameter of 1.5 cm. The distance between the wounds was 5 mm. At the same time, the central artery and the artery and vein of cranial bundle were ligated to create an ischemic environment. -----158

**Figure 5.2.** Would healing process up to nineteen days. The presence of oxygen-release patch promoted wound healing compared with control, and 50% (n=8) of the wounds healed after 19 d while only 25% (n=8) healed in control group. -----160

**Figure 5.3.** Quantified wound area of the samples at different time points. The wound size was smaller in the presence of oxygen delivery materials at all the time points compared with control. The decrease of wound size became significant ($P<0.05$) after 11 d. On the $14^{th}$ day, the wound area had dropped to 8 $mm^2$ from 44 $mm^2$ while the wound area in the control group was still 25 $mm^2$. -----161

**Figure 5.4.** H&E staining images of rabbit ear tissue with and without the oxygen-release patch. In the presence of oxygen-release patch, the wounds healed almost completely after 19 d, with only less collagen near the cartilage compared with health tissues. In contrast, the wound did not heal adequately without oxygen-release patch and demonstrated evidence of tissue remodeling on the convex side (empty arrow). The reepithelialization of the wounds was not complete (white arrow) either. -----162

**Figure 5.5.** Would healing process up to 17 d. In the presence of ODP tissue necrosis in the wounded area was inhibited and most of the ischemic wounds actually healed in the end. In contrast, the tissues in the wounded area experienced serious necrosis and only holes eventually remained in the control group. -----164

**Figure 5.6.** Quantification of non granulation tissue coverage ratio of the wounded area with and without oxygen-release materials (n=8). In the presence of oxygen-release materials, the granulation area kept increasing and after 17 d almost the whole wounded area was covered by

color changes around the microparticles were observed without hydrogel in all cases except for pH changes in culture medium. Very little color change was noticed in culture medium, suggesting that there was not much pH change caused by the oxygen-release material in culture medium. -----181

**Figure 6.4.** Fluorescent images of live/dead assay stained adipose tissue under various oxygen concentrations after 7 d. Adipose tissue preserved under anoxia with 2 mg/mL microparticles in 50% v/v hydrogel displayed very good viability (a), but tissue preserved under other conditions, such as 5 mg/mL (b) and 0 mg/mL (c) microparticles in 50% v/v hydrogel under anoxia and 50% v/v hydrogel under normoxia (d) showed poor viability. These results indicated that adipose tissue was sensitive to oxygen, and that both high and low oxygen concentrations could kill cells. Most of the red nuclei located on the edge of adipocytes, indicating that most of the dead cells were adipocytes. Quantified results (e) indicated that tissue preserved at the optimal condition had a significantly higher viability than the other samples. -----183

**Figure 6.5.** Fluorescent images of the live/dead assay stained tissue cultured with 25% v/v (a), 10% v/v (b), and 0% v/v hydrogel (c) containing 2 mg/mL microparticles after 3 d. The viability was also quantified (d). -----184

**Figure 6.6.** The effect of volume ratio of hydrogel in the scaffold on the distance among adipose tissue blocks. -----185

**Figure 7.4.** Alamer Blue assay results of islet viability preserved under different conditions for 2 d. The presence of oxygen-release material resulted in significantly higher cell viability in islets compared with control. -----196

**Figure 7.5.** Fluorescent images of mouse heart tissue stained by live/dead assay, including fresh heart tissue (a), tissue preserved in the self-oxygenating scaffold under anoxia (b) and tissue cultured under anoxia (c) for 3 h. The heart slices were encapsulated with 0.6 mL self-oxygenating scaffold containing 5 mg/mL microparticles. -----197

**Figure 7.6.** Fluorescent images of mouse brain tissue stained by the live/dead assay: fresh brain tissue (a), brain tissue preserved in self-oxygenating scaffold under anoxia for 3 h (b) and 24 h (c), and brain tissue preserved under anoxia for 3 h (d) and 24 h (e). In the presence of oxygen delivery material, very few dead cells were found after 3 h under anoxia and cell viability was about 90% after 24 h. In contrast, almost all the brain cells died after 3 h under anoxia without oxygen-release material. -----199

**Figure 7.7.** Fluorescent images of mouse liver tissue stained by the live/dead assay: fresh liver tissue (a), liver tissue preserved in self-oxygenating scaffold under anoxia (b) and liver tissue cultured under anoxia (c) for 1 d. Microparticles were suspended in a 1% w/v alginate solution at a concentration of 10 mg/mL and then injected into liver through a needle. The whole liver was further encapsulated with 0.6 mL self-oxygenating hydrogel by crosslinking. -----200

**Figure 7.8.** Fluorescent images of rat marrow tissue stained by live/dead assay. The marrow tissue was preserved in self-oxygenating scaffold with 20 mg/mL (a), 30 mg/mL (b) and 40 mg/mL (c) of oxygen-release microparticles, and without (d) oxygen-release microparticles

under anoxia for 3 d. Marrow tissue displayed the highest cell viability in the presence of 30 mg/mL microparticles in the scaffold. -----209

**Figure 7.3S.** Hematoxylin and eosin (H&E) staining of subcutaneously implanted scaffolds with and without oxygen delivery materials after 2 and 4 weeks. The presence of oxygen delivery material greatly improved vascularization in the scaffold. A larger number of blood vessels were observed in the oxygen generating scaffold compared with the scaffold without oxygen-release material. -----210

## List of Tables

## Chapter 1

# Introduction

### 1. Oxygen deficiency

Molecular oxygen is important for the metabolic activities of most aerobic cells. [1] It plays an essential role in oxidative phosphorylation, a main bioprocess that produces energy for cellular activities. Generally *in vitro* cell culture conditions are categorized into three groups based on various oxygen concentrations, so called normoxia, hypoxia and anoxia. [1] Normoxic culture refers to culturing cells with 20% $O_2$. Hypoxia uses oxygen concentrations lower than 20% but above 0% and anoxia 0% $O_2$. Insufficient oxygen inhibits the oxidative phosphorylation in mitochondria and cells cannot generate enough energy to meet their demands. As a result, cellular activities including proliferation, differentiation, and protein secretion are affected, and cell apoptosis and even necrosis can occur [2-5].

As mentioned previously, normoxia in *in vitro* culture employed 20% $O_2$, whereas physiological $O_2$ is 2-9.5%. [1, 6, 7] Therefore, *in vitro* normoxia employs an $O_2$ concentration 4-5 times higher than physiological normoxia. The physiological normoxia, however, is normally taken as hypoxia in *in vitro* culture. As a result, *in vitro* normoxia culture may alter cell activities compared with physiological normoxia. Cells cultured under normoxia change their shapes and have been found to have different functionality compared with cells *in vivo*. [8] Moreover, it has been found that the oxygen concentration influences cellular activities. [9-12] Therefore, special attention should be paid in tissue engineering and tissue and organ preservation to this difference between *in vitro* normoxia and physiological normoxia.

Hypoxia and even anoxia are common in tissue engineering, tissue and organ preservation, cell and tissue transplantation, and wound healing. [13-16] In these circumstances, oxygen

deficiency occurs either because the solubility of oxygen in culture medium and body liquids is extremely low and the effective diffusion distance of oxygen is limited or the blood supply, which carries oxygen, to the tissues and organs is interrupted due to the impaired blood vessels. Therefore, delivering oxygen to cells and tissues may alleviate hypoxia in the tissues and organs.

## 2. Current approaches for oxygen delivery

Oxygen delivery has been applied in tissue engineering, tissue and organ preservation, and wound healing [2, 17-20]. In tissue engineering, it has been found that oxygen delivery improves the oxygenation of engineered tissues, promotes cell proliferation, and augments cell metabolic activities [21, 22]. Oxygen delivery also prolongs tissue and organ preservation time and improves the functionality of preserved tissues and organs [23-26]. In addition, oxygen delivery has been found to promote the healing of various wounds, such as ischemic wounds caused by diabetes and radiation, chronic wounds, and burns [27, 28]. So far, various approaches have been developed to deliver oxygen to cells and tissues, including hyperbaric oxygen therapy, normobaric hypoxic therapy, persufflation, employing liquids with high oxygen solubility, administrating artificial hemoglobin, and inducing angiogenesis with growth factors [29-35]. However, all these methods have various disadvantages, such as limited availability and portability of equipment, oxidative toxicity, vasoconstriction, and nonconfirmed efficacy over other treatments [36-38]. Another approach for oxygen delivery is to use oxygen-generating agents, mainly peroxides that decompose to generate oxygen in the presence of water. Oxygen-release systems consisting of peroxides have been used to deliver oxygen to tissues and cells. It has been reported that oxygen delivery using peroxides improves cell viability and islet functionality under hypoxia, delays tissue necrosis in skin flaps, and promotes wound healing [2, 18, 39, 40]. Nevertheless, the reported materials to date are either

nondegradable, have inflexible shapes, which restricts the application of the materials, and cytotoxicity, or require toxic catalysts and high concentrations of catalase. Therefore, the current oxygen delivery systems based on peroxides still need to be improved.

## 3. Thesis objective

The aim of this work includes development of a biodegradable *in situ* oxygen delivery system with a controlled oxygen-release rate, evaluation of the oxygen-release capacity and cytotoxicity of the oxygen-release material using hypoxia resistant and intolerant cells, preservation of various tissues with the oxygen-release material, and treatment of ischemic wounds using the oxygen delivery system.

### 3.1 Preparation of oxygen delivery material

The oxygen delivery system was composed of calcium peroxide (CP), hydrophobic biodegradable polymers and biocompatible catalysts. CP were used as the oxygen generating agent, hydrophobic biopolymers were used to reduce the decomposition rates of the peroxide, and catalysts were incorporated into the system to remove the cytotoxicity of $H_2O_2$. Alginate hydrogel was employed to encapsulate the oxygen-release material to further reduce the oxygen-release rate.

### 3.2 Evaluation of oxygen release capacity and biocompatibility of the oxygen-release material

The oxygen-release capacity and cytotoxicity of the oxygen-release material was tested with hypoxia resistant primary human fibroblasts as well as hypoxia-sensitive Madin-Darby canine kidney (MDCK) cells under anoxic culture. Furthermore, MDCK cell transplantation, with and without oxygen-release material, was performed subcutaneously on rats. Hypoxia occurs in the

implants due to ischemia, which reduces cell viability in the transplanted scaffolds. In this work, the effects of oxygen delivery on cell viability in the transplants were examined.

### 3.3 Preservation of blood vessels at physiological temperature by oxygen delivery

Currently, the most common way to preserve tissues and organs is to keep them at low temperatures (hypothermia). Under hypothermia, the metabolic rate of cells is decreased, so is the oxygen consumption rate of the cells. Hence, the preservation time for tissues and organs is prolonged. However, reperfusion injuries take place after hypothermic preservation caused by both the cold temperature and hypoxia during preservation. In this work, oxygen delivery material was used to preserve rat aortas at physiological temperature to avoid reperfusion injuries. Blood vessels have a relatively simple composition and a geometric structure. They have a tube-like shape and are composed of smooth muscle and endothelial cells, and extracellular matrix. The functionality of the blood vessels can conveniently be tested by measuring endothelial mitochondrial membrane potential and biochemically stimulated contraction force. Therefore, the blood vessel is a good model for tissue preservation studies. So far, preservation of blood vessels has been performed under hypothermia and reperfusion injury due to cold preservation is alleviated by adding antioxidative agents into modified preservation solutions. I sought to preserve blood vessels at physiological temperature by oxygen delivery to avoid reperfusion injury.

### 3.4 Effect of topical oxygen delivery on ischemic wound healing

Hypoxia takes place in wounds due to the interrupted blood supply to the wounded area caused by the impairment of blood vessels. As a matter of fact, wounded tissue consumes more oxygen than healthy tissue because wounded tissue needs to generate new cells and extracellular matrix

to repair the wounds and produce enough reactive oxygen species to prevent infection in addition to macrophages. Hence, hypoxia inhibits wound healing for several reasons. In this work, an ischemic rabbit ear wound model was used to investigate the influence of an oxygen delivery patch on preservation of wounded tissue and wound healing.

### 3.5 Preservation of adipose tissue

Adipocytes in the adipose tissue die under hypoxia, which causes a big issue in reconstructive surgery: resorption of transplanted adipose tissue. Following optimized experiments in the preservation of blood vessels, preservation of adipose tissue using the self-oxygenating scaffold at physiological temperature was attempted. The effect of tissue volume on adipocyte viability was assessed, and changes were made to minimize the death of adipocytes.

### 3.6 Other applications

Hypoxia induces angiogenesis, the formation of new blood vessels, through hypoxia-inducible factor-1alph (HIF-1α), a type of protein that promotes the secretion of vascular endothelial growth factor. However, long-term hypoxia inhibits angiogenesis since cells cannot generate enough energy to support the growth of cells and production of extracellular matrix for blood vessel formation. In this work, I investigated the effects of hypoxia on vascularization in implants using the oxygen-release scaffolds as a non-hypoxic control. In addition, preservation of various other tissues, such as mouse islets, mouse heart slices, heart brain slices, mouse liver, and rat bone marrow, was performed using the self-oxygenating scaffold at physiological temperature. Finally, incorporation of the oxygen-release microparticles into 3D printed scaffolds was attempted.

## Chapter 2

# Oxygen delivery using materials and bloodless life

Huaifa Zhang[1], Jake Barralet[1,2]

1. Faculty of Dentistry, McGill University, Montreal, QC, Canada
2. Division of Orthopaedics, Department of Surgery, Faculty of Medicine, McGill University, Montreal, QC, Canada

## Preface

Oxygen is essential for the survival of aerobic cells. Oxygen accepts electrons during oxidative phosphorylation, enabling cells to generate enough energy to support cellular activities. However, lack of oxygen, i.e. hypoxia, is common during tissue engineering, tissue and organ preservation, and wound healing, due to the extremely low solubility and limited effective diffusion distance of oxygen in water and body liquid. Various strategies have been developed to deliver oxygen to tissues and cells. In this chapter, current approaches for oxygen delivery using biomaterials in the field of biomedical engineering was reviewed. Since waste removal is also one of the key issues in tissue engineering, tissue and organ preservation, and wound healing, biomaterials that have been used to remove wastes from cells and organisms were also discussed.

## Abstract

Blood delivers oxygen and nutrients to cells and tissues and removes metabolic wastes. For decades, researchers have been trying to develop approaches that mimic these two functions of blood. Oxygen is crucial for the survival of tissues and cells in vertebrates. Hypoxia (oxygen

deficiency) and even at times anoxia (absence of oxygen) occur during organ preservation, organ and cell transplantation, wound healing, tumors, and in engineering of tissues.

To date, different approaches have been developed to deliver oxygen to tissues and cells, including hyperbaric oxygen therapy (HBOT), normobaric hyperoxia therapy (NBOT), employing liquids with high oxygen solubility, administrating artificial hemoglobin and red blood cells (RBCs), using oxygen-generating agents, persufflation, and generating oxygen through biochemical reactions and electrolysis. Metabolic waste accumulation is another issue in biological systems. Metabolic wastes change the microenvironment of cells and tissues, and influence the metabolic activities of cells, and ultimately cause cell death. This review examines advances in blood mimicking systems in the field of biomedical engineering and summarizes applications of biomaterials in oxygen delivery and metabolic waste removal.

**Key words:** biomaterials, oxygen delivery, PFCs, red blood cell transfusion, artificial hemoglobin, peroxides

## 1. Introduction

Oxygen ($O_2$) is crucial to the survival and metabolism of aerobic cells [41]. Different types of cells need different oxygen tensions to maintain their normal metabolic activities (Table 2.1). Oxygen concentration influences cell activities, including oxygen consumption rates (Figure 2.1), cell proliferation [2], cell differentiation [3], glycolysis [4], apoptosis [5], angiogenesis [42, 43] and gene expression [4]. Under severe hypoxia, cell apoptosis or necrosis will occur. On the other hand, high oxygen concentrations can also result in apoptosis or necrosis. [44, 45] The hypoxic limit of several cells and tissues is well known, and some are shown in Figure 2.2. Some doubt exists as to precise hyperoxic limits because cells can adapt to some extent with

conditioning. In general, hyperoxia causes cell death by excessive ROS generation and hydrogen peroxide production.

Table 2.1. Cell sensitivity towards hypoxia

| Hypoxia tolerant | Prefer hypoxia | Hypoxia sensitive |
|---|---|---|
| Fibroblast[2] | Stem cells[3, 46] | Renal cells [47] |
| Marrow [a] [48, 49] | Osteoclast [b] [50] | Neurons[51] |
| Tumor cells [52] | Corneal limbal epithelium | Primary hepatocyte[53] |
| HTC, FU5 and HepG2[53] | Chondrocyte [c] [54-56] | Islets [39] |
| Myoblast [57] | Endothelial cells[58, 59] | Osteoblast [60] |
| MIN6 β cell [d] [39] | Smooth muscle cell [57] | Retinal ganglion cells[61] |
| Chondrocyte [e] [54-56] | Myosatellite cells [62] | |
| | Sp2/0-derived mouse hybridomas [10] | |
| | Human embryonic stem cells [63] | |

Note: [a]: marrow stem cells can survive under 1% $O_2$; [b]: 2% $O_2$ promotes osteoclast activity; [c]: 1% $O_2$ promotes chondrocytes growth; [d]: MIN6 β cells survive 5% $O_2$; [e]: 5% $O_2$ does not kill chondrocytes.

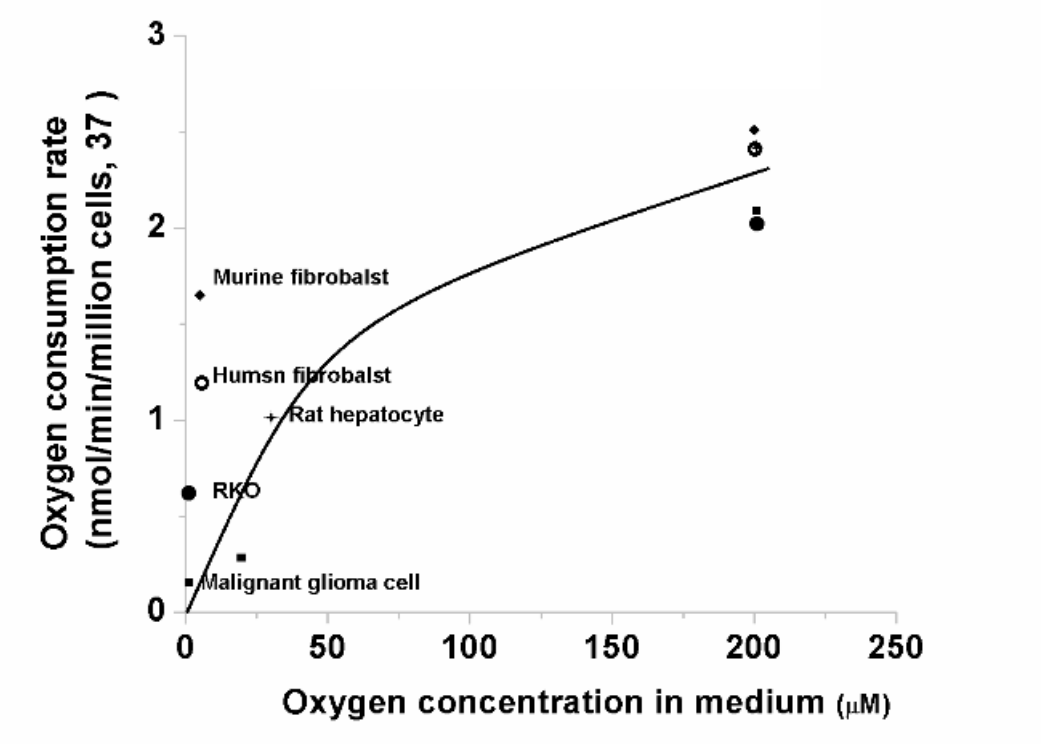


Figure 2.1. Oxygen consumption rates under different oxygen concentrations. [64-68] Generally, the consumption rates of oxygen of different kinds of cells increase as the oxygen concentration increases.

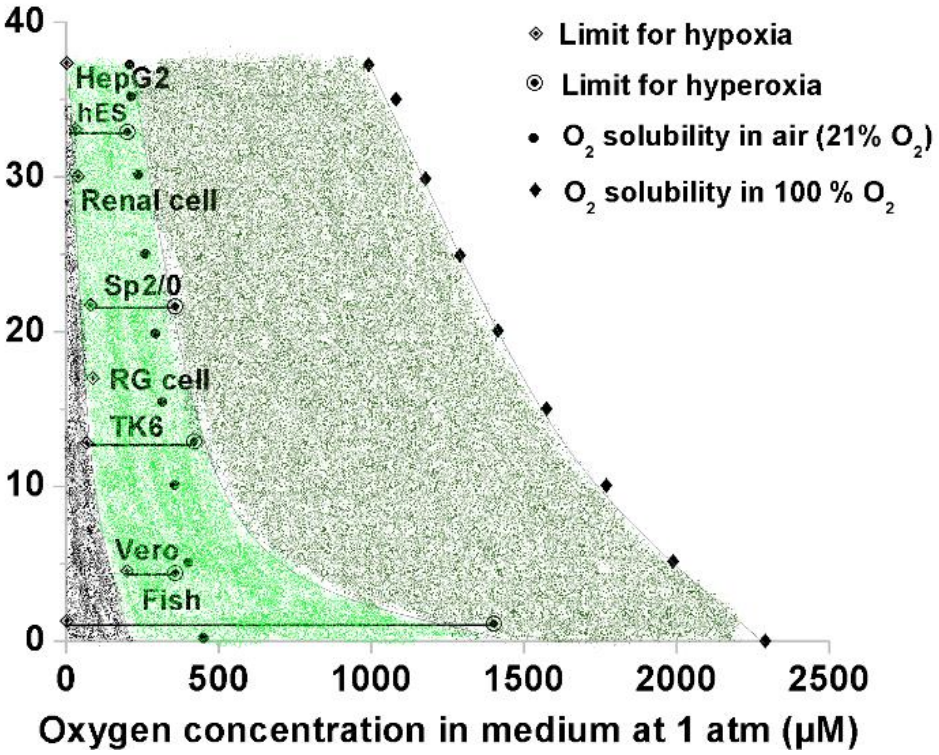


Figure 2.2. Oxygen tolerant of different kind of cells and organism. [69-71] From 37 ℃ to 0 ℃ in air the oxygen content of saturated water increases from 200 μM to 457 μM. In pure oxygen, however, their values are five times higher. Generally, cells and organisms can survive in the green area but cannot in the grey and dark green area.

Physiologically, oxygen is delivered to local tissues and cells by diffusion in the form of molecular oxygen dissociated from hemoglobin in red blood cells (RBCs). Soluble metabolic wastes will be removed from tissues and excreted from body mainly through the lungs and kidneys.

The oxygen tension of tissues ranges from 1% to 10% [1, 72, 73] while *in vitro* cell culture is normally carried out under 20% $O_2$ using a 5% $CO_2$ buffered solution. 1% $O_2$ is normally consider to be hypoxic in *in vitro* culture, although it is within the normal oxygen tension range

in tissues *in vivo*. Since the *in vivo* oxygen and $CO_2$ tension are much lower than that in *in vitro* culture, *in vitro* culture cannot represent physiological environment of cells. There is big difference between keeping cells alive and making cells to be comparable to physiological behaviors.

Given both the scientific and clinical interests of oxygen delivery, people have made numerous efforts to find suitable approaches for oxygen delivery. So far, methods, including hyperbaric oxygen therapy (HBOT), normobaric hyperoxia therapy (NBOT), employing oxygen soluble perfluorocarbons (PFCs), administrating artificial hemoglobin or RBCs, introducing oxygen-generating agents, persufflation, and generating oxygen through biochemical reactions and electrolysis have been explored to supply oxygen to tissues and cells under various circumstances (Table 2.2). In spite of the considerable research in the area, very few successes have been achieved in clinical practice.

Table 2.2. Methods for oxygen delivery

| Local oxygen release | *In situ* oxygen generation | Gaseous oxygen | Others |
|---|---|---|---|
| Perfluorocarbons | $CaO_2$ | Hyperbaric oxygen therapy | Porous scaffold |
| Artificial hemoglobin | $H_2O_2$ | Normobaric hyperoxia | Angiogenesis |
| Red blood cells | $Na_2CO_3$•1.5 $H_2O_2$<br>Urea•$H_2O_2$<br>Chlamydomonas reinhardtii | Persufflation | Biochemical reactions<br>Electrolysis |

Accumulation of metabolic wastes such as lactic acid, $CO_2$, and ammonia are toxic and can cause damages to cells and organs if the wastes are not removed in time. [74, 75] Although some efforts have been made to remove metabolic wastes using biomaterials, only several successes have been achieved. We will also discuss metabolic removal by biomaterials in this review.

## 2. Hyperbaric oxygen therapy

The amount of oxygen dissolved in tissues and liquid is proportional to the partial pressure of surrounding oxygen, according to Henry's law. Therefore, the oxygen concentration in tissues and blood can be increased by compressed oxygen. HBOT uses pure oxygen at two to three times of the atmospheric pressure at sea level in a chamber to increase the quantity of oxygen dissolved in interstitial fluid and plasma, thereby replacing at least some of the function of hemoglobin (Figure 2.3) [76]. HBOT has been used to treat carbon monoxide poisoning, decompression sickness, wound healing and organ preservation [77]. Henshaw [78] built the first hyperbaric atmosphere chamber in 1662, which formed the basis for the development of modern HBOT. Diseases that have been treated clinically with HBOT are listed in Table 2.3.

Figure 2.3. Hyperbaric oxygen therapy treatment chambers. Left: monoplace chamber; Right: multiple-place chamber. (Riess et al. [79] )

The first application of HBOT, which can be traced to 1895 [80], is to treat carbon monoxide (CO) poison by accelerating the removal of CO from blood and tissues [81]. In 1900, Mosso further confirmed the intoxication effects of HBOT on dogs and monkeys suffered from CO hypoxia [80]. Later in 1950, Pace et al. [81] conducted the first treatment on human volunteers and proved the beneficial effects of hyperbaric oxygen on CO intoxication in human. However, there is still no sufficient evidence to confirm the positive effects of HBOT on CO poisoning, based on the data until 2010 [82, 83]. Currently, hyperbaric oxygen therapy is not a commonly employed method for CO intoxication in clinic. According to Ku et al. [83], only 18.8% of the CO poisoned patients were treated with HBOT between 2000 and 2010. So far, there are no standardized protocols for HBOT for the treatment of CO poisoned patients. Very little information exists concerning the influence of different factors on the outcomes of HBOT for the treatment of CO poisoning, such as the delay of treatment, the treatment time period, gas pressure, treatment frequency and number of sessions, the severity of intoxication, and the condition of the patients [84-87]. Moreover, HBOT requires special instruments, which are

only available in a limited number of hospitals. Given the fact that normobaric-oxygen treatment through a face mask is the quite successful, HBOT is rarely a competitive method.

Decompression sickness is caused by formation of gas bubbles after the saturation of inert gas in blood and tissues after deep diving and high altitude ascending. Treatment of decompression sickness is one of the widely known applications of HBOT. [29] The United States Navy initiated the treatment of decompression sickness using HBOT in 1943. Now HBOT has become a standard method for the treatment of decompression sickness [29, 36] and standardized protocols have also been developed [88]. Nevertheless, the superiority of HBOT over the other available treatments for decompression sickness is not clear cut, following the data of randomized controlled clinical trials before 2011 [89]. Moreover, it has been suggested that different factors relate to the patient's physical conditions and the parameters in the therapy should be taken into consideration to get ideal results.[90]

Another application of HBOT is wound treatment through oxygenation, including late radiation injuries, chronic refractory osteomyelitis [91, 92], ulcers [93-95], burns [96-98], acute wounds, flaps and grafts [99, 100]. Late radiation injuries cause tissue deterioration by means of reduction in vascularity and formation of fibrous tissue. The use of HBOT to treat late radiation injuries started in the 1970s [101, 102]. HBOT improves recovery from osteoradionecrosis and bone death caused by radiation [103-106] and increases the survival rate of implants in patients subjected to irradiation from 46.3% to 91.9% [107]. However, it seems that the positive effects are tissue-type dependent. Clinical trials have indicated that HBOT benefits the healing of the head, neck, anus, rectum, and tooth sockets suffering from late radiation injuries [102, 108] but not tooth implant success in irradiated patients [109]. Chronic refractory osteomyelitis refers to bone infections lasting for more than six months under appropriate treatments. Although

HBOT has been reported to have beneficial effects on the healing of chronic refractory osteomyelitis, it cannot cure chronic refractory osteomyelitis alone. The main treatment for chronic refractory osteomyelitis is currently a combination of surgeries and administration of antibiotics. [110] HBOT has been used to treat ulcers, the most common type of chronic wounds, since 1970 [93]. However, no conclusive effects of HBOT on the healing of ulcers have been demonstrated. Some clinical data indicate HBOT is likely to assist the healing of diabetic leg ulcers in some patients as an adjunctive therapy [94] while some results show that HBOT improves the healing only in a short term [95]. Results from 29 patients with chronic wounds between 2009 and 2012 show that HBOT improved wound healing in 50% of the patients while patients with diabetes mellitus did not response positively.[111] HBOT has been employed to treat burning wounds since 1967 [96]. Some pre-clinical experiments on pigs and rats have shown positive effects of HBOT on the healing of burn wounds [97, 98]. However, it is not clear if it is the oxygen or simply the high pressure that works [98]. Moreover, negative results have also been reported where HBOT inhibits healing of burns in pigs while normobaric 100% $O_2$ promotes it [112]. Only several clinical trials have been reported using HBOT to treat burn wounds a decade ago [113-115]. Moreover, systemic reviews concerning the HBOT for thermal burns failed to find enough evidence supporting the positive effects of the therapy. [37, 116] Therefore, HBOT may not be a good approach to treat burning wounds. HBOT is believed to promote acute wound healing by producing oxidant through oxygenating tissues and inducing neovascularization. [117, 118] Nevertheless, its effects on acute wounding healing cannot be warranted based on the data before 2013 [119]. Interestingly, HBOT can only oxygenate the superficial layers of skin as gaseous oxygen cannot penetrate the skin. [120] Ischaemic stroke, mostly caused by focal cerebral ischemia [121], has been treated with HBOT in an attempt to oxygenate the brain [122-124]. Yet again the existing trials have shown

conflicting results [123, 125, 126] and cannot prove the efficacy of HBOT due to the small number of patients, based on the data before 2014. [127]

HBOT has also been used for organ preservation. Hatayama et al. reported that they managed to preserve rat hearts in a mixture of compressed CO (400 kPa) and oxygen (300 kPa) for 48 hours at 4 ℃ and the preserved hearts were able to beat after transplantation. [128] CO is believed to act beneficially by reducing inflammatory, alleviating apoptosis and suppressing metabolic activities of cells.

Table 2.3. Diseases treated by hyperbaric oxygen therapy clinically

| Diseases | Efficacy over other treatment options |
|---|---|
| CO poisoning [80-87] | Unconfirmed [82, 83] |
| Decompression sickness [29, 88, 89, 129] | Confirmed [89, 90] |
| Late radiation injuries [101, 103-109] | Inconclusive [102, 109] |
| Chronic refractory osteomyelitis [91, 92] | Unconfirmed [110] |
| Burning wounds [96-98, 112, 113, 115] | Negative [37, 114, 116] |
| Ulcers [93, 94] | Inconclusive [111] |
| Acute wounds [100, 118] | Unconfirmed [99, 119] |
| Acute ischaemic stroke [122-126] | Unconfirmed [123, 125, 127] |
| Femoral head osteonecrosis [130-133] | Not conclusive [132, 133] |
| Aseptic osteonecrosis [134, 135] | Not conclusive [134, 135] |

In summary, hyperbaric oxygen therapy has been used to treat various diseases in clinic. The main risks of HBOT include systemic oxygen poisoning, due to highly compressed oxygen (with a pressure higher than 2 atmospheres) and long exposure time to pure oxygen, ear damages caused by high pressure, neurotoxicity, and fire [79, 116, 136]. The other main disadvantages associated with HBOT include large and expensive devices, limited availability

and requirement of trained technician. Although superficially logical, much clinical use of HBOT is not supported by statistically trials and variations in protocols make frustrate comparison.

### 3. Normobaric hyperoxia therapy

Normobaric hyperoxia therapy (NBOT), unlike HBOT, oxygenates tissues and organs using high concentrations of oxygen at atmospheric pressure. NBOT normally uses 40-100% $O_2$, which is higher than atmospheric oxygen concentration. [137] The most important application of NBOT is to protect neurons during cerebral ischemia and acute ischemic stroke. [30, 137-139]

NBOT protects neurons by maintaining their oxygenation and does not show oxidative toxicity after 24 h perfusion with 100% $O_2$ in focal cerebral ischemia models. [140-142] Henninger et al. [30] found that early NBOT improved brain cell viability in penumbral in a rat embolic stroke model. However, early stage of NBOT is mandatory in these circumstances because neuron died very fast in ischemia and the damages are not reversible. [143] Data from 52 patients with traumatic brain injury in two different units show that NBOT improved tissue oxygenation and reduced intracranial pressure comparing to the patients' base line and other patients in control group. [144] Moreover, NBOT does not show oxidative toxicity in patients with traumatic brain injuries. [145] More recently, results from a phase II clinical trial show that the combination of HBOT and NBOT improve the oxidative metabolism of the brains and reduces mortality in patients with traumatic brain injuries compared with the standard treatment. [146] The reader is directed to the following reviews for more information concerning NBOT in cerebral ischemia and stroke treatment [137, 139, 147]. In addition, NBOT has been shown to alleviate acute renal failure caused by haemorrhagic shock in rats. [148]

Although many reports have shown NBOT does not cause oxidative toxicity when used for a short time to treat patients with brain ischemia, oxidative toxicity has been observed in organs and tissues of NBOT treated animals, especially when the treatment time is long (>12 h). [149-151] It has also been reported that the protective efficacy of NBOT on neurons is influenced by endothelial nitric oxide synthase dysfunction. [138] Moreover, NBOT has been found to change microcirculation in healthy people by decreasing capillary perfusion and oxygen concentrations in the muscles. [152]

In summary, NBOT can oxygenate tissues in ischemia and is neuroprotective. Because it is easy to administer and the devices for NBOT are portable, NBOT can be a very good method to treat ischemic brain injury and ischemic stroke at the very early stage to open the therapeutic time window. [153] Nevertheless, the efficacy of NBOT for the treatment of brain ischemia and stroke over other methods still needs to be confirmed based on more evidence, and guidelines for the administration need to be specified. [154]

## 4. Local oxygen release

Substances in which oxygen is highly soluble or binds reversibly, such as PFCs, artificial hemoglobin and RBCs may be used as oxygen delivery vehicles and even reservoirs of oxygen itself.

### 4.1 Perfluorocarbons

PFCs have a long history of clinical use. They are extremely chemically and biologically inert volatile liquids and possess a very high respiratory gas-dissolving capacity. [155] Therefore, PFCs have been employed as oxygen vehicles to deliver oxygen to tissues and cells. Among

the PFCs, perfluorodecalin (PFD, $C_{10}F_{18}$) and perflubron ($C_8F_{17}Br$) are two of the most widely studied products. They have high oxygen and $CO_2$ gas solubility and a high excretion rate through the lungs (Table 2.4) [155-158]. They are $CO_2$ sinks and dissolve $CO_2$ to release oxygen in tissues. PFCs have been used in various applications, including liquid ventilation, blood substitute, tissue/organ preservation, wound healing, *in vitro* cell culture and tissue engineering, which are discussed in the following sections.

Table 2.4. Physical properties of perfluorodecalin ($C_{10}F_{18}$) and perflubron ($C_8F_{17}Br$) [158]

| Properties (Units) | $C_{10}F_{18}$ | $C_8F_{17}Br$ |
|---|---|---|
| oxygen solubility (vol. %, 25 ℃) | 40 | 50 |
| $CO_2$ solubility (vol. %, 25 ℃) | ~140 | ~210 |
| melting point (℃) | -10 | 5 |
| vapor pressure (torr, 37 ℃) | 14 | 10.5 |
| interfacial tension vs. saline (mN/m) | ~60 | 51.3 |

4.1.1 Liquid ventilation

Liquid ventilation, an important treatment for acute lung injuries and acute respiratory distress syndrome, employs oxygenated liquids to fill the lungs to support the respiration of animals. [159, 160] In fact, liquid ventilation for gas exchange was the first demonstrated biomedical application of PFCs, initiated by Clark and Gollan in 1966 to supply oxygen to mice and cats [161]. In their ground-breaking experiment, mice survived up to 20 h after being submerged in a PFC liquid, perfluorobutyltetrahydrofuran or FX-80, saturated with oxygen (Figure 2.4). Liquid ventilation can be divided into two classes: total (or tidal) liquid ventilation (TLV) in which liquids fill the entire alveolar space and airways, and partial liquid ventilation (PLV), where only part of the alveolar is filled with liquids. [162]

Figure 2.4. Mouse breathing the liquid PFC (FC-80) saturated with oxygen (Pr. L. C. Clark, Jr., Department of Pediatrics, University of Cincinnati). (Lowe [163] Copyright 2006, Royal Society of Chemistry)

Extensive studies concerning the interaction between PFCs and tissues during ventilation have been carried out, such as distribution and elimination of the liquids in tissues and effects of retained PFCs on tissues. [164-171] PFCs can be eliminated by the lungs and the amount of PFCs retained in tissues depends on the type of inhaled PFCs, organs, and species. [164, 165] Nevertheless, the residue in the case of FX-80 does not affect the growth of animals. [166, 167] PFCs can reduce the response of alveolar macrophages to potent stimuli, enhance surfactant phospholipid synthesis and secretion, and decrease the formation of reactive oxygen species (ROS). [168-171] Animal experiments have shown that liquid ventilation of PFCs improves gas exchange in tissues. [167, 172-174] Partial liquid ventilation alleviates acute allograft dysfunction after lung transplantation in dogs and results in better outcomes than conventional mechanical ventilation. [31]. Similar results have been reported in juvenile piglets with endotoxin induced acute lung injuries. [175] However, the outcome of PLV can be affected by

both the volume of PFC used and the filling rate [176]. These parameters should therefore be optimized to improve the outcomes. In contrast, liquid ventilation of PFCs performed on humans showed conflicting results. Greenspan et al. [165], Shaffer et al. [177] and Leach et al. [178] reported that liquid ventilation improved gas exchange on preterm neonates or infants. On the contrary, Kacmarek et al. [179] reported that PLV did not show improvements in terms of 28-d mortality when administrated on patients with acute respiratory distress syndrome, either at high or low doses. In summary, encouraging results have been reported about liquid ventilation with PFCs. Nevertheless, concerns still exist about applying liquid ventilation clinically given that the physiology of PFC is still not clear. [180] Moreover, liquid ventilation also causes lung injuries. [173, 175] This technique still needs to be improved to get good clinical results by optimizing parameters like oxygenation levels of administrated PFCs, volume of PFCs used, filling rates, and ventilation time period.

### 4.1.2 Blood substitute

Blood substitutes largely only undertake a small part of the real blood function, i.e. to transport respiratory gases oxygen and $CO_2$. Therefore, they mainly replace the role of hemoglobin in RBCs. They are intended to solve issues surrounding the traditional blood transfusion methods, such as shortage of blood supply in acute situations [182], immunologic risks, infectious safety issues [182, 183], and also religious objections. [184-186]

Perfluorocarbon emulsions have good oxygen solubility and are biologically inert and relatively stable in blood, and thus they are promising blood substitutes (Table 2.5) [182]. There have been many research articles and reviews concerning blood substitute using PFCs [187-198]. Geyer carried out the first whole blood substitute using PFC emulsions (FC-47), when he kept rats in excellent condition for at least 9 months. [198] The problem was that their

products retained in the animals for lifetime. Afterwards, PFD was found to be excreted rapidly by both Clark [199] and Naito [200], which enlightened the future of PFCs in biomedical applications.

So far, several PFC blood substitute products have been developed, including Fluosol-DA 20%, Perftoran, Oxygent, and Oxycyte. Among them, only Fluosol-DA 20% and Perftoran have been used clinically. Fluosol-DA 20% was approved in 1990 in USA and some European countries, but production stopped in 1994 [163] because of defects such as a low oxygen-carrying capacity (approximately 40% of that of red cells), poor stability, and adverse effects of its surfactant. [182, 201-203] Perftoran was approved for clinical application in Russia in 1996 and is the only PFC based blood substitute still being used clinically [204]. Oxygent is the most advanced oxygen-carrier under development from Alliance Pharmaceuticals (La Jolla, CA) [205]; it has a greater oxygen-carrying capacity and improved stability and shelf life compared with former products. However, the product encountered setbacks in the phase 3 trial [206] and the company's partner refused to fund them to resume the trial. Oxycyte is another blood substitute under development from Tenax Therapeutics. In 2014, FDA approved the company's request to do clinical testing of Oxycyte, however, the company stopped their phase 2b trial six-month later. Meanwhile, people keep working on developing new PFC blood substitutes that are able to carry more oxygen. [207, 208]

Table 2.5. Summary of main PFC emulsions [197, 201, 209-212]

| Name | Producer | Clinical application or year of invention | Adverse effects | Storage |
|---|---|---|---|---|
| Fluosol-DA 20% | Green Cross Corporation | Approved by FDA in 1989 | Flu-like symptoms, platelet level decrease | Frozen |
| Perftoran | Perftoran | Approved by Russia in 1996 | Hypotension, Pulmonary complications | Frozen |
| Oxypherol | Green Cross Corporation | Invented in 1970s | Long time retention in body | Cold |
| Oxycyte | Oxygen Biotherapeutics, Inc | Halted phase 2b trial in 2014 | Potential transient mild thrombocytopenia | Cold |
| Oxygent | Alliance Pharmaceuticals | Stopped Phase 3 trial in 2003 | Headache, nausea and delayed onset fever | Cold |

In fact, analysts are not optimistic towards the development of blood substitutes. They do not expect there will be successful blood substitutes within the next several years, at least in the commercial market. Because the blood substitutes are much more expensive than donated blood [206]. In addition, the blood substitutes have other problems, like flu-like symptoms and macrophage hypertrophy and recruitment. More information concerning different kinds of PFC products used for blood substitute and the problems encountered in the area can be found in the following reviews. [189, 213, 214]

### 4.1.3 Tissue/Organ preservation

PFCs have been used to preserve tissues and organs based on the assumption that deterioration of organ function following harvest is due to oxygen deficiency. PFCs have been used as

oxygen suppliers to various tissues and organs, including islets, brains, pancreas, hearts and kidneys, either by static preservation or perfusion [215-224]. Preservation outcomes of organs with PFCs seem to depend on the type of organs and species (Table 2.6). [225]

Cold static preservation using PFCs has been performed on islets, pancreas, and kidneys. Both PFD and perflubron emulsions improve the functionality and viability of islets. [23, 24, 226] However, perfluorodecalin failed to show improvements in long-term preservation and after transplantation [227-229]. Oxygenated PFCs have been found to improve the outcomes of pancreas preservation in most cases compared with preservation buffers. Oxygenated PFC-UW showed beneficial effects on the preservation of rat kidneys but not pig kidneys. [230, 231].

PFCs have also been used to preserve brains, kidneys, hearts and livers through perfusion. In 1967, Sloviter and Kamimoto [25] first reported the perfusion of an isolated rat brain with perfluorocarbon emulsion (FX-80) and maintained the brain's function and metabolism for one hour. In 1980, Dirks et al. [232] perfused an isolated rat brain with perfluorotributylamine (FC 43) emulsions and kept the brain alive for more than 7 h, whereas blood perfused brains only survived for 4.5 h. PFC emulsions have been used to preserve kidneys by perfusion since 1970s. [233] Cold oxygenated Perftoran perfusion may minimize the reperfusion injury of preserved human kidneys. [234] Kidneys from brain-dead pigs have been preserved for 18 h [235] by hypothermic perfusion using an oxygenated mixture containing PFC emulsion. The beneficial effects of PFC emulsions on heart preservation have been shown in different species, such as rats, pigs, dogs, and rabbits. [236-239] However, the preservation results of hearts depend on the type of PFC emulsions. [240] PFC emulsion perfusion has been proven to be beneficial in rat liver preservation but is not helpful for the preservation of pig livers. [241-245]

In summary, PFCs have been used to preserve tissues and organs and have showed positive results. Nevertheless, most of the work is still at the preliminary stage.

Table 2.6. Perfluorocarbon emulsions for tissue/organ preservation

| | Species | Outcomes | Clinical practice |
|---|---|---|---|
| Islet | Human, rat, dog, pig | Oxygenation improved *in vitro* preservation in short term (24 hours), no improvement in long term or after transplantation [23, 24, 227, 229, 246, 247] | No |
| Brain | Rat, pig | Sustained survival of brain by perfusion [25, 232, 248] | No |
| Pancreas | Human, pig, rat, dog | Certain types of PFCs improved the yielding of isolated islets from pancreas (7 hours) [228, 249], some did not make many improvements [223]; OLM was better than TLM [250, 251]; | Yes [252, 253] |
| Kidney | Human, pig, rat, dog | Perfusion with PFC emulsions improved preservation outcomes [233-235, 254] | No |
| Liver | Rat, pig | Improved liver preservation outcomes in rat livers but not in pig livers [241-245] | No |
| Heart | Rat, pig, dog, rabbit | Perfusion with PFC emulsions preserved hearts for at least 4 hours [236-240] | No |
| Lung | Pig, dog | PFCs improved lung preservation outcomes [255, 256] | No |

4.1.4 Wound healing

The process of wound healing requires oxygen [14]. Oxygen is believed to facilitate wound healing by promoting anti-inflammatory effects, preventing infection from anaerobic pathogens, and improving formation of collagen [257, 258]. Oxygenated PFCs have been found to promote wound healing. A topical oxygen emulsion (TOE) containing oxygen-saturated

perfluorocarbon has been employed to treat ischemic secondary-burns on porcine and was found to assist the epithelialization and collagen deposition of the wound and also promoted vasculogenesis. [259] Pieter et al. [257] and Shinzeki et al. [27] reported that intrarectally administrated oxygenated PFD promoted murine colitis healing. Wijekoon et al. [260] developed a hydrogel system consisting of PFC chains which was able to absorb and then release oxygen. Such a system could be used for wound dressing, however, no such study has been reported yet. PFCs have been employed to accelerate or improve wound healing by oxygen delivery, but no PFC products for wound healing is available so far.

#### 4.1.5 *In vitro* cell culture

Lack of oxygen is common during tissue engineering (in constructs with a dimension > 2 mm) and high-density cell culture, due to the limited solubility of oxygen in culture medium and the restricted diffusion distance of oxygen from culture medium towards cells. [261] Suboptimal levels of oxygen eventually affects the overall health of the cells [45]. PFCs have been employed during cell culture to supply oxygen to cells. They increase oxygen concentrations in the culture system, improve cell metabolic activities, and change cell functionality. For example, oxygenated perfluoromethyldecalin (FlutecR pp11) improved mouse-mouse hybridoma cell growth as well as antibody production [262]. In addition, the presence of oxygenated PFCs improves viability, proliferation, and differentiation of other cell lines and stem cells. [263-265] PFCs also improved the metabolic activities of HepG2 cells encapsulated in hydrogel and the growth of CP5 bovine chondrocytes in polylactide (PLA) scaffolds [266, 267]. Fluorinated polymers have been developed to deliver oxygen to cells in scaffolds. [260, 268] Nevertheless, PFCs were found to have dose-dependent toxic effects on mouse spleen cells and higher doses reduced cell viability [269]. In summary, PFCs are able to supply oxygen

to cells and adjust oxygen tension in the culture system. No products or work related to clinical applications have been reported so far.

### 4.1.6 Tissue engineering

Compared with *in vitro* cell culture systems, lack of oxygen can be much more severe in tissue engineering. Due to the large dimension of the constructs and the limited diffusion distance of oxygen, even anoxia occurs in the core area of the engineering tissues. PFCs have been introduced to tissue engineering to alleviate hypoxia and anoxia. A guideline for preparing perfluorocarbon emulsions for biological applications has been proposed, i. e. choose the perfluorocarbon with the highest oxygen loading capacity, maximize the perfluorocarbon fraction, and use the smallest emulsion droplets. PFCs have been used in tissue engineering in different ways, such as perfusion, incorporation into scaffolds or addition to culture medium. [17] In 2009, Tan et al. [21] reported that Oxygent perfusion increased epithelial partial oxygen tension of tissue-engineered trachea (TET), which improved epithelial metabolism and tended to slow cartilage tissue formation without impairing angiogenesis. Moreover, fluorinated zeolite has been embedded into polyurethane scaffolds to improve human coronary artery smooth muscle cell growth in the scaffold as well as cell infiltration depths into the scaffold. [270] It has also been found that oxygenated Oxycyte$^{R}$ increases oxygen capacity of culture medium and cell activities in the 3D bioartificial device. [22] Recently, it has been reported that PFD emulsions improve the viability of transplanted rat islets. [251]

In conclusion, enormous efforts have been made to oxygenate tissues and cells using PFCs in various applications. Encouraging experimental results have been obtained *in vitro* and in animal experiments. However, a gap still exists between the development of PFC products and the expectation of the realm. Moreover, the side effects caused by PFCs themselves or by the

additives in emulsions retard the development of PFC based products. [203, 271, 272]. In addition, PFCs are expensive to manufacture and recover [273]. It is also necessary to optimize the delivered oxygen amount [274] to avoid over oxygenation [229]. Further work is required to get a better understanding of the interaction between the PFC products and biological systems, control the oxygen delivery process, find suitable clinical applications, and carry out clinical trials wisely.

### 4.2 Allogeneic red blood cells

RBCs are responsible for the task of oxygen delivery in animals. Isolated RBCs have been used as blood substitute to improve oxygenation. They are the most commonly transfused blood compound in clinic. RBCs can be stored for up to 42 days at 2 ℃ in citrate-dextrose-phosphate solution normally. [275] RBCs are not biomaterials but are supposed to be the baseline for the best oxygen delivery results one can get. Although the first case of RBC transfusion in patients was performed in 1964 [276], there are still problems concerning RBC transfusion, such as screen of applicable patients and principles for RBC administration. Marik and Corwin [277] found that RBC transfusions were associated with increased morbidity and mortality in adult, intensive care unit, trauma, and surgical patients after analyzing current data and suggested assessing every patent before conducting RBC perfusion. The adverse effects associated with RBC transfusion have been reviewed [278] and recommendations about RBC transfusion under various circumstances have also been proposed [279]. In 2014, Wilkinson et al. [280] suggested that larger patient sample sizes were required to assess the efficiency of RBC perfusion for the treatment of specific types of diseases with standardized perfusion procedures.

In summary, RBC perfusion has been used to improve the oxygenation of blood. However, the efficacy of RBC perfusion for the treatment of some diseases is not clear based on the current

data. This therapy also has some risks, including the introduction of exogenous blood-borne disease, transfusion reaction, and exposure of foreign blood cells [281]. Careful evaluation is necessary before transfusing RBCs to patients.

### 4.3 Stabilized (Artificial) hemoglobin

Hemoglobin is the basic oxygen delivery vehicle in blood. It is able to bind and release oxygen at different oxygen and $CO_2$ concentrations. In 1925, Adair et al. [282] successfully imitated the $CO_2$ dissociation curves of blood with a mixture of hemoglobin and sodium bicarbonate, which demonstrated the potential of hemoglobin being used without the red corpuscle. However, outside RBCs, hemoglobin molecules are easy to dissociate into sub-proteins, which cause renal toxicity. Therefore, it is necessary to stabilize hemoglobin. The most commonly employed methods for hemoglobin stabilization include using intra-molecular cross-linking to stabilize the tetramer [283], initiating intra- and intermolecular polymerization to increase molecular size and surface conjugation. Another approach is to encapsulate hemoglobin into delivery vehicles (Figure 2.5).

Stabilization of hemoglobin was initiated in 1929 by Haurowitz and Waelsch [284]. The performance of polymerized hemoglobin is influenced by different factors, such as molecular mass, concentrations of circulated hemoglobin, and temperature. [285-287] The main problems with hemoglobin based blood substitutes include oxidative stress and vasoconstriction, which causes hypertension and reduces blood supply to tissues. To reduce oxidative stress, hemoglobin has been copolymerized with peroxidases or antioxidants. [288, 289] Bäumler et al. [38] reported that vasoconstriction can be eliminated by narrowing size distribution (around 700 nm). PEG surface coating has been found to eliminate macrophage uptake, prolong blood circulation and reduce cytotoxicity of hemoglobin [290]. Encapsulated hemoglobin has been

reported to improve the cerebral oxygenation of various species, such as rats, pigs, and nonhuman primates, and maintain normal cerebral metabolism. [291-293] Different kinds of materials have been employed to encapsulate hemoglobin to improve the performance of hemoglobin. Cationic amylose has been used to improve both the stability and oxygen-loading capacity of encapsulated hemoglobin. [294] Liposome encapsulated hemoglobin is able to maintain systemic oxygen uptake in rabbits and may accelerate wound healing after gastric incision and anastomosis in rats. [33, 295] Lumbricus terrestric erythrocruorin (LtEc), a natural extracellular hemoglobin, has also been used for oxygen delivery. LtEc also has a low autoxidation rate and a limited nitric oxide dioxygenation activity. [296]

Silverman and Weiskopf [297] summarized the existing information on hemoglobin-based oxygen carriers, including their characteristics and clinical properties, and addressed the serious adverse events observed during clinical trials which did not appear in animal experiments. Among the diverse opinions concerning applying hemoglobin-based products as oxygen carriers, the prevailing view is that the most substantial challenge is to find appropriate applications for the products which have a favorable balance of benefits and risks. So far, only one hemoglobin-based product developed by Biopure has been approved in South Africa to treat perioperative anemia in clinic. [298]

So far, intensive studies have been conducted to use modified hemoglobin for oxygen delivery and encouraging progresses have been achieved in terms of reducing side effects and enhancing oxygenating ability of the products. Nevertheless, their application in clinical practice is still limited.

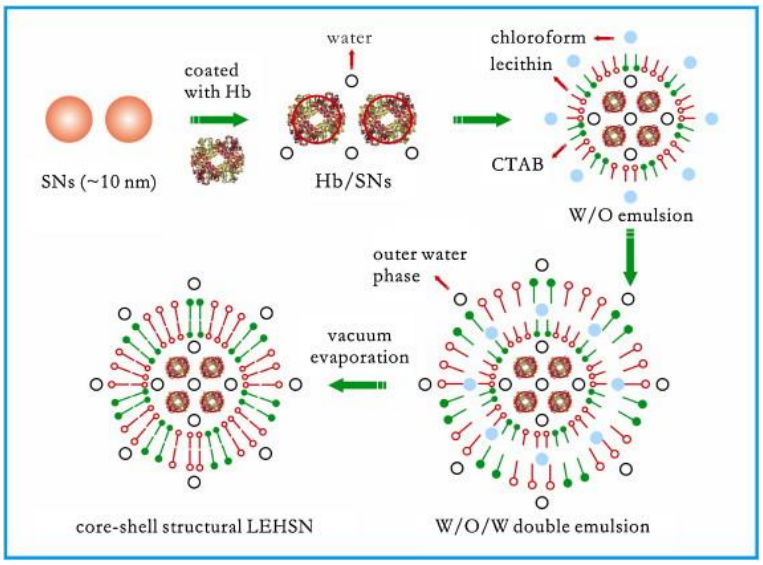


Figure 2.5. A schematic diagram of hemoglobin encapsulation in liposome. (Liu et al. [299] Copyright 2012 with permission from Elsevier)

**5. Oxygen-generating agents**

This category mainly refers to peroxyanions, including metal peroxides and hydrogen peroxide. Peroxides are often unstable and can decompose to produce molecular oxygen when in contact with water. [300] It is possible to control the decomposition rate of metal peroxides by adjusting the available amount of water. In this way, they can be used to supply oxygen to cells sustainedly with tunable gas release rate. They have been used in agri- and aqua-culture to supply oxygen to plants and aquatic animals. [301-303] The main chemical reactions involved in the decomposition of peroxides are presented using CP as an example (Equation 1-3). It is often neglected that peroxides produce radicals during decomposition and these radicals have not been treated well. Under the 5% $CO_2$ atmosphere used in cell culture, the alkaline reaction product further reacts to form calcite.

Peroxides, including sodium percarbonate ($[Na_2CO_3]_2 \bullet 3H_2O_2$), CP, and $H_2O_2$, have been used to deliver oxygen to tissues and cells in different applications (Table 2.7), such as *in vitro* cell culture [2, 39, 40] and tissue preservation [39, 304]. Although promising results have been obtained, the present methods still need to be improved. Harrison et al. [304] embedded $[Na_2CO_3]_2 \bullet 3H_2O_2$ into Poly(d,l-lactide–*co*–glycolide) (PLGA) films and found that the material was able to delay the necrosis process of skin flaps during the first three days *in vivo*. However, there was no difference between the experimental groups and control groups after seven days, possibly because the material failed to generate enough oxygen for such a long period. CP has been used to supply oxygen to fibroblasts in PLGA scaffold and reported to improve cell growth compared with cells cultured under hypoxia (1% $O_2$). However, one of the problems was that very high concentrations of expensive catalase (around $10^6$ times that of catalase in blood) were required to alleviate the cytotoxicity of $H_2O_2$ generated by CP. Moreover, the authors did not compare the experimental group with cells cultured under normoxic conditions. [2] Pedraza et al. [39] encapsulated CP in silicon rubber plates and employed their plates to deliver oxygen to β cells and islets under hypoxia (1% $O_2$). They found that the oxygen-release plates improved both the MTT reduction activity and LDH release of islets for short time periods. However, LDH release increased ten times for both experimental and control groups. Few data beyond two days were presented. With β cell culture, the presence of CP improved cell proliferation but the hypoxic control did not show cell death. In addition, the PMDS used in their system was not biodegradable, which compromised the *in vivo* applications of the material. Moreover, the size of the material was quite large and its shape was inflexible. Another kind of peroxide that has been used to deliver oxygen for tissue engineering is $H_2O_2$, which has been encapsulated into PLGA microspheres. It enhanced the viability of cardiosphere-derived cells (CDCs) under hypoxia (1% $O_2$). Again, high concentrations of catalase (at least $2\times10^7$ times of that in blood) were used to catalyze the

decomposition of $H_2O_2$ and minimize its cytotoxicity. [40] Peroxides based oxygen delivery has been reviewed and the reader is directed to the following review[305]. More recently, Chandra et al. [18] developed a wound dressing using $[Na_2CO_3]_2 \bullet 3H_2O_2$ and CP as the oxygen source, probably to use the combined fast and low oxygen-release rates. The authors found that the oxygen generating dressing facilitated wound healing using a pig wound model. Nevertheless, this article is currently under review, no data can be seen yet. Moreover, they used $MnCl_2$ as the catalyst to remove $H_2O_2$, but $MnCl_2$ is soluble in water and cytotoxic, making it very easy to diffuse out of the system into tissues and kill cells. [306]

Peroxides as oxygen delivery agents have the following advantages, including low prices, easy to store, controlled amount of oxygen in their formulas, *in situ* release of oxygen, adjustable oxygen-release rates, and metabolizable byproducts. Nevertheless, one big problem with peroxides is the cytotoxicity of $H_2O_2$, which exists in all the peroxide-based oxygen delivery systems. $H_2O_2$ generates radicals, which are very cytotoxic. Very low concentrations of $H_2O_2$ (as low as 0.03 mM) can kill cells. [307, 308] Moreover, peroxides decompose very fast and result in burst release of oxygen or hydroxyl ions, which can also kill cells. Therefore, it is essential to reduce the decomposition rate of peroxides and minimize the concentration of $H_2O_2$. So far, there are only two reported *in vivo* experiments.

Table 2.7. Peroxides used for oxygen delivery in tissue engineering

| Peroxides used for tissue engineering | Applications | Catalysts |
|---|---|---|
| $CaO_2$ [2, 39] | β Cells, rat islets, fibroblasts | No catalysts; Catalase |
| $H_2O_2$ [40] | Cardiosphere-derived cells | Catalase |
| $Na_2CO_3$•1.5 [304] | Skin flap preservation | No catalysts |
| $Na_2CO_3$•1.5 and $CaO_2$ [309] | Pig dermal wounds | $MnCl_2$ |

$$CaO_2 + 2H_2O \rightarrow Ca(OH)_2 + H_2O_2 \quad (1)$$

$$2H_2O_2 \rightarrow 2H_2O + O_2 \quad (2)$$

$$Ca(OH)_2 + CO_2 \rightarrow CaCO_3 \downarrow + H_2O \quad (3)$$

In addition to peroxides, researchers also tried to use photosynthetic biomaterials to produce oxygen (Figure 2.6). Schenck et al. [310] seeded microalgae *Chlamydomonas reinhardtii* cells into a collagen scaffold. They found that those cells continued to grow during incubation and produced oxygen in the presence of white light. They further engrafted the scaffold into a mouse full skin defect. The microalgae survived five days and did not cause a native immune response in both mouse and zebrafish models. Chimetric tissues were also generated composed of algae and murine cells while interesting the requirement for light is clearly an obstacle to application.

Oxygen-generating agents are receiving more and more attentions to deliver oxygen to tissues and cells, usually as a more practical alternative to HBOT. Although some research work has been done, the utilization of oxygen-generating agents in the biomedical field has just started and further work is required to improve the oxygen delivery systems.

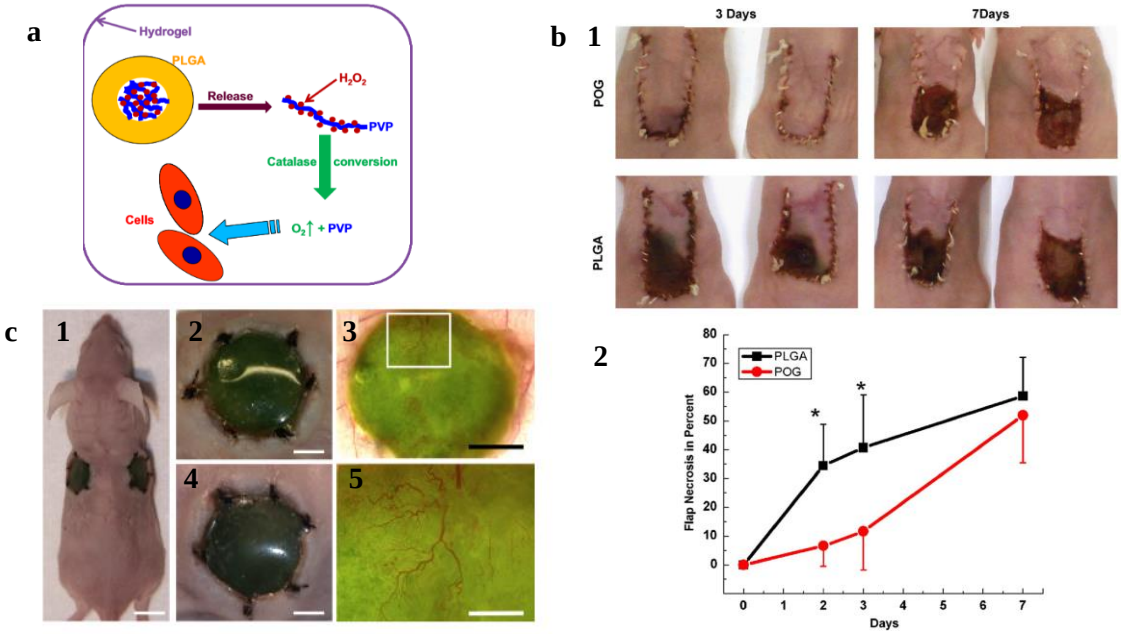


Figure 2.6. Application of peroxides and photosynthetic biomaterials for oxygen delivery. [304, 310] a: schematic of preparation of $H_2O_2$-based oxygen-release particles (Li et al. [40] Copyright 2012 with permission from Elsevier); b: tissue necrosis in skin flaps with (POG) and without (PLGA) $[Na_2CO_3]_2 \cdot 3H_2O_2$ (1) and the quantified necrosis percentage (2) (Harrison et al. [304] Copyright 2007 with permission from Elsevier); c: Photosynthetic materials engrafted *in vivo* (1), no infection or inflammation was observed (2 and 4) and blood vessels were formed in the material (3 and 5). (Schenck et al. [310] Copyright 2015 with permission from Elsevier)

## 6. Other oxygen delivery methods

### 6.1 Topical oxygen delivery

Several products are available or in development for oxygen delivery to wounds (Table 2.8). Among these products, different methods are employed to generate oxygen, including water electrolysis, precharging with pure oxygen, biochemical reactions, and $H_2O_2$ decomposition.

Epiflo (Ogenix Corp, USA), NATROX™ (Inotec Amd Limited, UK), and TransCu $O_2$® ($EO_2$ Concepts®, USA) extract oxygen from air using an electrochemical oxygen concentrator. Those devices are activated by a battery and can generate oxygen continuously. [311] Epiflo is about 2″x 2.5″x 1″in size and around 100 g in weight. [311] Both Epiflo and NATROX™ deliver gaseous oxygen through a thin flexible tube to an oxygen delivery system which is in contact with the wound surface. Extra dressings that absorb fluids may be required. The cost is normally below $1,000 per patient using NATROX™ as indicated on their website [312]. None of the three types of devices can be reused. Among these devices, Epiflo is the most studied oxygen generator. [19, 313, 314] It has been reported to promote the healing of sickle cell ulcers [314], warfarin induced skin necrosis [315], and chronic wounds [316] but not in the wound following cardiac surgery or in dermal wounds on health horse [317, 318].

Another commercial product, OxyBand (OxyBand Technologies, Inc. USA), delivers prefilled pure oxygen to wound sites through dressing. [319] OxyBand uses a barrier layer to load oxygen and allows oxygen to diffuse to the wound through a permeable porous layer and can sustain oxygen delivery for 5 d. This dressing has been reported to accelerate the healing of burn wounds in humans and reduce pain scores as well. [319] OxygeneSys™ from Halyard Health (USA) has also been used to deliver dissolved oxygen directly to the treatment site via wound dressing. It has a closed cell foam matrix enriched by pre-filled oxygen and sustains 48 h. [320] New research showed that OxygeneSys™ reduced inflammation and necrosis in pig skin flaps compared with flaps treated with normal hydrogel dressing. [320] Oxyzyme™ (Insense Ltd, UK) is a hydrogel dressing incorporating a biochemical system which increases the dissolved oxygen concentration at the wound surface. It consists of two separate components which must be applied together to activate the biochemical process. The two gel sheets are presented in individual aluminium foil laminate pouches. The first gel containing

glucose and iodide ions is placed directly upon the wound surface. The second gel contains glucose oxidase, which catalyzes the oxidation of (beta)-D-glucose to D-gluconic acid and hydrogen peroxide. Hydrogen peroxide oxidizes iodide ions thereby liberating oxygen. [321] The dressing is typically changed every 2-3 d. The product is considered safe for patients [321, 322], has been reported to promote the healing of ulcers, and is more cost effective compared with standard care. [28, 323] Dermox$^{TM}$ (Med-e-Cell, USA) is a topical oxygen wound treatment device. It can maintain oxygen-rich or oxygen-depleted micro-environments over the wound electrochemically (Med-e-Cell) and generate a time-dependent oxygen concentration profile. However, Dermox$^{TM}$ is still under early stage preclinical testing. In 2014, Ochoa et al. [324] developed an oxygen generating film consisting of parchment paper, $MnO_2$ catalyst and PDMS microfluidic network. They circulated $H_2O_2$ into the network and generated oxygen through $H_2O_2$. This system could be used for wound healing in certain circumstances.

These topical oxygen delivery systems all produce oxygen and are mostly only used for wound healing treatment. Nevertheless, none of them are implantable, and the majority of them are single use and expensive. Compared with the electrical devices, the dressing systems are more convenient to apply, but it is difficult to control oxygen-release rates for the dressing systems. In fact, these systems are derived from HBOT while no clear evidence can support that HBOT promotes wound healing. These systems have not proven to surpass HBOT. [325] Moreover, delivering oxygen by surface flushing is not effective at penetrating skin. [317] Therefore, more studies are required to evaluate the efficiency of these products. [326, 327]

Table 2.8. Topical oxygen delivery products on the market

| Name | Manufacturer | Working principle | Regulatory status |
|---|---|---|---|
| Epiflo | Ogenix Corp, USA | Electrolysis | FDA approved [311] |
| NATROX™ | Inotec Amd Limited, UK | Electrolysis | Approved in Europe [328] |
| TransCu $O_2$® | $EO_2$ Concepts®, USA | Electrolysis | FDA approved [329] |
| OxyBand | OxyBand Technologies, Inc. USA | Prefilled oxygen | Clinical trials [330] |
| OxygeneSys™ | Halyard Health, USA | Prefilled oxygen | Pre-clinical study [331] |
| Oxyzyme™ | Insense Ltd, UK [332] | Biochemical reactions | Approved in UK [312] |
| Dermox™ | Med-e-Cell, *USA* | Electrolysis | Early stage on rat [333] |

6.2 Persufflation

Persufflation refers to the use of gaseous oxygen to flush the tissues via arteries or veins to alleviate or eliminate hypoxia. It was first reported by Rudolf Magnus in 1902 when he found that a cat heart continued to beat when it was perfused by gaseous oxygen. [334] So far, persufflation has been employed to preserve hearts [335-339], kidneys [26, 32, 340], livers [341-344], pancreas [345, 346] and small intestines [347]. Encouraging positive experimental results have been reported for the preservation of those organs and tissues. There are two types of persufflation: anterograde persufflation and retrograde persufflation. Anterograde persufflation follows the physiologic flow path while retrograde persufflation introduces gas to the organs and tissues from the opposite direction of physiological flow. It has been suggested that each kind of persufflation may be suitable for different organs and tissues. [348] For example, it is better to oxygenate the coronary with anterograde persufflation to preserve hearts, while for the preservation of kidneys and livers retrograde persufflation should be employed. [348]

Persufflation has been reported to preserve hearts for up to 14.5 h [349]. Mownah et al. [20] recently reported that porcine hearts preserved by persufflation during cold storage had a better chance to functionally recover compared with hearts preserved by static cold preservation. Isselhard et al. [350] investigated the metabolic activities of canine kidneys persufflated with pure oxygen and found a very small deviation of metabolic activities from the regular status. The decrease rate of ATP level in kidneys was greatly reduced. The ATP level of kidneys stored at 6 ℃ under anaerobic ischemia (no perfusion) decreased 50% within 30 min, whereas it took 48 hours for kidneys preserved at 6 ℃ by persufflation to reach similar ATP levels. Treckmann et al. [26] compared the preservation results of porcine kidneys using static cold storage, machine perfusion and persufflation. They found that persufflation preservation resulted in a higher seven-day survival rate, faster functional recovery and better preserved tissue architecture after transplantation compared with the other two methods. Minor et al. [351] tried to preserve rat livers at 4 ℃ with the assistance of venous oxygen persufflation for 24 hours. They found that oxygen persufflation resulted in better preserved mitochondria and sinusoidal endothelial lining compared with static cold preservation. Moreover, persufflation has been reported to be superior to TLM, static cold preservation, and hypothermic perfusion for the preservation of the pancreas in terms of tissue integrity, *in vitro* function and islets yielding. [352, 353] Persufflation has also been reported to increase ATP levels in the pancreas [354]. More information about persufflation in organ preservation can be found in a review written by Suszynski et al. [355] In spite of these efforts made by researchers, persufflation is still limited to animal experiments.

Persufflation has been used in combination with cold storage to preserve various tissues, such as porcine hearts, canine kidneys, porcine kidneys and rat livers, and encouraging results have

been obtained. In general, persufflation has a better oxygenation effect than other preservation methods and results in improved tissue integrity, better functionality, higher levels of ATP, and enhanced post transplantation survival rates. However, the barrier to use persufflation in humans is an embolism. This method also has some inherent disadvantages. For example, it can neither provide nutrients to the cells nor remove non-gaseous metabolic wastes, and is therefore not able to preserve tissues for long time. Moreover, persufflation causes embolization after transplantation. Interestingly, no hyperoxia toxicity caused by persufflation has been reported while 95% $O_2$ induces inflammatory lung injuries and lung cell apoptosis in rats. [356]

### 6.3 Peritoneal oxygenation

Oxygenation of the peritoneal cavity utilizes the peritoneum's large surface area and high vascularity as a gas exchanger to replace the role of lung. Intraperitoneal oxygenation has been attempted using oxygen since 1970 [357]. Faithfull et al. [358] circulated 20% Fluosol-DA to deliver oxygen to rabbits by peritoneal perfusion. They found that the product increased oxygen tension and decreased $CO_2$ tension in arteries. Feshitan et al. [359] developed oxygen microbubbles (OMBs) coated with phospholipid and injected the OMBs into the intraperitoneal space of rats. This method enabled all the rats with acute lung trauma to survive at least two hours and kept the hemoglobin saturation and heart rate at normal levels during that timeframe. Peritoneal oxygenation improves short-term oxygenation of the body to replace lung function. The application of peritoneal oxygenation on humans has not been reported yet.

## 7. Metabolic waste removal

Although supplying oxygen prevents hypoxia, another crucial role of the blood is the removal of metabolic wastes. Accumulated wastes such as lactic acid, $CO_2$, and nitrogen wastes, change

local pH and ion concentrations, alter cell activities, and can ultimately kill cells in tissues and organs. (Table 2.9) Nitrogen wastes, including ammonia, urea, creatinine, uric acid, and indoxyl sulfate, are important toxic wastes. Among them, ammonia is the most toxic substance [360] and can even be lethal. [361] It induces inflammation and brain edema, poisons neurons, and causes metabolic disorders, which can kill cells. [362-365] It can also change pH in cells, interrupt energy metabolism, and damage organs. [361, 366] Urea and creatinine have been reported to reduce survival time of anephric rats. [367] Increased creatinine in old patients with breast cancer induces fever and neutropenia toxicity. [368] Uric acid concentration in serum related to mortality from cardiovascular diseases and ischemic heart disease in women. [369, 370] Uric acid is also related to hypertension, coronary heart disease, cardiovascular diseases, and renal diseases. [371-374] More information about nitrogen toxins can be found in the following reviews. [375, 376] *In vitro* experiments show that lactic acid impairs T cell function and changes proliferation and differentiation behaviors of osteoblasts. [377, 378] Elevated $CO_2$ levels increase respiratory minute volume, arterial pressure, and heart rate. [379]

Table 2.9. Cytotoxicity of various metabolite wastes

| | Cytotoxicity | Serum concentrations | Removal approaches |
|---|---|---|---|
| Ammonia | Inflammation, brain edema, neuron poison, oxidative stress, cell death, liver and renal pathology [361-366] | 0.039-0.09 mg/dL [380] | Liver, kidney, activated carbon, zeolite, and renal tubule cell assist device [381-384] |
| Urea | Reduced viability of anephric rats [367] | 20-45 mg/dL [385] | Kidney, cell therapy, dialysis, and activated charcoal [386, 387] |
| Uric acid | Coronary heart disease, hypertension, cardiovascular disease, renal diseases [369-374] | 5.4-6.7 mg/dL [388] | Activated charcoal, and dialysis [389, 390] |
| Creatinine | Fever, neutropenia toxicity [368] | 0.9 ± 0.1 mg/dL [391] | Kidney, activated charcoal, and dialysis [390, 392] |
| Indoxyl sulfate | endothelial dysfunction, oxidative stress, cardiac fibrosis, kill cells [393-398] | 2.9 ± 2.0 mg/dL [399] | Kidney, carbon, and dialysis [400-402] |
| Lactic acid | Impairs tumor immunogenicity, change cardiac output [377, 378, 403] | 3.3 ± 1.9 mg/dL [404] | Biocarbonate, dialysis, and administration of base [405] |
| $CO_2$ | Increase respiratory minute volume, arterial pressure and heart rate [379] | | Lung and blood [406] |

The most common way to remove waste in *in vitro* is simply by changing the culture medium or using sufficiently high volumes of culture medium so that toxic levels of wastes will not be reached. In high-density cell culture, perfusion is normally used to remove metabolic wastes and products. [407] Zeolites are molecular sieves with good cationic absorbent properties,

especially for ammonia [408, 409]. They have been used to remove ammonia wastes in high-density cell culture and reduce the concentration of ammonia to the safe range. [410]

Activated carbon has been used to remove nitrogen wastes from blood and rat intestine [411, 412]. Encapsulated activated charcoal has been used to replace some of the kidney's function to remove nitrogen metabolites and has been found to improve the kidney function of rats with chronic renal failure. [387, 390] Microencapsulated genetically transfected cells have also been used to remove urea and successfully reduced plasma urea levels in uremic rats by oral administration. [386, 413] Researchers have found that incorporation of renal tubule cells into filtering fibers improves ammonia excretion in uremic dogs. [414] In clinic, activated carbon has been used in hemodialysis as an absorbent to remove toxins in patients. [415] An oral adsorbent (AST-120) made of porous carbon has been used to remove nitrogen toxins from patients with chronic kidney disease. [400, 416, 417]

Dialysis, which uses semi-permeable membranes to remove metabolic waste (small molecules and ions) from blood, has been used in clinic since 1950s. [418, 419] The reader is directed the following literature for more information. [419-421]

PFCs can be used to remove $CO_2$ since $CO_2$ is highly soluble (can be more than 160 % v/v) in PFCs. [422] Metal peroxides can also remove acidic wastes, such as lactic acid and $CO_2$, as they generate alkaline byproducts during decomposition and might reasonably be expected to form calcium salts of acidic metabolites. [300]. Another approach is to induce new blood vessels in the engineered tissues or use porous scaffolds so that local metabolic wastes can be easily removed from tissues and cells. [42, 423, 424]

The problem with perfusion is that it exerts shear stresses onto cells, which can kill cells. Zeolites and activated carbon can remove ammonia without killing cells but absorb valuable bioproducts at the same time. [425] PFCs can remove $CO_2$ but cannot remove other wastes. Metal peroxides are able to neutralize acidic products but decompose very fast, and the resulting hydroxides can over neutralize lactic acid and $CO_2$. Therefore, it is necessary to control the decomposition rates of peroxides. As to the dialysis, it is very expensive. Patients normally cannot afford to use dialysis for a long time, although it is unavoidable in most cases. The life quality of patients is greatly reduced due to the frequent and time-consuming dialysis. Long-term dialysis can also cause lethal infective endocarditis. [426] AST-120 delays the initiation of dialysis in patients but does not guarantee improved survival rates after dialysis. [400] For the removal of accumulated lactic acid, different ways of base administration have been used. Nevertheless, the beneficial effects of base administration have not been confirmed yet. [405]

In summary, although different approaches have been explored to remove metabolic wastes from cells and tissues, they are either expensive, non-effective, or non-confirmative.

## 8. Conclusions and work to do

A variety of approaches have been developed to deliver oxygen to tissues and cells. Various materials and methods have been used for oxygen delivery, such as HBOT, BNOT, PFCs, artificial hemoglobin, RBCs, peroxides, topical oxygen-release devices, persufflation of gaseous oxygen, and peritoneal oxygenation. Nevertheless, the results are not very satisfactory. These approaches either cannot get approved in clinic, have no conclusive positive effects, cause oxidative toxicity, or are expensive and have limited availability. Developing a product with controlled oxygen-release rate, acceptable cost, and minimal side effects is necessary.

More efforts should be made to determine the appropriate applications for each kind of method. There is also a gap between the oxygen requirement of different kinds of tissues and the oxygen-release behavior of various oxygen delivery methods.

Among the different approaches, HBOT has been used in clinic and showed beneficial effects on several diseases. However, HBOT requires special devices, has limited availability, needs specially trained operators, and has the risk of oxidative toxicity. Therefore, more research is required to evaluate its efficacy over other treatments. NBOT is more convenient to perform compared with HBOT and has proven to be beneficial for early brain ischemia and stroke, but it is not suitable for long-term use. Intensive efforts have been made to use PFCs for oxygen delivery, ranging from liquid ventilation to blood substitute to organ preservation to tissue engineering. Nevertheless, very limited success has been obtained in clinic so far. More work is required to find suitable applications for the PFC products, reduce side effects, and avoid over oxygenation. RBC transfusion has been used in clinic to improve oxygenation, but its positive influence on patients with certain types of diseases is still inconclusive. It also possesses risks including introduction of exogenous blood-borne disease, transfusion reaction, and exposure of foreign cells. Artificial hemoglobin has also been intensively studied but again with little success in clinic. One of the main problems with artificial hemoglobin is side effects. Oxygen generating peroxides are receiving more and more attentions in recent years, but the current systems are still immature, more work is required to push forward towards clinical applications instead of a proof of concept. Several products for topical oxygen therapy are available on the market, but they are expensive, single-use and non-infective. Persufflation of gaseous oxygen can oxygenate tissues and organs more effectively compared with other methods, however, it can only work in a short term since it can neither supply nutrients to the

cells nor remove wastes from the cells. Peritoneal oxygenation is only suitable for short-term use as well.

Metabolic wastes can cause serious damages to tissues and organs and can even be lethal. Although some achievements have been obtained by removing metabolic wastes with extracorporeal devices, with dialysis as the most important example, not much work has been done to remove the wastes with biomaterials either *in vitro* or *in vivo*.

We find a phenomenon that exists in every oxygen deliver method, i.e. many clinical trials cannot be used to estimate the positive effects on the investigated topics due to the defects in the experimental design. This is a waste of resources, including time, money, and human efforts. We argue that researchers and surgeons should work together closely so that the experiments could be designed and conducted properly and that valuable clinical data could be generated.

## Chapter 3

### Comparison of oxygen delivery to hypoxia resistant and intolerant cells in anoxia

Huaifa Zhang[1], Daisuke Sato[1], Svetlana Komarova[1], Simon Tran[1], Jake Barralet[1,2]

1. Faculty of Dentistry, McGill University, Montreal, QC, Canada

2. Division of Orthopaedics, Department of Surgery, Faculty of Medicine, McGill University, Montreal, QC, Canada

### Preface

As described in Chapter 1, the current methods for oxygen delivery have various drawbacks, such as side effects, oxidative toxicities, high costs, restricted availabilities of equipment, and limited penetration depths through the skin. Peroxides have been used to oxygenate tissues and cells, but the current systems either use toxic catalysts, require extremely high concentrations of catalase, or cannot be cultured with cells at a close distance. In this work a biodegradable oxygen delivery system that was capable of supporting cell growth under anoxia was developed. The oxygen delivery system maintained a normal growth rate of human primary fibroblasts and Madin-Darby canine kidney (MDCK) cells under anoxia, protected human primary fibroblasts from apoptosis and necrosis caused by anoxia, and greatly reduced the expression level of hypoxia related genes in human primary fibroblasts under anoxia. In addition, the oxygen-release material could encapsulate MDCK cells and sustained cell growth *in vivo*.

### Abstract

A biodegradable oxygen delivery material system (ODS) was prepared using calcium peroxide (CP) as the oxygen-generating agent, and hydrophobic biopolymers and alginate hydrogel to adjust the oxygen-release rate. Removal of cytotoxic $H_2O_2$ was achieved using manganese

dioxide ($MnO_2$) or iron (II, III) oxide ($Fe_3O_4$) catalysts. The oxygen delivery capacity and biocompatibility of ODS were evaluated with human primary fibroblasts and the very $O_2$ sensitive Madin-Darby canine kidney (MDCK) cells under anoxia. The ODS surprisingly maintained the viability of primary fibroblasts whereas the cells gradually died under anoxia. Furthermore, the ODS restored the activity and functionality of the cells to a normal level. The normal expression level of the gene associated with the glycolysis was maintained while a great reduction in the expression level of the apoptosis and angiogenesis related genes was observed. The ODS was further developed into a self-oxygenating scaffold (SOS) that supported the viability of encapsulated MDCK cells under anoxia. Furthermore, it was found that the SOS supported cell growth and promoted vascularization in the scaffold after subcutaneous implantation. Here, we developed a biodegradable oxygen delivery system with controlled oxygen-release rate and successfully rescued $O_2$ sensitive cells under anoxia and sustained cell growth *in vivo*.

**Keywords:** oxygen delivery, peroxide, anoxic culture, primary human fibroblast, Madin-Darby canine kidney, cell transplantation, vascularization

## 1. Introduction

Oxygen ($O_2$) is essential for mammalian cells and tissues in terms of cell proliferation and differentiation, gene expression, and molecular modulations. [1, 427] In tissue engineering, hypoxia often occurs because of the extremely low solubility of oxygen in the culture medium and the limited effective diffusion distance of oxygen inside the constructs. Consequently, oxygen is insufficient in the deeper area of a three dimensional (3D) tissue construct especially for tissues with large sizes or containing highly metabolically active cells. As a result, cell apoptosis and necrosis were induced due to the lack of oxygen. Furthermore, during wound

healing, the blood vessels are usually impaired, leading to a low or no blood supply to tissues. Being one of the major obstacles for the development of tissue engineering and wound healing, oxygen shortage could be alleviated with oxygen therapy. [428]

So far, mainly two strategies have been employed to deliver oxygen to tissues and cells. The first one aims to decrease the oxygen diffusion distance to cells with a bioreactor [429], by promoting angiogenesis [34], and by using a porous scaffold [430]. The second one focuses on increasing oxygen concentration surrounding the cells and tissues, with hyperbaric oxygen therapy [76], oxygenated perfluorocarbons (PFCs) [197], artificial haemoglobin [431] and oxygen generating agents [39]. Although bioreactors alleviate hypoxia by perfusing oxygenated culture medium through the scaffold, the perfusion exerts lethal shear stresses to the cells. The angiogenesis method induces formation of new blood vessels using growth factors and cells, nevertheless this approach is time consuming. [432, 433] Hyperbaric oxygen therapy, which is usually performed in sealed tanks, uses compressed oxygen to oxygenate tissues and obviously requires special equipment, and may cause systematic oxygen toxicity. [434] PFCs have long been used as oxygen delivery agents. They are chemically and biologically inert and have an exceptional oxygen loading capability, making them good candidates to serve as oxygen delivery vehicles for tissues and cells. Nevertheless, being highly dense, they will settle down to the bottom during culture and some side effects could occur [197]. Artificial haemoglobin has also been used to supply oxygen to tissues and cells. Nevertheless, their instability in the blood circulation requires their surface to be modified and this leads to adverse effects on the cells [431]. Another approach for oxygen delivery is to use oxygen-generating peroxides. Peroxides spontaneously decompose in water into oxygen. Several peroxides including hydrogen peroxide ($H_2O_2$) [435], sodium percarbonate ($Na_2CO_3$•1.5 $H_2O_2$) [304] and especially calcium peroxide (CP) [2] have been employed to

supply oxygen to the cells and the tissues. [436, 437] A major disadvantage is that they usually decompose very fast. In addition to the prevention of a sustainable oxygen supply, a fast decomposition rate causes accumulation of cytotoxic $H_2O_2$ in the culture medium. CP has a relatively low decomposition rate because of its low solubility in water and the re-precipitation of $Ca(OH)_2$ by-product onto the surface of CP, and thus is a good candidate for oxygen delivery. [2, 39, 438] Previous work using CP as oxygen delivery materials only rescued cells partially [2, 39, 304]. Additionally a well-controlled oxygen release from CP in a biodegradable scaffold has rarely been achieved in tissue engineering. [2, 304] The use of biodegradable materials *in vivo* is of emotional, financial and clinical interests for the patient as well as for the society where a second surgery could be avoided.

We developed a biodegradable *in situ* ODS with a tuneable oxygen-release rate to oxygenate the tissues and cells sustainably. CP powders were chosen as the oxygen generating agent and polycaprolactone (PCL) or poly(lactide-co-glycolide) (PLGA) and alginate hydrogel to control the oxygen-release rate. PCL and PLGA have already been approved by US Food and Drug Administration (FDA) and their hydrophobic characteristic slows down the decomposition rate of CP. Furthermore, PCL and PLGA reduce the surface area of CP powders as well, which further inhibits CP decomposition. In addition to limiting the amount of water available to CP, alginate hydrogel prevents the generation of oxygen bubbles in culture medium, which kill cells and cause blood clotting *in vivo* [439], and serves as a barrier to oxygen, avoiding burst release of oxygen towards cells. [440] Since the direct decomposition product of CP is the cytotoxic $H_2O_2$ [441], a catalyst ($MnO_2$ or $Fe_3O_4$) has been introduced in the ODS. The ODS is either presented as i) a sandwich-structured chunk with an oxygen-release slab in the middle, or ii) a self-oxygenating scaffold (SOS) consisting of oxygen-release microparticles and hydrogel.

Fibroblasts, existing in many organs and tissues, are very common cells and have been widely used as the reference in tissue engineering. In addition, they play an important role during wound healing by inducing angiogenesis, initiating anti-infection events, and taking part into the regeneration of tissues. Here human primary fibroblasts were chosen as the model to evaluate the material's ability to rescue cells under severe hypoxic circumstances (anoxia). The more oxygen sensitive Madin-Darby canine kidney (MDCK) cells, were then employed to further demonstrate the oxygen-release capability of the ODS. MDCK cells were successfully encapsulated within the SOS and the effects of oxygen delivery on cell growth evaluated *in vivo*. In summary, we successfully invented a biodegradable *in situ* ODS that sustainably supplied oxygen to cells and tissues with adjustable gas release rates.

## 2. Materials and methods

### 2.1 Preparation of sandwich-structured slab

CP-PCL slabs were prepared by mixing CP powders (Sigma, USA) with PCL (Mw 70,000-90,000, Sigma, USA) in chloroform (with fixed CP to PCL ratio) first. Then, a certain amount of CP-PCL mixture was added into a round foil mold with a diameter of 2 cm. Finally CP-PCL slabs would be obtained after the evaporation of chloroform in a fume hood at room temperature. Likewise, CP-$MnO_2$-PCL composites were prepared with the addition of a certain amount of $MnO_2$ (Fisher Scientific, Canada) into the mixture.

The sandwich-structured oxygen-release material was prepared according to Figure 3.1. 0.5 mL 1% sodium alginate (FMC BioPolymer, Philadelphia, USA) solution was used to prepare the first piece of hydrogel by spreading the solution onto a piece of filter paper wetted by 0.1 M $CaCl_2$ (Fisher Scientific, Canada); then CP powders or the material composites containing CP were put onto the prepared hydrogel; subsequently, another piece of alginate hydrogel was

made from 0.5 mL 3% sodium alginate solution similarly and put on top of the composite; in the end, the two pieces of alginate hydrogel were cross-linked by 1 M $CaCl_2$ for 5 min to form an intact structure.

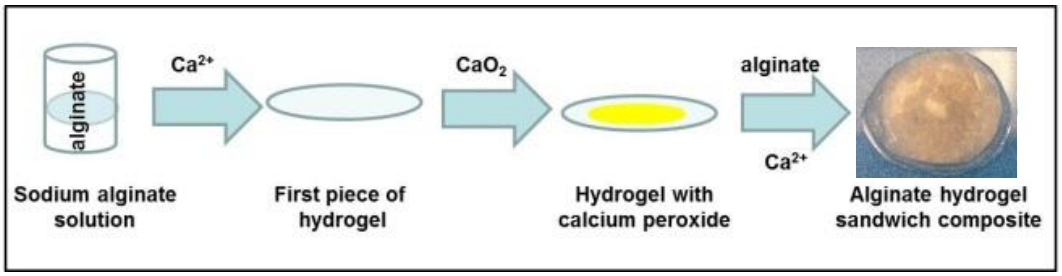


Figure 3.1. Preparation of the sandwich-structured material.

2.2 Preparation of oxygen-release microparticles

Oxygen-release microparticles (CP-$Fe_3O_4$-PLGA, weight ratio 1:10:10) were prepared using a phase separation method [442] in the absence of $H_2O$. CP powders and $Fe_3O_4$ (Aldrich, USA) were first mixed in PLGA (50/50, Mw 28,000, Advanced Polymer Materials Inc, Canada) solution in chloroform, then the suspension was added into glycerol (Fisher Scientific, Canada) with 1 % w/v polyvinyl alcohol (Mw 89,000-98,000, Aldrich, USA) (PVA) and stirred for 10 min at room temperature. When the particles became dry in a fume hood, the CP-$Fe_3O_4$-PLGA microspheres were collected by centrifuging the suspension at 4000 rpm, washed with alcohol three times, and dried at room temperature.

The morphology as well as the microstructure of the microparticles was examined under a scanning electron microscope (FE-SEM, FEI Inspect F-50, USA). Potassium iodide (KI, Fisher Scientific, Canada) and starch solution (Fisher Scientific, Canada) was used to detect $H_2O_2$ in the system and the solution became blue in the presence of $H_2O_2$.

2.3 Oxygen-release behaviors of the materials

To investigate the effect of PCL, $MnO_2$ and alginate hydrogel on oxygen-release behaviors of the material, oxygen release from the sandwich-structured slab was recorded using a bench pH/Ion meter (pH2100, Oakton, USA) and a Clark type micro-oxygen electrode (MI-730, Microelectrodes, Inc. USA) in a sealed reactor. At the beginning, 110 mL deionized $H_2O$ was added into the flask and flushed by $N_2$ from the bottom until almost all of the oxygen was removed (the meter reading became stable). Then, the oxygen-release material was put into flask and the reactor sealed. The composition of oxygen-release materials was listed in Table 3.1. Accumulated oxygen concentration in $H_2O$ was recorded every 15 min for 24 h. The measurement for each sample was repeated three times.

Table 3.1. Material composition

| | CP (wt %) | PCL (wt %) | $MnO_2$ (wt %) | Weight (mg) |
|---|---|---|---|---|
| CP-PCL | 25 | 75 | 0 | 45.3±3.49 |
| CP-$MnO_2$-PCL | 12.5 | 37.5 | 50 | 89.6±4.81 |

2.4 *In vitro* cell culture

Human primary fibroblasts (derived from foreskins after written informed consent which was approved by the Centre Hospitalier Universitaire de Quebec (CHUQ)'s Ethics Committee) were used to evaluate the ability of the oxygen-release material to support cell metabolic activities under anoxia. Fibroblasts were seeded in 6-well plate wells, which had been separated through cutting, with a density of $1.5\times10^5$ cells/well and left to attach to the wells overnight. Then the oxygen-release material was added into the well in insert with the 1% hydrogel side facing towards cells and the culture medium replaced by the one that had been pre-degased in $N_2/CO_2$ (10% $CO_2$) (buffered $N_2$) for 20 h. The process was carried out in the biological sage cabinet by putting the individual wells into a 50 mL jar which had been flushed by buffered $N_2$

beforehand and sealed with a rubber stopper. The jar was flushed by a balloon filled with buffered $N_2$ in the cabinet during operation. Cells were cultured under anoxia by putting the jars in a desiccator with grounded joint at 37 ℃. The desiccator was constantly flushed by buffered $N_2$ at a flow rate of 200 mL/min and the culture time was up to 4 d. Dulbecco's Modified Eagle Medium (DMEM) supplemented with 10% FBS and 1% penicillin-streptomycin was used for cell culture. Normoxia culture was carried out in a normal cell incubator with 20% $O_2$ and 5% $CO_2$ at 37 ℃. MDCK cells were cultured in a similar way at a density of $1.0\times10^4$ cells/well for up to 6 h. Two kinds of ODS, CP-hydrogel and CP-$MnO_2$-PCL-hydrogel, were used for MDCK cell culture.

Fibroblast viability was estimated through Alamar Blue staining (Invitrogen, USA). Alamar Blue is non-toxic to cells and generates fluorescent signals upon reduction by live cells. All the samples were stained before the experiments started and when the experiments were finished. Cells were washed with fresh culture medium three times before being stained; then 1 mL of Alamar Blue working solution was added to each well and incubated for 3 h under 5% $CO_2$ and 37 ℃; finally the solution was collected and measured on a plate reader (Spectramax M2E Microplate reader, Molecular Devices, USA) with an exciting wavelength of 540 nm and emission wavelength of 585 nm. Each sample was read three times by the plate reader and the average value was used. Cell viability was expressed as the percentage of the readings before experiments. Each experiment was repeated triplicate.

Alternatively, fibroblast viability was also examined by trypan blue staining (Gibco, USA). Trypan blue enters cells with compromised membranes and stains the nuclei of cells dark blue. Cells were washed with PBS twice after the removal of culture medium. Subsequently the cells were stained with 1% trypan blue in PBS and observed under a microscope (Leica DMIL, Leica,

Germany). The images were recorded using a digital camera (QICAM Fast 1394, QImaging, Canada). Another set of cells were used to quantify the cell viability. Firstly the culture medium was removed and cells were washed with PBS. Both the culture medium and PBS was collected. Successively the cells were detached by 0.25% Trypsin-EDTA, which would be counteracted with culture medium containing 10% FBS. Afterwards the cell suspension was centrifuged, together with the collected culture medium and PBS at the beginning, for 5 min at 1500 rpm/min. Next the supernatant was discarded and cells were re-suspended in PBS. Finally the cells were stained with trypan blue and counted with a hemacytometer [443]. Each sample was repeated three times. The viability of MDCK cells was also examined following the same method.

Cell viability was further observed through a fluorescent microscope (Imager.M2, Zeiss, Germany) after being stained by the live/dead assay. The live/dead assay (life science, USA) employs Calcein AM to stain live cells green and Ethidium homodimer-1 to stain the nuclei of dead cells red.

The apoptosis of fibroblasts was examined by a terminal deoxynucleotidyl transferees (TdT)-mediated dUTP nick end labeling (TUNEL) kit (GenScript, USA). TUNEL stains cells with impaired DNAs. Cells were seeded onto a glass coverslip in 6-well plate wells with a density of $1.5\times10^5$ cells/well and subsequently stained according to the provided instruction. Afterwards the slides were examined under a microscope (Leica DM4000B, Leica, Germany) and photographed by a digital camera (Retiga 2000R Fast, QImaging, Canada). The ratio of apoptosis cells was estimated by counting both the stained and unstained cells. Three random view fields were counted for each sample.

The proliferation behaviors of fibroblasts were assessed using a BrdU Immunohistochemistry Kit (Abcam, Canada), which stains cells that synthesize new DNA, i. e. cells that are mitotically active in S phase. Cells were seeded onto glass coverslips with the same method with TUNEL and stained following the given protocol at designed time points. The samples were then examined under a microscope (Leica DM4000B, Leica, Germany) and photographed by a digital camera (Retiga 2000R Fast, QImaging, Canada). The ratio of dividing cells was estimated by counting both the stained and unstained cells. Three view fields were counted for each sample.

q-PCR was performed to investigate gene expression of the fibroblasts cultured under different conditions. The expression of genes related to glycolysis, apoptosis and angiogenesis, which were glucose transporter 1 (GLUT 1), Bcl-2/adenovirus E1B 19kD-interacting protein 3 (BNIP3) and vascular endothelial growth factor (VEGF), respectively, was inspected. Beta-2-microglobulin (B2M) was chosen as the house-keeping gene, which has been shown to have a stable expression level under the hypoxic environment. [444] RNA isolation was performed using the RNeasy Mini Kit (Qiagen) following the instructed procedures. Successively, cDNA was prepared through reverse transcription using a High Capacity cDNA Reverse Transcription Kit (Applied Biosystems, USA). In the end, q-PCR was carried out on a real time PCR machine (7500 Real Time PCR System, Applied Biosystems, USA) with the DNA being labeled by Sybr green (Power SYBR Green PCR Master Mix, Applied Biosystems, USA). Primer sequences for the genes were listed in Table 3.2. Three replicates were performed and triple measurements done for each sample. Cells cultured under normoxia were set as the standard during analysis. The average value was used.

Table 3.2. Primer sequences of the genes

| | Forward | Reverse |
|---|---|---|
| GLUT 1[445] | 5'-CAA CTG GAC CTC AAA TTT CAT TGT GGG-3' | 5'-CGG GTG TCT TAT CAC TTT GGC TGG-3' |
| BNIP3[446] | 5'-CTG AAA CAG ATA CCC ATA GCA TT-3' | 5'-CCG ACT TGA CCA ATC CCA-3' |
| VEGF[445] | 5'-CAG CGC AGC TAC TGC CAT CCA ATC GAG A-3' | 5'-GCT TGT CAC ATC TGC AAG TAC GTT CGT TTA-3' |
| B2M[447] | 5'-AGGCTATCCAGC GTACTCCA-3' | 5'-CCAGTCCTTGCTGAAAGACA-3' |

Reactive oxygen species (ROS) produced by MDCK cells were measured using a DCFDA-Cellular Reactive Oxygen Species Detection Assay Kit (Abcam, Canada) following the instruction. The cells were seeded in 6-well plate wells at a density of $1.0\times10^4$ cells/well and left to attach to wells overnight. Then the cells were labeled with DCFDA for 45 min. Afterwards the cells were cultured under different conditions. In the end, the culture medium was collected and a plate reader (Spectramax M2E Microplate reader, Molecular Devices, USA) was used to measure the ROS with an exciting wavelength of 485 nm and emission wavelength of 535 nm. Triplicates were performed for each sample.

2.5 Cell encapsulation

MDCK cells were encapsulated in SOS at a density of $1\times10^6$ cells/mL. Briefly, MDCK cells were mixed with 1% w/v alginate solution containing CP-$Fe_3O_4$-PLGA microparticles, then the mixtures were extruded into 0.1 M $CaCl_2$ solution to form beads of 5 mm in diameter. Cells were also encapsulated in 1% w/v alginate hydrogel with $Fe_3O_4$-PLGA microparticles as the negative control. Encapsulated cells were cultured under anoxia to evaluate the effect of oxygen-release materials on cell viability.

2.6 Cell transplantation

Athymic "nude" male rats (Crl: NIH-Foxn1) supplied by Charles River Laboratories, which were 6- to 7-week old and 200-220 g in weight, were used for subcutaneous implantation. All experiments followed Canadian Institutional Animal Care Guidelines and were approved by the Animal Care Committee at McGill University. For subcutaneous implantation, MDCK cells were labeled with carboxyfluorescein succinimidyl ester (CFSE, Abcam, Canada) and encapsulated in hydrogel with and without oxygen-release materials before surgery and kept on ice. Before the surgery, the rats were anesthetized using isoflurane. Two places on the dorsal surface were shaved. A 4 cm skin incision was made and one pocket was created on each side of the incision to yield a total of 2 pockets, where scaffolds with (right side) and without (left side) oxygen-release microparticles were implanted. Implants were taken out after 2 and 4 weeks.

Cell viability in the implants was examined under the fluorescent microscope. To examine cell growth after transplantation, implants were retrieved and cells in the alginate hydrogel released by dissolving the hydrogel with a 100 µl 55m M potassium citrate and 90 mM NaCl (pH 7.4) solution for 20 min at room temperature. The cells were stained with trypan blue exclusion

staining and counted under a microscope with a haemocytometer to assess their population. [448]

For histological characterization, the implants were fixed in 4% paraformaldehyde in PBS overnight and then embedded in paraffin. Haematoxylin and eosin staining (H&E) was performed to examine the structure and cell density of the implants. Vascularization and vascular endothelial growth factor (VEGF) secretion in the scaffold were examined using immunohistochemistry.

## 3. Results

### 3.1 Effects of PCL, hydrogel and $MnO_2$ on oxygen release

Figure 3.2 shows the direct effects of the polymer and catalyst composition in the ODS on the oxygen release. According to Figure 3.2a, the oxygen-release rate of CP-Gel was the fastest whereas CP-PCL in the hydrogel decomposed the slowest, i.e. the lowest oxygen-release rate. PCL greatly decreased the amount of released oxygen by 265% in only 24 h (Figure 3.2a). The addition of $MnO_2$ catalyst to the CP-PCL composite increased the release of oxygen by 46% in 24 h (Figure 3.2b). Nevertheless, the alginate hydrogel capsule further reduced the released oxygen amount by 85% in 24 h (Figure 3.2c).

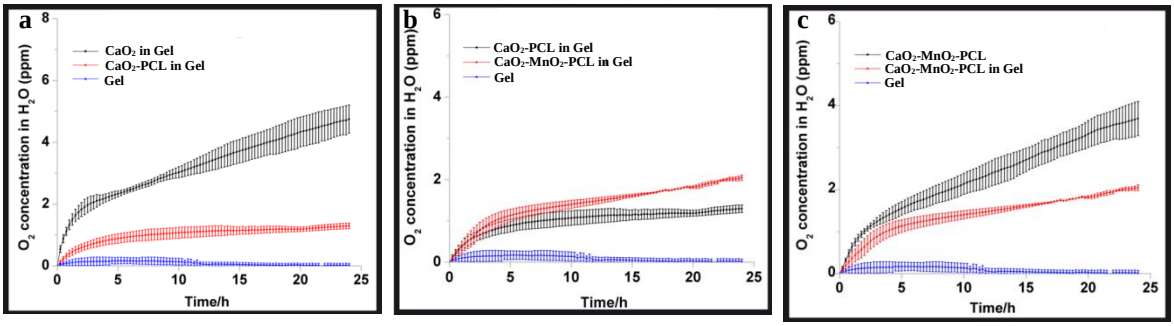


Figure 3.2. Oxygen release results of the composites showing the effect of PCL (a), $MnO_2$ (b) and hydrogel (c) on oxygen release.

3.2 Fibroblast viability under anoxic culture (Alamar Blue)

Cell number was measured with the non-toxic Alamar Blue staining. According to Figure 3.3, ODS under anoxia resulted in roughly the same cell number with normoxic culture after 1 and 4 days, indicating that ODS under anoxia maintained a similar growth rate compared with cells cultured under normoxia. In contrast, without ODS cell number decreased by 40% after only 1 day under anoxia and nearly all the cells died after 4 d (Figure 3.3). Therefore, the oxygen-release material successfully rescued cells in anoxic culture.

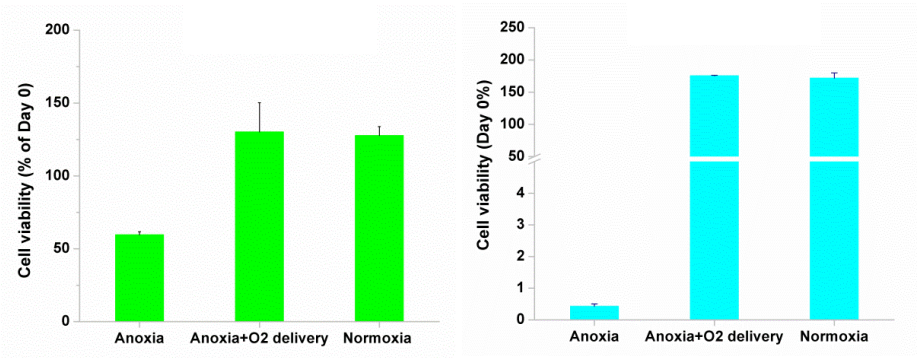


Figure 3.3. Alamar Blue results of cell number cultured for 1 day (left) and 4 days (right) under anoxia with and without ODS.

3.3 Fibroblast viability under anoxic culture (trypan blue)

Trypan blue penetrates into dead cells and stains the nuclei of dead cells dark blue. Positively stained dead cells were observed after 1 day under anoxia (Figure 3.4 a) whereas no positively stained cells were found under normoxia (Figure 3.4 c) and in the presence of ODS under anoxia (Figure 3.4 b). After 4 d under anoxic culture, most of the cells were dead. These results suggested that the cells were prone to die under anoxia without ODS. Quantified results showed similar results. After 1 d and 4 d, the cell viability under anoxia decreased by 78% and 91%,

respectively. Nevertheless, the cells cultured with ODS under anoxia maintained similar viability to those cultured under normoxia. The discrepancy between the images and the quantified results in Figure 3.4 might be due to the detachment of some dead from the cover slips that could not be observed under the microscope.

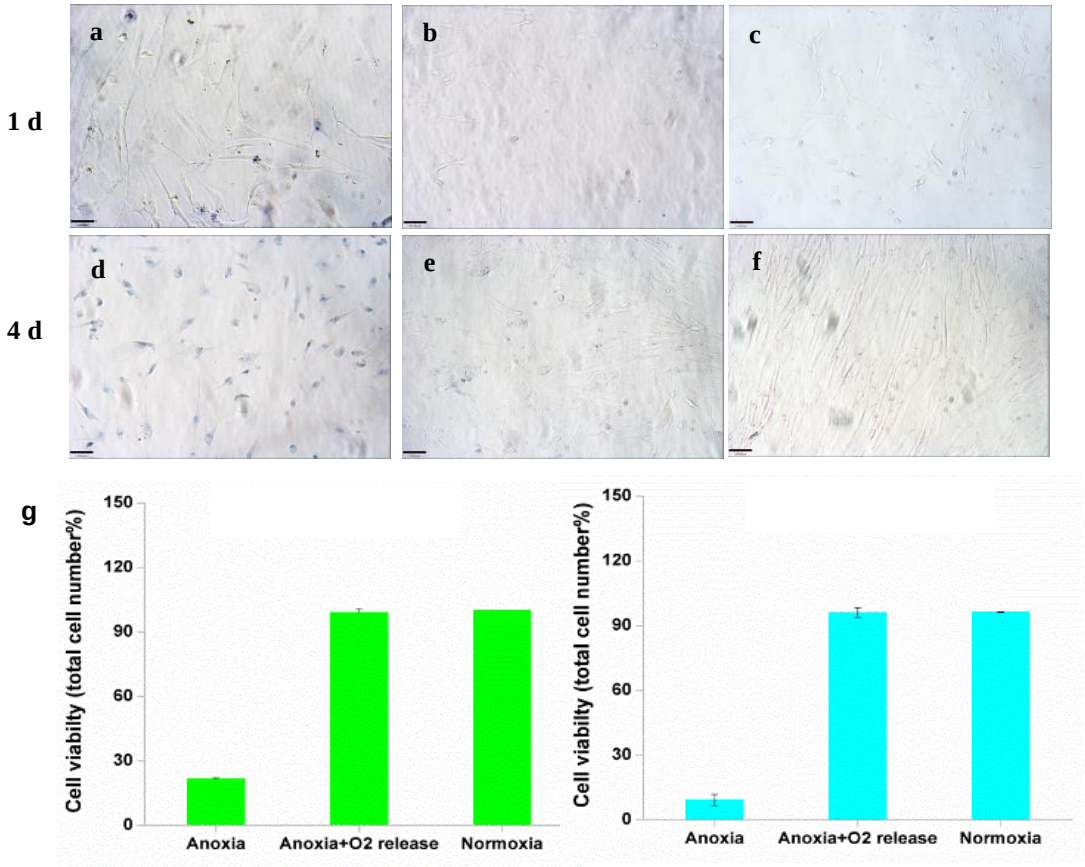


Figure 3.4. Trypan blue staining images of cells cultured for 1 d and 4 days under various conditions and quantified cell viability; a and d: anoxia; b and e: anoxia with ODS; c and f: normoxia; g: quantified results after 1 (left) and 4 d (right).

## 3.4 Fibroblast viability (live/dead assay)

The fluorescent live/dead staining results are shown in Figure 3.5. Only a few dead cells were found in the samples cultured with ODS under anoxia and under normoxia. In contrast, many

cells were found dead in the negative control (under anoxia) after 1 d and nearly all the cells died after 4 d. This study confirmed our previous results of Alamar Blue and trypan blue staining.

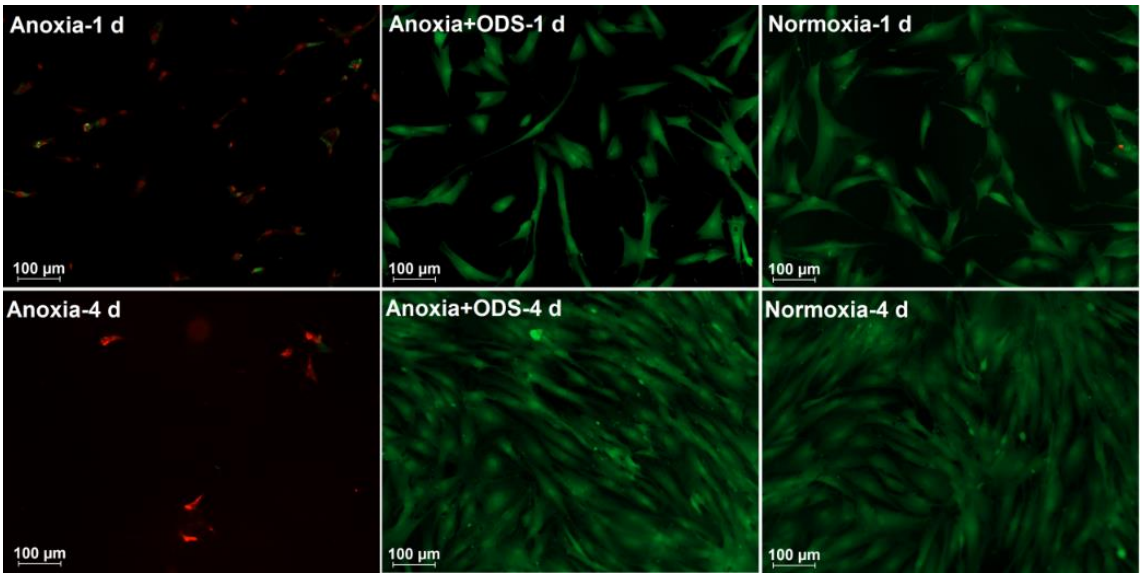


Figure 3.5. Fluorescent images of fibroblasts cultured under various conditions; red: dead cells; green: live cells.

3.5 Fibroblast apoptosis stained by the TUNEL assay

TUNEL staining studies the DNA fragmentations in the cells undergoing apoptosis. The majority of cells cultured under anoxia suffered DNA injuries (Figure 3.6a and d) whereas the cells cultured with ODS under anoxia (Figure 3.6b and e) and under normoxia (Figure 3.6c and f) only showed few DNA damages, indicating that ODS protected the cells from apoptosis under anoxia. The quantified results showed that less than 2% cells displayed DNA injuries when they were cultured under anoxia with ODS and under normoxia. However, more than 80% cells cultured under anoxia without ODS exhibited DNA injuries. The percentage of apoptotic cells was under estimated due to the detachment of dead cells from the culture plate.

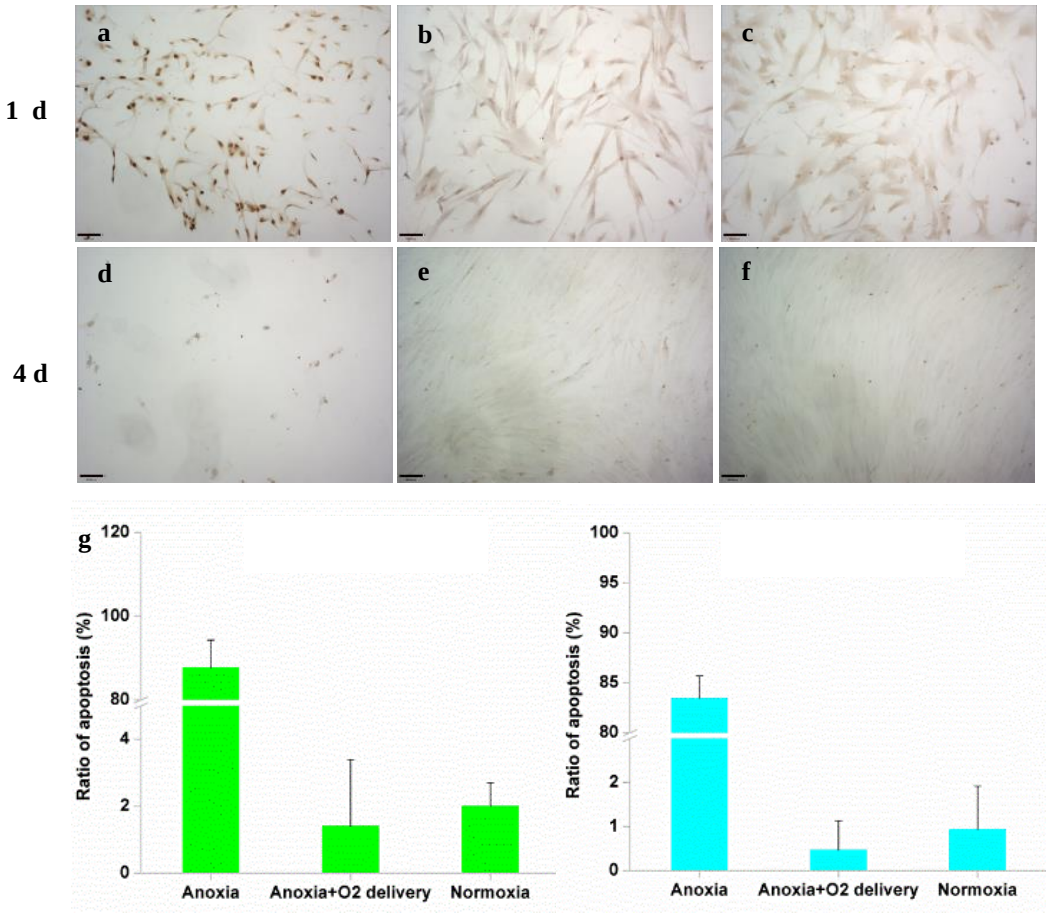


Figure 3.6. TUNEL staining images of cells cultured for 1 d and 4 d under various conditions and quantified results; a and d: anoxia; b and e: anoxia with ODS; c and f: normoxia; g: quantified results after 1 (left) and 4 d (right).

3.6 Fibroblast proliferation stained by the BrdU assay

Figure 3.7 shows that after 1 day, the majority of the cells in all the three samples were positively stained, indicating that new DNA molecules were being synthesized in the cells. Nevertheless, the percentage of positively stained cells under anoxia without ODS after 1 d was smaller compared with the other samples (Figure 3.7a-c). After 4 d, however, no positively stained cells were observed in the sample cultured under anoxia without ODS (Figure 3.7d) whereas 30% cells cultured under the other two conditions namely anoxia with ODS (Figure

3.7e) and normoxia (Figure 3.7f). In the presence of ODS under anoxia the cells exhibited a similar DNA synthesis level to that of cells cultured under normoxia. The ratio of the positively stained cells decreased after 4 d, probably because the high cell density inhibited DNA synthesis activities of the cells.

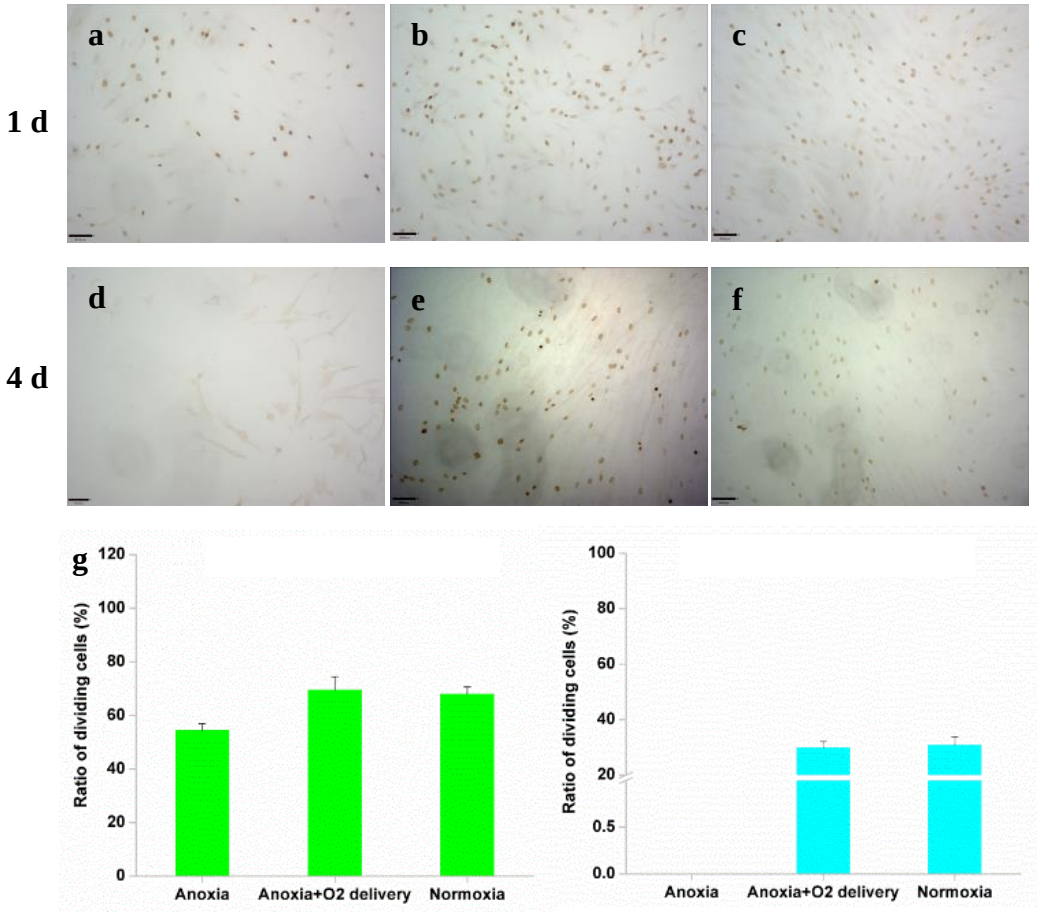


Figure 3.7. BrdU staining images of cells cultured for 1 d and 4 d under different conditions and quantified results; a and d: anoxia; b and e: anoxia with ODS; c and f: normoxia; g: quantified results after 1 (left) and 4 d (right).

## 3.7 q-PCR results of fibroblasts

Figure 3.8 describes the expression of hypoxia related genes of the cells cultured under anoxia with and without ODS, and normoxia. The results showed that the presence of ODS restored

the expression of Glut 1 to a normal level under anoxia while anoxic culture without ODS increased the expression level of Glut 1 by 12 folds after 1 day (Figure 3.8a) and 6 folds after 4 days compared with the experimental group (Figure 3.8a and b). Similarly, the expression of BNIP3 gene of the cells increased around 12 times after 1 day and 21 times after 4 days under anoxia compared with that of cells cultured under normoxia. However, the expression of BNIP3 gene in the cells cultured with ODS only increased 2.5 times after 1day and 4.5 times after 4 days (Figure 3.8a and b). Nevertheless, it seems that the increase of the BNIP3 gene expression did not affect cell apoptosis and proliferation (Figure 3.6b, e and 3.7b, e). VEGF expression of the cells amplified 11.5 folds after 1 day and 6.5 folds after 4 days under anoxia without ODS compared with that of cells under normoxia. As to the cells cultured with ODS, the VEGF expression increased about 30% after 1 day and 1 fold after 4 days.

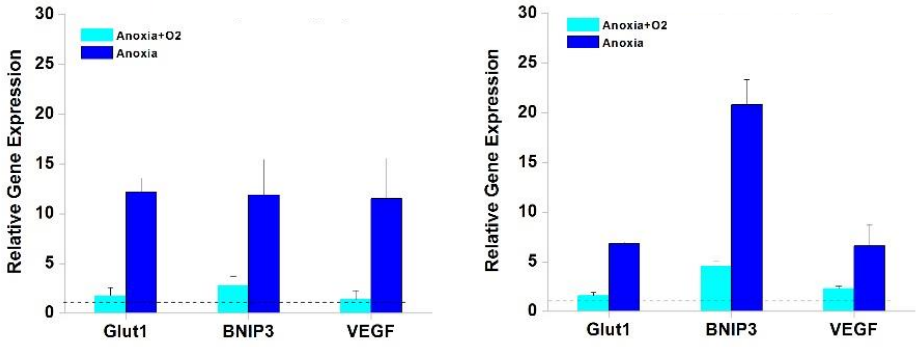


Figure 3.8. q-PCR results of hypoxia-related gene expression at day 1 (left) and day 4 (right), the dashed line indicated the expression level of cells under normoxia.

## 3.8 MDCK viability (trypan blue)

The fast decomposition of CP generates a large amount of $H_2O_2$ that accumulates in the culture system, leading to cell death. Figure 3.9 shows the viability of cells under anoxia (Figure 3.9a and e), in the presence of CP-hydrogel (Figure 3.9b and f) and CP-$MnO_2$-PCL hydrogel (Figure

3.9c and g). The cells cultured under anoxia and in the presence of CP-hydrogel lost their viability after 3 h whereas the cells cultured with CP-$MnO_2$-PCL-hydrogel under anoxia maintained a similar viability to cells culture under normoxia (Figure 3.9i), indicating that $MnO_2$ catalyst reduced the $H_2O_2$ concentration in the system.

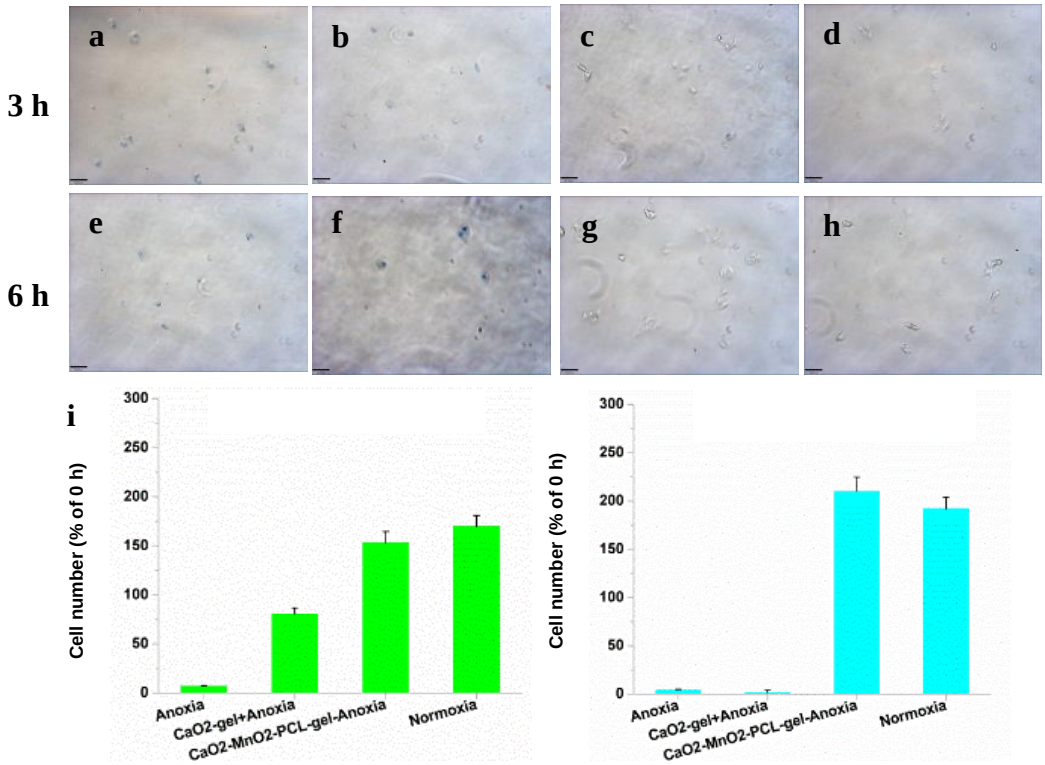


Figure 3.9. Trypan blue staining images of MDCK cells cultured for 3 h and 6 h under various conditions and quantified cell number changes; a and e: anoxia; b and f: CP-hydrogel in anoxia; c and g: CP-$MnO_2$-PCL-hydrogel in anoxia; d and h: normoxia; i: quantified cell number changes after 3 (left) and 6 h (right).

## 3.9 MDCK viability (live/dead assay)

Figure 3.10 shows that the cells exhibited a good viability under anoxia in the presence of ODS under anoxia. In contrast, a large number of cells died under anoxia both with and without CP-hydrogel. The quantity of dead cells in the samples cultured under anoxia without oxygen-

release materials was similar to the samples cultured with CP-hydrogel under the same conditions. This result confirmed the importance of the $MnO_2$ catalyst on the cell viability under anoxia with CP used as the oxygen source.

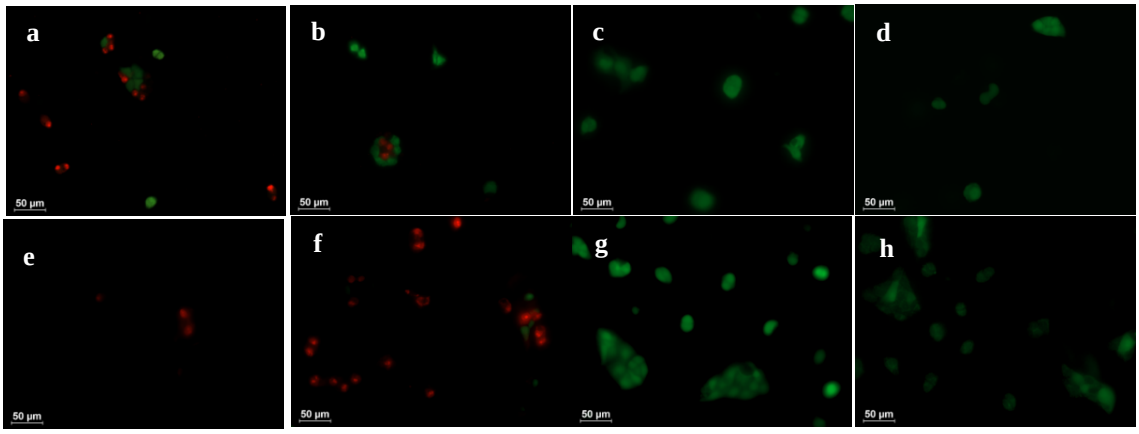


Figure 3.10. Fluorescent images of MDCK cells cultured for 3 h (up) and 6 h (bottom) under different conditions; a and e: anoxia, b and f: CP-hydrogel in anoxia, c and g: ODS in anoxia, d and h: normoxia.

3.10 ROS production by MDCK

Figure 3.11 shows the production of ROS under different conditions. The maximum production of ROS in MDCK cells was found in the presence of CP-hydrogel under anoxia. This result, combined with the cell viability, confirmed that the toxic effect of the CP-hydrogel leading to the cell death was the result of a high ROS production. In contrast, the amount of ROS in cells cultured with the oxygen-release materials containing $MnO_2$ and PCL was greatly reduced, suggesting that $MnO_2$ and PCL effectively alleviated ROS generation in cells.

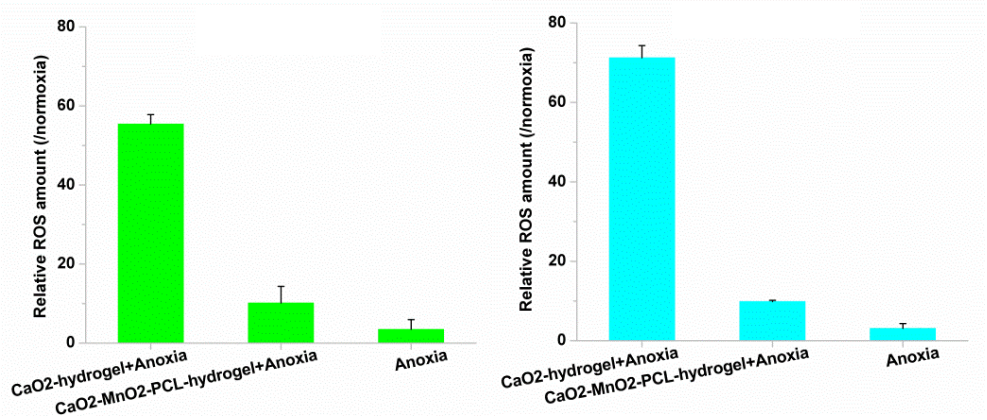


Figure 3.11. ROS generation in MDCK cells under different conditions after 3 (left) and 6 h (right). A much higher level of ROS was detected in cells cultured with CP-gel under anoxia.

## 3.11 Oxygen-release microparticles

SEM images of the as-prepared CP-$Fe_3O_4$-PLGA microparticles in Figure 3.12 shows that the particles had a size between 5-20 µm. This allowed more flexibility application and handling of the material  without being restricted by the shape and size of the material, unlike the slab and other reported scaffolds [2, 39].

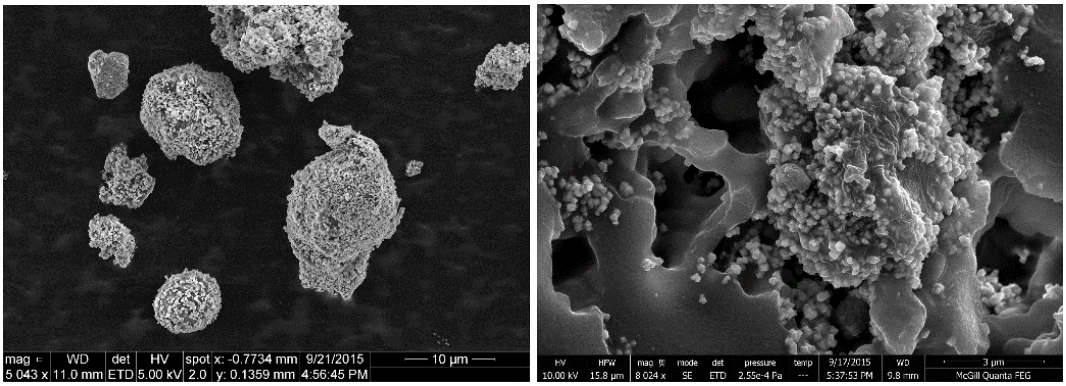


Figure 3.12. SEM images of the CP-$Fe_3O_4$-PLGA microparticles.

## 3.12 Decomposition of CP in microparticles

The release of $H_2O_2$ from CP in microparticles was further investigated (Figure 3.13). A blue color was observed in both cases, meaning that $H_2O_2$ was produced in the microparticles either with or without the hydrogel. The fact that the microparticles without the hydrogel generated a darker blue color than the microparticles within the hydrogel suggested that more $H_2O_2$ was released from the microparticles, and therefore that the hydrogel inhibited the decomposition of CP. Furthermore, Figure 3.13 shows that the presence of alginate hydrogel greatly reduced the amount of $H_2O_2$ accumulated in the system and that the presence of hydrogel decreased the decomposition rate of CP, preventing the burst release of oxygen and increasing the lifetime of the oxygen-release materials.

Figure 3.13. Photos of the microparticles with and without alginate hydrogel in KI-starch solution after 30 min.

## 3.13 Encapsulation of MDCK cells in SOS

Alginate hydrogel beads were prepared by dropping the alginate solution into the $CaCl_2$ solution and the MDCK cells were successfully encapsulated in the SOS beads (Figure 3.14).

The black color of the bead resulted from the presence of $Fe_3O_4$ catalyst. Beads with a diameter of 5 mm were prepared based on optimized results from the cell viability study (data were not shown).

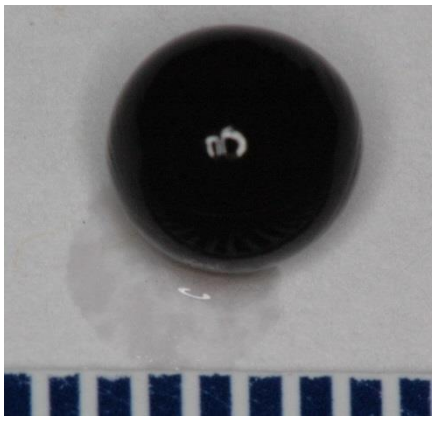

Figure 3.14. Photo of an SOS bead containing MDCK cells.

Figure 3.15 shows that green live cells in the samples cultured in the presence of oxygen-release material whereas only a small number of live cells were observed under the same conditions without the oxygen-release material. Therefore, cells encapsulated in SOS had much higher viability under anoxia compared with cells in the control group. The presence of oxygen-release materials successfully improved cell viability under the anoxic culture. Cell viability could be impaired by lack of nutrients and hypoxia. The present results indicated that in hydrogel scaffolds hypoxia was a more potent issue to cells compared with the nutrient shortage.

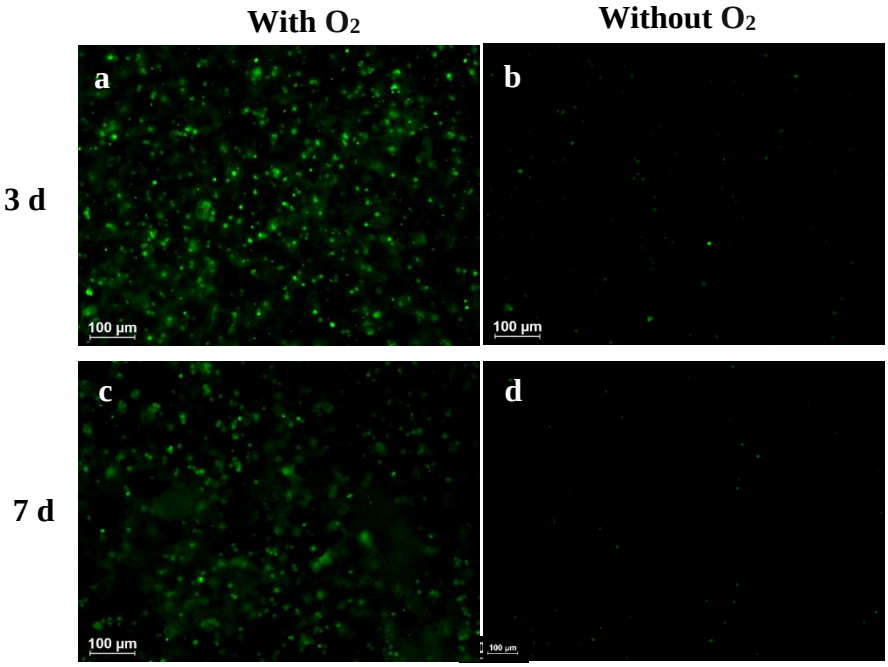


Figure 3.15. Fluorescent images of MDCK cells stained by CFSE cultured under anoxia with (a and c) and without (b and d) the oxygen-release material.

3.14 MDCK transplantation in self-oxygenating scaffold

Figure 3.16 shows that cells cultured with SOS displayed stronger green signals after 4 weeks compared with the cells in the control group. This indicated that the presence of oxygen-release material successfully rescued cells *in vivo* before the vascularization event whereas most of the cells died in the absence of oxygen-release material (Figure 3.16).

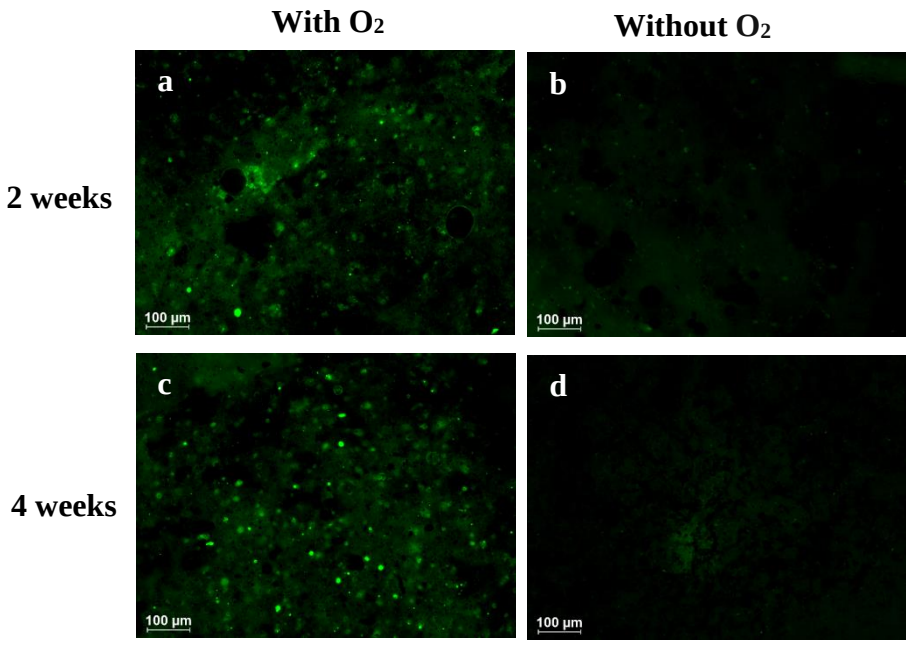


Figure 3.16. Fluorescent images of MDCK cells after transplantation with (a and c) and without (b and d) oxygen-release materials.

The supply of oxygen and nutrients is indispensable for the survival of cells. The cell number was quantified after transplantation (Figure 3.17). The cell number steadily increased with time in the experimental group and reached 4 times of its initial value after 4 weeks. In contrast, cell number decreased in the control group.

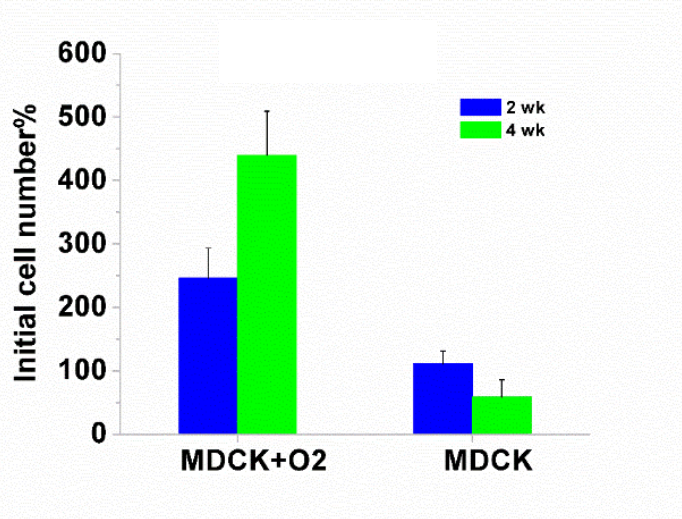


Figure 3.17. Quantified MDCK cell number in retrieved implants in the presence and the absence (control) of oxygen-release materials.

After 4 weeks the cell density was high on the edge in the both kinds of implants because of the presence of oxygen and nutrients in this area from surrounding tissues (Figure 3.18b and e). Nevertheless, in the core area and more particularly around the oxygen-release material, the samples with oxygen-release material exhibited a higher cell density (Figure 3.18 d-f) than the samples without oxygen-release material. This suggested that oxygen delivery was able to support cell growth in transplants by supplying oxygen. Similar experimental results were observed at the 2-week time point (Figure 3.1S).

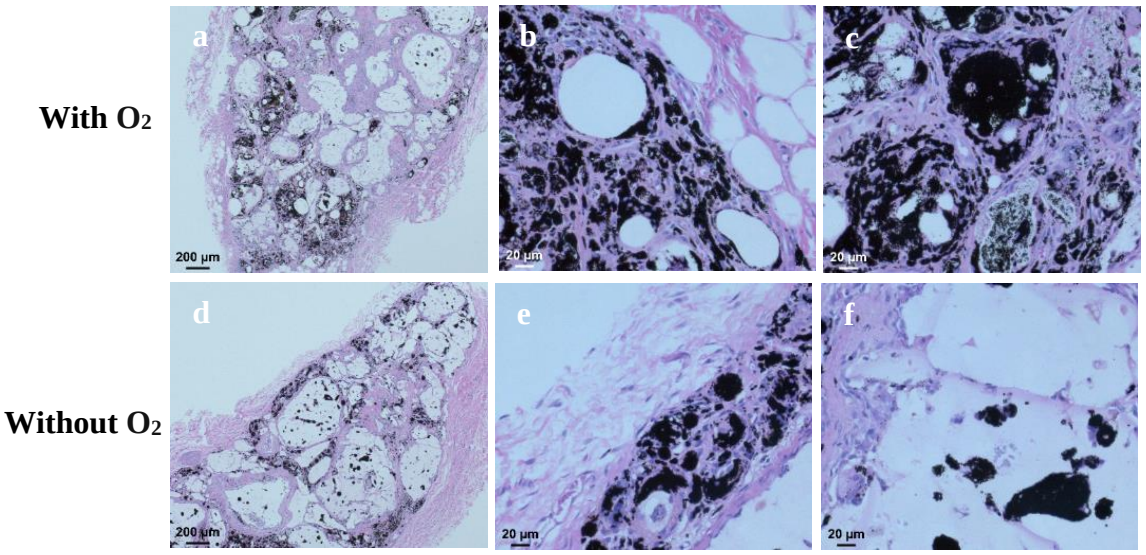


Figure 3.18. H&E staining of the implants with (a, b and c) and without (d, e and f) oxygen-release material after 4 weeks. a and d were low magnification images of the samples, b and e were taken at the edge of the scaffold and e and f in the central area.

Vascular endothelial growth factors (VEGF) play an important role in the formation of new blood vessels and it is generally thought that the hypoxia inducible factor-α (HIF-α) induced by hypoxia stimulates their expression. Although the VEGF staining (Figure 3.19) was positive in both samples, the saturation density of the stain appeared to be stronger in the sample with oxygen-release material, suggesting that more growth factors may be secreted by cells in the experimental group. Similar results were observed in samples retrieved after 2 weeks (Figure 3.2S)

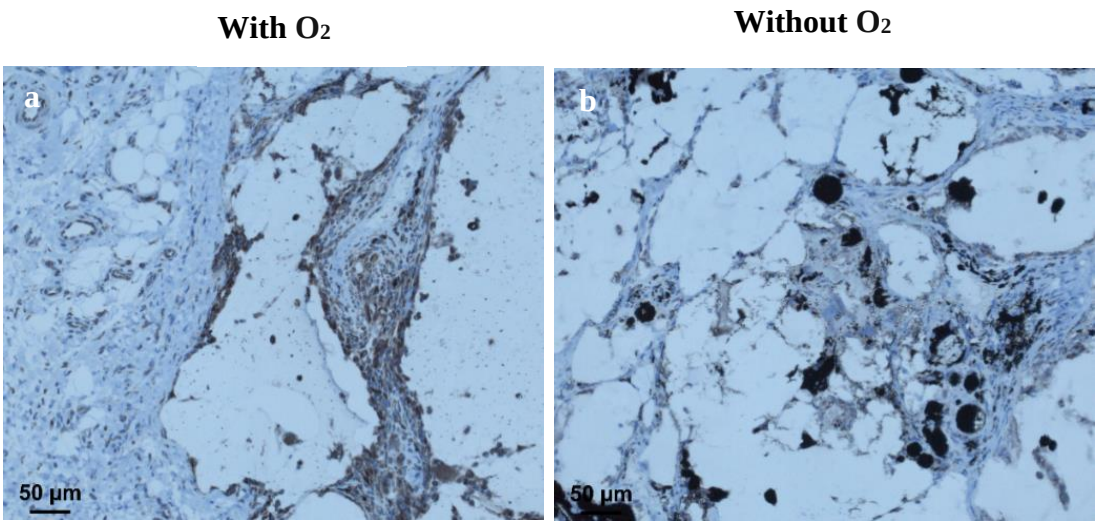


Figure 3.19. Vascular endothelial growth factor (VEGF) staining images of the samples with (a) and without (b) oxygen-release materials after 4 weeks.

The formation of blood vessels in the scaffold is crucial considering that they can supply cells with oxygen and nutrients and remove local metabolic wastes of the survival of transplanted cells in the scaffold. Figure 3.20 shows the effect of the oxygen-release materials in the scaffold on the blood vessel density compared with the scaffold without oxygen-release material. The results indicated that the density of capillaries in the experimental group was much higher than that in the control group, and that the density increased with time in the experimental group whereas it did not vary in the control group. This confirmed the positive effects of the oxygen-release material in promoting vascularization in the scaffold. Stained images for the samples after 2 weeks can be found in the supplemental information (Figure 3.3S).

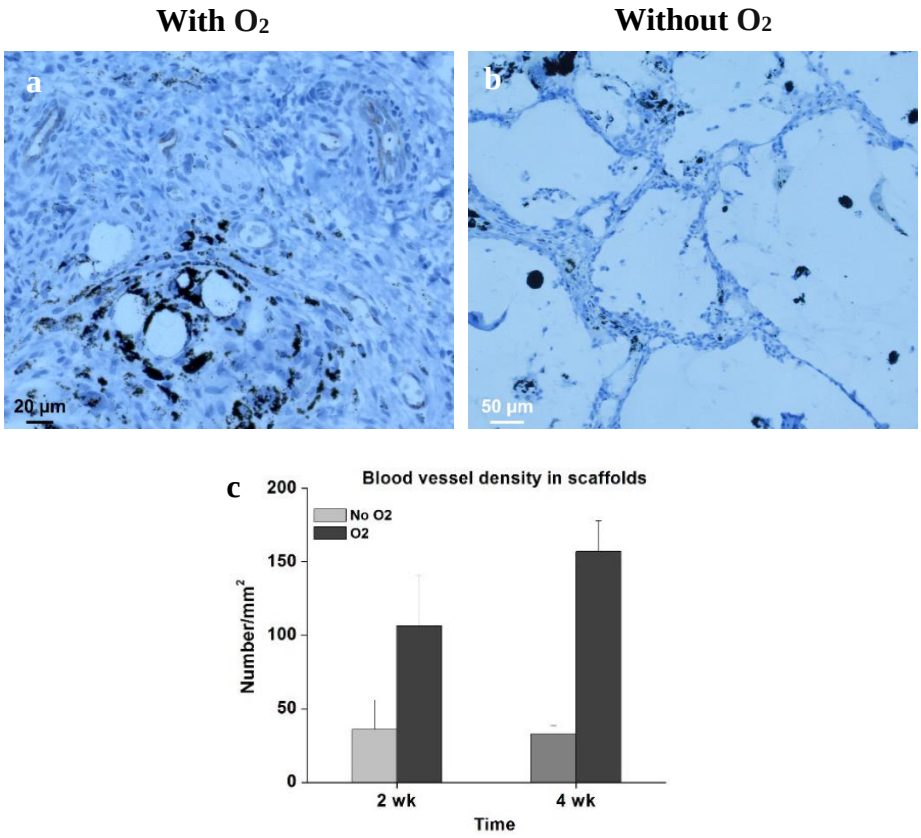


Figure 3.20. Blood vessel staining results of the transplanted scaffolds (a and b) after 4 weeks and the quantified blood vessel density in the scaffolds (c). Endothelial cells in blood vessels were stained dark brown.

## 4. Discussion

Cells require oxygen during normal respiration to produce enough ATP to maintain their normal metabolic activities. Meanwhile, many cells have the ability to adapt to the hypoxic environment through increasing the glycolytic activity [449]. Hypoxia is very common during tissue engineering and in wound healing, causing energy outage of cells. As a result, cell necrosis in the core area of tissue constructs, delayed wound healing, severe inflammation, and even chronic wounds often occur.

Normally, *in vitro* cell culture is carried out under 20% $O_2$ supplemented with 5% $CO_2$ to buffer the culture medium. Oxygen concentrations under 20% are considered to be hypoxic *in vitro* [1]. So far, the most majority of research work concerning oxygen delivery was carried out under hypoxia, usually under 1-5% $O_2$. Nevertheless, the oxygen concentrations of cells are 1-2.5 % *in vivo*, [450] which are within the range of *in vitro* hypoxia. In fact, commonly used *in vitro* cell models are tolerant to hypoxia, such as fibroblasts, stem cells and β cells. [2, 3, 39, 451] These cells can stay alive for days under the hypoxic culture and hypoxia can promote fibroblast proliferation in a short period. [14] Anoxic culture, where no oxygen is provided, is a more severe environment than hypoxia. Aerobic cells are fragile without oxygen and certain types of cells, such as primary cells and MDCK cells [452, 453], die within hours under anoxia.

As an oxygen-generating agent, CP has been used to deliver oxygen to tissues and cells. The main problems associated with CP include the formation of gas bubbles and burst release of cytotoxic $H_2O_2$ and hydroxyl ions due to the high decomposition rate of CP. Therefore, it becomes essential to reduce the decomposition rate of CP and minimize the amount of $H_2O_2$ and hydroxyl ions in the culture system. So far, the decomposition rate of CP has been deliberately reduced by encapsulating the powders into hydrophobic silicon rubbers. [39] Both catalysts and catalase have been used to remove the generated $H_2O_2$. However, either very high concentrations of catalase were required to remove the cytotoxicity of generated $H_2O_2$ or the catalysts used in literature were toxic. [2, 18, 309] In this work, we developed a biodegradable ODS that overcame all these obstacles. In our system, biodegradable and hydrophobic polymers were used to reduce the CP decomposition rate by compelling water available to the powders. Biodegradable $Fe_3O_4$ was used as the catalyst to remove $H_2O_2$. Alginate hydrogel was employed to further slowdown the decomposition rate of CP and inhibit the formation of gas bubbles in culture medium. Moreover, the hydrogel also served as a barrier to oxygen and

radicals generated during the decomposition of $H_2O_2$, and thus protected cells from burst release of cytotoxic agents.

Hypoxic culture (1% $O_2$) of fibroblasts has been previously performed to evaluate the oxygen delivery capacity of CP. [39] The authors reported that CP improved cell growth in PLGA porous scaffold under 1% $O_2$. Nevertheless, no comparison with normoxic culture was presented. Moreover, culture medium containing a very high concentration of catalase (around $10^6$ times of that in blood) was required to remove the cytotoxicity of $H_2O_2$, which compromised the economic merit of the system and may cause adverse effects such as paradoxical reductive stress on cells [454]. Interestingly, there was not much difference in terms of cell number between the control and experimental groups under hypoxia after three days, but the presence of CP resulted in a larger cell number than the control group under normoxia at the same time point. The possible reason was either that the reported oxygen-release system was unable to correct the oxygen concentration to the level that promoted cell growth under hypoxia or the burst release of cytotoxic agents at the beginning compromised the beneficial effects of the material. Therefore, our ODS was evaluated under anoxia so that a shorter experimental period would be required to observe the effects of our material. In addition, the acute cytotoxicity of our system and its oxygen-release efficacy can also be examined. Only a one-day experiment was enough to find a significant decrease in cell number and viability in the control group compared with the experimental group. Moreover, the experimental group maintained a similar level of cell number and viability to that of cells cultured under normoxia. (Figure 3.3-3.5) Consequently, anoxic culture is a more efficient way to evaluate oxygen delivery systems. In addition, our oxygen-release system displayed little cytotoxicity to cells and was able to correct cell growth to normoxic levels under anoxia. TUNEL and BrdU staining results (Figure 3.6 and 3.7) further confirmed that our ODS protected cells from anoxia induced

apoptosis and maintained normal DNA production. The q-PCR results (Figure 3.8) showed that ODS minimized the expression levels of hypoxia related genes.

The quantified cell viability under anoxia after 1 day from trypan blue staining was lower than that from Alamar Blue staining. The possible reason is that the viability obtained from trypan blue staining was the ratio of live cells to total cells while the Alamar Blue staining results were normalized to the cell number at 0 day. Although many cells died under anoxia, some cells may continue to divide as shown by the BrdU staining. As a result, the obtained cell viability from Alamar Blue was higher than that from trypan blue since the total number of cells increased. Interestingly the trypan blue results exhibited larger cell viability than Alamar Blue staining after 4 days. This result can be justified by the fact that that many dead cells lost their integrity after 4 days and became debris (data not shown). As a result, a number of dead cells could not be collected, which increased the quantified ratio of live cells. The discrepancy between the images of trypan blue stained cells and the quantified cell viability because a large number of dead cells detached from the wells and could not be observed under the microscope. Consequently, the images under microscope displayed larger cell viability. The fluorescent live/dead staining images further proved excellent cell viability under anoxia in the presence of oxygen-release material. Cells augment the expression of genes related to glycolysis, apoptosis and angiogenesis in response to hypoxia. The q-PCR results confirmed these effects of anoxia on cells. Anoxia greatly increased the expression level of Glut 1 gene in the cells. Nevertheless, ODS restored the expression of Glut 1 gene to a normal level (Figure 3.8). Although the expression level of BNIP3 gene in cells cultured under anoxia with ODS was higher than that in cells cultured under normoxia, cell apoptosis behavior was not influenced as shown in TUNEL staining (Figure 3.6 and 3.7). The possible reason is that either the level of BNIP3 gene expression of normal cells was very low or the cells were relatively tolerant to

BNIP3 gene expression. Therefore, even the BNIP3 gene expression level of the cells cultured with ODS increased by several folds, cell apoptosis still did not occur. VEGF gene expression was greatly reduced when the cells were cultured under anoxia in the presence of ODS, compared with cells cultured under anoxia.

After testing our ODS with primary fibroblasts, we further examined the system using oxygen sensitive MDCK cells. We also wanted to use it as a model to test the possible mechanism of cytotoxicity caused by the oxygen-release material through measuring the generation of ROS in the cells. The experimental results showed that ODS was able to rescue MDCK cells under anoxia. Although peroxides have been used to supply oxygen to cells and tissues, the cytotoxicity associated with the decomposition of peroxides has rarely been investigated. All the peroxides involve $H_2O_2$, which induces apoptosis, during the generation of oxygen. [455] According to our experimental results, the composition of oxygen-release material affected ROS production in the cells and influenced cell viability (Figure 3.9 and 3.10). Therefore, the death of cells might be the result of ROS production induced by the oxygen-release material. The addition of hydrophobic polymers and catalysts greatly reduced ROS levels in the cells, suggesting that ROS in cells may be induced by high oxygen tension or high concentrations of $H_2O_2$ released from the oxygen-release material. The experimental results in this work indicated that both a suitable decomposition rate of CP and catalysts were required to remove the cytotoxicity of oxygen-release material.

Afterwards, we developed oxygen-release microparticles consisting of CP, hydrophobic PLGA, $Fe_3O_4$ catalysts, and alginate hydrogel (Figure 3.12). The optimised system was further used to create an SOS to encapsulate cells and deliver oxygen *in situ*. Hypoxia or even anoxia is an obstacle in cell and tissue transplantation due to the impaired or absence of blood vessels in the

implants. Different approaches have been developed to alleviate hypoxia upon transplantation, such as prevascularization of the scaffold [456], pre-treatment of the implants under hypoxia [457], and induction of vascularization in the scaffold using growth factors, endothelial and vascular smooth muscle cells, stem cells and transfected cells [432, 433, 458, 459]. However, after transplantation, there is still a time period during which the cells are deprived of oxygen. Even when the scaffold is prevascularized, a two-day period is necessary to maximise the oxygen concentrations in the implants. Furthermore, clotting in the preformed vessels is common leading to non-functional vessels that generally require a seven-day period to form a functional network in the implants. [456] According to the other methods, more than one week is necessary to form new blood vessels in implants. [457-459] Being currently non-efficient, an approach to supply directly oxygen after transplantation is a matter of the utmost importance. This study confirmed that our SOS sustained cell survival after implantation before the vascularization was completed in the scaffold. With the oxygen-release scaffold, transplanted cells showed improved cell viability and continued to grow *in vivo* (Figure 3.16 and 3.17). Moreover, our experimental results showed that the presence of oxygen-release material promoted vascularization (Figure 3.20) in the scaffold. The reason could be that the supply oxygen supported the cellular activities related to capillary formation.

White et al [456] transplanted prevascularized scaffold containing endothelial cells and lung fibroblasts into mouse and found that prevascularization improved oxygen concentrations in the scaffold after two days. The cells in the scaffold maintained their viability after transplantation but did not show much increase in cell number. Their approach required long *in vitro* culture time (seven days) to achieve prevascularization with specific cell types in specialized culture medium. Moreover, the cells needed to be added into the scaffold upon polymerization. The density of cells used to stimulate vascularization in their scaffold was

already very high (around $0.5\times10^9$ cells/mL), which made it difficult to incorporate other cells into the scaffold. In addition, the size of the implants was limited to 0.5×1.2 mm. With our SOS, cells could be encapsulated in the scaffold and continue to grow in scaffolds thicker than 2.4 mm. No *in vitro* culture was required. Moreover, oxygen delivery promoted vascularization in the scaffold, which further improved the survival environments of transplanted cells.

## 5. Conclusions

An *in situ* ODS was developed and used to rescue human primary fibroblasts and the oxygen sensitive MDCK cells under the anoxic environment. ODS was composed of biocompatible and biodegradable materials and had adjustable oxygen-release rates. The results showed that ODS was able to restore the cell function and activities to a normal level under the anoxic circumstances. Furthermore, an SOS was developed to support cell growth *in vivo* and to promote vascularization in the implants. Since the alginate hydrogel have been used as drug delivery vehicles, alginate hydrogel-based ODS and SOS have the potential to serve as an "all in one" delivery system to deliver oxygen and other drugs to cells and tissues at the same time.

## 6. Acknowledgements

The authors would like to thank Dr. Charles Doillon (Laval University, Quebec) for the kind donation of fibroblast cells used in this study. This work is supported by the *Natural Sciences and Engineering Research Council* of Canada (*NSERC*) and China Scholarship Council (CSC). The authors also would like to acknowledge BioPloymer and Advanced Polymer Materials Inc. for providing us with sodium alginate and PLGA, respectively.

## Supplemental information

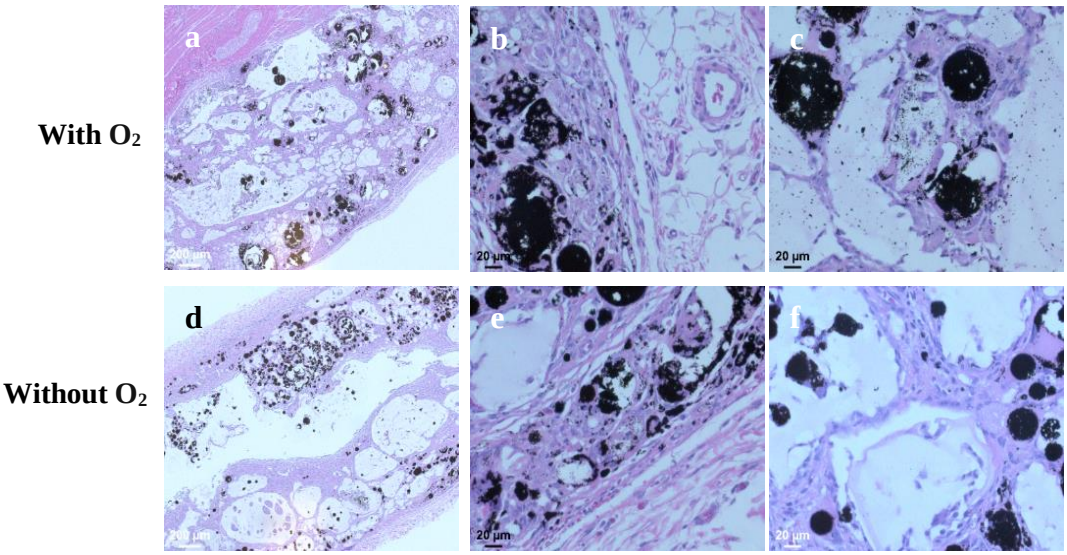


Figure 3.1S. H&E staining of the implants with and without $O_2$ release material after 2 weeks. a and d were low magnification images of the samples, b and e were taken at the edge of the scaffold and e and f in the central area with a higher magnification.

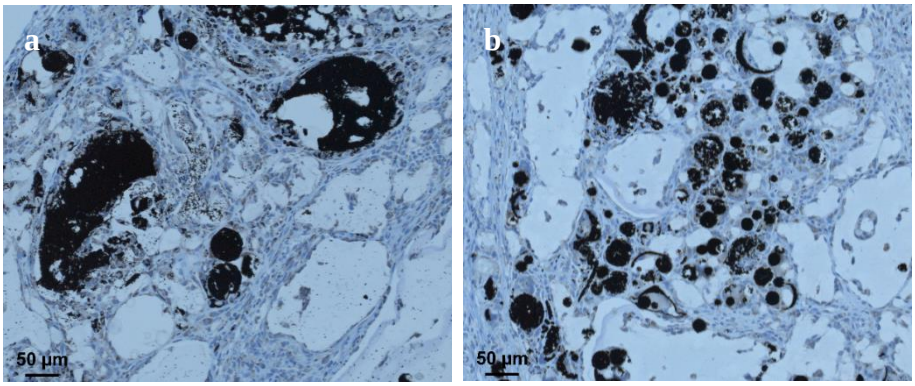


Figure 3.2S. Vascular endothelial growth factor (VEGF) staining images of the samples with (a) and without (b) $O_2$ release material after 2 weeks. VEGF was stained dark brown. Both kinds of sample were VEGF positive.

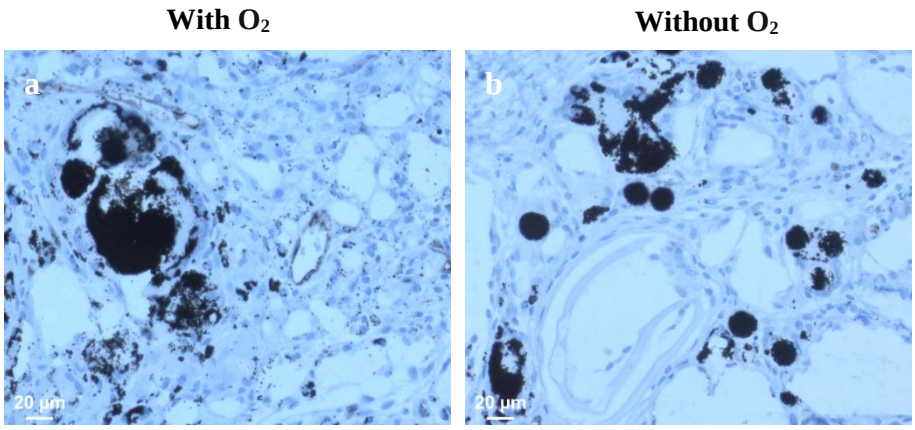


Figure 3.3S. Blood vessel staining images of the transplanted scaffolds (a and b) after 2 weeks. Endothelial cells in blood vessels were stained dark brown. A higher density of blood vessels was found in the sample with $O_2$ release materials.

## Chapter 4

### Blood vessel preservation with a self-oxygenating scaffold

Huaifa Zhang[1], Simon Tran[1], Jake Barralet[1,2]

1. Faculty of Dentistry, McGill University, Montreal, QC, Canada

2. Division of Orthopaedics, Department of Surgery, Faculty of Medicine, McGill University, Montreal, QC, Canada

### Preface

Hypoxia is one of the major issues during tissue and organ preservation. Generally, tissues and organs are preserved at low temperatures (hypothermia) to reduce metabolic activities of the cells so that they will consume less oxygen. Although this method prolongs the preservation time of tissues and organs, reperfusion injury occurs after transplantation due to hypoxia and the low temperature during preservation, jeopardizing the functionality of the tissues and organs. The reperfusion injury is thought to be caused by the generation of reactive oxygen species when the cells are re-exposed to oxygen. Another preservation approach is perfusion, i.e. circulation of oxygenated preservation solutions in the tissues and organs under hypothermia through blood vessels. Perfusion of preserved tissues and organs improves preservation outcomes, but perfusion can result in damage to blood vessels in the tissues and organs. Since the oxygen-release material was able to support cell growth under anoxia and to maintain cell growth *in vivo*, it may also be able to preserve tissues. In this chapter, I sought to preserve blood vessels at physiological temperature with the self-oxygenating scaffold. The self-oxygenating scaffold successfully maintained high cell viability in rat aortas for up to seven days under anoxia and preserved normal endothelial mitochondrial membrane potentials and maintained original KCl induced contraction force as well.

**Abstract**

Damage caused by oxygen deficiency (hypoxia) is one of the major factors limiting tissue and organ preservation time. The most common approach to prolonging preservation under hypoxia is the reduction of metabolic rate of the tissue by cooling (hypothermia), but it creates an additional issue namely reperfusion injury upon warming. Warm perfusion avoids reperfusion injury but can cause shear damage to blood vessels and requires hard ware. Preservation of a functioning vasculature is therefore a fundamental impediment to any new approaches for normothermic tissue and organ preservation and tissue engineering. Here, we developed a self-oxygenating scaffold (SOS) with controlled release rate that was introduced in and around a blood vessel lumen and culture with oxygen deprivation was performed at 37 ℃ compared with the standard preservation protocol. After optimization of the peroxide content at 37 ℃, almost no dead cells were observed in blood vessels, the mitochondrial membrane potential of the endothelial cells was maintained and the vessels retained 90% of their original KCl stimulated contraction force compared with the hypothermia control, which had 15% viability, 5% membrane potential, and 50% contraction force after rewarming. This approach then appeared to overcome a key obstacle in tissue and organ preservation and tissue engineering.

**Key words:** tissue preservation, oxygen delivery, anoxia, peroxide

## 1. Introduction

To date, organs are often preserved temperately under hypothermia either by static cold preservation or cold perfusion [460-462]. Although these methods can preserve organs for a short period, the preservation time is limited, being less than thirty-six hours for kidneys [463], less than eight hours for lungs [464, 465], and less than six hours for hearts [466]. Besides, reperfusion injury occurs when the tissues and organs are transplanted, [467-469] which can

delay and even compromise the functions of the transplants [29, 470]. The injury is believed to be partially caused by oxygen shortage [83, 471], which is one of the major challenges during organ preservation [472]. Organs require a suitable amount of oxygen to sustain their normal functionality, neither too much nor too little [274]. So far, many efforts have been made, employing different approaches, to supply oxygen to tissues and organs during preservation, such as introducing oxygen carriers into the preservation solutions [473, 474], using oxygen-generating materials [39], and gaseous persufflation [350, 354]. One group of the oxygen carriers is perfluorocarbons (PFCs). PFCs have a high capacity to dissolve oxygen [155, 188] and have been used to oxygenate tissues and organs, by means of perfusion or the static two-layer method (TLM) [473, 475, 476]. Nevertheless, oxygen release from PFCs depends on the gas partial pressure, and thus it is difficult to control the oxygen-release rate during culture. Perfusion produces shear stresses and causes vascular damages [477]. Moreover, the TLM, in which tissues were put into the preservation buffers above oxygenated PFCs and received oxygen diffused from the PFCs, cannot oxygenate tissues homogeneously due to the oxygen gradient in the system caused by diffusion. The beneficial effects of TLM have not been conclusively proved yet [222, 478]. Other carriers, such as blood, red blood cells and artificial hemoglobin, have also been used to improve the preservation of tissues and organs through perfusion [474, 479]. Nevertheless, no data have shown the superiority of the oxygen carriers over preservation buffers without the oxygen carriers. [474] Besides, *in situ* oxygen-release materials have been used for tissue preservation, however, the current systems require either toxic catalysts or extremely high concentrations of catalase, do not have adjustable shapes, and are large (in the range of 10 mm) [2, 18, 39]. Gaseous persufflation uses pure oxygen to perfuse organs and causes oxygen toxicity and thus cannot preserve tissues and organs more than 24 h. [346, 350, 351, 354] In summary, oxygen delivery improves the outcome of tissue and organ

preservation, however, methods that are able to supply oxygen sustainedly in a practical manner and at a controlled rate are still required.

Blood vessels are composed primarily of smooth muscle cells, endothelial cells, collagen and elastin. Blood vessel transplants are required in coronary artery bypass surgery. According to WHO (World Health Organization), nearly 7.3 million people die of coronary heart diseases and this will continue to increase to 23.3 million by 2030. Blood vessels are normally stored at the low temperature (4 ℃). Although the metabolic activities of cells are greatly reduced at 4 ℃, 10-12% of their normal metabolic activities are still in operative. [235, 480, 481] Therefore, hypoxia occurs during preservation and cell damages take place after reperfusion [482]. Re-introduction of molecular oxygen to the cells during reperfusion, which results in burst generation of reactive oxygen species, is believed to be one of the causes of the injuries [483]. Moreover, hyperthermia itself is also reported to cause damages to endothelial cells by inducing reactive oxygen species (ROS) [482, 484]. Consequently, it will be very helpful if blood vessels could be preserved at the physiological temperature with adequate oxygen supply. We intended to evaluate the feasibility of preserving blood vessels, by providing oxygen at a constant rate to them, cultured in buffered nitrogen in the normothermic environment. Inorganic peroxides decompose in water to release hydrogen peroxide that in turn can be catalytically decomposed to form oxygen and have been widely used in aqua- and agri-culture [303, 485]. Recently this technology has been applied to biomaterials and the topic been recently reviewed [305]. There have been several attempts to sustain cells in hypoxia using peroxides embedded in polymers, which were used to reduce the oxygen-release rate by retarding the water diffusion rate. Nonetheless, none of the reported *in situ* oxygen-release systems were suitable for clinical applications. All the reported oxygen delivery systems that employed calcium peroxide (CP) as the oxygen-generating agent had an inflexible physical

shape and a large size, either in the form of plates (or film) or nonflexible scaffolds, which seriously restricted their applications [2, 39, 304]. Besides, those oxygen delivery systems either used non-degradable polymers [39] or required a high concentration of catalase (up to $10^7$ times of that in blood) in the culture system [2, 486] or could not generate satisfactory results [304]. Although some of the oxygen-release systems have proven to improve cell viability under hypoxia, none of the experiments had positive controls. Therefore, the efficacy of those oxygen-release materials were not really clear. Moreover, none of the systems paid attention to prevent the formation of bubbles, which are lethal to cells [487], due to the release of oxygen. In addition to CP, hydrogen peroxide ($H_2O_2$) has also been used to deliver oxygen to cells after being encapsulated into microparticles [40]. However, the problem with this system was that it needed an extremely high concentration of catalase (at least $2\times10^7$ times higher than that in blood) to reduce the cytotoxicity of the released $H_2O_2$ [40, 486]. Therefore, the performance of current *in situ* oxygen-release systems were not satisfactory. We sought to develop a biodegradable oxygen-release system that had a tunable physical shape, a controlled oxygen-release rate, and eliminated bubble formation without use of catalase.

Here an oxygen-release system was made of oxygen-generating microparticles and alginate hydrogel. For the first time, we prepared oxygen-generating microparticles consisting of CP, manganese dioxide ($MnO_2$) and polycaprolactone (PCL). CP produces hydrogen peroxide ($H_2O_2$) in moisture [300]. $MnO_2$ was used to catalyze the decomposition of $H_2O_2$ produced by CP, since cells are very sensitive to the toxic $H_2O_2$ [441]. PCL is hydrophobic and biodegradable and can reduce the decomposition rate of CP. Alginate hydrogel retards the diffusion of generated oxygen [488] and thus avoids burst release of oxygen. Meanwhile, the presence of hydrogel avoided formation of bubbles and further reduced oxygen release. The decomposition of peroxides generates radicals, which are very cytotoxic. Since the radicals

have an extremely short lifetime ($10^{-9}$ s) [489], the presence of hydrogel may also protect cells from radicals.

The oxygen-release system was used to preserve thoracic aortas from rats under anoxia. The optimal loading levels of the oxygen-generating microparticles and whether lumen only, lumen and adventitial or adventitial oxygen delivery was optimal for arterial preservation were investigated. The functionality of the preserved aortas was also examined using endothelial mitochondrial membrane potential staining and mechanical testing.

## 2. Materials and methods

### 2.1 Procurement of blood vessel tissue

Thoracic aortas from rats (5-8 months old) were collected immediately after the euthanization of animals used in other non-pharmaceutical medical studies and kept in phosphate buffer solution (PBS) on ice for a maximum of three hours. Following dissection of connective tissues, the aortas were cut into 5 mm in length and preserved under one of following different conditions, anoxia (95% nitrogen ($N_2$), 5% carbon dioxide ($CO_2$), 37 ℃), hypothermia (20% oxygen ($O_2$), 4 ℃) and normoxia (20% $O_2$, 5% $CO_2$, 37 ℃).

### 2.2 Preparation of oxygen-release microparticles

Oxygen-release microparticles (CP-$MnO_2$-PCL, weight ratio 1:10:10) were prepared using a phase separation method [442] in the absence of $H_2O$. CP powders (Aldrich, USA) and $MnO_2$ (Fisher Scientific, Canada) were first mixed in PCL (Mw 70,000-90,000, Aldrich, USA) solution in chloroform (Fisher Scientific, Canada), then the suspension was added into glycerol (Fisher Scientific, Canada) with 1 wt% polyvinyl alcohol (Mw 89,000-98,000, Aldrich, USA) (PVA) and stirred for 10 min at room temperature. When the particles became dry in a fume

hood, the CP-$MnO_2$-PCL microspheres were collected by centrifuging the suspension at 4000 rpm, washed with alcohol three times and dried at room temperature.

2.3 Encapsulation of blood vessels

Before the experiments, a mathematical simulation of oxygen transportation in the scaffold and across the artery wall was performed. [490] According to the modeling results, oxygen gradients could be created across the blood vessel wall, and it was possible to adjust the oxygen gradient by changing oxygen distribution in the scaffold via changing the amount of peroxides in the scaffold. Moreover, burst release of oxygen towards blood vessels was minimized using hydrogel.

Oxygen-release microspheres were mixed with 1% w/v sodium alginate (FMC BioPloymer, USA) solution and sterilized by ultraviolet (UV) light for 20 min; next 350 µl of the mixture was added onto a piece of filter paper that had been moistened with 100 mM $CaCl_2$, using a 24-well plate well as the module; then a piece of aorta with a length of 5 mm filled with the particle-alginate mixture was put on the mixture; afterwards, another 350 µl of the mixture was added on top of the aorta; finally, 100 µl of 100 mM $CaCl_2$ was added into the plate to cross link the alginate (Figure 4.1). Various concentrations of microparticles (from 10 mg/mL to 40 mg/mL) in the alginate solution were used to estimate the optimal oxygen concentration. Samples with only scaffold inside or outside of the aorta lumen were also prepared to examine the effects of oxygen distribution on the viability of blood vessels. The aortas were cultured in Dulbecco's Modified Eagle Medium (DMEM) supplemented with 10% FBS and 1% Penicillin/Streptomycin solution (P/S). Anoxic culture was carried out by putting the samples in a sealed jar (that had been flushed with 95% $N_2$ and 5% $CO_2$) in a desiccator which was constantly flushed with $N_2$. Preservation at 4 ℃ in Hanks' balanced salt solution (HBSS) with

10 mM glucose was taken as the positive control [482]. Aorta segments alone were also preserved under anoxia and normoxia in culture medium to serve as negative controls. The culture medium was changed every three days. Anoxic environment was created by flushing the jar with balloons filled with $N_2$ during the change of culture medium.

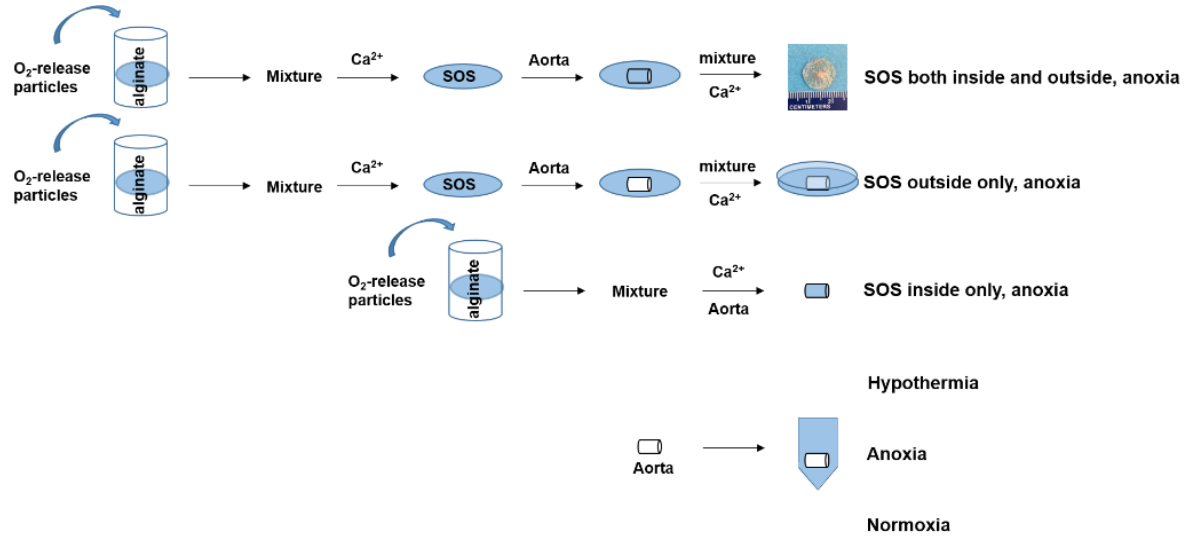


Figure 4.1. Schematic of blood vessel culture under different conditions.

## 2.4 Characterization

A field emission scanning electron microscope (FE-SEM, FEI Inspect F-50, FEI, USA) was employed to examine the morphology of CP, $MnO_2$ and the prepared microparticles. The microstructure of the microparticles was inspected under SEM as well. A pycnometer (AccuPyc 1330, Micromeritics, USA) was used to measure the density of prepared microparticles following the instruction. The specific surface area of the microparticles was measured as well using a gas adsorption analyzer (TriStar, MicroMeritics, USA).

N,N-dimethyl-p-phenylenediamine (DMPD, Sigma, USA) was employed to detect radicals released from the material. [491, 492] The microparticles with and without alginate hydrogel

were put into 2.5 mg/mL DMPD solution and the released radicals turned the solution into red. Potassium iodide (Fisher Scientific, Canada) and starch solution (Fisher Scientific, Canada) was used to detect $H_2O_2$ in the system and the solution became blue in the presence of $H_2O_2$. The change of colorless culture medium was detected by a pH indicator (Riedel-deHaen (pH 4-10), Aldrich, USA)). 7 mg microparticles and 3 mL solution containing dyes were used in all the experiments. To encapsulate the microparticles, 500 µL 1% w/v alginate was used. The color changes were recorded with a camera (D70S, Nikon, Japan).

The viability of endothelial cells and smooth muscle cells was examined using fluorescent staining after 150-minute incubation in HBSS with 10 mM glucose at 37 ℃ and examined under a fluorescence microscope (Imager.M2, Zeiss, Germany). Ethidium bromide-1 (Life technologies, USA) was used to stain the nuclei of dead cells and Hoechst 33258 (Life technologies, USA) the nuclei of all cells in the tissue. The ratio of dead cells in both the cross section and lumen side of blood vessels was quantified by counting the stained dead cells and all cells.

The mitochondrial membrane potential of endothelial cells was also measured using tetramethylrhodamine methyl ester (TMRM, Setareh Biotech, USA) staining [482]. The samples were rewarmed at 37 ℃ in HBSS with 10 mM glucose for 150 min and then stained with TMRM (500 nmol/L) for 30 minutes in HBSS with 10 mM glucose. Afterwards the stained samples were kept in 250 nmol/L TMRM for maintenance. The aortas were placed into incubation chambers with a coverglass bottom with the endothelial side being downside. Fluorescence of the mitochondria of the endothelial cells was inspected using an inverted confocal microscope (LSM 510, Zeiss), under the condition of 116 µm pinhole, at $\lambda$exc. = 543 nm, $\lambda$em. = 585 nm. [482]

Smooth muscle contraction force, stimulated by 120 mM KCl, was measured with a Mach-1$^{TM}$ mechanical testing system (Biomomentum Inc. Canada) fitted with a 150 g load cell. The rat aortas were cut into 5-mm ring segments. Each ring segment was suspended in a tissue bath containing 300 mL of Krebs Henseleit (KH) solution (122 mM NaCl, 4.7 mM KCl, 1.2 mM $MgCl_2$, 15.4 mM $NaHCO_3$, 1.2 mM $KH_2PO_4$ and 5.5 mM glucose) and mounted between 2 stainless steel wire hooks. One hook was fixed to the bottom of the bath and the other hook was connected to the force transducer. The KH buffer was gassed continuously with 95% $O_2$ and 5% $CO_2$ at 37 ℃ and changed every 20 min. The baseline tension of all vessel rings was adjusted to around 1.0 g. After 1 h of equilibration, KH solution supplemented with 120 mM KCl was used to stimulate the contraction of the aorta tissue rings. Contraction force of the aorta tissue rings was recorded by a tensiometer. [493] The stimulated contraction force of all the samples was expressed as the percentage of the stimulated force before preservation. Four replicates were performed for each sample. The results were expressed as an average ± standard deviation.

## 3. Results

### 3.1 Material characterization

According to Figure 4.2c, the oxygen-release particles were spherical with a diameter ranging from 20-300 μm. They had a porous structure on the surface (Figure 4.2d) and CP particles dispersed on the surface and in the pore structures (Figure 4.2d arrow). The microparticles had a large size range possibly due to the large size distribution of $MnO_2$ particles (Figure 4.2b).

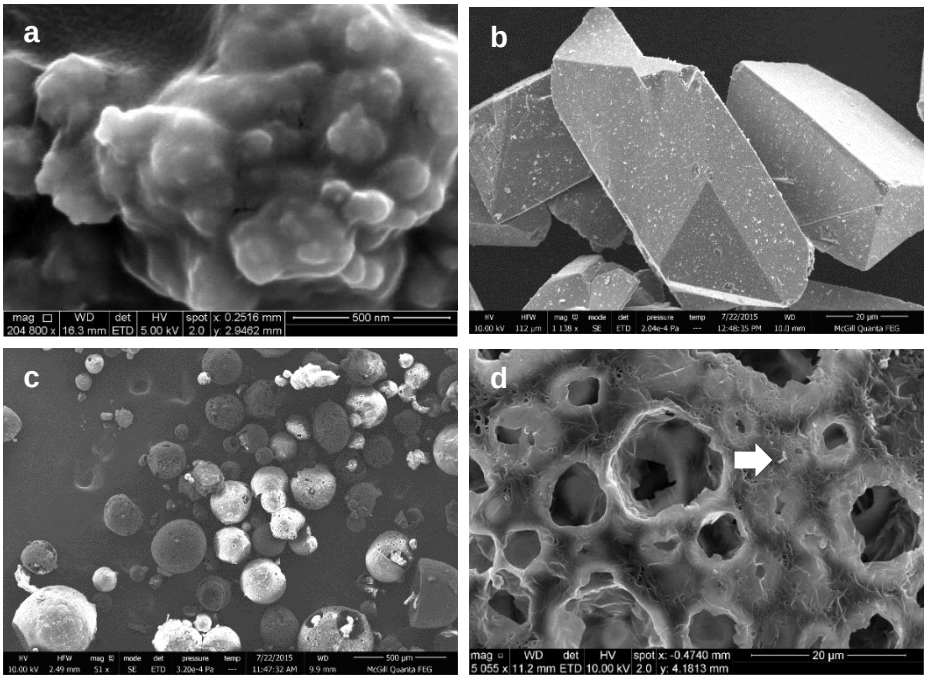


Figure 4.2. SEM image of CP powders (a), $MnO_2$ (b) and oxygen-release microparticles (c and d). The oxygen-release microparticles had a spherical shape and were porous. CP powders were nano particles. $MnO_2$ particles are polyhedrons with a size ranging from 20-80 µm. The prepared oxygen-release microparticles had a spherical shape and a porous structure (Figure 4.2d).

The specific surface area of CP powders and the prepared microparticles was measured. Figure 4.3 shows the measured specific surface area of the samples. The microparticles had a 50% smaller specific surface area compared with CP powders (Figure 4.3). The measured density of the microparticles indicated that the particles only had 20% closed porosity (Supplemental Table 4.2S), suggesting that the particles had connective pore structures.

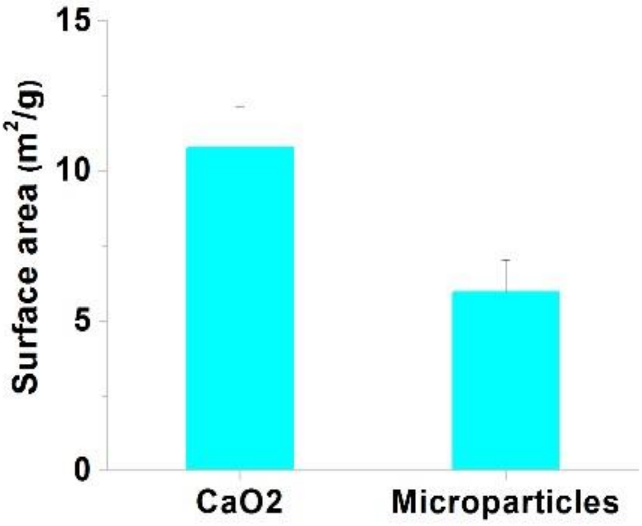


Figure 4.3. Specific surface area of CP powders and CP-$MnO_2$-PCL microparticles. The specific surface area of microparticles was 50% of that of CP powders.

For the free radical release test (Figure 4.4a), the color only changed inside the hydrogel from pink to red when the microparticles were encapsulated in alginate hydrogel, indicating that all the released radicals were trapped inside the hydrogel. The intensity of red color in the hydrogel was less than that in water caused by microparticles without hydrogel, and therefore, alginate hydrogel reduced the release rate of free radicals from microparticles. The presence of alginate hydrogel greatly reduced the released amount of $H_2O_2$ (Figure 4.4b), suggesting that alginate hydrogel inhibited the decomposition rate of CP in the microparticles. The microparticles did not cause pH change in culture medium (Figure 4.4c), indicating that the released hydroxyl ions were consumed by the buffer system in culture medium.

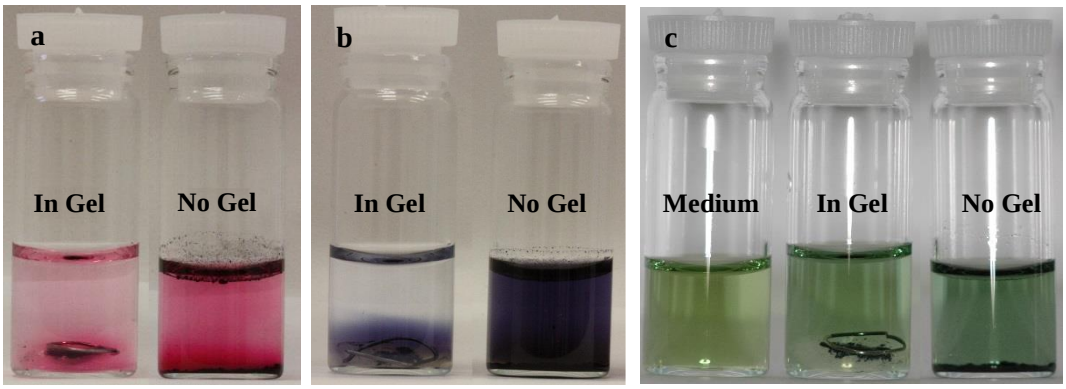


Figure 4.4. Release of radicals (a) and $H_2O_2$ (b) from the materials as well as pH changes in culture medium (c) after 60 min. The presence of alginate hydrogel greatly mitigated color changes in a and b, suggesting there were less $H_2O_2$ and free radicals release when the microparticles were in hydrogel. In contrast, significant color changes around the microparticles were observed without hydrogel in a and b. For pH changes (c), however, no color change was noticed in culture medium, either with or without hydrogel, suggesting that pH did not change much in culture medium.

3.2 Viability of arterial cells at 37 ℃

From the cross section fluorescent image of freshly procured aorta (Figure 4.5a), well-aligned smooth muscle cells were observed in tunica media with almost no dead smooth muscle cells; dead cells were barely detected in the endothelial ring in tunica intima, locating at the lumen side, as well. The fluorescent image from lumen side showed parallel aligned elongated endothelial cells (Figure 4.5b). The image also confirmed that there were very few dead endothelial cells in freshly procured aortas. Nevertheless, after being cultured for seven days under the standard cell culture condition (37 ℃, DMEM culture medium supplemented with 10% FBS and 1% P/S, 20% $O_2$, 5% $CO_2$), nearly all the cells, either from tunica media or tunica intima, were stained dead (Figure 4.5c). Endothelial cells on the aorta wall were also mostly stained dead (Figure 4.5d). In the case of anoxic culture, similar results were observed. Around

85% cells on the cross section surface were stained dead and around 95% of endothelial cells died on the lumen side (Figure 4.5e and f). Moreover, the endothelial layer of aortas cultured under anoxia lost its integrity and exhibited a lower cell density compared with that of fresh aortas.

For the purpose of further experiments, both the standard cell culture and anoxic culture were used as the negative control culture conditions. This loss of viability occurred rapidly, even after three days (Figure 4.3S). Under the anoxic culture conditions, 45% of cells died on the cross section surface and 55% of endothelial cells died on the lumen side. Nearly all the cells, including smooth muscle cells and endothelial cells, already died under normoxia after three days.

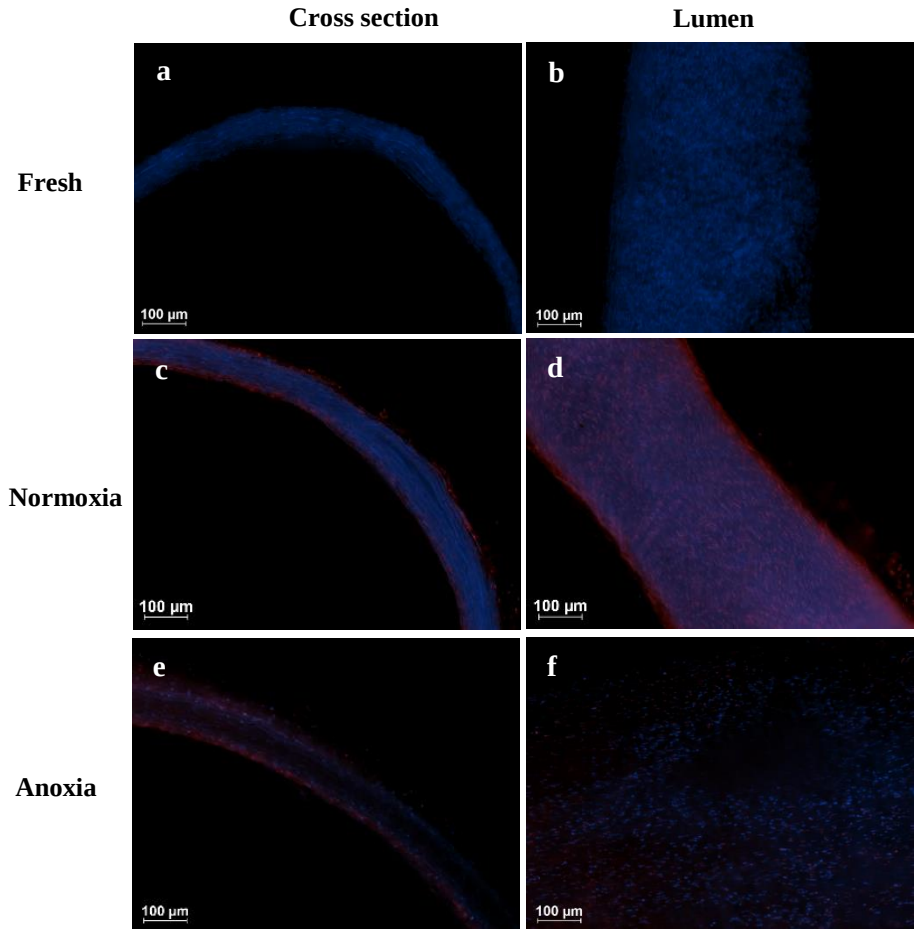


Figure 4.5. Fluorescent images of the aorta tissue, preserved under various conditions for 7 d, stained by Ethidium bromide-1 and Hoechst 33258. Dead cells were stained red, and all the nuclei were stained blue. The cross section images (a, c and e) exposed both smooth muscle cells (in the ring) and endothelial cells (inner side). The lumen-side images (b, d and f) showed the layer of endothelial cells. After 7 d, most cells died in aortas preserved under either normoxia (c and d), i.e. 20% $O_2$, 37 ℃, or anoxia (e and f), i.e. 0% $O_2$, 37 ℃.

3.3 Cold preservation

As expected, cold preservation improved cell viability compared with standard culture conditions (Figure 4.5c and d and Figure 4.6). After three days, both smooth muscle cells in tunica media and endothelial cells in tunica intima maintained high cell viability immediately after retrieval from storage (around 90%), however, rewarming reduced cell viability very rapidly to 45% (Figure 4.6a and b). After seven days, cell viability had decreased to 65%, again this was exacerbated by rewarming such that only 15% viable cells were detected (Figure 4.6c and d).

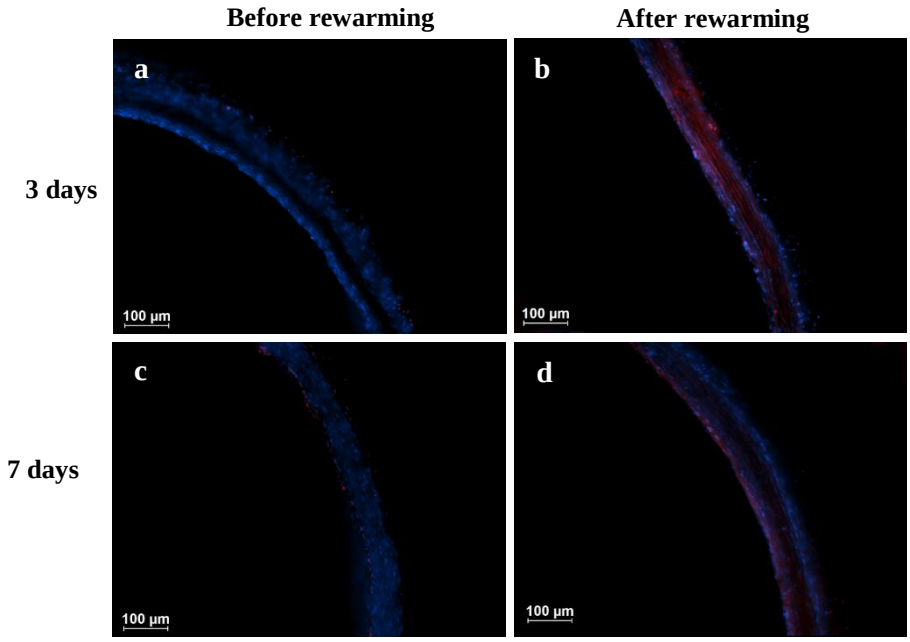


Figure 4.6. Fluorescent images of aortas stored under hypothermia before and after rewarming. After three days, very few cells were stained dead from cold preserved aorta (a), after rewarming, however, a large amount of dead cells were found, including both endothelial cells and smooth muscle cells (b). After seven days, a majority of endothelial cells died but most of the smooth muscle cells stayed alive (c). Nevertheless, after rewarming for 150 min many smooth muscle cells were found to be dead (d).

### 3.4 Effect of SOS location

Of the three permutations of location possible, namely lumen-side, adventitial side, and both sides, the combined inside and outside appeared optimal compared with the other locations (Figure 4.4S). When the SOS was introduced only on the luminal side, about 65% of the cells in aorta were stained dead even after one day. The endothelial cells in tunica intima appeared to die completely. The closer smooth muscle cells were to tunica intima, the greater the proportion died. (Figure 4.4Sa) In the case of placing SOS only outside of the blood vessel, cells in both tunica intima and tunica media died. (Figure 4.4Sb)

### 3.5 Effect of peroxide concentration on cell viability

The composition of SOS were selected from 10, 20 and 40 mg/mL of microparticle suspension concentrations. 700 µl SOS was used per 5 mm aortic section, representing a total potential oxygen load of 28, 56 and 112 µg of molecular oxygen sufficient to fully saturate 35, 70 and 140 mL medium, respectively, i. e., 4 orders of magnitude more than the tissue volume itself (around 6 µL).

When a concentration of 10 mg/mL microparticles were in SOS, 20% dead cells were observed after three days (Figure 4.7a). The dead cells are mainly endothelial cells in tunica intima and smooth muscle cells close to tunica intima. When the concentration of microparticles was increased by three times to 40 mg/mL, 80% of the cells were detected to be dead (Figure 4.7c). This time almost all of the endothelial cells in tunica intima and the majority of smooth muscle cells in tunica media died. On the other hand, aortas preserved in SOS with 20 mg/mL microparticles displayed nearly 95% viability (Figure 4.7b), on the basis of this observation, 20 mg/mL was selected for further experiments.

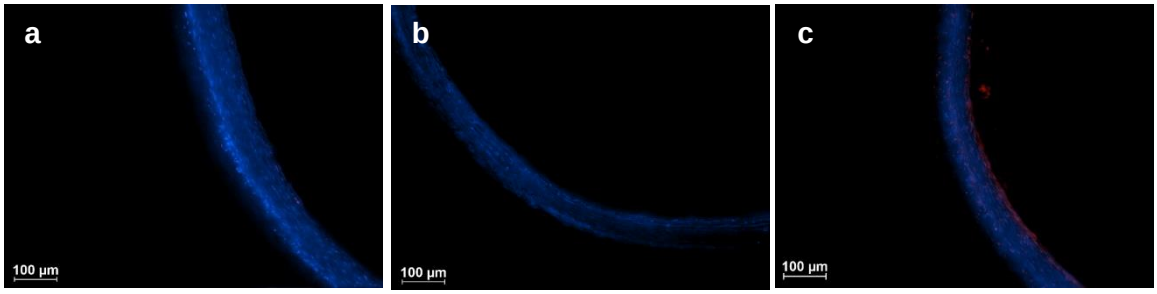


Figure 4.7. Cross sectional images of fluorescently stained aortas preserved by self-oxygenating scaffolds (SOS) with different concentrations of microparticles under anoxia, i.e. 0% $O_2$, 37 ℃, after 3 d. Dead cells were stained red, and all the nuclei were stained blue. a: 10 mg/mL, b: 20 mg/mL microparticles, c: 40 mg/mL microparticles. Dead cells were observed in a and c.

3.6 Mitochondrial membrane potential of endothelial cells in blood vessels under various conditions

Unlike human endothelial cells, rat endothelial cells are elongated rather than cobblestoned as shown in Figure 4.8. The potential of mitochondrial membrane of the endothelial cells in aortas was much better preserved in the presence of SOS under anoxia for up to seven days, compared with that of aortas stored under anoxia, normoxia, and hypothermia. (Figure 4.8a-d) The endothelial cells in the tissues of the experimental group had a significantly higher membrane potential than that of endothelial cells in control groups. Moreover, endothelial cells in aortas preserved under anoxia and normoxia lost their mitochondrial membrane potential even after 3 days (Figure 4.5S).

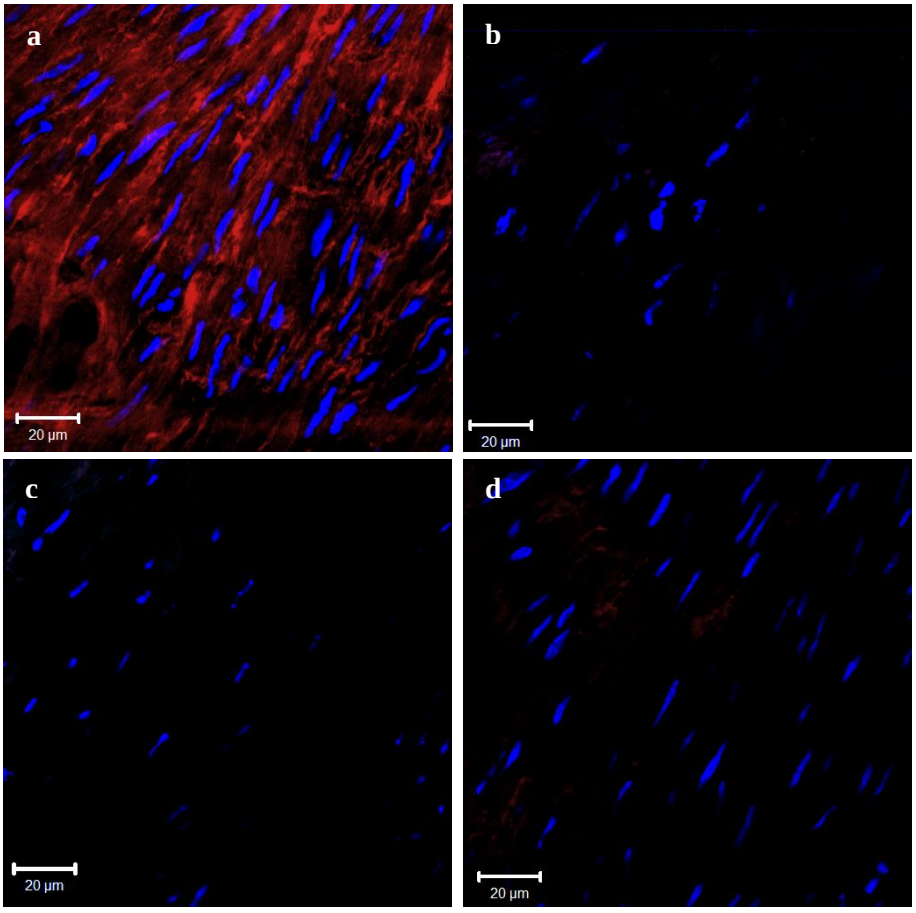


Figure 4.8. Fluorescent images of tetramethylrhodamine methyl ester (TMRM) stained endothelium mitochondrial membrane potential after seven days. The aorta preserved under anoxia, i.e. 0% $O_2$, 37 ℃, in the presence of the self-oxygenating scaffold (SOS) maintained a normal endothelium mitochondrial membrane potential (a) while samples preserved under anoxia (b), normoxia (c), i.e. 20% $O_2$, 37 ℃, and hypothermia (d) lost their endothelium mitochondrial membrane potentials.

3.7 Effects of oxygen supply on mechanical properties of aortas

The presence of SOS maintained about 90% of KCl stimulated contraction force of aortas after three days (Figure 4.6S). Consistent with the cell viability results, the other conditions

preserved no more that 60% of KCl stimulated contraction force. The contraction force detected from samples preserved under normoxia may be due to the osmosis changes upon the addition of KCl. Smooth muscle cells play a key role in the regulation of blood vessel wall structure and geometry. Therefore, the viability of smooth muscle cells in preserved vessels determines the functionality of the blood vessels and is an essential criterion to assess the preservation outcome of the vessels.

Even after seven days, aortas stored in anoxia in the presence of self-oxygenating scaffolds still maintained about 90% of KCl stimulated contraction force (Figure 4.9). In contrast, the KCl stimulated contraction force of aortas preserved under the other conditions was no more that 50% (Figure 4.9).

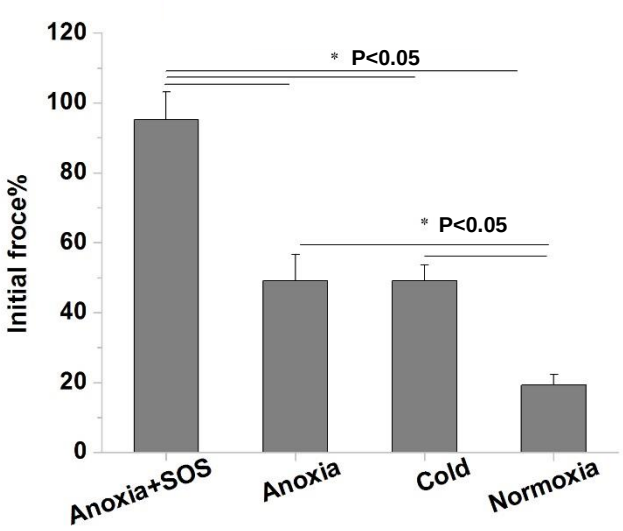


Figure 4.9. KCl stimulated contraction force of aortic rings after seven days. The presence of self-oxygenating scaffold (SOS) under anoxia (0% $O_2$, 37 ℃), maintained normal stimulated contraction force for up to seven days, however, the other conditions, namely anoxia, normoxia (20% $O_2$, 37 ℃) and cold (20% $O_2$, 4 ℃) failed to retain the KCl stimulated contraction force.

## 4. Discussion

Warm perfusion or cold preservation have achieved blood vessel preservation time of up to forty eight hours and fourteen days. [482, 494, 495] Extension of viability limit described in our study has been achieved by chemically mitigating damage by reactive oxygen species (ROS) [482]. A hypoxic environment induces the increase of glycolytic activities [175], which reduces the amount of generated ATP through respiration and causes the depletion of ATP. The depletion of ATP generates hypoxanthine, which is converted into xanthine under hypoxia. [470] When the cells are brought back to normal oxygen tensions, xanthine reacts with oxygen and generates ROS. [470] The burst generation of ROS by xanthine can kill cells [496, 497]. As oxygen shortage occurs under both anoxic and cold conditions, cell death after rewarming occurs in both cases. On the other hand, when the environmental oxygen tension is higher than normal oxygen tension, ROS are also produced. [498] Therefore, normoxia also failed to prevent cell death in preserved aortas. We determined that only when the oxygen tension of aortas is maintained within the normal level, damage caused by rewarming is avoided. Reactive oxygen species can be reduced by superoxide dismutase or adenosine [499]. Nevertheless, these additives are usually expensive.

Most tissue and cell engineering culture approaches evolve from commercial bioreactors and rely on fluid flow for gas, nutrient supply, and waste transportation. While many attempts have been made to deliver oxygen from materials to cells, most of the materials were themselves adapted from aquaculture technique or synthetic blood products. The vast majority of previous work has focused on ways to introduce oxygen in a sustained manner into culture systems without considering where this oxygen goes if it is not consumed by the cells. In addition, while several researchers have attempted to use polymer encapsulated peroxides, they have to either use toxic $MnCl_2$ or extremely high concentrations of catalase to remove $H_2O_2$, a cytotoxic

compound, generated by the peroxides. [304, 309, 500] Just like the lung and leaves and other natural gas exchange structures, the inherently low solubility of atmospheric gases at physiological conditions necessitates the use of high surface areas for rapid transfer without buildup of toxic decomposition products and the hydrogen peroxide intermediate.

Aortas need an appropriate amount of oxygen, possibly close to the oxygen tension in blood (around 13%) on the luminal side [41], which is 80% lower than normoxia but much higher than anoxia, to maintain their normal activities. Although many efforts have been made to oxygenate tissues and organs during preservation [39, 216, 217, 228, 232, 235, 270, 304, 501-503], supplying of a suitable amount of oxygen to tissues and organs has rarely been studied [166].

According to the mathematical simulated results, burst release of oxygen towards the blood vessels could greatly be alleviated by alginate hydrogel (Figure 4.2Sa). Moreover, the oxygen gradient across the blood vessel wall could be adjusted by controlling oxygen-release rate in SOS so that various oxygen concentrations could be provided to different types of cells (Figure 4.2Sb).

The detected $H_2O_2$ release from the microparticles with and without hydrogel confirmed the inhibiting effects of hydrogel towards CP decomposition. (Figure 4.4b). In addition, the free radicals released during the decomposition of peroxides were trapped within the hydrogel so that cells could be protected from toxic radicals, and the released hydroxyl ions were readily neutralized by the buffer system in culture medium (Figure 4.4a and c), eliminating the toxicity of the alkaline byproduct.

In this work, rat aortas were cultured under different conditions with various oxygen concentrations, namely anoxia with SOS, anoxia, normoxia, and cold preservation. The tissue-protective capacity of our SOS in anoxic circumstances was tested. The commonly used cold preservation was chosen as the positive control. The results from Figure 4.7 showed that the presence of self-oxygenating scaffold successfully prevented cell death in the tissue under anoxia (Figure 4.7b), while aortas kept in other conditions showed much lower cell viability (Figure 4.5 and 6). Moreover, a suitable amount of oxygen, i.e. 20 mg/mL microparticles in the scaffold, was essential to keep cells alive in the tissues (Figure 4.7a, b and c).

Supplying oxygen only from one side of the artery, either from the lumen side or the adventitial side, resulted in very poorly preserved artery tissues (Figure 4.4S). Only a very small volume (about 16 μL in our case) of SOS could be added into the lumen of the artery considering the small diameter of the blood vessel. As a results, the amount of oxygen generated from SOS was very small, about $6.8\times10^{-5}$ mL in total. More importantly, a large ratio of released oxygen for SOS may diffuse out of the lumen since the artery was in an anoxic environment. When the artery was encapsulated by SOS only from the outside, the endothelial cells could not be oxygenated. According to the simulated results, the oxygen concentration in the artery wall decreased abruptly when SOS only existed on the adventitial side, which may result in nonsufficient oxygenation of smooth muscle cells. As a result, poor cell viability was observed when SOS was only supplied from one side of the artery. When there was SOS both inside and outside of the artery, a more homogeneous and stable oxygen environment was created around the artery. Hence, the artery was well preserved.

In addition to cell viability results, the TMRM stained endothelial cell mitochondrial membrane potential results indicated that the endothelial cells in aortas preserved in the presence of SOS

were healthy (Figure 4.8 and Figure 4.5S). In contrast, endothelial cells in aorta tissue preserved under the other conditions showed much lower membrane potentials. The loss of mitochondrial membrane potential led to irreversible cell death through caspase activation, release of death effectors such as cytochrome c and metabolic changes. [504, 505] Endothelial cells in the control groups may either die of hypothermic and reperfusion injury or hyperoxic injury. The results of KCl stimulated contraction force of preserved aortas further confirmed the healthy status of smooth muscle cells kept in SOS under anoxia (Figure 4.9 and Figure 4.6S). These results indicated that the endothelial and smooth muscle cells were not only alive after preservation in anoxia with SOS but also in healthy status.

## 5. Conclusions

Rat aortas were successfully preserved in buffered nitrogen with the assistance of SOS at physiological temperature. The *in situ* oxygen-release scaffold was able to maintain high cell viability, normal mitochondrial membrane potentials of endothelial cells, and healthy smooth muscle cells in the aorta. Based on the results in this work, we argue that the technique of tissue and organ preservation can be improved by oxygen delivery on condition that an appropriate amount of oxygen is supplemented to tissues and organs.

## Acknowledgements

This work was supported by the Natural Sciences and Engineering Research Council of Canada (*NSERC*) and China Scholarship Council (CSC). The authors also would like to acknowledge the Animal Resource Division of the Research Institute of the McGill University Health Center for providing animals to us and BioPloymer for providing us with sodium alginate. Last but not least, the authors would like to acknowledge Fields-Mprime Industrial Problem Solving Workshop at the University of Toronto.

## Supplemental information

Mathematical modeling

The oxygen diffusion process from CP-$MnO_2$-PCL microparticles through alginate hydrogel as well as the oxygen concentration gradients across the blood vessel wall was mathematically simulated. Oxygen concentration at a certain point in the alginate hydrogel at certain time point (Equation 1 first term on the left) was determined by the diffusion of oxygen in hydrogel (Equation 1 first term on the right) and the amount of oxygen generated by the particles (Equation 1 second term on the right). The amount of generated $O_2$ depended on the amount of CP in the particles, the decomposition rate of CP, the amount of $H_2O$ available to the reaction, the presence of catalysts, local pH, and the diameter of the particles. Given the complexity of the oxygen-generating process, the modeling mainly focused on the diffusion of oxygen away from the particles through hydrogel. The dimension of the embedded aorta tissue was measured to be 1.9 mm in inner wall diameter and 2.14 mm in outer wall diameter (Table 4.1S) and cut into 5 mm in length. To simulate oxygen gradients across the blood vessel wall, the model was reduced to an axially symmetric geometry because of its thin wall (Figure 4.1S). The oxygen concentrations in blood vessel wall at certain time points (Equation 2 first term on the left) were determined by oxygen diffusion through the blood vessel (Equation 2 first term on the right) as well as the $O_2$ consumption rate of the tissue (Equation 2 second term on the right). The oxygen diffusion coefficient in the aorta tissue was taken as $2\times10^{-4}$ $mm^2/s$. The oxygen consumption rate of the arteriolar tissue was taken as $5.71\times10^{-5}$ ($mol\cdot100\ cm^{-3}$ $tissue\cdot min^{-1}$) [506], endothelial cells $1.5\times10^{-17}$ $mol\ cell^{-1}\ s^{-1}$, and smooth muscle cells 2.6 times of that of endothelial cells [507]. The endothelial cells in arteriolar wall was assumed to be one layer with a thickness of $10^{-3}$ mm [508] and their cross-section area was $2\times10^{-4}$ $mm^2$ [509]. The rest

of aorta wall was treated as average tissue comprising smooth muscle cells, of which the cross-section area was $5.6\times10^{-4}$ $mm^2$ [509].

Table 4.1S. Dimension of the thoracic aorta

| | Diameter (mm) |
|---|---|
| Outer wall | 2.14±0.07 |
| Inner wall | 1.91±0.05 |

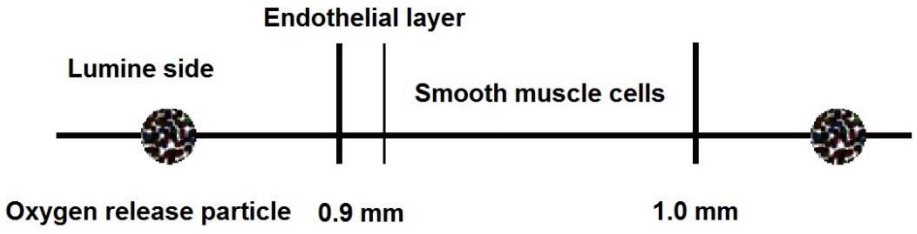


Figure 4.1S. Schematic geometry of oxygen diffusion through the aorta wall.

$$\frac{\partial c}{\partial t} = \nabla\left(\kappa_{gel}\nabla c\right) + \sum_i f_i\left(r,t\right) \quad (1)$$

$$\frac{\partial c}{\partial t} = \nabla\left(\kappa_{artery}\nabla c\right) - S\left(r,t\right) \quad (2)$$

where c is the oxygen concentration, t is time, **κ** is the oxygen diffusion coefficient, r is the distance from the center of the aorta ring, S is the consumed oxygen.

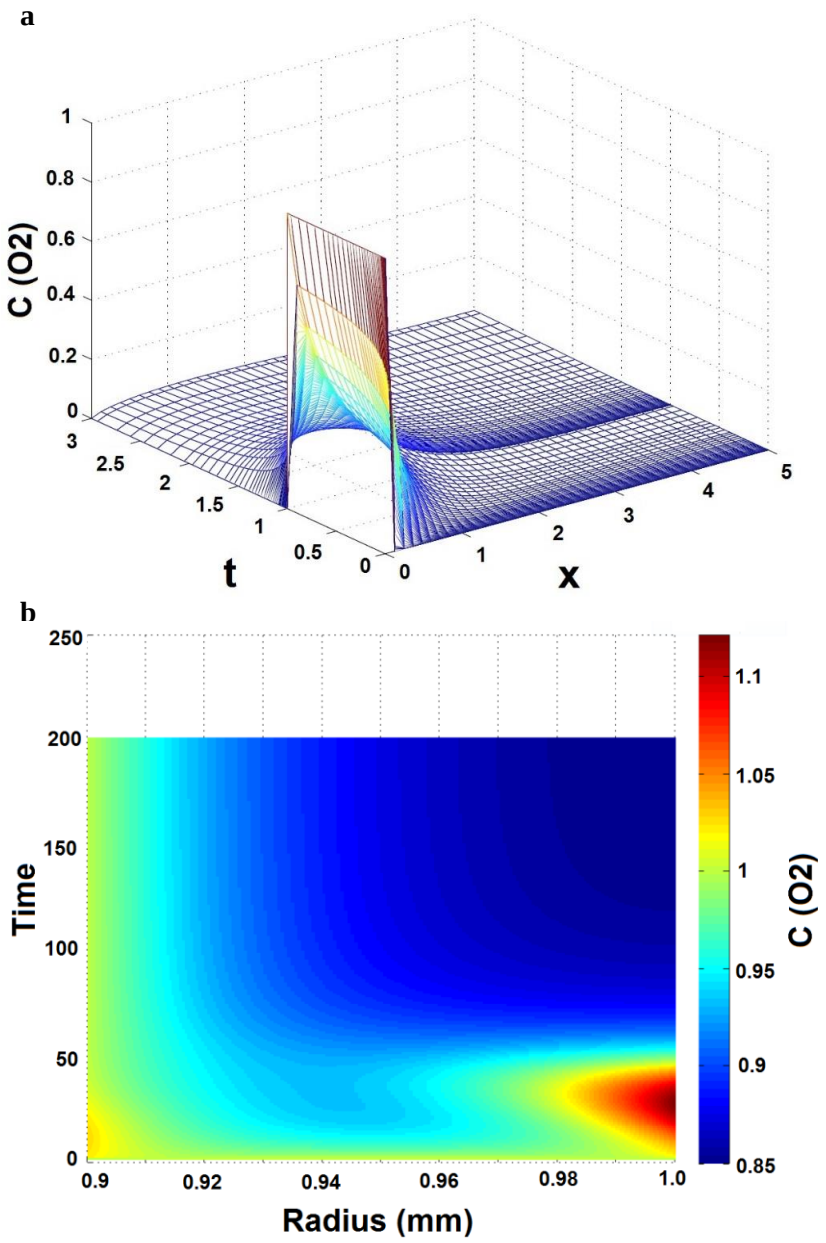


Figure 4.2S. Mathematically simulated oxygen concentration gradients versus time and position in hydrogel (a) and the oxygen gradients across the aorta wall (b). The oxygen concentration decreased exponentially away from the microparticles in hydrogel and then stayed at a relatively stable level (a). Therefore, burst release of oxygen towards the aorta tissue was mitigated and the tissue received a relative stable oxygen supply. The oxygen gradient across the artery wall could also be adjusted to fit the needs of both endothelial cells and smooth muscle cells.

Mathematical simulation results showed that burst release of oxygen occurred only in the area adjacent to the oxygen-release particles, the oxygen concentration decreased abruptly away from the core of microparticles, and the presence of alginate hydrogel smoothed oxygen-release profile (Figure 4.2Sa). Therefore, the burst release of oxygen was alleviated. The simulated oxygen gradient results across the blood vessel wall showed that the oxygen concentration decreased gradually from inside of the blood vessel to outside (Figure 4.2Sb). Given the fact that endothelial cells are more tolerant to high oxygen concentrations than smooth muscle cells, this seems to be a more physiological oxygen profile.

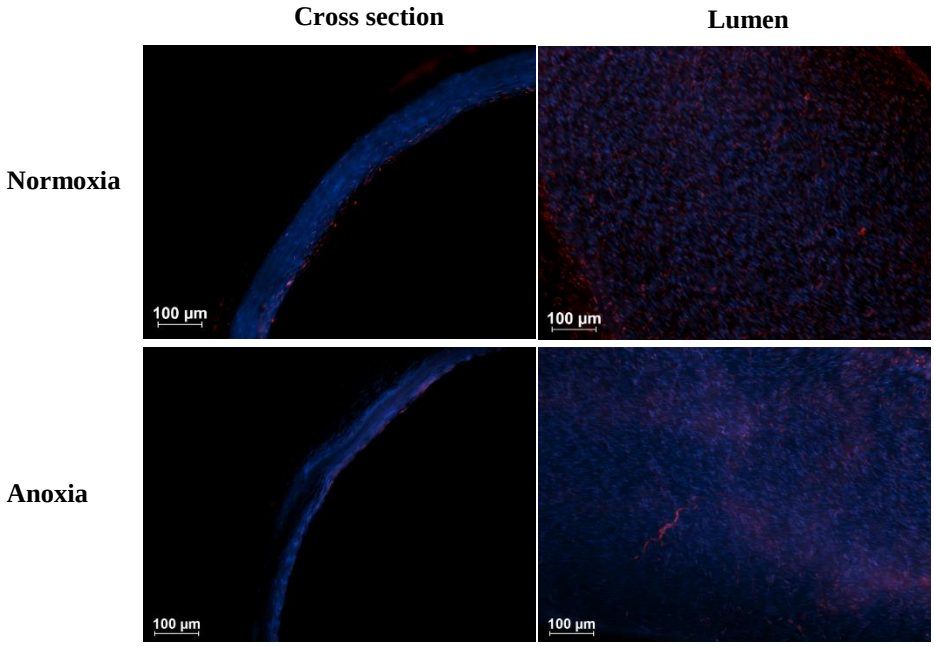


Figure 4.3S. Fluorescent images of Ethidium bromide-1 and Hoechst 33258 stained aorta preserved under normoxia and anoxia, after three days. Dead cells were stained red, and all the nuclei were stained blue.

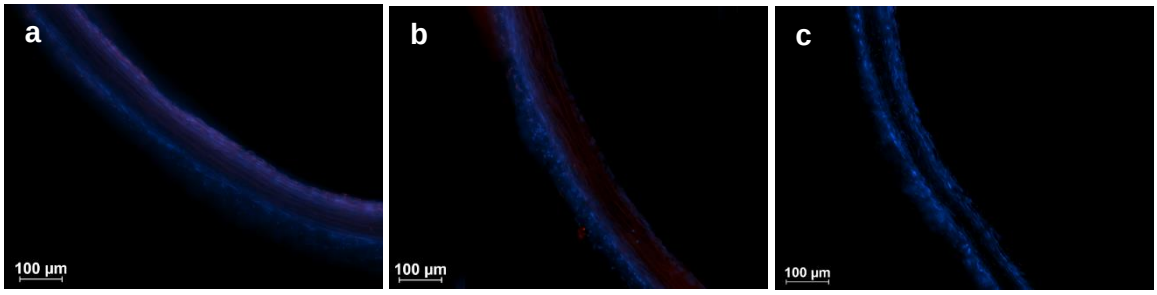


Figure 4.4S. Cross section images of Ethidium bromide-1 and Hoechst 33258 stained aorta preserved by self-oxygenating scaffolds (SOS, 20 mg/mL microparticles in the scaffold) with oxygen supply only from lumen-side (a) or adventitial side (b) or both sides (c) under anoxia, i.e. 0% $O_2$, 37 ℃, after one day. 16 µL SOS was used to fill the lumen of the artery. In the other two samples, 700 µL SOS was used. Dead cells were stained red, and all the nuclei were stained blue. Supplying oxygen from only one side, either from the lumen side or adventitial side, to the blood vessels resulted in a large number of dead cells, while oxygen delivery from both sides successfully preserved blood vessels.

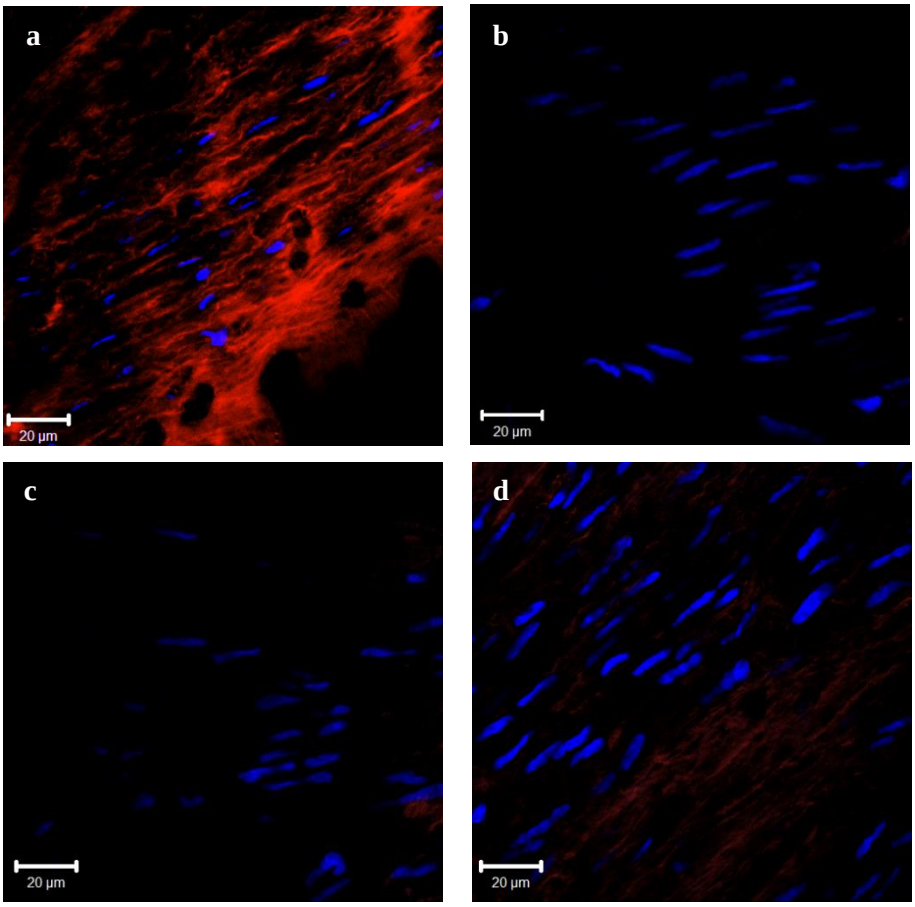


Figure 4.5S. Fluorescent images of tetramethylrhodamine methyl ester (TMRM) stained endothelium mitochondrial membrane potential after three days. The aorta preserved under anoxia, i.e. 0% $O_2$, 37 ℃, in the presence of self-oxygenating scaffold (SOS) maintained a normal endothelium mitochondrial membrane potential (a) while samples preserved under anoxia (b) and normoxia (c), i.e. 20% $O_2$, 37 ℃, lost their endothelium mitochondrial membrane potentials. The aorta kept at 4 ℃, 20% $O_2$ (d) retained partial of their endothelium mitochondrial membrane potentials.

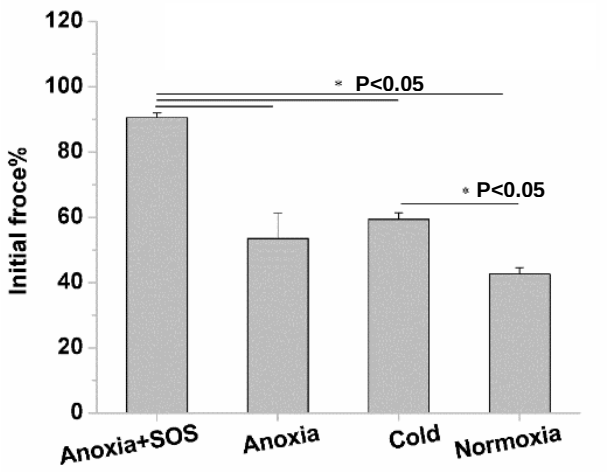


Figure 4.6S. Potassium chloride (KCl) stimulated contraction force of aorta tissue rings after three days. The presence of self-oxygenating scaffold (SOS) under anoxia (0% $O_2$, 37 ℃, 20 mg/mL microparticles in the scaffold) maintained 90% of the aortas' stimulated contraction force after three days, however, the other conditions, namely anoxia, normoxia (20% $O_2$, 37 ℃) and cold (20% $O_2$, 4 ℃) retained less than 60% of the tissue's stimulated contraction force.

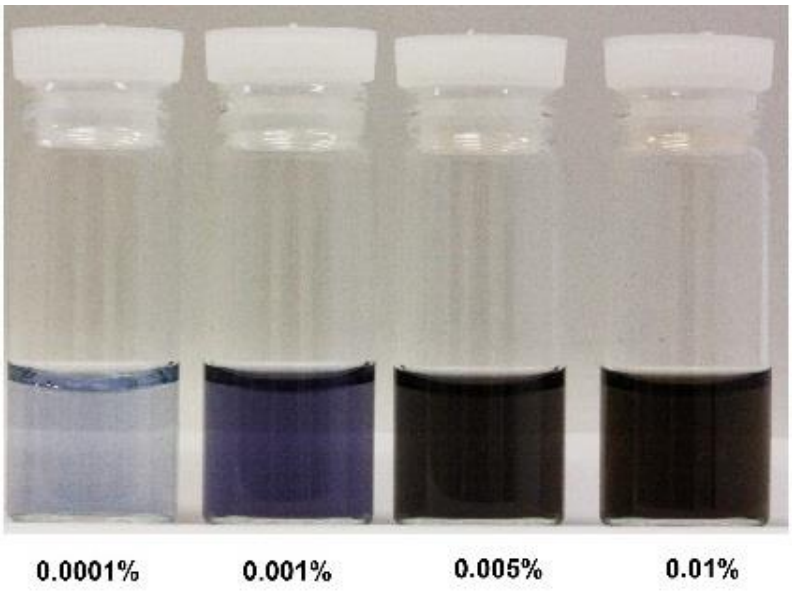


Figure 4.7S. Color changes of KI-starch solution in the presence of different concentration of $H_2O_2$. The color of the solution changed from light blue to dark blue as the concentration of $H_2O_2$ increased from 0.0001% to 0.005%.

Table 4.2S. Measured density of the microparticles and calculated ineffective porosity

| | Microparticles | Ineffective porosity |
|---|---|---|
| Density (g/mL) | 1.55±0.13 | 22% |

## Chapter 5

### Oxygen delivery effectively prevented tissue necrosis in ischemic wounds

Huaifa Zhang[1], Hani Shash[2], Amal Al-Odaini[3], Mirko Gilardino[2], Jake Barralet[1,4]

1. Faculty of Dentistry, McGill University, Montreal, QC, Canada

2. Division of Plastic and Reconstructive Surgery, Department of Surgery, Faculty of Medicine, McGill University, Montreal, QC, Canada

3. Division of Medical Oncology, Faculty of Medicine, McGill University, Montreal, QC, Canada

4. Division of Orthopaedics, Department of Surgery, Faculty of Medicine, McGill University, Montreal, QC, Canada

### Preface

Like tissue preservation, wound healing also requires extra oxygen supply. Hypoxia and even anoxia can happen in wounds due to the interruption of blood supply. Oxygen plays an important role in anti-infection, extra cellular matrix production, collagen deposition, cell proliferation, and vascularization. Therefore, oxygen therapy has been used to treat wounds, such as hyperbaric oxygen therapy and topical oxygen therapy. However, these methods are either inconvenient to perform, expensive, or ineffective. The previous experimental results have shown that the developed oxygen delivery materials are able to support cell growth and preserve blood vessels under anoxia. An oxygen-release patch for wound treatment, which was capable of delivering dissolved oxygen to wounds, was further developed using the same oxygen-release material. The oxygen-release patch was evaluated with an ischemic rabbit ear wound model and was found to preserve wounded tissues and accelerate wound healing.

**Abstract**

Oxygen is essential for tissue survival and wound healing. Following trauma, hypoxia and even anoxia can occur due to the lack of blood supply. Wounds related to ischemia, such as diabetic ulcers and radiation injuries, often heal poorly. In this work, we developed an oxygen delivery patch (ODP) for wound healing and evaluated the patch on an ischemic rabbit ear full thickness wound model. The ODP employed calcium peroxide as the oxygen-generating agent and alginate hydrogel as the dressing material. The experimental results showed that the ODP increased wound healing rate and prevented tissue necrosis in large wounds. Moreover, the presence of oxygen eliminated the adverse effects of ischemic wounds on neighbouring tissues. The oxygen-release patch promoted ischemic wound healing, prevented ischemic tissues from necrosis, and protected tissues adjacent to the wounds. Of fundamental significance was the demonstration that biomaterial mediated topical oxygen delivery could sustain tissue viability for sufficient time before a new vasculature was established.

**Key words:** Oxygen delivery, peroxide, wound dressing, wound healing, ischemia

## 1. Introduction

Oxygen is essential for wound healing, in terms of cell viability, collagen production, anti-infection, inflammation process, and angiogenesis. [15, 510-512] However, oxygen deficiency is common in wounded areas due to the damage of blood vessels, which leads to the impairment of blood supply and a reduction or cessation of oxygen supply. In fact, wounded tissue demands more oxygen than normal tissues, because of the enhanced cellular metabolic activities related to the production of new tissues and antibacterial activities. [513-516] The interrupted oxygen supply to the wounded area worsens the situation, increases the risk of infection, and further inhibits the process of wound healing.

The use of wound dressing materials to treat wounds is common in clinic. The dressing can prevent infection, keep the wounds hydrated, and absorb exudates. [517] Hydrogels contain a large amount of water and can rehydrate the wound bed thereby reducing pain. In addition, they are gas permeable and bacteria impermeable, and thus have been used for dressing various kinds of wounds, such as pain wounds, ulcers, radiation injuries, and necrotic wounds. [518-523]

Oxygen delivery is believed to promote wound healing. The topical supply of oxygen to wounded area promotes fibroblast proliferation [524], improves the production rate and quality of collagen [525-528], facilitates angiogenesis, and augments the antibacterial activities of macrophages [316, 524, 529]. So far, various efforts have been made to promote wound healing by means of oxygen delivery, including hyperbaric oxygen therapy, topical oxygen delivery and oxygen-release dressings. However, they are either not effective enough, expensive, inconvenient to access, or in some cases have potential oxidative toxicities. [304, 530-532]

Calcium peroxide (CP) reacts to produce oxygen in moisture and has been employed for oxygen delivery in agri- and aqua-culture. Recently, it has also been used to supply oxygen to mammalian cells and tissues. [39] CP has a defined amount of oxygen in its formula and a relatively low decomposition rate. Furthermore, all its byproducts can be metabolized by the body. Calcium cross-linked sodium alginate is known to be biodegradable and biocompatible and has been used in numerous biomedical applications including wound dressings. We employed alginate hydrogel to encapsulate CP in hydrophobic biopolymers to control oxygen diffusion and to act as a barrier between the calcium hydroxide decomposition product and cells. This system then used the water in the hydrogel to conduct the oxygen to the wound

surface. [120, 533, 534]. In the biological system, pH is maintained at a stable level by buffering system. Similarly, we used $Ca(HPO_4)_2$ and $NaHCO_3$ to buffer our ODP.

In this work, attempts were made to ascertain if the *in situ* ODP was capable of preserving wounded ischemic tissues and promoting wound healing.

## 2. Material and methods

### 2.1 Preparation of the oxygen delivery patch

The patch was consisted of $CaO_2$, $Fe_3O_4$, PCL, $NaHCO_3$, $Ca(HPO_4)_2$ and an alginate hydrogel. $CaO_2$, $Fe_3O_4$, PCL, $NaHCO_3$ and $Ca(HPO_4)_2$ were first mixed in chloroform, next the mixtures were transferred into a 3.5×3.5 cm foil mold. After that, chloroform was removed by evaporation to get a piece of $CaO_2$-$Fe_3O_4$-PCL plate, which was encapsulated by 6 ml 3% alginate hydrogel cross-linked with 1 M $CaCl_2$ subsequently. Briefly, two pieces of identical raw alginate hydrogel were prepared by spreading 3 mL 3% alginate solution on a piece of filter paper (cut into 50×50 mm) wetted by 1 M $CaCl_2$, respectively, then the plate was placed in between the two pieces of raw alginate hydrogel, finally the alginate solution was cross-linked by 1 M $CaCl_2$ to obtain the oxygen-release patch with a sandwich structure. Control dressing patches were prepared using a similar method without oxygen-release plates. All the patches were sterilized by UV for 20 min before being used.

### 2.2 Chronic wound model

Male New Zealand white rabbits (3-3.5 kg) were used in this study. All procedures were performed in accordance with the animal care and use committee. Each animal was anesthetized by intramuscular injection of 10 mg/kg of xylazine and 1 mg/kg of acepromazine followed by intramuscular injection of 35 mg/kg of ketamine. Isoflurane mask was also used

for anesthesia induction. The ears of the rabbits were shaved and the cutaneous surface was disinfected with a povidone iodine solution. Afterwards, three vertical incisions were made about 1 cm from the base of the ear, close to the 3 main bundles composed of the artery, vein and nerves. The central artery as well as the artery and vein of cranial bundle was ligated to induce ischemia in the ear. Two different kinds of wound models were created. One of them was made following reported procedures with ischemic wounds on the concave side. [531] Briefly, four full thickness round wounds with a diameter of 7.5 mm were created on each rabbit ear after the central artery of the ear had been ligated. The distance between the wounds was 20 mm. Two ears on each rabbit were treated with oxygen-release patch and hydrogel patch only, respectively. 3M™ Tegaderm™ transparent film dressings were used to fix the ODP onto the wounds and keep moisture of the wounds at the same time. A larger ischemic wound model with a larger size (15 mm in diameter) was created on the convex side to further examine the effect of oxygen-release patch on wound healing (Figure 5.1). The ears on each rabbit were treated with the oxygen-release patch and hydrogel patch only, respectively. The patches were fixed in the same way as previously described. The rabbits received 0.05 mg/kg buprenorphine 30 minutes prior to the end of surgery and then a post-operative injection of buprenorphine every 8 to 12 hours was administered (0.02-0.05 mg/kg), for a minimum of 72 hours. The patches were changed every three days.


Figure 5.1. Ischemic wound on a rabbit ear. Four full thickness wounds were created with a diameter of 1.5 cm. The distance between the wounds was 5 mm. At the same time, the central artery and the artery and vein of cranial bundle were ligated to create an ischemic environment.

The healing process was observed and photographed. The wound area on the concave side at different time points was measured using an image analysis software (Image J, NIH). The area of the wounds without granulation tissue on the convex side was inspected using the same software and expressed as the percentage of initial area of the wounds.

For histological examination, the ear tissues were fixed with 4% paraformaldehyde in PBS and then embedded in paraffin. Hematoxylin and eosin (H&E) staining was performed. The stained slides were observed under a microscope (Imager.M2, Zeiss, Germany). A scoring system was adopted from the literature to analyze the histologic results (score 0-3, 3 high, 0 absent). [535]. The presence of inflammation, tissue architecture, collagen deposition, and granulation tissue formation was assessed by a pathologist under blinded conditions. Statistical results were expressed as average ± standard deviation. Two-way Anova test, with the patch type and time

as the main factors, was used to examine variance among the samples and $p<0.05$ was considered to be significantly different.

## 3. Results

### 3.1 Wound healing on the concave side of ischemic rabbit ears

The prepared patches were about 50×50 mm. As they were not adhesive to the wounds, extra materials were required to fix the patches onto wounds. In this experiment, we used the 3M™ Tegaderm™ transparent film dressing. Since the film dressings are made of impermeable plastic they reduced water loss, which was additionally essential for the release of oxygen from the patch.

In the experimental group granulation already started on the 4$^{th}$ day (Figure 5.2 arrow) and the granulation tissue area increased with time. A majority (75%) of the wounds closed after 19 days (Figure 5.2). In the control group without oxygen-release material, however, scarcely any granulation tissues was found on the 4$^{th}$ day (Figure 5.2). After 19 days, only 25% wounds completely closed (Figure 5.2). In addition, infection occurred in one rabbit in control (Figure 5.1S), which suggested but did not prove that the oxygen-release patch may also have antibiotic properties.

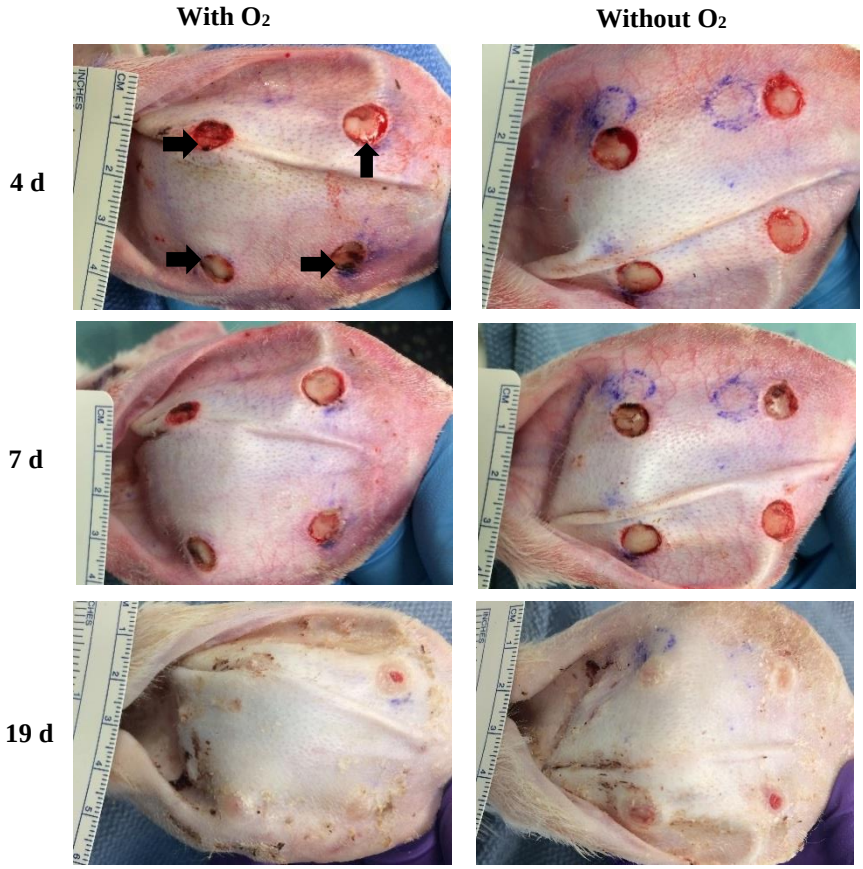


Figure 5.2. Would healing process up to nineteen days. The presence of oxygen-release patch promoted wound healing compared with control, and 50% (n=8) of the wounds healed after 19 d while only 25% (n=8) healed in control group.

The supply of oxygen increased wound healing rates. The wound size reduced faster in the experimental group than the control group at all the time points (Figure 5.3). Furthermore, the wound size in the presence of oxygen-release materials became significantly smaller than control after 11 days. However, after 19 days the wound size in the control group also greatly decreased (Figure 5.3). The results of two-way Anova test showed that oxygen delivery significantly improved wound healing. The healing of the wounds was also significantly improved with time. Nevertheless, there was no patch type and time interactions for the healing of wounds.

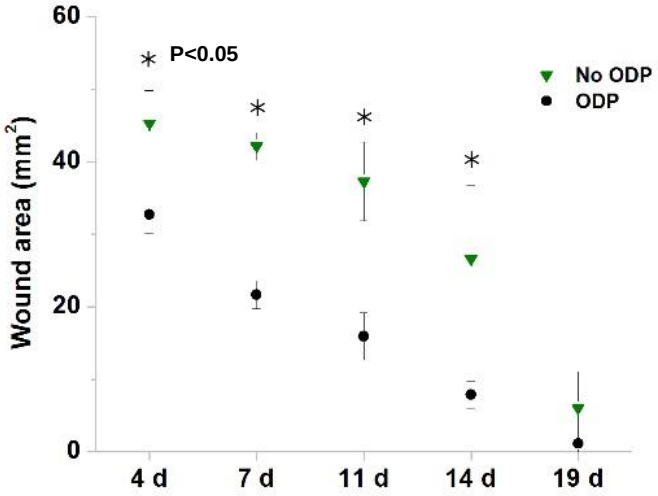


Figure 5.3. Quantified wound area of the samples at different time points. The wound size was smaller in the presence of oxygen delivery materials at all the time points compared with control. The decrease of wound size became significant ($P<0.05$) after 11 d. On the 14$^{th}$ day, the wound area had dropped to 8 mm$^2$ from 44 mm$^2$ while the wound area in the control group was still 25 mm$^2$.

Wounds in the experimental group healed very well. A large amount of aligned collagen was deposited in the wounded area (Figure 5.4 black arrow). New epithelial cells covered the wounds completely. The newly formed tissues were well vascularized as well. In contrast, the control group did not heal completely. The epithelialization was neither complete nor smooth (Figure 5.4 white arrow). Tissue remodeling on the opposite side of the wound was observed in the control group (Figure 5.4 empty arrow) but not in the experimental group, suggesting that the ischemic wound jeopardized the health of adjacent tissues and that oxygen delivery to the wounds protected the neighboring tissues.

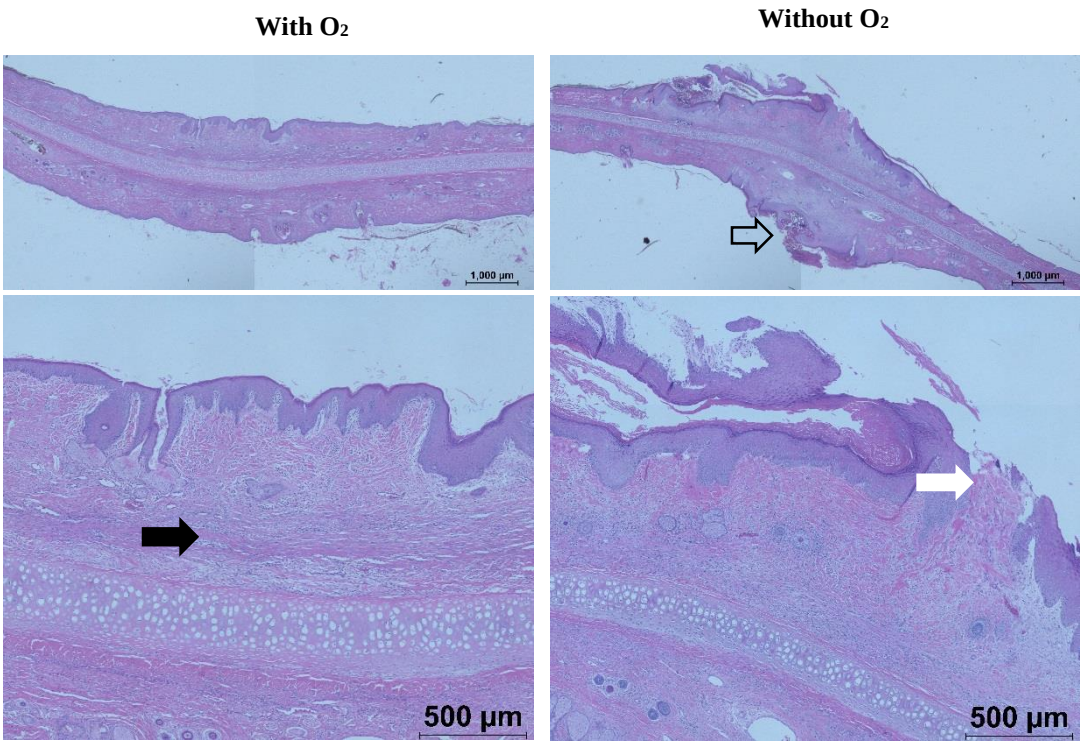


Figure 5.4. H&E staining images of rabbit ear tissue with and without the oxygen-release patch. In the presence of oxygen-release patch, the wounds healed almost completely after 19 d, with only less collagen near the cartilage compared with health tissues. In contrast, the wound did not heal adequately without oxygen-release patch and demonstrated evidence of tissue remodeling on the convex side (empty arrow). The reepithelialization of the wounds was not complete (white arrow) either.

According to histopathological scores, wounds showed mild acute and chronic inflammations in average, indicating that all the wounds were in the process of healing. [536] And there was no significant difference between the two groups in both cases (Table 5.1). The amount of granulation tissue in experimental group was higher than that in control group but having no significant difference (Table 5.1). Oxygen treated wounds displayed lower levels of granulation tissue maturation and collagen deposition than control but still there was no significant

difference (Table 5.1). The experimental group exhibited significant higher levels of reepithelialization and neovascularization compared with the control group (Table 5.1).

Table 5.1. Histopathological scores of the wounds after 19 d

| | Oxygen-release patch (n=8) | Hydrogel patch (n=8) |
|---|---|---|
| Acute inflammation | 0.75±0.46 | 0.75±1.03 |
| Chronic inflammation | 0.12±0.35 | 0.25±0.46 |
| Granulation tissue amount | 2.25±0.89 | 1.88±1.13 |
| Granulation tissue fibroblast maturation | 1.63±0.74 | 2±1.07 |
| Collagen deposition | 1.88±0.83 | 2.13±0.99 |
| Reepithelialization | 2.86±0.38* | 2.25±1.17 |
| Neovascularization | 2.38±0.92* | 1.5±0.92 |

Note: * significant difference ($p<0.05$).

3.2 Would healing on the convex side of ischemic rabbit ears

In the experimental group, tissue necrosis was avoided or greatly reduced (Figure 5.5). Moreover, the wounds were actually healing and 50% (n=8) of the wounds even closed after 17 d (Figure 5.5). In contrast, after 4 days, the wounded tissues changed color from white to dark, a clinical sign of tissue necrosis, with an oxygen-free patch (Figure 5.5). It deteriorated after 7 days and signs of tissue degradation became increasingly evident, as the wounds became more transparent and some of them were breaking through the entire ear (Figure 5.5 arrow). After 11 days, more holes through the ear were observed and all the wounds became holes after 14 days (data not shown).

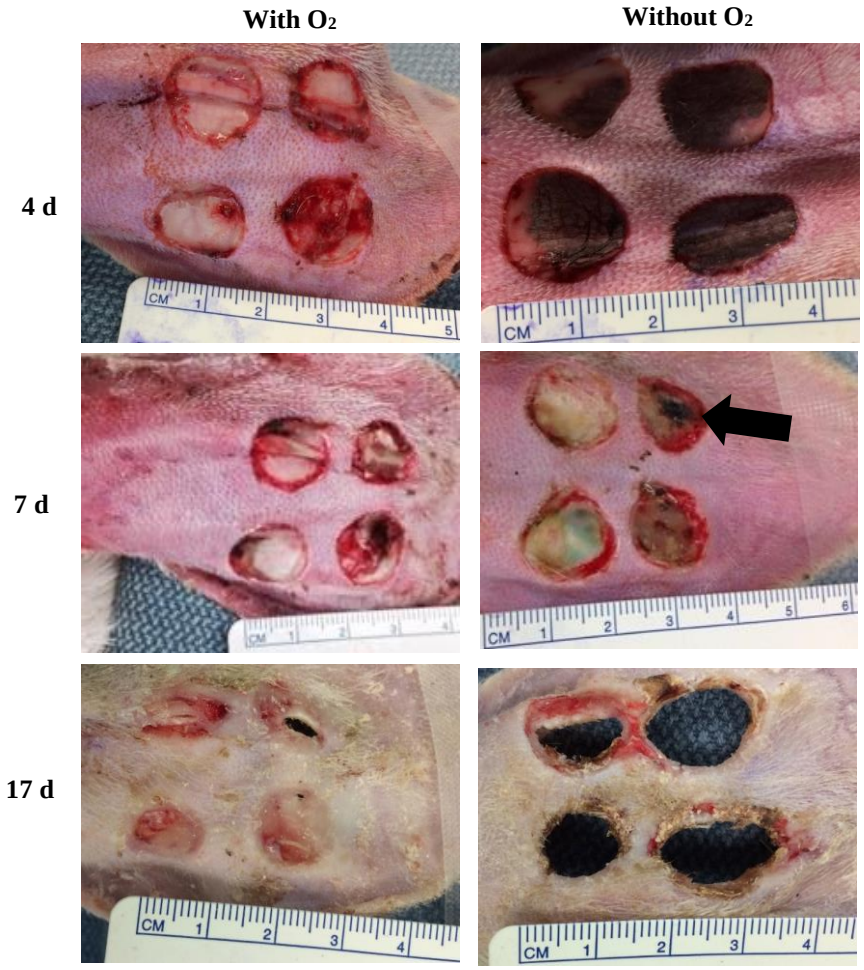


Figure 5.5. Would healing process up to 17 d. In the presence of ODP tissue necrosis in the wounded area was inhibited and most of the ischemic wounds actually healed in the end. In contrast, the tissues in the wounded area experienced serious necrosis and only holes eventually remained in the control group.

The granulation area in the wounds was measured as shown in Figure 5.6. In the experimental group, the wound area covered by granulation tissue increased with time and after 17 d almost all the wounds were covered (Figure 5.6). In the control, however, granulation tissue formation was very little. Moreover, the percentage of granulation tissue area decreased with time until 11 d (Figure 5.6). The wounded area began to reduce after 11d. The results of Anova test

showed that there was significant difference among different groups. The interaction effects of patch type and time also existed.

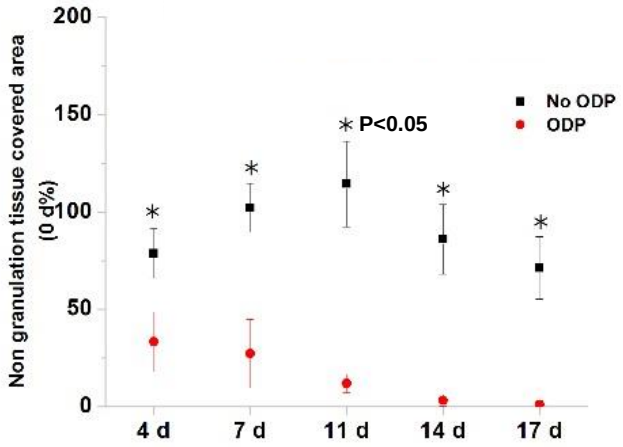


Figure 5.6. Quantification of non granulation tissue coverage ratio of the wounded area with and without oxygen-release materials (n=8). In the presence of oxygen-release materials, the granulation area kept increasing and after 17 d almost the whole wounded area was covered by granulation tissue. In contrast, the majority of the wounded area could not be epithelialized in the control group.

As assessed by H&E staining (Figure 5.7), the oxygen-release patch not only protected wounded tissues from necrosis but also promoted wound healing. The granulation tissue completely filled the space of the excised tissues and the wounds were covered by new epithelial cells (Figure 5.7 dark arrow). Collagen deposition and blood vessels generated by neovascularization were also observed in the newly formed tissues. In the control group, however, tissues necrosis destroyed the wounded tissues through the entire ear. Very little granulation tissue was formed in the wounded area.

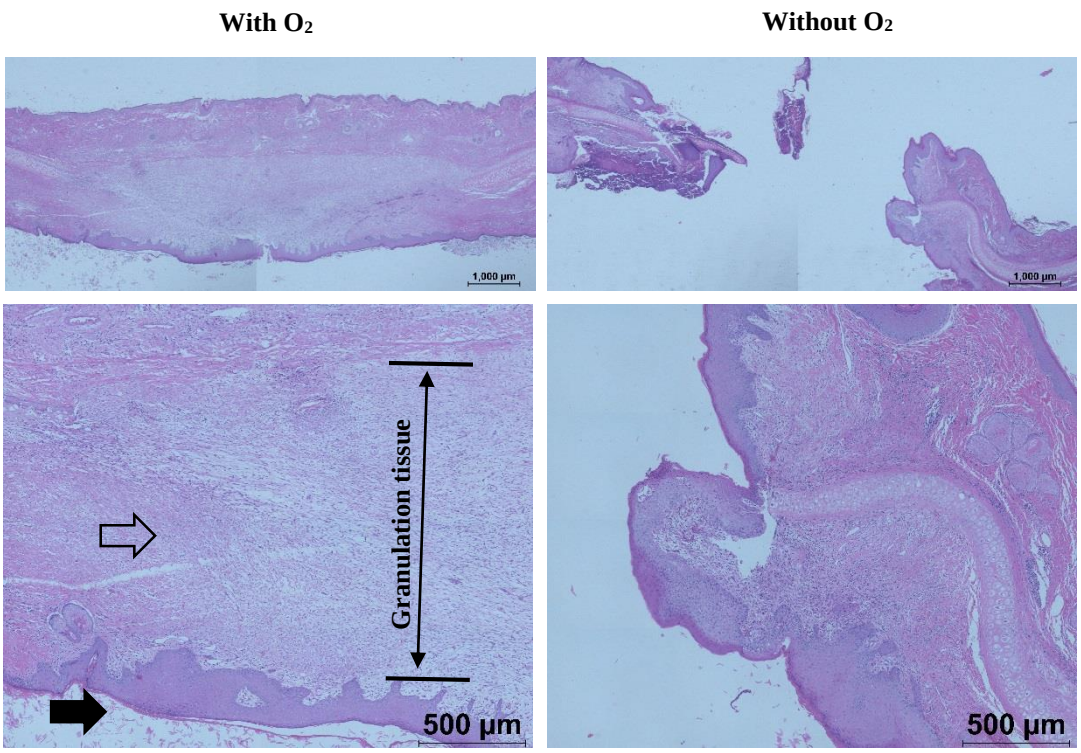


Figure 5.7. Histology of the wounded area after 17 d with and without oxygen-release patches. Granular tissue formation, collagen deposition (empty arrow) and neovascularization were observed in the wounded area in the experimental group. Complete epithelialization (dark arrow) was observed in the oxygen treated wounds.

The histopathological scores of the wounds treated with oxygen-release patches were listed in Table 5.2. After 17 d, wounds treated with oxygen-release patches showed only mild inflammations, suggesting that the wounds were in the process of healing. The amount of granulation tissue formation as well as granulation tissue maturation was moderate. Collage deposition and neovascularization rankings were between the mild and the moderate levels. The level of reepithelialization was above moderate. All these results indicated that the wounds were healing. Control group could not be scored due to the absence of any tissue following necrosis.

Table 5.2. Histopathological scores of the wounds treated with oxygen-release patches (Tissue was lost due to necrosis in the control group)

| | Score (0-3) (n=8) |
|---|---|
| Acute inflammation | 0.75±0.46 |
| Chronic inflammation | 0.875±0.35 |
| Granulation tissue amount | 2±0.75 |
| Granulation tissue fibroblast maturation | 1.88±0.35 |
| Collagen deposition | 1.63±0.74 |
| Reepithelialization | 2.38±0.74 |
| Neovascularization | 1.63±0.52 |

**4. Discussion**

In addition to sustaining aerobic respiration, oxygen is believed to be essential for the healing of wounds, due to its important role in the process of inflammation, anti-infection, collagen deposition and fibroblast proliferation. [14, 537] Since the effective oxygen diffusion distance in tissues is less than 100 μm [14, 538], cells are generally considered not to be able to get enough oxygen from capillaries out of this range. Nevertheless, blood supply is normally interrupted following wounding as blood vessels are impaired. Although it is thought that hypoxia itself induces neovascularization in wounds by inducing the generation of vascular endothelial growth factor (VEGF) through hypoxia-inducible factor-1alpha (HIF-1α) stabilisation, cells require oxygen to form capillaries. [539] Moreover, oxygen enhances VEGF levels in wounds. [540] Collagen deposition in the wounded area is also essential for wound healing because it forms the matrix for neovascularization and wound remodeling. Oxygen plays an essential role in collagen synthesis. It has been found that oxygen delivery improves collagen synthesis *in vivo*. [541, 542] In addition, oxygen promotes epidermal and fibroblast cell growth. [543-545] In this case, oxygen therapy can be a good approach to promote wound healing.

Data supporting the use of locally delivered oxygen has been generated from the literature using *in situ* oxygen generating devices to accelerate wound healing. For example EpiFLO is one such portable oxygen delivery device that has been used for wound healing. [313, 316, 546-548] Similar devices have been reported to improve the healing of chronic wounds, ulcers and ischemic wounds [316, 527, 546-548].

Harrison et al [304] developed an *in situ* oxygen delivery system by incorporating sodium percarbonate into poly(D,L-lactide-co-glycolide) (PLGA) films. They used their system to preserve ischemic skin flaps in a mouse model and found that their oxygen delivery material reduced tissue necrosis and cellular apoptosis for at least 3 d. Nevertheless, no improvement was observed after 7 d, possibly because there was not sufficient oxygen supply to meet the tissue's demand.

According to the literature, the average healing time for 6 mm wounds on the concave side of healthy rabbit ears is about 15 d. For the ischemic wounds with the same size and location, the healing time was reported as being between 17 and 27 d. [549] Said et al. [548] found that the supply of gaseous oxygen improved the deposition of glycosaminoglycan and epithelialization but showed no improvement in collagen deposition. The oxygen treatment resulted in 156% higher epithelial coverage of the wounds compared with the control after 8 d. The oxygen treated wounds healed about 50% after 8 d, and wounds in the control group healed around 20% after 8 d. However, no data for longer time points were presented. In our experiment, wounds healed around 50% (n=8) after 7 d when they were treated with oxygen and half of these wounds (n=8) closed after 19 d. In the absence of oxygen-release materials, however, the wounds only healed 10% after 7 d and 25% (n=8) of the wounds were closed after 19 d with

one ear being infected. Moreover, oxygen delivery significantly improved vascularization in the newly formed tissues (Table 5.1), which was expected to accelerate the wound healing process. Because more newly formed blood vessels could provide more nutrients and oxygen for tissue regeneration in the wounded areas. Data from longer time points in our work indicated that the ischemic rabbit ear had some regenerative abilities (Figure 5.3 and 5.6) indicating the blood system remodelled to compensate the wounds, however, the presence of oxygen-release materials significantly accelerated wound healing after 11 d. A similar healing phenomenon was also observed previously. [531]

According to the histology slides, the oxygen-release patch resulted in higher levels of neovascularization and epithelialization compared with the control group in the standard ischemic wound model. The supply of oxygen to the ischemic wounds also successfully preserved neighboring tissues. The tissue adjacent to the wounds was damaged in the control possibly due to the high demand of oxygen in the wounds, which in turn deprived the oxygen supply to other tissues given the limited available oxygen in the ischemic ear. Our oxygen-release patch showed better results compared with topical oxygen therapy, possibly because of two reasons. One reason may be that our oxygen-release patch delivered dissolved oxygen to the wounds, and the dissolved oxygen had a better ability to penetrate the tissue than gaseous oxygen, which was used in topical oxygen therapies. [120, 533] Therefore, the wounds was better oxygenated by our oxygen-release patch. Another possible reason was that our oxygen-release patch generated hydrogen peroxide, which was able to recruit leukocytes to the wounds and prevent infections. [550, 551] Our experimental results showed that the oxygen-release patches may reduce the infection risks.

The ischemic wound model with a larger wound size was more challenging. Serious tissue necrosis occurred in the control group and holes formed eventually in the ischemic ears. In contrast, the presence of ODP successfully preserved the wounded tissues in most cases, and the wounds were able to heal with oxygen supply.

Based on our experimental results, our oxygen-release patches were able to keep the host tissue alive with inadequate oxygen supply until such time that the blood supply was re-established. Normally, it takes two weeks for the restoration of blood supply to ischemic wounds. [552] Consequently, tissues in the wounded area suffer from hypoxia for at least two weeks, and this long period of oxygen deficiency can cause serious inhibition to wound healing. Our experimental results indicated that oxygen delivery to ischemic wounded tissue was important for the preservation of injured tissue and promoted wound healing.

## 5. Conclusion

We successfully developed an oxygen-release patch for wound dressing. This oxygen-release patch was easy to prepare and was capable of preserving wounded ischemic tissues and promoting ischemic wound healing in ischemic rabbit ears. Our experiment proved that *in situ* oxygen delivery was able to promote wound healing by promoting vascularization and reepithelialization while inhibiting tissue necrosis.

## Acknowledgement

This work is supported by the Natural Sciences and Engineering Research Council of Canada (NSERC) and China Scholarship Council (CSC). The authors also would like to acknowledge BioPloymer for providing us with sodium alginate.

**Supplemental information**

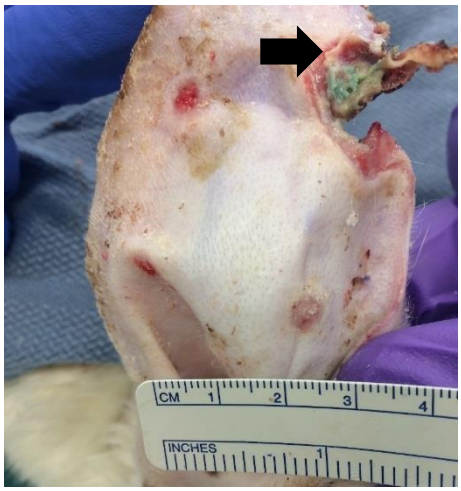


Figure 5.1S. Infected wound on ischemic ear. The up right wound experienced serious infection (arrow). The tissues adjacent the wound became thinner, which may be a sign of tissue degeneration.

## Chapter 6

# Effect of hydrogel volume ratio on *ex vivo* adipose tissue viability in a self-oxygenating scaffold

Huaifa Zhang[1], Simon Tran[1], Jake Barralet[1,2]

1. Faculty of Dentistry, McGill University, Montreal, QC, Canada

2. Division of Orthopaedics, Department of Surgery, Faculty of Medicine, McGill University, Montreal, QC, Canada

## Preface

Adipose tissue resorption post transplantation is an obstacle in reconstructive surgery. The main cause of the adipocyte post-transplantation death is ischemia. The main current approaches to increase adipose reconstruction volume is the used of adipose-derived stem cells and growth factor. These methods only improve the regenerating ability of the transplanted tissue. The oxygen delivery system (ODS) has been found to support cell growth under anoxia, promote vascularization in the scaffold, preserve blood vessels at physiological temperature, and protect ischemic wounds from necrosis. In this chapter, the self-oxygenating scaffold was further used to preserve large volumes of adipose tissue under anoxia. The efficacy of the self-oxygenating scaffold for anoxic adipose tissue culture was investigated.

## Abstract

Resorption of adipose tissue due to the death of adipocytes is a significant issue in reconstructive surgery. Oxygen deficiency in the transplanted adipose tissue caused by

ischemia is one of main reasons for cell death. This work sought to culture adipose tissue with a volume of up to 0.33 mL under anoxia by encapsulating the adipose tissue into a self-oxygenating scaffold (SOS). Furthermore, adipocyte viability in rat adipose tissue after transplantation with oxygen delivery material will be investigated. Experimental results from *in vitro* tissue culture under anoxia showed that oxygen delivery maintained high cell viability in adipose tissue even under anoxia in a scaffold with a diameter of 7 mm and a length of 10 mm. Moreover, adipose tissue was found to be sensitive to oxygen concentrations and only a suitable concentration of oxygen-release microparticles in the scaffold was able to maintain the viability of the cells in adipose tissue. The effect of hydrogel volume percentage in the scaffold on cell viability was further examined and culture of 0.33 mL adipose tissue for 7 d with 15 % v/v scaffold was achieved.

**Key words:** Reconstructive surgery, adipose tissue preservation, oxygen delivery, peroxides

## 1. Introduction

Adipose tissue transplantation in plastic surgery has been increasingly practiced, [553] either for cosmetic or trauma reconstruction purposes. [554, 555] Although adipose tissue transplantation has been conducted for more than a century, tissue resorption after transplantation is still a major issue. [556] Adipocytes die after only one day of tissue transplantation. [16] Different approaches have been developed to alleviate resorption after transplantation. One of the methods is cell transplantation. [557, 558] Adipose-derived stem cells have been found to retain the volume of transplanted adipose tissue by generating new adipocytes. The stem cells have been mixed with adipose tissue and transplanted into patients. However, this method was found to improve tissue retention in breasts but not in faces [559,

560] and further data are required to confirm the positive effects of the stem cells. Another method is to incorporate growth factors into the transplants to reduce tissue loss. [561, 562] For example, basic fibroblast growth factor (bFGF), which induces the differentiation of preadipocyte into the adipocyte, has been added into adipose grafts and has been reported to improve the weight maintenance of transplanted adipose tissue after transplantation [561]. However, specialized carriers are required for the growth factor to exhibit beneficial effects, and the carriers seem to be non-resorbable. [561]

Although long term *in vitro* culture of adipose tissue has been reported, the cultured tissue is usually a monolayer and is very thin. [563, 564] In the clinical setting, however, large volumes of fat tissue transplantation is common. It is believed that the death of adipocytes after transplantation occurs as a result of ischemia. [16] Therefore, oxygen deficiency can be one of the factors that impair cell viability except for lack of nutrients. [565] Oxygen delivery has been used to improve the outcome of tissue engineering and organ preservation, such as islets, skin, and the brain [2, 39, 232], but preserving adipose tissue by oxygen delivery appears to have never been studied. Preservation of large volumes of adipose tissue with biodegradable oxygen-release materials may provide an approach to alleviate cell death in transplanted adipose tissue.

In the work, a biodegradable self-oxygenating scaffold (SOS) consisting of calcium peroxide (CP), iron oxide ($Fe_3O_4$), poly(lactide-co-glycolide) (PLGA) and alginate hydrogel was developed. CP decomposes in the presence of water and generates hydrogen peroxide ($H_2O_2$), which in turn produces oxygen after decomposition. Although CP has a relatively low decomposition rate compared with other peroxides, it still decomposes too fast, causing burst

release and accumulation of cytotoxic $H_2O_2$ and hydroxyl ions. Since cells are extremely sensitive to $H_2O_2$, iron oxide ($Fe_3O_4$) was used to catalyze the decomposition of $H_2O_2$. poly(lactide-co-glycolide) (PLGA) was used to reduce CP decomposition rate by reducing water. Alginate hydrogel was used to further inhibit CP decomposition by reducing the amount of water available to the oxygen generating agent. The hydrogel also served as a barrier to further protect cells from radicals produced during the decomposition of peroxides. Moreover, the hydrogel controlled oxygen diffusion from the microparticles towards cells, which reduced oxidative toxicity from oxygen.

Development of a method to maintain the viability of large volumes of adipose tissue was attempted so that adipocyte viability after transplantation could be improved. An SOS composed of oxygen-release microparticles (CP-$Fe_3O_4$-PLGA) and alginate hydrogel was employed to encapsulate adipose tissue and examined cell viability after anoxic culture.

## 2. Materials and methods

### 2.1 Preparation of self-oxygenating scaffold

Oxygen-release microparticles composed of calcium peroxide (CP), $Fe_3O_4$ and PLGA were prepared using a phase separation method [442] in the absence of $H_2O$. CP powders (Aldrich, USA) and $Fe_3O_4$ (Fisher Scientific, Canada) were first dispersed in PLGA (50/50, Mw 28,000, Advanced Polymer Materials Inc, Canada) solution in chloroform (Fisher Scientific, Canada) with a weight ratio of 1:10:10 (CP:$Fe_3O_4$:PLGA), then the suspension was added into glycerol (Fisher Scientific, Canada) containing 1% w/v polyvinyl alcohol (PVA, Mw 28,000-98,000, Aldrich, USA) and stirred for 10 min at room temperature. After being dried in a fume hood, the CP-$Fe_3O_4$-PLGA microparticles were collected by centrifugation at 4000 rpm, which were

then washed with alcohol three times and dried at room temperature. The SOS was prepared by suspending the oxygen-release microparticles into 1% w/v sodium alginate solution and then crosslinking the mixtures with 0.1 M $CaCl_2$.

2.2 Adipose tissue preparation and culture

Male Wistar rats (35-40 d, 126-150 g) from Charles River Laboratories were used as the adipose donor. All experiments followed Canadian Institutional Animal Care Guidelines and were approved by the Animal Care Committee at McGill University. White adipose tissue was collected immediately after the euthanization of rats and kept in phosphate buffer solution (PBS) on ice. Adipose tissue encapsulation with SOS was performed as shown Figure 6.1. The tissue was then cut into 3×3 mm pieces by a scissor to make it easier to encapsulate the adipose tissue into SOS. Generally, the smaller the adipose tissue blocks, the easier for them to be encapsulated, meanwhile more cells would be damaged since more cells were exposed on the surface of the tissue blocks. For example, to get a 3×3 mm block about 0.5% cells were exposed to the risk of being damaged while cutting when the size of adipocytes was about 50 μm. Afterwards the adipose tissue was mixed with the microparticle-alginate suspension. In the end, the mixtures were transferred into a silicon tube with an inner diameter of 3 mm and a length of 10 mm and cross-linked using 0.1 M $CaCl_2$ for 10 min. Different concentrations of microparticles in the scaffold were used to investigate the effects of oxygen concentration on cell viability. Scaffolds with different volume percentages of alginate hydrogels were studied to maximize the volume percentage of adipose tissue in the scaffold (adipose volume percentage 50%, 75% and 85%). Adipose tissue encapsulated in alginate only was used as the control. The scaffolds were cultured under anoxia (95% $N_2$, 5% $CO_2$, 37 ℃) for up to 7 d in Dulbecco's Modified Eagle Medium (DMEM) supplemented with 10% fetal bovine serum

(FBS) and 1% Penicillin/Streptomycin (P/S). The culture medium was changed every 3 d. Three replicates were performed for each sample.

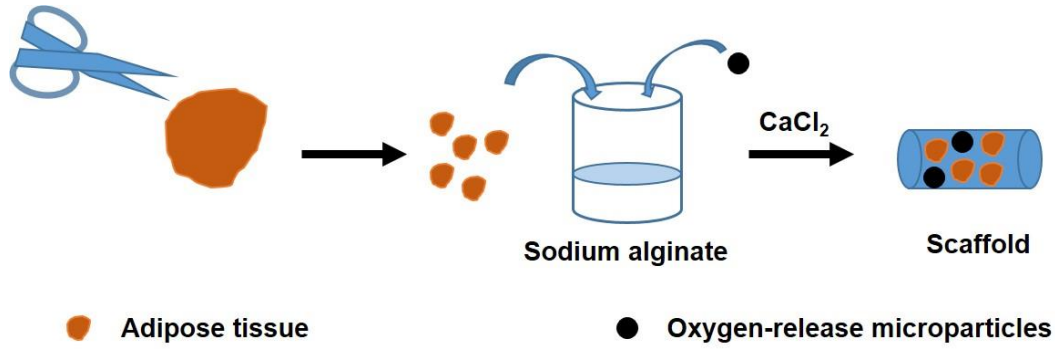


Figure 6.1. Encapsulation of rat adipose tissue into oxygen-generating scaffold.

2.3 Characterization

The morphology as well as the microstructure of the microparticles was examined with a field emission scanning electron microscope (FE-SEM, FEI Inspect F-50, USA). The density of the microparticles was measured by a gas pycnometer (Micromeritics AccuPyc 1330, USA). Moreover, the specific surface area of the microparticles was also examined (Micromeritics TriStar 3000, USA).

N,N-dimethyl-p-phenylenediamine (DMPD, Sigma, USA) was employed to detect free radicals released from peroxides. [491, 492] The microparticles with and without alginate hydrogel were put into 2.5 mg/mL DMPD solution and the released radicals turned the solution red. The potassium iodide (Fisher Scientific, Canada) and starch solution (Fisher Scientific, Canada) was used to detect $H_2O_2$ in the system and the solution became blue in the presence

of $H_2O_2$. The change of pH caused by the oxygen-release material in both water and colorless culture medium was detected by a pH indicator (Riedel-deHaen (pH 4-10), Aldrich, USA)). 7 mg microparticles and 3 mL water or medium were used in all these experiments. The color changes were recorded with a camera (D70S, Nikon, Japan).

The viability of cells in adipose tissue was examined by a live/dead assay and observed under a fluorescent microscope (Imager.M2, Zeiss, Germany). Live cells were stained green by Calcine AM and nuclei of dead cells red by Ethidium homodimer-1. In addition, Hoechst 33258 was used to label all the nuclei. Cell viability was quantified by counting live and dead cells in the images. More than 5 fields were counted each sample. The results were expressed as an average ± standard deviation.

## 3. Results

### 3.1 Characterization of oxygen-release microparticles

The size of the oxygen-release material plays an important role in practice, since a large size restricts the application of the material. The $Fe_3O_4$ particles were cubes smaller than 300 nm. (Figure 6.2a) The prepared microparticles had a size similar to cells (Figure 6.2b and c), making them readily be mixed with cells during application. The application of microparticles are no longer restricted by their size and shape, which are big problems for the previous oxygen delivery systems using metal peroxides. The microparticles appeared to have a porous structure (Figure 6.2d), which increased the penetration of water into the microparticles to react with CP, and thus improves the reaction efficiency of CP. The abundant amount of $Fe_3O_4$ particles on the surface of the microparticles increased efficacy of the catalysts.

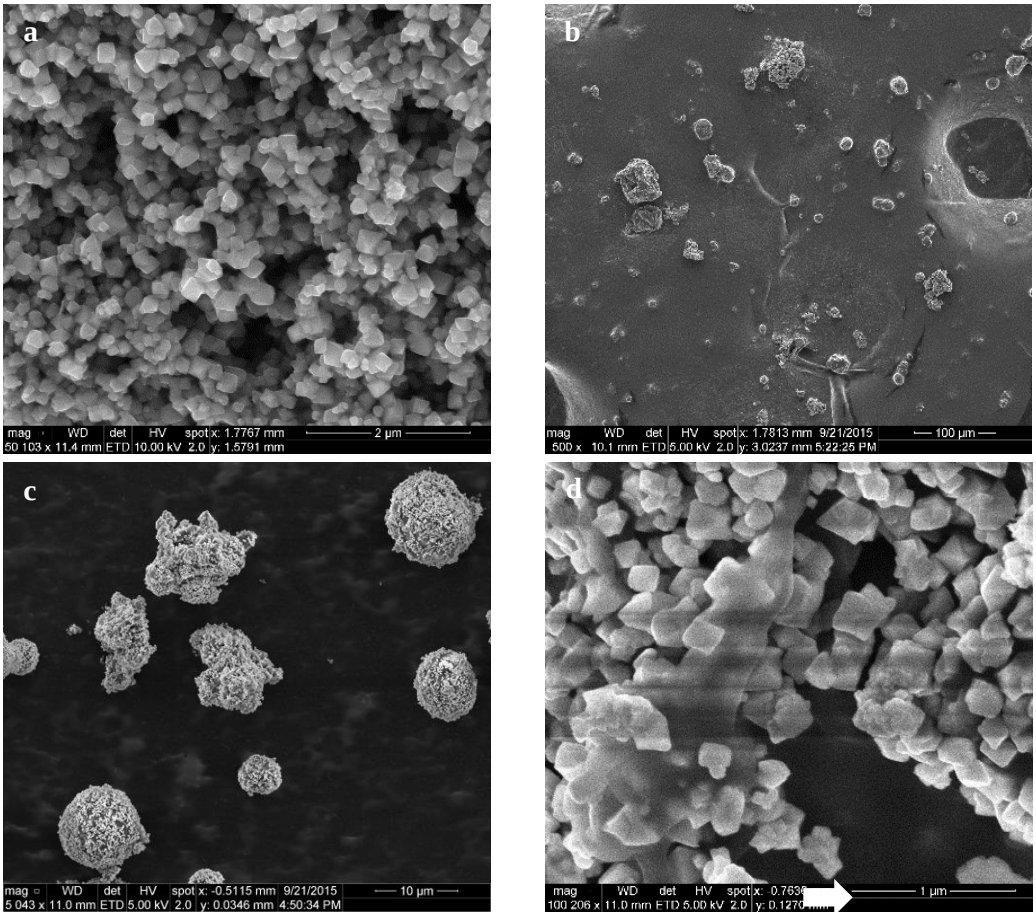


Figure 6.2. SEM image of $Fe_3O_4$ nanoparticles (a) as well as the prepared oxygen-release microparticles (b-d) under different magnifications. $Fe_3O_4$ particles were nano cubes sized between 100-280 nm. The microparticles were covered with a layer of $Fe_3O_4$ nanoparticles (d arrow) and had a diameter of 5-60 µm. Moreover, the microparticles had a porous structure.

In order to investigate the structure of the prepared microparticles, their density was measured. The calculated low close porosity according to the measured density of the microparticles (Table 6.1) suggested that the microparticles were either solid particles or had a connective porous structure. When combined with SEM images, the microparticles were more like to have a connective porous structure.

Table 6.1. Surface area and density of the microparticles

| | CP powders | $Fe_3O_4$ | PCL | Microparticles |
|---|---|---|---|---|
| Density (g/mL) | 2.96±0.08 | 5.90±0.16 | 1.16±0.03 | 1.78±4.12 |
| Closed porosity | | | | 10.00% |

The effect of hydrogel on the decomposition of CP was investigated by detecting color changes caused by $H_2O_2$, radicals, and hydroxyl ions. In Figure 6.3a, only a small area on top of the material became blue in the presence of hydrogel, indicating that a very small amount of $H_2O_2$ was released from the material. In contrast, the microparticles without hydrogel changed the whole solution into dark blue, suggesting that much more $H_2O_2$ was produced in naked microparticles compared with the microparticles in hydrogel. A similar phenomenon was observed for the pH changes in water. Therefore, the presence of alginate hydrogel greatly reduced the amount of generated hydroxyl ions. For the radical staining, when the microparticles were encapsulated in hydrogel only the hydrogel was stained red (Figure 6.3b), indicating that radicals were trapped by the hydrogel. The microparticles without hydrogel, however, generated a thick band of red color above the particles. The fact that the microparticles either with or without hydrogel did not cause obvious color changes in culture medium suggests that the hydroxyl ions generated by the materials can readily be neutralized by the buffering system in culture medium.

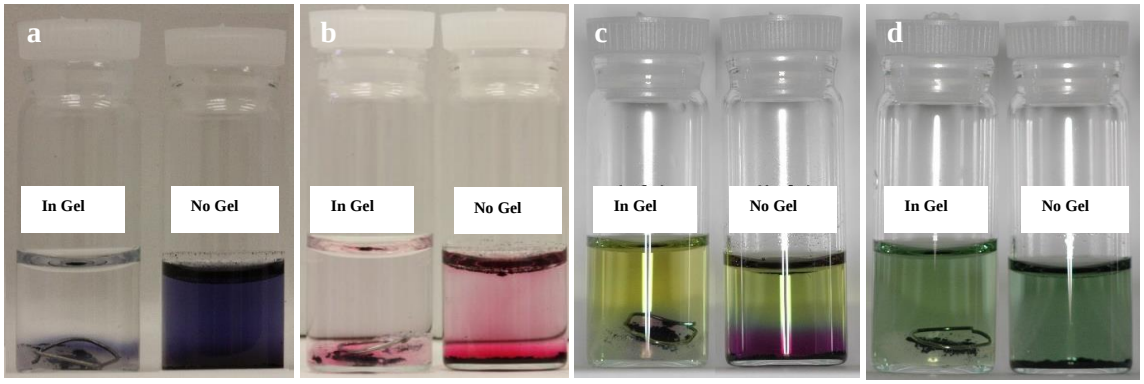


Figure 6.3. Release of $H_2O_2$ (a) and radicals (b) from the materials as well as pH changes in water (c) and culture medium (d) after 30 min. The presence of alginate hydrogel greatly mitigated color changes in a, b and c, suggesting there were less $H_2O_2$, radicals and hydroxyl ions release when the microparticles were encapsulated in the hydrogel. In contrast, significant color changes around the microparticles were observed without hydrogel in all cases except for pH changes in culture medium. Very little color change was noticed in culture medium, suggesting that there was not much pH change caused by the oxygen-release material in culture medium.

3.2 Cell viability in preserved adipose tissue

Physiologically, adipose tissue is very well vascularized. Therefore, it is logical to expect good oxygenation of adipose tissue *in vivo*. However, too much oxygen could cause oxidative toxicity and kill cells, as shown in Figure 6.4b. The high oxygen concentration killed all types of cells after 7 d (Figure 6.4d), although death mainly occurred in adipocytes after 3 d (Figure 6.1S). Cells death may also be caused by hypoxia in the scaffold as shown in Figure 6.4d. Adipocytes are the most oxygen-sensitive cells in adipose tissue and account for the most of the dead cells in anoxic (Figure 6.4c) and normoxic culture. Adipose-derived stromal cells were resistant to hypoxia [566], and thus survived in anoxic and normoxia culture in this experiment.

Nevertheless, it seems that those cells were not resistant to hyperoxia. With a suitable concentration of microparticles in the scaffold, cells in the adipose tissue maintained high viability (Figure 6.4a).

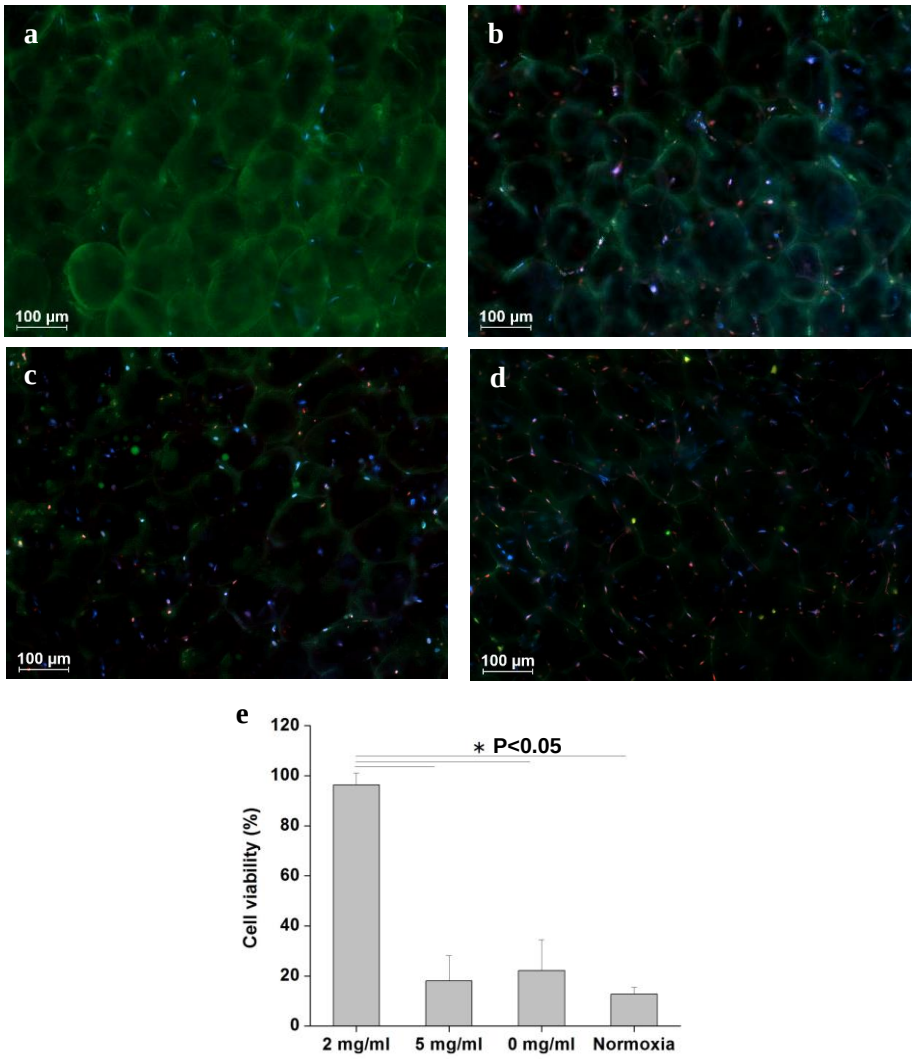


Figure 6.4. Fluorescent images of live/dead assay stained adipose tissue under various oxygen concentrations after 7 d. Adipose tissue preserved under anoxia with 2 mg/mL microparticles in 50% v/v hydrogel displayed very good viability (a), but tissue preserved under other conditions, such as 5 mg/mL (b) and 0 mg/mL (c) microparticles in 50% v/v hydrogel under anoxia and 50% v/v hydrogel under normoxia (d) showed poor viability. These results indicated that adipose tissue was sensitive to oxygen, and that both high and low oxygen concentrations could kill cells. Most of the red nuclei located on the edge of adipocytes, indicating that most of the dead cells were adipocytes. Quantified results (e) indicated that tissue preserved at the optimal condition had a significantly higher viability than the other samples.

The volume ratio of hydrogel in the scaffold also affected cell viability in the adipose tissue. When compared with the results in Figure 6.5, the decreased volume ratio of hydrogel in the scaffold impaired cell viability in tissue. The cell viability decreased by 50% when the percentage of hydrogel volume dropped from 50% v/v to 25% v/v (Figure 6.5a) and continued to decrease as the volume of hydrogel was further reduced (Figure 6.5b and c).

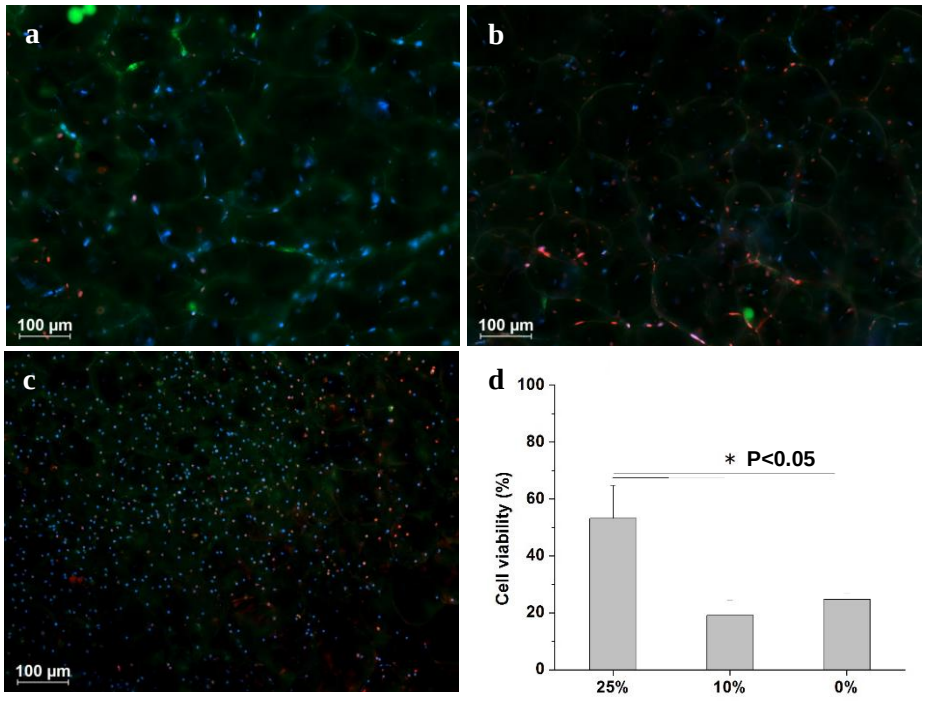


Figure 6.5. Fluorescent images of the live/dead assay stained tissue cultured with 25% v/v (a), 10% v/v (b), and 0% v/v hydrogel (c) containing 2 mg/mL microparticles after 3 d. The viability was also quantified (d).

The volume ratio of hydrogel in the scaffold influenced the distance among the encapsulated adipose tissue blocks as shown in Figure 6.6. The relationship between the distance among the adipose tissue blocks and the volume ratio of hydrogel in the scaffold was expressed in Equation 1. As the volume ratio of hydrogel decreased, the distance among the adipose tissue

blocks also reduced, leading to decreased distance between the oxygen-release microparticles and the adipose tissue. Since hydrogel acted as a barrier of cytotoxic radicals released from the microparticles, the protective effect of hydrogel on adipose tissue would reduce when the layer of hydrogel between the source of radicals and the tissue became thinner. Consequently, cell viability in stored adipose tissue reduced as the volume ratio of hydrogel in the scaffold decreased.

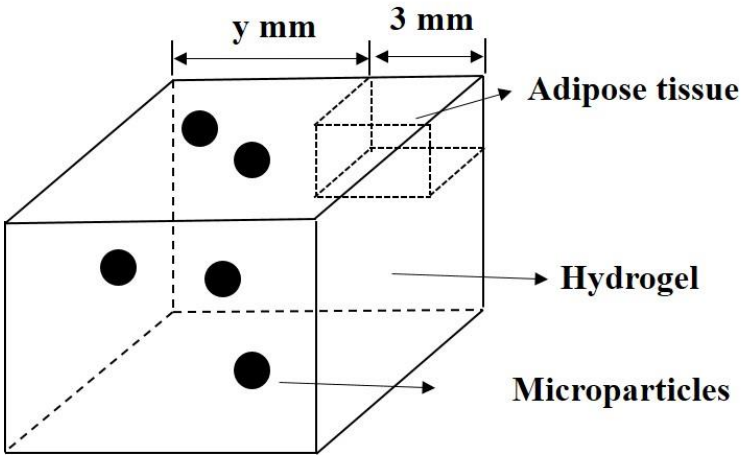


Figure 6.6. The effect of volume ratio of hydrogel in the scaffold on the distance among adipose tissue blocks.

$$y = 3 \times \left(1 - V_{Gel}\right)^{-1/3} - 3 \qquad (1)$$

Where y (mm) was the distance among the adipose tissue blocks, and $V_{Gel}$ was the volume ratio of hydrogel in the scaffold. The adipose tissues blocks were taken as 3×3×3 mm cubes and supposed to be dispersed evenly in the scaffold.

## 4. Discussion

Oxygen-release microparticles were prepared with a size of 5 to 60 μm, which was close to the size of cells. The small size made it possible to apply the particles in broader circumstances

with more flexible ways, unlike reported work in which oxygen-release materials were either in the form of big slabs or hard porous scaffolds. [2, 39] The presence of alginate hydrogel greatly reduced the decomposition rate of CP in water. Subsequently, the release rate of $H_2O_2$ and hydroxyl ions from the oxygen-release material in hydrogel was significantly reduced (Figure 6.3a and c). The radical staining results (Figure 6.3b) suggested that the alginate hydrogel trapped the cytotoxic radical ions, and thus cells could be protected from the radicals by the alginate hydrogel. Moreover, the hydroxyl ions produced by CP did not change the pH of culture medium, therefore, the toxicity of hydroxyl ions could be removed by culture medium.

Adipose tissue is very sensitive to hypoxic environments. Hypoxia induces chronic inflammation in adipose tissue in obesity and causes adipose tissue dysfunction and insulin resistance. [567] Cells in adipose tissue, such as adipocytes, vascular endothelial cells, and blood derived cells, cannot survive under 3% oxygen. [565] Nevertheless, adipose-derived stromal cells can survive under 1.3% oxygen and are activated to repair the tissue by the low oxygen concentration. [565] Adipocytes in transplanted adipose tissue start to die on the first day, with only some adipocytes on the surface area up to 300 μm in depth surviving. [16] Furthermore, adipose tissue regeneration occurs in the zone where adipose-derived stromal cells are alive. Therefore, the transplanted adipose tissue is able to repair itself through the regenerative abilities of the stromal cells. In the core of the tissue, however, all kinds of cell lose viability and tissue necrosis occurs. [16]

In this work *in vitro* culture results showed that adipose tissue was able to maintain high cell viability for up to 7 d under anoxia in the presence of oxygen-release microparticles. Moreover,

the amount of oxygen-release materials had great effects on cell viability. Cells in adipose tissue failed to survive under anoxia. Although much work has been done concerning the adverse effects of hypoxia on adipose tissue, the influence of hyperoxia on adipose tissue has rarely been studied. In this work high concentrations of oxygen-release materials were found to jeopardized cell viability, suggesting that cells in adipose tissue were sensitive to over oxygenation. The experimental results from normoxia showed very poor cell viability in adipose tissue (Figure 6.4d). A possible reason was that hypoxia occurred in the scaffold because of the limited diffusion efficacy of oxygen through hydrogel.

In summary, the oxygen delivery material was able to preserve adipose tissue under anoxia for up to 7 d. A variety of factors, including the concentration of oxygen-release material in the scaffold, the volume ratio of hydrogel in the scaffold, and the addition of albumin, were shown to affect cell viability in preserved adipose tissue.

## 5. Further work

Cell viability under anoxia will be further examined by a Lactate Dehydrogenase (LDH) assay (Abcam, Canada) with a plate reader (Spectramax M2E Microplate reader, Molecular Devices, USA) following the provided instruction. Each sample will be read three times by the plate reader and the average value will be used. Cell apoptosis in the preserved adipose tissue will be examined using a caspase 3/7 assay kit (CellEvent®, molecular probes, USA). The *in vitro* cultured adipose tissue will also be fixed in 4% paraformaldehyde in PBS overnight and be embedded in paraffin. Hematoxylin and eosin (H&E) staining and perilipin staining will be carried out to examine the tissue structure and live cells in the tissue.

*In vivo* evaluation of the effect of *in situ* oxygen supply on adipocytes viability and fat tissue resorption will be performed by subcutaneous implantation. Male Wistar rats (35-40 d, 126-150 g) from Charles River will be used. Before the surgery, the rats will be anesthetized with isoflurane. Two places on the dorsal surface will be shaved along the spine. A 4 cm skin incision will be made and one pocket created on each side of the incision to yield a total of 2 pockets, where scaffolds containing adipose tissue with (right side) and without (left side) oxygen-release microparticles will be implanted. The scaffolds will be weighed before surgery. Implants will be retrieved after 2 and 4 weeks. The retrieved scaffolds will also be weighed to measure weight changes of the implants. The volume changes of the transplants both before and after transplantation will be assessed by immersing the transplants in saline solution. [568] Cell apoptosis in the transplants will be detected with a caspase 3/7 assay kit. Then the implants will be fixed and embedded as previously described. H&E staining and perilipin staining will be used to examine tissue structure and live cells, repectively. Immunohistochemistry staining will be used to label blood vessels, hypoxia-inducible factor 1-alpha (HIF-1α) and secreted vascular endothelial growth factor (VEGF) in the scaffold.

**Acknowledgement**

This work is supported by the Natural Sciences and Engineering Research Council of Canada (NSERC) and China Scholarship Council (CSC). The authors also would like to acknowledge BioPloymer and Advanced Polymer Materials Inc. for providing us with sodium alginate and PLGA, respectively.

**Supplemental information**

Table 6.1S. Specific area of the prepared microparticles

| | CP powders | Microparticles |
|---|---|---|
| Surface area ($m^2/g$) | 10.76±1.36 | 2.92±0.58 |

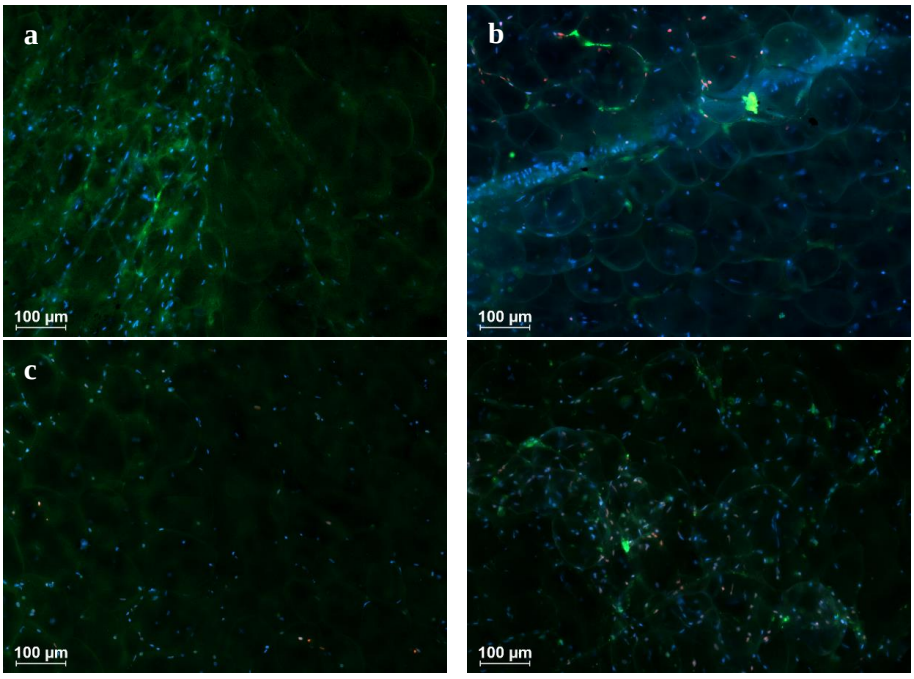


Figure 6.1S. Fluorescent images of the live/dead assay stained adipose tissues cultured under anoxia supplied with various $O_2$ concentrations after 3 d. Adipose tissues preserved under anoxia with 2 mg/mL microparticles in 50% v/v hydrogel displayed very good viability (a), but tissues preserved under other conditions, such as 5 mg/mL (b) and 0 mg/mL (c) microparticles in 50% v/v hydrogel under anoxia and 50% v/v hydrogel under normoxia (d) showed poor viability. Most of the nuclei stained red located on the edge of adipocytes, indicating that most of the dead cells were adipocytes.

# Chapter 7

## Ongoing work

### Preface

The previous chapters showed that the developed oxygen delivery material had excellent biocompatibility and was capable of supporting cell growth under anoxia, of promoting vascularization in implants, of preserving blood vessels and adipose tissue under anoxia, of preserving ischemic tissue, and of accelerating ischemic wound healing. Since hypoxia and even anoxia are common issues during tissue engineering, tissue and organ preservation, and cell transplantation, there are many other applications for our oxygen delivery materials. In this chapter, the oxygen delivery material was applied to other areas. Preliminary experiments on the preservation of mouse islets, mouse heart slices, mouse brain slices, and mouse livers at physiological temperature using the self-oxygenating scaffold was performed, an initial investigation about the effects of oxygen delivery on vascularization in scaffold *in vivo* investigated, and incorporation of the oxygen-release material into a three-dimensional printed scaffold explored.

### 1. Introduction

Vascularization is crucial for the functionality and long-term survival of cells. Many efforts have been devoted to improving vascularization in transplants, including prevascularization the scaffolds with endothelial cells and fibroblasts [569, 570], introduction of stem cells [571, 572], and addition of angiogenesis growth factors [573]. Although encouraging results have been obtained, these methods still require more than one week to form new blood vessel networks. The problem is that the transplanted cells may already die during that week. It is well known that hypoxia induces angiogenesis through hypoxia-inducible growth factor-1alfa (HIF-1α),

which augments the secretion of vascular endothelial growth factor (VEGF) from cells and promotes blood vessel formation. However, long-term hypoxia inhibits vascularization, possibly because under hypoxia cells cannot produce adequate raw material to build blood vessels, such as cells, collagen and elastin. Therefore, oxygen delivery may promote vascularization by supporting the activities of blood vessel related cells.

Tissue and organ preservation has long been investigated due to the growing demand for tissue and organ transplantation and drug screening. So far, various approaches have been developed to preserve organs and tissues. Most approaches used low temperature to reduce oxygen consumption in preserved tissues and organs and to alleviate hypoxia. However, hypoxia still occurs during preservation and reperfusion injuries take place due to the low temperature and hypoxia during preservation. Perfusion of tissues and organs at temperatures close to the physiological temperature has been used for heart and kidney preservation, but perfusion causes damage to blood vessels in the organs. The ability of the oxygen delivery material to preserve tissues and organs at physiological temperature under severe oxygen deficiency was tested. Moreover, transplanted tissues and organs suffer from ischemia due to limited blood supply, which causes delayed functionality from the transplants and even loss of cells. If the oxygen delivery material can support cell survival in tissues and organs, the material can be implanted together with tissues and organs to retain the viability of the tissues and organs before blood vessels reconnect with the host vasculature.

Hypoxia is also common in tissue engineering and has become a major obstacle for constructing tissues large enough for clinical practice. Oxygen solubility in water and culture medium is extremely low and the effective diffusion distance of oxygen from culture medium into scaffolds is limited, so cells in the core of engineered tissues cannot get enough oxygen.

We attempted to construct a 3D scaffold that releases oxygen *in situ* so that hypoxia in large scaffolds can be eliminated.

**2. Tissue and organ preservation**

Hypoxia is one of the major issues in tissue and organ preservation. Hypoxia in organs and tissues results in ATP depletion in cells. The depletion of ATP generates hypoxanthine, which is converted into xanthine in the hypoxic environment. When the cells are brought back to normal oxygen tensions, xanthine reacts with oxygen and generates reactive oxygen species (ROS). [470] Burst generation of ROS occurs during reperfusion due to the accumulation of xanthine under hypoxia [496, 497]. Since ROS can kill cells, rewarming injury is a major issue in tissue and organ preservation. Various methods have been used to alleviate the damage caused by rewarming, such as adding antioxidants into the preservation solution and oxygenating tissues and organs during preservation by perfusion or persufflation. Oxygen delivery agents like perfluorocarbons and peroxides have been used to improve the results of tissue and organ preservation. However, those methods either require expensive additives, damage blood vessels in the tissues and organs, have limited valid time, or are currently at a very early stage of development. In this work, oxygen-release microparticles were prepared, which could be incorporated into hydrogel scaffolds with flexible shapes, and used to deliver oxygen to various tissues and organs, including mouse islets, mouse heart slices, mouse brain slices, mouse livers, and rat marrow tissue.

All the tissues and organ slices tested were encapsulated into the oxygen-release alginate hydrogel scaffold by cross-linking with $Ca^{2+}$ and cultured under anoxia. For mouse liver preservation, an alginate solution containing oxygen-release microparticles was injected into the organ and then the liver was encapsulated with the oxygen-release alginate hydrogel

scaffold through cross-linking. Samples cultured under anoxia without the oxygen-release scaffold were used as a control.

## 2.1 Mouse islet preservation

The purity of isolated mouse islets was examined with dithizone staining, which stained the Zn element in islets. [574] Figure 7.1 shows the dithizone staining of the isolated islets. The staining confirmed that the isolated islets had a high purity and most of the clusters were stained red by dithizone.

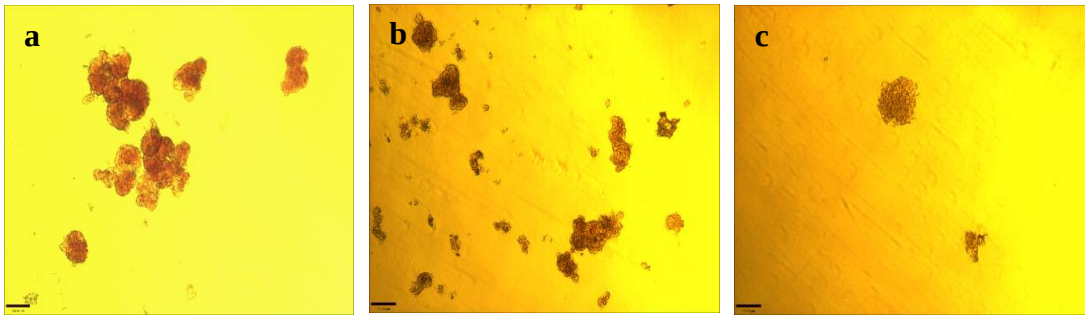


Figure 7.1. Images of dithizone stained islets at 0 d (a) and islets cultured under anoxia with (b) and without (c) oxygen-release material after 2 d. Dithizone binds zinc ions in the islet and stains the islet red. Almost all the clusters were stained by dithizone, suggesting the isolated islets had a high purity. Scale bar is 200 µm.

The integrity of the islets is an easy way to identify the viability of islets, as dead islets lose their integrity. The morphology of the islets cultured under different conditions (Figure 7.2) suggested that the presence of oxygen-release material maintained the integrity of the islets under anoxia while the islets cultured without the oxygen-release material lost their integrity under the same conditions. The loss of integrity indicates the islets were undergoing necrosis.

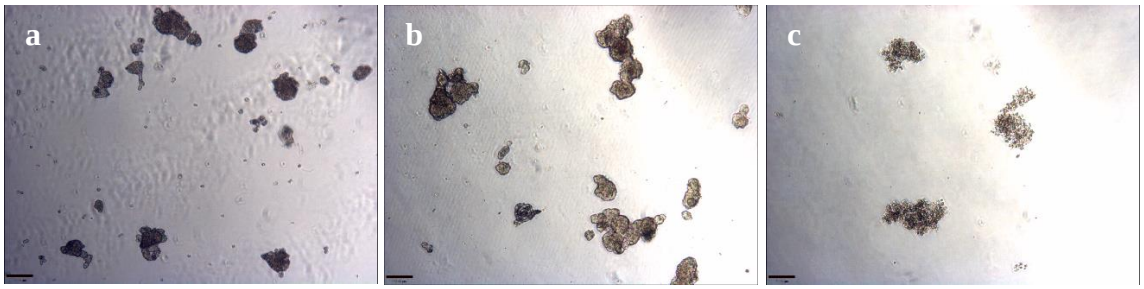


Figure 7.2. Morphology of islets at 0 d (a) and islets cultured under anoxia with (b) and without (c) oxygen-release material after 2 d. Islets preserved under anoxia with oxygen-release material maintained their integrity, while those without oxygen-release material lost their integrity. Scale bar is 200 μm.

Cell viability in the islet was assessed using the live/dead assay. The live/dead assay staining results (Figure 7.3) indicated that the addition of oxygen-release material improved cell viability in islets under anoxia compared with control samples. All the cells died under anoxia (Figure 7.3c) whereas the presence of oxygen-release material maintained high cell viability (Figure 7.3b).

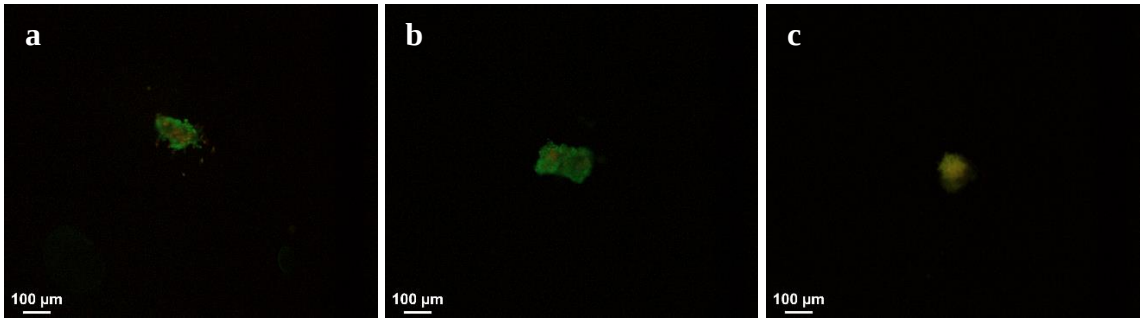


Figure 7.3. Fluorescence images of live/dead assay stained islets at 0 d (a) and islets cultured under anoxia with (b) and without (c) oxygen-release material after 2 d. The majority of cells in islets cultured with oxygen-release material were stained green, suggesting they maintained their viability under anoxia. However, without oxygen-release material almost all the cells were stained red. The cluster displayed a yellow color due to the overlap of stained red color and green background.

In addition, cell viability in the stored islets was assessed using Alamar Blue staining. The Alamar Blue staining results (Figure 7.4) showed that the presence of oxygen-release material increased cell viability in the islets from 20% without oxygen-release material under anoxia to 60% with oxygen-release material under anoxia.

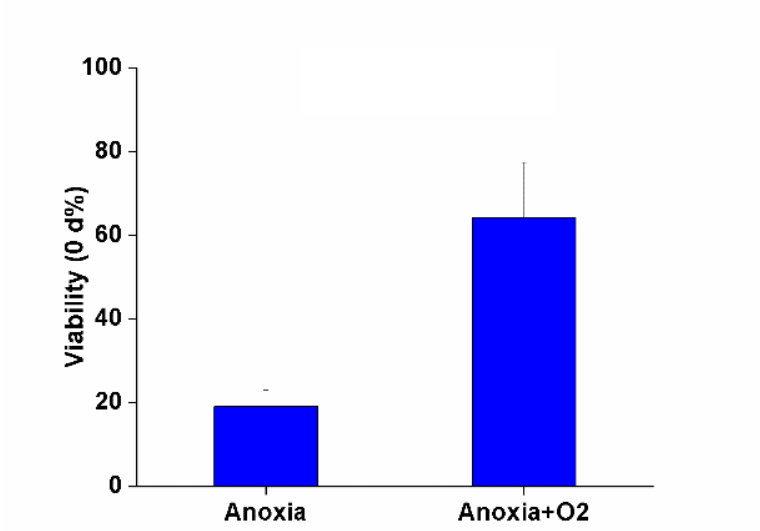


Figure 7.4. Alamer Blue assay results of islet viability preserved under different conditions for 2 d. The presence of oxygen-release material resulted in significantly higher cell viability in islets compared with control.

2.2 Mouse heart slice preservation

The mouse heart was manually cut into slices and the slices encapsulated in the oxygen-release scaffold. The heart slices were obtained by cutting across the heart and were about 1-2 mm in thickness. The slices were then encapsulated with the oxygen-release hydrogel scaffold.

Cell viability in the mouse heart slice was examined by the live/dead assay staining. According to Figure 7.5, the oxygen-release scaffold successfully maintained high cell viability in the mouse heart slice under anoxia (Figure 7.5b) while the heart slices in control groups lost most of their cell viability (Figure 7.5c), suggesting that oxygen delivery may be used to preserve heart or muscle tissue. The experimental results also suggested that the oxygen-release material was not toxic to heart cells. Heart ischemic disease is one of the main causes for heart failure, which leads to morbidity and mortality. [575] Autologous bone marrow cells have been

injected into the ischemic area of heart to promote vascularization, but this method requires tedious cell isolation and characterization procedures. Moreover, the isolated cells need to be injected as soon as possible. [576] Therefore, it will be much more convenient if the oxygen-release microparticles could be used to treat heart ischemic disease.

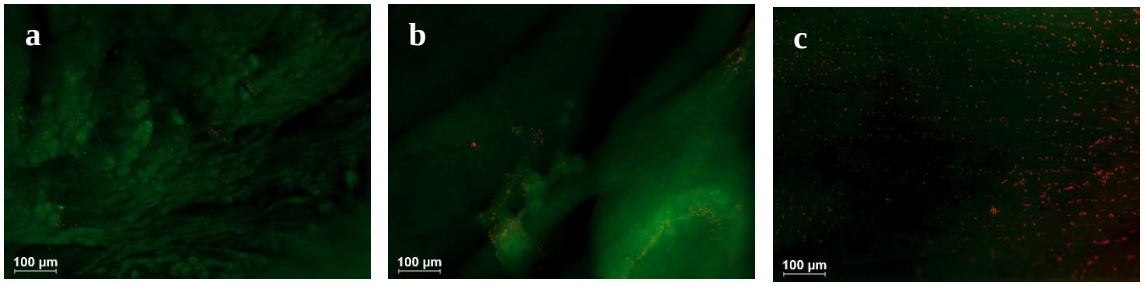


Figure 7.5. Fluorescent images of mouse heart tissue stained by live/dead assay, including fresh heart tissue (a), tissue preserved in the self-oxygenating scaffold under anoxia (b) and tissue cultured under anoxia (c) for 3 h. The heart slices were encapsulated with 0.6 mL self-oxygenating scaffold containing 5 mg/mL microparticles.

Electrical stimulation was tried to evaluate the functionality of the stored heart tissue but failed to stimulate the tissue. Possibly because the machine used for stimulation could not generate suitable electrical signals, including the shape, frequency, current and voltage of the signals. [577-580] Square wave pulses (30 μA; 2 ms) at a frequency between 1 and 40 Hz have been used to stimulate the mouse heart. [578] For the rat heart tissue, electrical signals with a 100-ms-long square wave pulse of amplitude 100 V and at frequencies of 1 and 2 Hz are used [577]. Evaluation of functionality of the heart through perfusion was also attempted. Fresh heart re-beating was achieved, however, the stored heart could not re-beat under the same conditions although cell viability in the stored heart remained high (Figure 7.1S).

2.3 Mouse brain slice preservation

The mouse brain was cut into slices and the slices encapsulated in the oxygen-release scaffold. The brain slices were obtained by manually cutting with a blade across the brain into slices about 2 mm in thickness. The slices were encapsulated with oxygen-release hydrogel scaffold by cross-linking.

Brain tissue contains a large number of neurons, which are very sensitive to hypoxia. So far only very thin brain tissue slices with a thickness of several micrometers have been preserved by perfusion. [581] In this work, as shown in Figure 7.6, the oxygen-release scaffold successfully maintained high cell viability in thick mouse brain slices under anoxia for up to 24 h (Figure 7.6b, c), while the brain slices in the control group lost most of their cell viability after 3 h (Figure 7.6d), suggesting that oxygen delivery could be used to preserve brain slices under the severely oxygen deficient environment. Brain tissue is sensitive to free radicals and iron, which can cause damage to brain tissue by inducing oxidative stresses. [582-584] The experimental results in this work indicated that the potential cytotoxicity of free radicals release from the peroxides, i.e. CP and $H_2O_2$, was successfully removed and that $Fe_3O_4$ catalyst in the oxygen-release material did not cause toxicity to brain tissue.

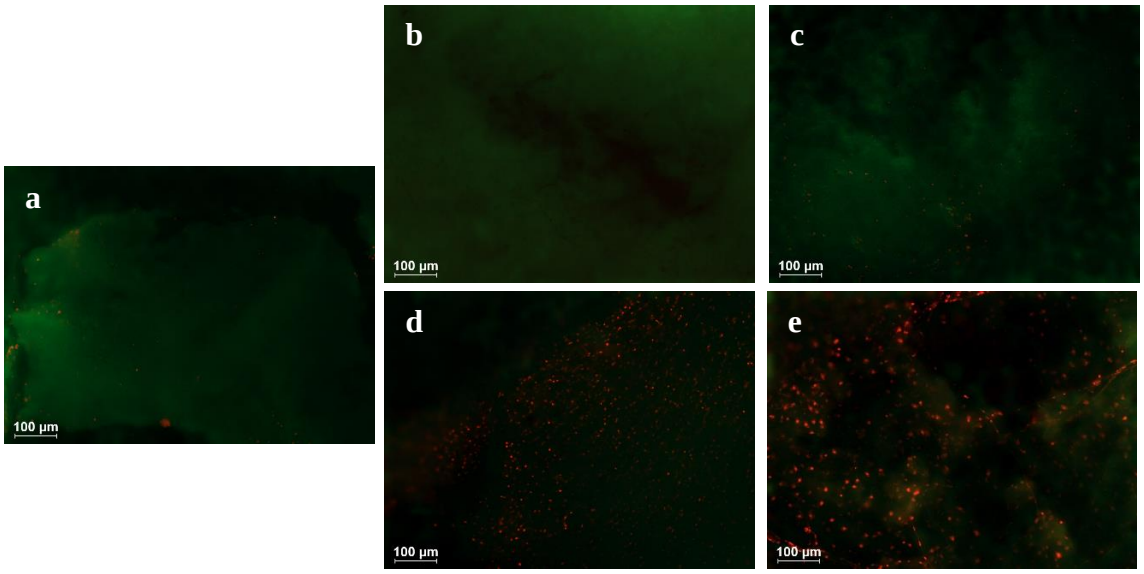


Figure 7.6. Fluorescent images of mouse brain tissue stained by the live/dead assay: fresh brain tissue (a), brain tissue preserved in self-oxygenating scaffold under anoxia for 3 h (b) and 24 h (c), and brain tissue preserved under anoxia for 3 h (d) and 24 h (e). In the presence of oxygen delivery material, very few dead cells were found after 3 h under anoxia and cell viability was about 90% after 24 h. In contrast, almost all the brain cells died after 3 h under anoxia without oxygen-release material.

2.4 Mouse liver preservation

Livers play an important role in detoxification, digestion, and blood circulation. In addition, livers are able to regenerate by themselves. Since liver transplantation has become an import way to treat liver related diseases, growing new liver tissue *in vitro* can be very attractive. In this preliminary experiment, oxygen-release scaffolds, being both inside and outside of the liver, successfully maintained high cell viability in mouse livers under anoxia for up to 24 h (Figure 7.7b) while the livers in the control group already lost most of their cell viability (Figure 7.7c), suggesting that oxygen delivery could be used to preserve livers under the severely oxygen deficient environment. Moreover, the oxygen-release material was not toxic to liver

cells according to the experimental results. It may be possible to regenerate livers *in vitro* with the oxygen delivery material.

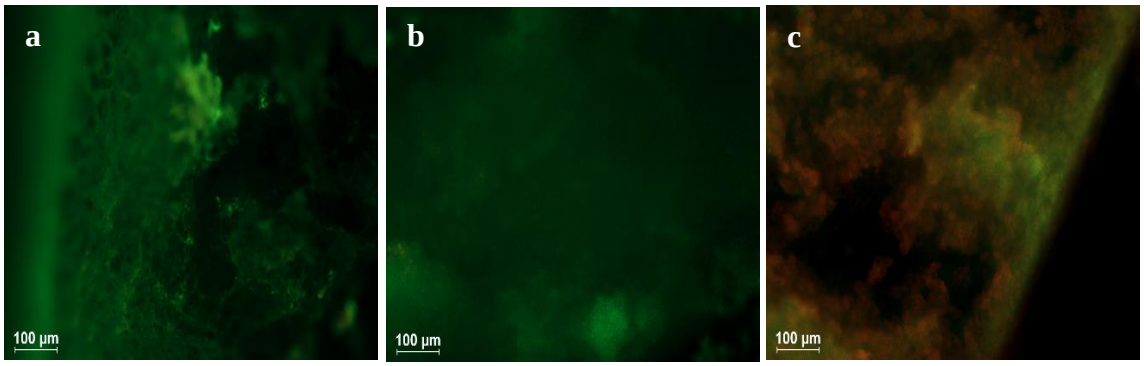


Figure 7.7. Fluorescent images of mouse liver tissue stained by the live/dead assay: fresh liver tissue (a), liver tissue preserved in self-oxygenating scaffold under anoxia (b) and liver tissue cultured under anoxia (c) for 1 d. Microparticles were suspended in a 1% w/v alginate solution at a concentration of 10 mg/mL and then injected into liver through a needle. The whole liver was further encapsulated with 0.6 mL self-oxygenating hydrogel by crosslinking.

2.5 Rat bone marrow preservation

Marrow tissue contains different kinds of cells, such as adipocytes, hematopoietic stem cells and mesenchymal stem cells. [585-587] Marrow tissue plays an important role in bone formation and blood cell generation. Marrow-derived cells have been used for cell therapy. [588] However, cell viability is low after transplantation because of hypoxia. Our experimental results showed that marrow tissue could be preserved by the oxygen-release material and that a suitable amount of microparticles was required to obtain high cell viability in cultured marrow tissue (Figure 7.8 and Figure 7.2S). Therefore, this oxygen-release system could be used for bone marrow-derived cell transplantation and bone marrow transplantation.

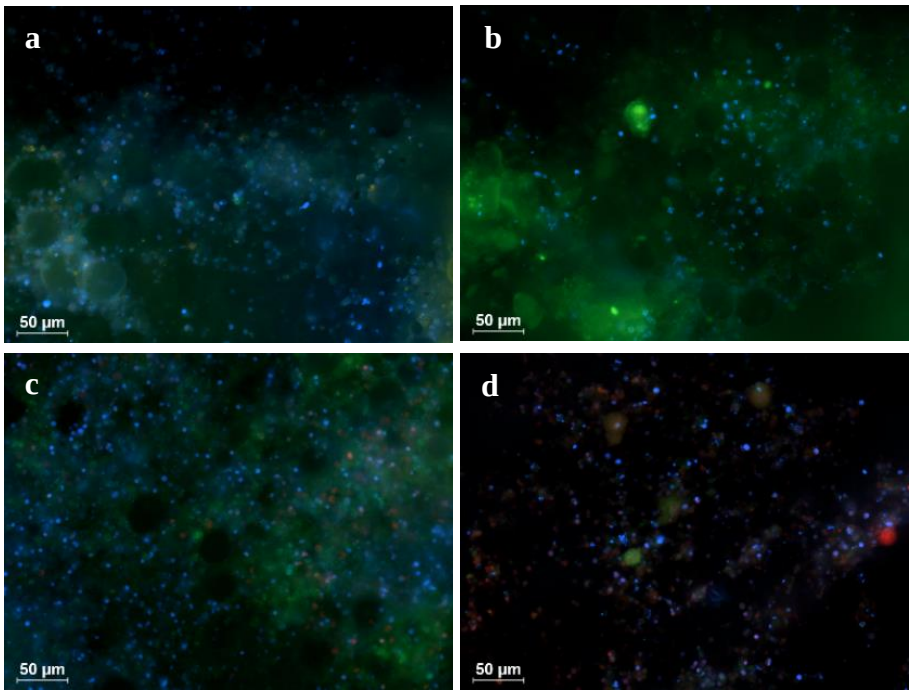


Figure 7.8. Fluorescent images of rat marrow tissue stained by live/dead assay. The marrow tissue was preserved in self-oxygenating scaffold with 20 mg/mL (a), 30 mg/mL (b) and 40 mg/mL (c) of oxygen-release microparticles, and without (d) oxygen-release microparticles under anoxia for 7 d. The cultured marrow tissue displayed the highest cell viability in the scaffold with 30 mg/mL oxygen-release microparticles.

In summary, ischemia is the most obvious event in extracorporeal tissues and organs since there is no blood supply to the tissues and organs. As a result, the tissues and organs lose the source of oxygen and nutrients. During tissue and organ preservation, one of the common practice is to reduce the demand of oxygen and nutrients from preserved tissues and organs under hypothermia. Although tissues and organs can be preserved under hypothermia for prolonged periods of time, the occurrence of reperfusion injuries, caused by low temperature and hypoxia during preservation, brings new problems. This preliminary experimental work showed that the oxygen-release material was not toxic to various tissues, and that tissue and organs were preserved at physiological temperature by being provided with extra oxygen. In

this way, reperfusion injuries could be prevented. Keeping tissue and organs alive at physiological temperature can be useful for drug screening as well.

### 3. Effects of oxygen delivery on vascularization in implants

Vascularization is very important to the survival of tissue and cells in tissue and cell transplantation. It is well known that hypoxia induces angiogenesis [589, 590], but it is not clear whether oxygen delivery promotes vascularization. Oxygen delivery may improve vascularization because angiogenesis related cells need energy to differentiate, grow, and synthesize raw materials to build the vessel networks. Normally, angiogenesis related growth factors or stem cells are used to promote vascularization in the scaffold. This process usually takes more than one week. It would be a great advantage if the oxygen delivery material could promote the formation of blood vessels in implants and keep cell alive in the scaffold at the same time.

A porous oxygen-release scaffold was prepared by dispersing calcium peroxide (CP) (Aldrich, USA), iron oxide ($Fe_3O_4$) (Fisher Scientific, Canada) and ammonia chloride ($NH_4Cl$, 250-500 μm) (Fisher Scientific, Canada) particles in a poly(lactic-co-glycolic acid) (PLGA) (50/50, Mw 28,000, Advanced Polymer Materials Inc, Canada) solution in chloroform. The mixtures were then transferred into a glass tube with an inner diameter of 5 mm and a thickness of 2 mm. A cylinder was obtained when the sample dried. $NH_4Cl$ was used as a pore-making agent and then removed by ethanol. In the end, a porous scaffold that released oxygen was obtained containing 5 % w/v CP. In the scaffold, CP was the oxygen generating agent and $Fe_3O_4$ the catalyst of $H_2O_2$ produced by CP.

Male Wistar rats (35-40 d, 126-150 g) from Charles River were used for subcutaneous implantation. The porous scaffolds with and without oxygen-release materials were implanted subcutaneously into rats on the dorsal side. After 2, 4 and 12 weeks, the scaffolds were retrieved and subjected to histological examination.

The micro-structure of the porous scaffold as well as the distribution of CP and $Fe_3O_4$ particles was examined using SEM. As shown in Figure 9, the porous scaffold had a connective pore structure (Figure 7.9a) and its surface was covered with a large amount of $Fe_3O_4$ particles (Figure 7.9b, c). The connective pore structure allowed tissue infiltration into the scaffold. $Fe_3O_4$ particles on the scaffold surface could increase efficacy of the catalysts.

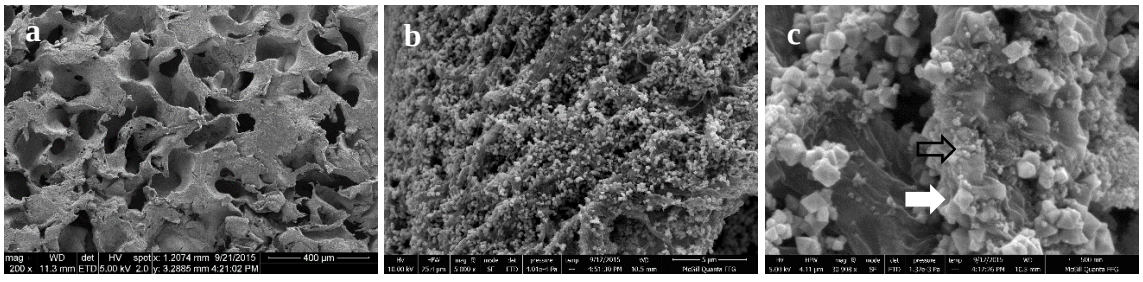


Figure 7.9. SEM images of the porous CP-$Fe_3O_4$-PLGA scaffold. The scaffold had a porous structure. The pores appeared to be connected. The pore size ranged from nano- to micro-meters. An abundance of $Fe_3O_4$ particles (white arrow) were observed on the surface of the polymers, and CP particles were observed on the surface of the polymer as well (empty arrow).

According to histological staining, the presence of oxygen-release material improved vascularization in the subcutaneously implanted scaffolds. A larger number of blood vessels in the oxygen-release scaffolds were found compared with the scaffold without extra oxygen supply at various time points. (Figure 7.10 and Figure 7.3S) After 12 weeks, blood vessel networks (black arrows) were observed in the experimental group. In contrast, a much smaller

amount of blood vessels could be seen in the control group compared with the experimental group. The *in vivo* experimental results suggested that oxygen delivery promoted vascularization in the scaffold.

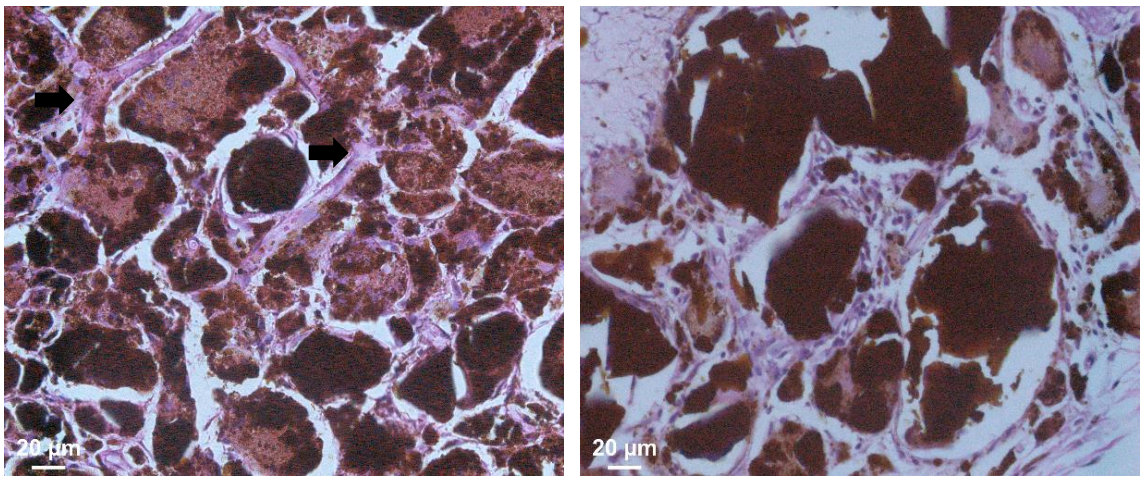


Figure 7.10. Hematoxylin and eosin (H&E) staining of subcutaneously implanted scaffolds with (left) and without (right) oxygen delivery materials after 12 weeks. The supply of oxygen greatly improved vascularization in the scaffold.

Hypoxia induces vascularization in the scaffold through HIF-1α and VEGF. However, long-term hypoxia cannot support blood vessel formation in the scaffold. Blood vessel formation includes cell proliferation and differentiation and generation of collagen and elastin. All these activities require energy and only oxidative phosphorylation is able to generate enough energy to support these activities. Moreover, the oxygen concentration affects the quality of generated collagen and the formation of tube-like structure. [591, 592] It has been reported that vascularization is inhibited in PLGA scaffolds possibly due to the production of acidic byproducts during the biodegradation of PLGA. In this work, the presence of CP could remove the acidic substances by the hydroxyl ions released during the decomposition of the metal peroxide. Moreover, oxygen supply may support cell activities related to vascularization. Hence, the process of vascularization in the scaffold was accelerated by the oxygen delivery

material based on the metal peroxide. This part of work is delayed by the histological characterization due to the technical difficulties with sample cutting.

**4. 3D printing**

Constructing three-dimensional (3D) scaffolds is a novel technique for tissue engineering. It enlightened the future of tissue engineering in building tissue constructs with a 3D structure. As mentioned previously, oxygen deficiency is common in large tissue constructs. Construction of a 3D scaffold that can oxygenate itself was attempted, enabling the engineered tissue to maintained high cell viability.

Sodium alginate is widely used for tissue engineering and is biodegradable and biocompatible. Sodium alginate pastes containing oxygen-release microparticles were prepared for 3D printing. The microparticles were mixed with sodium alginate (LF200, FMC BioPolymer, USA) powders first. Then the mixtures were wetted with 6% w/v polyvinyl alcohol (PVA) (Aldrich, USA) in water with a ratio of 8:1(mixture/liquid) in weight to form a paste. The paste was used to produce a 3D scaffold using a Bioplotter (regenHU) by dispensing. A 20×20×3 mm scaffold was obtained. The pore size in the scaffold was examined under a stereomicroscope (SteREO Discovery.V20 Carl Zeiss, Germany).

The photos of the platform used for 3D printing as well as the printed scaffold was shown in Figure 7.11. Figure 7.11a shows the platform for 3D printing. Briefly, sodium alginate pastes containing oxygen-release microparticles were filled in a syringe and then extruded onto a flat surface through a needle. By moving the needle in both horizontal and vertical directions, a porous scaffold with a defined structure was produced. The scaffold has a regular porous

structure (Figure 7.11b). The pore size on the edge of the scaffold was smaller compared with the pore size in the inner area due to the shrinkage of alginate paste.

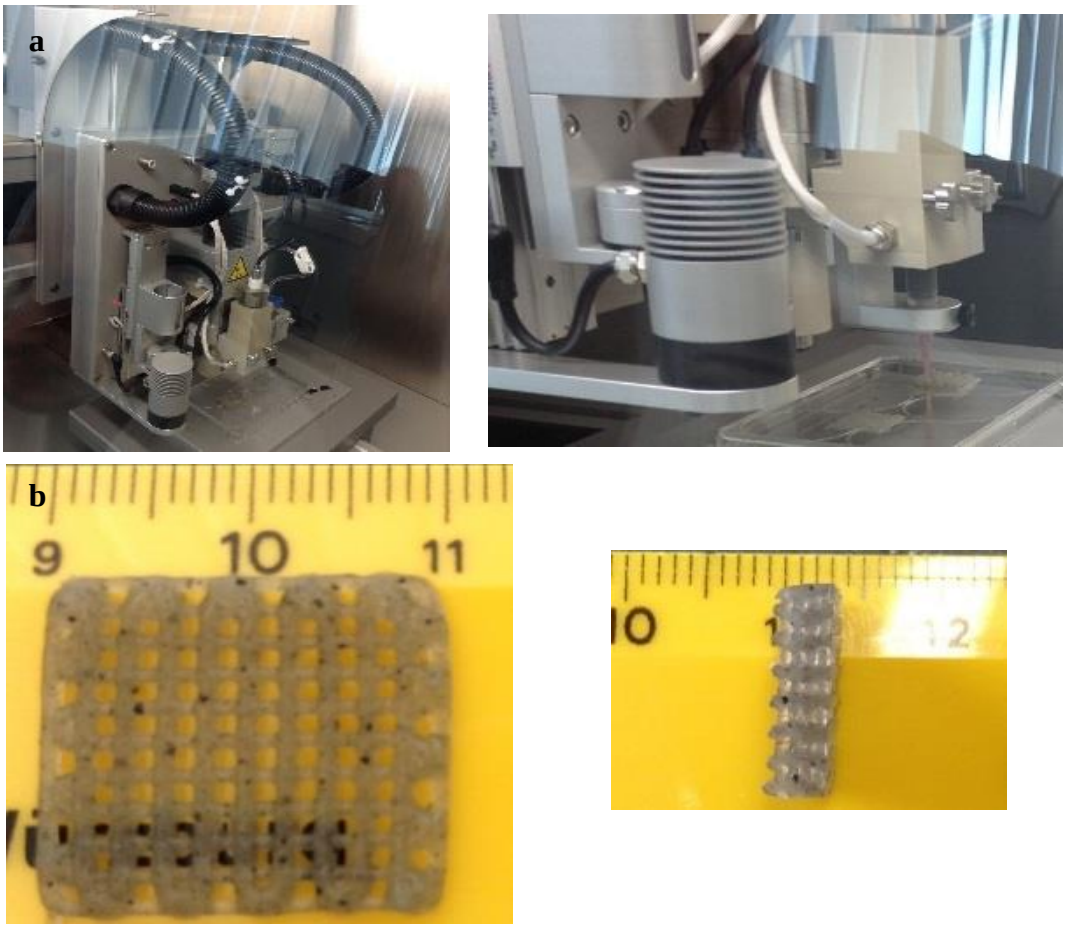


Figure 7.11. Photos of the 3 D printing machine (a) and the printed 3D scaffold (b).

The microscopic images of the printed scaffold were shown in Figure 7.12. The 3D scaffold had an interspace of about 1 mm between lines and 0.1-0.25 mm between layers.

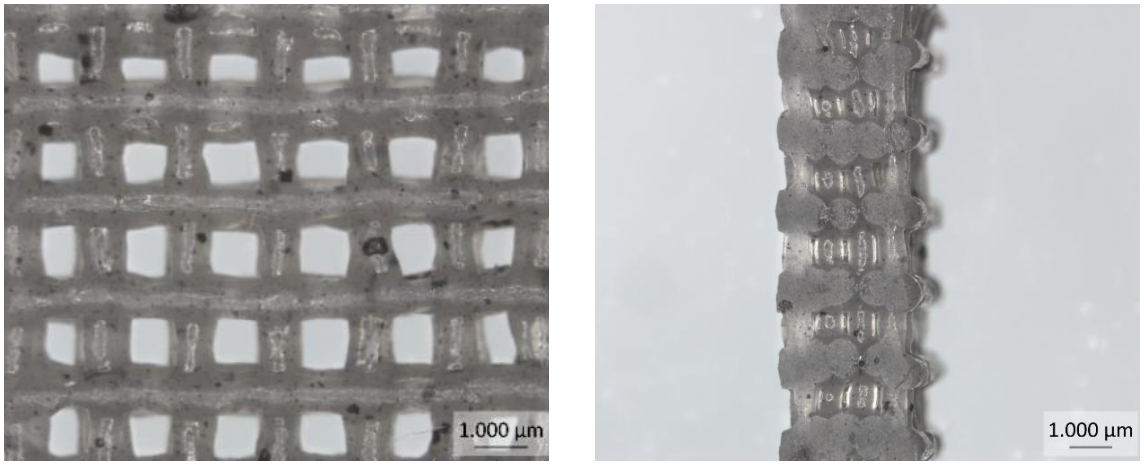


Figure 7.12. Image of 3 D printed alginate scaffold containing oxygen-release microparticles (black dots).

This was only the initial work and more like a proof of concept. It suggested that it was possible to create a scaffold with various oxygen concentrations. Therefore, the effects of oxygen concentrations on cells activities, like migration, proliferation and differentiation, apoptosis, and necrosis, in the scaffold could be investigated. In addition, it made it possible to build tissue constructs with a large enough size for clinical practice by providing a more homogeneous oxygen environment to cells in the scaffold.

## Supplemental information

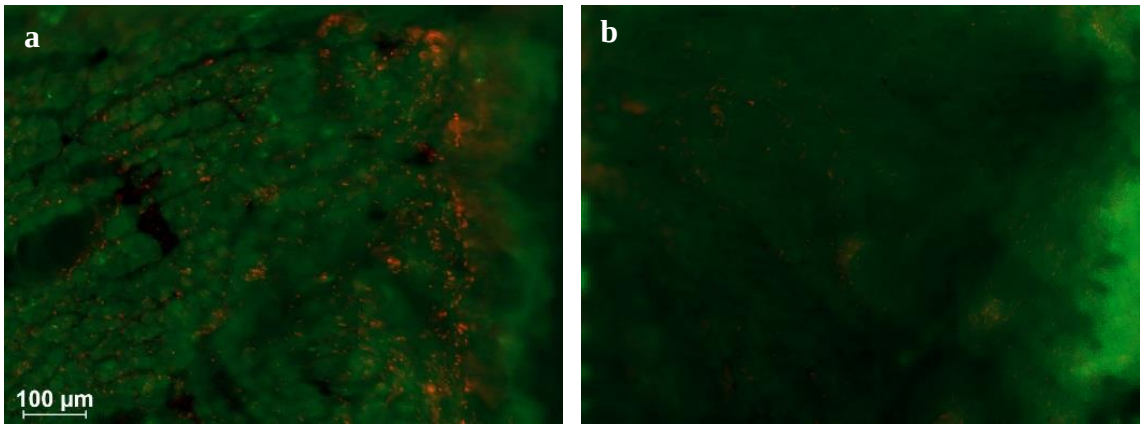


Figure 7.1S. Fluorescent images of perfused beating mouse heat tissue (a) and preserved mouse heart tissue (b) stained by the live/dead assay. The preserved heart tissue displayed better cell viability than perfused heart tissue.

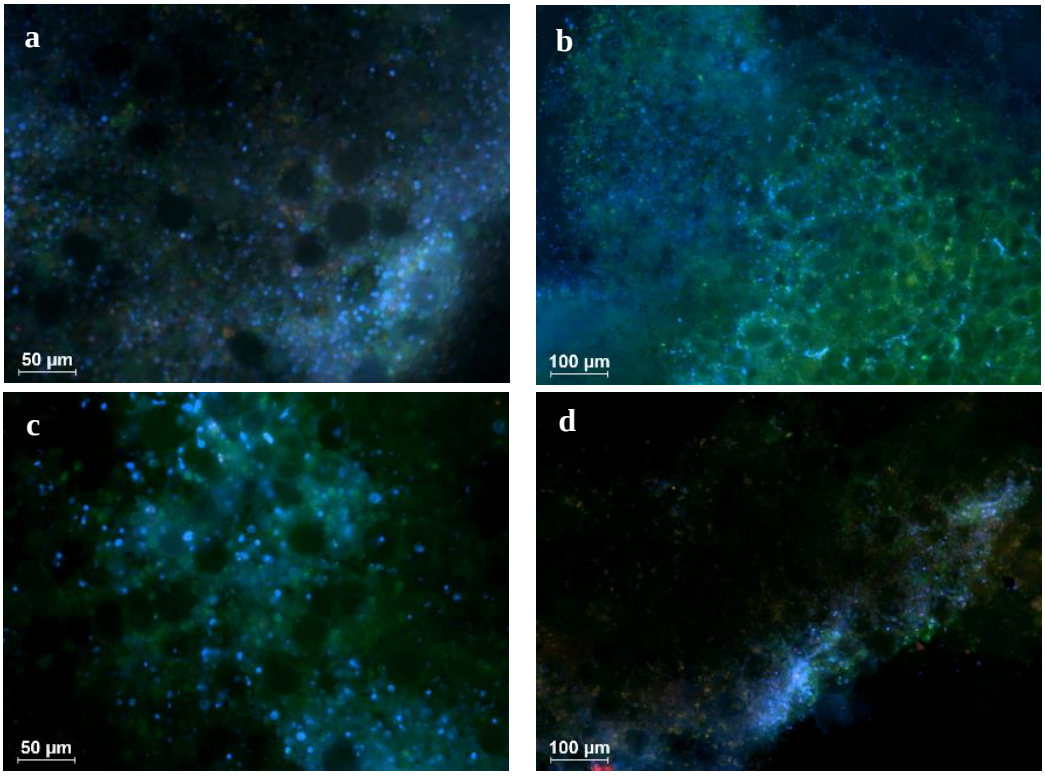


Figure 7.2S. Fluorescent images of rat marrow stained by the live/dead assay. The marrow tissue was stored in the self-oxygenating scaffold with 20 mg/mL (a), 30 mg/mL (b) and 40 mg/mL (c) of oxygen-release microparticles, and without (d) oxygen-release microparticles under anoxia for 3 d. Marrow tissue displayed the highest cell viability in the presence of 30 mg/mL microparticles in the scaffold.

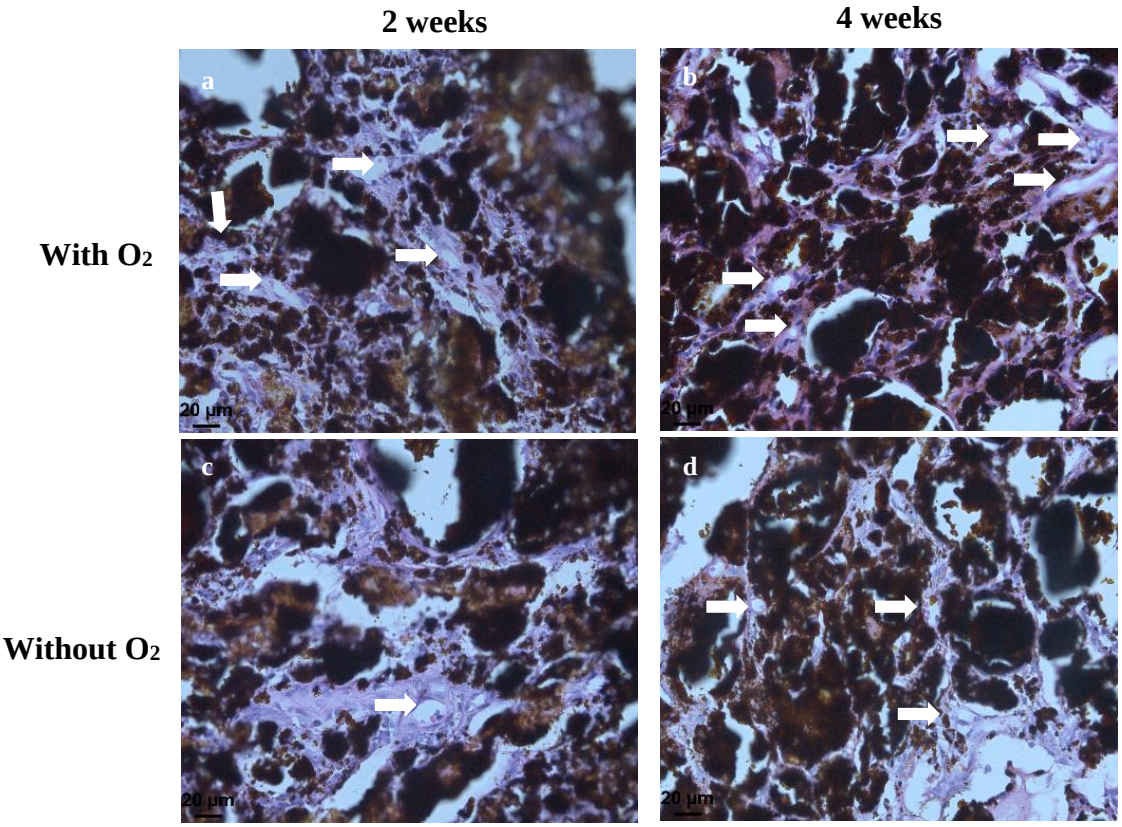


Figure 7.3S. Hematoxylin and eosin (H&E) staining of subcutaneously implanted scaffolds with and without oxygen delivery materials after 2 and 4 weeks. The presence of oxygen delivery material greatly improved vascularization in the scaffold. A larger number of blood vessels were observed in the oxygen generating scaffold compared with the scaffold without oxygen-release material.

## Chapter 8

### Final conclusions and future work

The main contributions of this thesis to the peroxide-based oxygen delivery system for tissue engineering include:

1. Improved the oxygen delivery system and the culture method to evaluate the system

In the previous reports using metal peroxides as the oxygen generating agent, the oxygen-release material was either made into disks (10 mm in diameter), porous scaffolds (10 mm in diameter), or films. The physical shapes and sizes restricted the application of the oxygen-release systems. In this work, oxygen-release microparticles were developed with a size similar to that of cells, therefore, the application restriction caused by the shape and size of oxygen-release material was greatly reduced. In addition, the reported peroxide-based oxygen delivery systems either neglected the cytotoxicity of $H_2O_2$ generated during the decomposition of peroxides or used toxic catalyst or extremely high concentrations of catalase, which could cause side effects such as paradoxical reductive stress on cells, to remove $H_2O_2$. Therefore, none of them was able to deal with the toxicant in an acceptable way. In this work, biocompatible $MnO_2$ and biodegradable $Fe_3O_4$ were successfully used to catalyze the decomposition of $H_2O_2$. Moreover, alginate hydrogel was introduced into the oxygen-release system to control oxygen diffusion and protect cells from oxidative toxicity. Last but not the least, a proper method is required to evaluate the oxygen delivery systems. Except for one recent report in which anoxic culture was used to evaluate the oxygen-release from hyperbarically loaded microtanks, all the previous work used hypoxic culture to evaluate their oxygen-release systems. The problem was that most of the cells could survive in the hypoxic environment. Moreover, no comparison with normoxic culture was presented in those reports. In this work, anoxic culture was employed to evaluate the oxygen-release efficacy of the

developed oxygen delivery system, and a comparison with normoxic culture was also performed.

2. Eliminated cytotoxicity

As mentioned before, cytotoxic byproducts are generated during the decomposition of peroxides. These byproducts include free radicals and hydroxyl ions in addition to $H_2O_2$. The cytotoxic free radicals were generally ignored in the previous reports. In this work, the alginate hydrogel was employed to isolate free radicals from cells. The experimental results confirmed that alginate hydrogel was able to trap free radicals. Given the extremely short lifetime of the radicals, alginate hydrogel may protect cells from free radicals. The toxicity from hydroxyl ions was avoided by reducing the decomposition rate of the metal peroxide, using hydrophobic biopolymers and alginate hydrogel, so that the released hydroxyl ions could be consumed by the buffer system in culture medium. The developed oxygen delivery system was tested on a various tissues and cells in a sealed system and exhibited excellent biocompatibility.

3. Towards the development of *in vivo* degradable systems

The reported peroxide-based oxygen delivery systems either used silicon rubbers, toxic catalysts, or high concentrations of catalase additives. Hence, none of them were suitable to be used as *in vivo* biodegradable oxygen delivery systems. In this work, attempts were made to develop an *in vivo* degradable oxygen-release system. The relatively cheap polycaprolactone (PCL) with a slow biodegradation rate and insoluble $MnO_2$ were used at the beginning to optimize the system. Afterwards, poly(lactic-co-glycolic acid) (PLGA), which had a faster *in vivo* degradation rate, and biodegradable $Fe_3O_4$ were used to replace the PCL and $MnO_2$, respectively, so that an oxygen delivery system that could fully degrade *in vivo* was obtained.

Although complete degradation of the oxygen-release system has not been achieved yet, it is very promising to be fulfilled given a longer time period *in vivo*.

4. Summary of the experimental results

An *in situ* oxygen delivery system was developed using calcium peroxide (CP) as the oxygen generating agent. An oxygen-release slab consisting of CP, $MnO_2$ and PCL was developed first and encapsulated in the alginate hydrogel to rescue human primary fibroblasts and Madin-Darby canine kidney (MDCK) cells under the anoxic condition. The oxygen-release system greatly reduced expression levels of hypoxia related genes in human primary fibroblasts and maintained normal growth rates of human primary fibroblasts and MDCK cells. Afterwards, a more advanced oxygen-release system, namely a self-oxygenating scaffold (SOS) composed of oxygen-release microparticles and alginate hydrogel, was developed. The SOS successfully encapsulated MDCK cells and supported cells growth *in vivo*, preserved thoracic aortas, adipose tissue, islets, heart slices, brain slices, the liver, and marrow from rats at physiological temperature. Moreover, a topical oxygen-release patch was developed based on CP and successfully preserved ischemic tissues and promoted the healing of ischemic wounds. In addition, oxygen delivery was found to improve vascularization in the implants. The oxygen-release microparticles were also incorporated into 3D printed scaffolds.

In spite of these encouraging results, there is still space to improve this oxygen delivery system. The technique for preparation of oxygen-release microparticles needs to be refined. Centrifugation was used to collect the microparticles, but some very small microparticles were lost because a very high centrifugation speed was required to collect them. Nevertheless, very high centrifugation speeds resulted in serious aggregations. Some particles were lost during washing as well. Therefore, it is worthy to find a better way to collect the microparticles. With

current technique, it takes 4-5 weeks to dry the microparticles at room temperature, possibly due to the low diffusion rate of chloroform in glycerol. Although several methods have been tried to reduce the time for drying, such as vacuum and heating, no obvious improvements were obtained. In addition, the ratio of catalysts in the microparticles could be further optimized so that the minimum amount of catalysts would be used.

Encouraging experimental results have been obtained using the oxygen delivery system in tissue engineering, cell transplantation, tissue and organ preservation, and wound healing. However, some information is still missing in this study. The experimental results suggested that different kinds of tissues and cells required various oxygen concentrations to stay alive. Although the amount of released oxygen was adjusted by changing the concentration of oxygen-release microparticles in the scaffold, the exact concentration of oxygen in the scaffolds has not been studied yet. It will be very valuable if the optimum oxygen concentrations for various cells, tissues and organs could be determined. The experimental results showed that oxygen delivery improved ischemic wound healing. Again, the amount of oxygen delivered to wounds was not measured.

Preliminary experimental results showed that the oxygen delivery system maintained high cell viability in various tissues, but the functionality of the preserved tissues was not evaluated, including the functionality of preserved mouse islets, mouse heart slices, mouse brain slices, and mouse liver. Moreover, oxygen-release scaffolds with optimized compositions, namely the CP amounts, biopolymer ratios, and alginate amounts, may further improve preservation results. Although the oxygen-release microparticles have been successfully incorporated into 3D printing scaffolds, the concentration of the microparticles in the scaffold still needs to be optimized for different types of cells.

## Chapter 9

## Bibliography


[1] A. Carreau, B.E. Hafny-Rahbi, A. Matejuk, C. Grillon, C. Kieda, Journal of Cellular and Molecular Medicine, 15 (2011) 1239-1253.
[2] S.H. Oh, C.L. Ward, A. Atala, J.J. Yoo, B.S. Harrison, Biomaterials, 30 (2009) 757-762.
[3] N. Haque, M.T. Rahman, N.H. Abu Kasim, A.M. Alabsi, The Scientific World Journal, 2013 (2013).
[4] A. Greijer, P. Van Der Groep, D. Kemming, A. Shvarts, G. Semenza, G. Meijer, M. Van De Wiel, J. Belien, P. Van Diest, E. van Der Wall, The Journal of pathology, 206 (2005) 291-304.
[5] G.M. Saed, M.P. Diamond, Fertility and Sterility, 78 (2002) 144-147.
[6] N.R. Forsyth, A. Musio, P. Vezzoni, A.H.R. Simpson, B.S. Noble, J. McWhir, Cloning and stem cells, 8 (2006) 16-23.
[7] N.R. Forsyth, A. Kay, K. Hampson, A. Downing, R. Talbot, J. McWhir, Regenerative Medicine, 3 (2008) 817-833.
[8] A.C. Boquest, A. Shahdadfar, K. Frønsdal, O. Sigurjonsson, S.H. Tunheim, P. Collas, J.E. Brinchmann, Molecular biology of the cell, 16 (2005) 1131-1141.
[9] L. Packer, K. Fuehr, (1977).
[10] W.M. Miller, C.R. Wilke, H.W. Blanch, Journal of cellular physiology, 132 (1987) 524-530.
[11] S.J. Morrison, M. Csete, A.K. Groves, W. Melega, B. Wold, D.J. Anderson, The Journal of Neuroscience, 20 (2000) 7370-7376.
[12] J. Estrada, C. Albo, A. Benguria, A. Dopazo, P. Lopez-Romero, L. Carrera-Quintanar, E. Roche, E. Clemente, J. Enriquez, A. Bernad, Cell Death & Differentiation, 19 (2012) 743-755.
[13] M. Lovett, K. Lee, A. Edwards, D.L. Kaplan, Tissue Engineering Part B: Reviews, 15 (2009) 353-370.
[14] A.A. Tandara, T.A. Mustoe, World J. Surg., 28 (2004) 294-300.
[15] F. Gottrup, World J. Surg., 28 (2004) 312-315.
[16] H. Eto, H. Kato, H. Suga, N. Aoi, K. Doi, S. Kuno, K. Yoshimura, Plastic and reconstructive surgery, 129 (2012) 1081-1092.
[17] F. Moolman, H. Rolfes, S. Van der Merwe, W. Focke, Biochemical engineering journal, 19 (2004) 237-250.
[18] P.K. Chandra, C.L. Ross, L.C. Smith, S.S. Jeong, J. Kim, J.J. Yoo, B.S. Harrison, Wound Repair and Regeneration, (2015) n/a-n/a.
[19] D.G. Kemp, M.H. Hermans, J Diabetic Foot Complications, 3 (2011) 6-12.
[20] O. Mownah, M. Khurram, C. Ray, A. Kanwar, D. Rees, J. Brassil, S. Stamp, N. Carter, J. Dark, D. Talbot, Transplantation, 94 (2012) 928.
[21] Q. Tan, A.M. El-Badry, C. Contaldo, R. Steiner, S. Hillinger, M. Welti, M. Hilbe, D.R. Spahn, R. Jaussi, G. Higuera, Tissue Engineering Part A, 15 (2009) 2471-2480.
[22] G. Shi, R.N. Coger, Biotechnology progress, 29 (2013) 718-726.
[23] E. Maillard, M. Sanchez-Dominguez, C. Kleiss, A. Langlois, M. Sencier, C. Vodouhe, W. Beitigier, M. Krafft, M. Pinget, A. Belcourt, Transplantation proceedings, Elsevier, 2008, pp. 372-374.
[24] E. Maillard, M.T. Juszczak, A. Clark, S.J. Hughes, D.R. Gray, P.R. Johnson, Biomaterials, 32 (2011) 9282-9289.
[25] H.A. Sloviter, T. Kamimoto, Nature, 216 (1967) 458-460.
[26] J. Treckmann, M. Nagelschmidt, T. Minor, F. Saner, S. Saad, A. Paul, Cryobiology, 59

(2009) 19-23.
[27] M. Shinzeki, Y. Takeyama, T. Ueda, T. Yasuda, S. Kishi, Y. Kuroda, KOBE JOURNAL OF MEDICAL SCIENCES, 49 (2003) 17-24.
[28] B. Lafferty, L. Wood, P. Davis, Wounds UK, 7 (2011) 14-23.
[29] D.M. Barratt, P.G. Harch, K. Van Meter, The Neurologist, 8 (2002) 186-202.
[30] N. Henninger, B.T. Bratane, B. Bastan, J. Bouley, M. Fisher, J Cereb Blood Flow Metab, 29 (2008) 119-129.
[31] H. Itano, M. Aoe, S. Ichiba, M. Yamashita, H. Date, A. Andou, N. Shimizu, The Annals of thoracic surgery, 67 (1999) 332-339.
[32] W. Isselhard, M. Berger, H. Denecke, J. Witte, J. Fischer, H. Molzberger, C. Freiberg, D. Ammermann, M. Brunke, Pflügers Archiv, 337 (1972) 87-106.
[33] H. Ikegawa, Y. Kuwagata, K. Hayakawa, K. Noguchi, H. Ogura, H. Sugimoto, Artificial organs, 36 (2012) 130-138.
[34] M.W. Laschke, Y. Harder, M. Amon, I. Martin, J. Farhadi, A. Ring, N. Torio-Padron, R. Schramm, M. Rücker, D. Junker, Tissue Engineering, 12 (2006) 2093-2104.
[35] P. Cabrales, G. Sun, Y. Zhou, D.R. Harris, A.G. Tsai, M. Intaglietta, A.F. Palmer, Journal of applied physiology, 107 (2009) 1548-1558.
[36] J.C. Davis, T. Hunt, J Intensive Care Med, 4 (1989) 7.
[37] E. Villanueva, M.H. Bennett, J. Wasiak, J.P. Lehm, The Cochrane Library, (2004).
[38] H. Bäumler, Y. Xiong, Z.Z. Liu, A. Patzak, R. Georgieva, Artificial organs, 38 (2014) 708-714.
[39] E. Pedraza, M.M. Coronel, C.A. Fraker, C. Ricordi, C.L. Stabler, Proceedings of the National Academy of Sciences, 109 (2012) 4245-4250.
[40] Z. Li, X. Guo, J. Guan, Biomaterials, 33 (2012) 5914-5923.
[41] A. Carreau, B.E. Hafny-Rahbi, A. Matejuk, C. Grillon, C. Kieda, Journal of cellular and molecular medicine, 15 (2011) 1239-1253.
[42] S.-k. Park, A.M. Dadak, V.H. Haase, L. Fontana, A.J. Giaccia, R.S. Johnson, Molecular and Cellular Biology, 23 (2003) 4959-4971.
[43] H. Pilch, K. Schlenger, E. Steiner, P. Brockerhoff, P. Knapstein, P. Vaupel, International Journal of Gynecological Cancer, 11 (2001) 137-142.
[44] A. Boveris, B. Chance, Biochem. J., 134 (1973) 707-716.
[45] C. Rappaport, In Vitro Cellular & Developmental Biology-Animal, 39 (2003) 187-192.
[46] H.-F. Chen, H.-C. Kuo, S.-P. Lin, C.-L. Chien, M.-S. Chiang, H.-N. Ho, Tissue Engineering Part A, 16 (2010) 2901-2913.
[47] A.C. Breggia, J. Himmelfarb, Oxidative medicine and cellular longevity, 1 (2008) 33-38.
[48] B. Annabi, Y.T. Lee, S. Turcotte, E. Naud, R.R. Desrosiers, M. Champagne, N. Eliopoulos, J. Galipeau, R. Beliveau, Stem Cells, 21 (2003) 337-347.
[49] H. Ren, Y. Cao, Q. Zhao, J. Li, C. Zhou, L. Liao, M. Jia, Q. Zhao, H. Cai, Z.C. Han, Biochemical and biophysical research communications, 347 (2006) 12-21.
[50] H.J. Knowles, A.-M. Cleton-Jansen, E. Korsching, N.A. Athanasou, The FASEB Journal, 24 (2010) 4648-4659.
[51] F.J. Northington, R. Chavez-Valdez, L.J. Martin, Annals of neurology, 69 (2011) 743-758.
[52] S. Young, R. Marshall, R. Hill, Proceedings of the National Academy of Sciences, 85 (1988) 9533-9537.
[53] D. Hugo-Wissemann, I. Anundi, W. Lauchart, R. Viebahn, H. de Groot, Hepatology, 13 (1991) 297-303.
[54] C.B. Foldager, A.B. Nielsen, S. Munir, M. Ulrich-Vinther, K. Søballe, C. Bünger, M. Lind, Acta orthopaedica, 82 (2011) 234-240.
[55] R.L. Dahlin, V.V. Meretoja, M. Ni, F.K. Kasper, A.G. Mikos, AIChE Journal, 59 (2013) 3158-3166.

[56] R. Das, G. Van Osch, M. Kreukniet, J. Oostra, H. Weinans, H. Jahr, Journal of Orthopaedic Research, 28 (2010) 537-545.
[57] W. Liu, Y. Wen, P. Bi, X. Lai, X.S. Liu, X. Liu, S. Kuang, Development, 139 (2012) 2857-2865.
[58] K.M. Porter, B.-Y. Kang, S.E. Adesina, T.C. Murphy, C.M. Hart, R.L. Sutliff, PLoS ONE, 9 (2014) e98532.
[59] B. Chen, V.E. Nelin, M.L. Locy, Y. Jin, T.E. Tipple, Thioredoxin-1 mediates hypoxia-induced pulmonary artery smooth muscle cell proliferation, 2013.
[60] C. Liu, A.L. Tsai, Y.C. Chen, S.C. Fan, C.H. Huang, C.C. Wu, C.H. Chang, Journal of cellular biochemistry, 113 (2012) 148-155.
[61] C. Kaur, V. Sivakumar, W.S. Foulds, C.D. Luu, E.-A. Ling, Journal of Neuropathology & Experimental Neurology, 71 (2012) 330-347.
[62] L. Urbani, M. Piccoli, C. Franzin, M. Pozzobon, P. De Coppi, PloS one, 7 (2012) e49860.
[63] T. Ezashi, P. Das, R.M. Roberts, Proceedings of the National Academy of Sciences of the United States of America, 102 (2005) 4783-4788.
[64] C. Crocker, J.J. Cech, Jr., Environmental Biology of Fishes, 50 (1997) 383-389.
[65] I. Papandreou, R.A. Cairns, L. Fontana, A.L. Lim, N.C. Denko, Cell Metabolism, 3 (2006) 187-197.
[66] I. Papandreou, A.L. Lim, K. Laderoute, N.C. Denko, Cell Death Differ, 15 (2008) 1572-1581.
[67] M.J. Allalunis-Turner, A.J. Franko, M.B. Parliament, British Journal of Cancer, 80 (1999) 104-109.
[68] P.T. Schumacker, N. Chandel, A.G. Agusti, Oxygen conformance of cellular respiration in hepatocytes, 1993.
[69] A. Oller, C. Buser, M. Tyo, W. Thilly, Journal of cell science, 94 (1989) 43-49.
[70] A. Mohyeldin, T. Garzón-Muvdi, A. Quiñones-Hinojosa, Cell stem cell, 7 (2010) 150-161.
[71] B. Speers-Roesch, M. Mandic, D.J. Groom, J.G. Richards, Journal of Experimental Marine Biology and Ecology, 449 (2013) 239-249.
[72] W. Wang, C. Winlove, C. Michel, The Journal of physiology, 549 (2003) 855-863.
[73] M. Muller, W. Padberg, E. Schindler, J. Sticher, C. Osmer, S. Friemann, G. Hempelmann, Anesthesia & Analgesia, 87 (1998) 474-476.
[74] G. Marcaida, V. Felipo, C. Hermenegildo, M.-D. Miñana, S. Grisolia, FEBS Letters, 296 (1992) 67-68.
[75] K.A. Athanasiou, G.G. Niederauer, C.M. Agrawal, Biomaterials, 17 (1996) 93-102.
[76] P.M. Tibbles, J.S. Edelsberg, New England Journal of Medicine, 334 (1996) 1642-1648.
[77] W.F. Bernhard, R.M. Filler, The American Journal of Surgery, 115 (1968) 661-668.
[78] N. Henshaw, Dublin, Dancer, 1664.
[79] C.R. Mortensen, Current Anaesthesia & Critical Care, 19 (2008) 333-337.
[80] M.E. Sluijter, The Treatment of Carbon Monoxide Poisoning by Administration of Oxygen at High Atmospheric Pressure, in: H. Bour, A.L. Mc (Eds.) Progress in Brain Research, Elsevier, 1967, pp. 123-182.
[81] N. Pace, E. Strajman, E.L. Walker, Science, 111 (1950) 652-654.
[82] N.A. Buckley, D.N. Juurlink, G. Isbister, M.H. Bennett, E.J. Lavonas, Cochrane Database Syst Rev, 4 (2011).
[83] C.-H. Ku, H.-M. Hung, W.C. Leong, H.-H. Chen, J.-L. Lin, W.-H. Huang, H.-Y. Yang, C.-H. Weng, C.-M. Lin, S.-H. Lee, I.K. Wang, C.-C. Liang, C.-T. Chang, W.-R. Lin, T.-H. Yen, PloS one, 10 (2015) e0118995.
[84] W.I.I. Done.
[85] G. Garrabou, J.M. Inoriza, C. Morén, G. Oliu, Ò. Miró, M.J. Martí, F. Cardellach, Intensive Care Med, 37 (2011) 1711-1712.

[86] S.R. Thorn, L.W. Keim, Clinical Toxicology, 27 (1989) 141-156.
[87] L.K. Weaver, R.O. Hopkins, K.J. Chan, S. Churchill, C.G. Elliott, T.P. Clemmer, J.F. Orme, F.O. Thomas, A.H. Morris, New England Journal of Medicine, 347 (2002) 1057-1067.
[88] R. Moon, Undersea Hyperb Med, 41 (2014) 151-157.
[89] M.H. Bennett, J.P. Lehm, S.J. Mitchell, J. Wasiak, The Cochrane Library, (2012).
[90] G. Cantarella, G. La Camera, V. Carnemolla, D.C. Grasso, D. Akhshik, C. Bonsignore, P. Di Marco, ACTA MEDICA MEDITERRANEA, 30 (2014) 369-370.
[91] C.-E. Chen, S.-T. Shih, T.-H. Fu, J.-W. Wang, C.-J. Wang, Chang Gung medical journal, 26 (2003) 114-121.
[92] N. Skeik, B.R. Porten, E. Isaacson, J. Seong, D.L. Klosterman, R.F. Garberich, J.Q. Alexander, A. Rizvi, J.M. Manunga Jr, A. Cragg, J. Graber, P. Alden, T. Sullivan, Annals of vascular surgery, 29 (2015) 206-214.
[93] B.H. Bass, Postgraduate Medical Journal, 46 (1970) 407-408.401.
[94] M. Löndahl, Diabetes/metabolism research and reviews, 28 (2012) 78-84.
[95] P. Kranke, M.H. Bennett, M. Martyn-St James, A. Schnabel, S.E. Debus, The Cochrane Library, (2012).
[96] S. Ketchum 3rd, A. Thomas, A. Hall, Surgical forum, 1967, pp. 65.
[97] I. Bilic, N.M. Petri, J. Bezic, D. Alfirevic, et al., Undersea & Hyperbaric Medicine, 32 (2005) 1-9.
[98] H.N. Korn, E.S. Wheeler, T.A. Miller, Archives of Surgery, 112 (1977) 732-737.
[99] P.B. Dauwe, B.J. Pulikkottil, L. Lavery, J.M. Stuzin, R.J. Rohrich, Plastic and reconstructive surgery, 133 (2014) 208e-215e.
[100] S. Stefanidou, M. Kotsiou, T. Mesimeris, Diving and hyperbaric medicine, 44 (2014) 243-245.
[101] E. Mainous, P. Boyne, G. Hart, Naval Hospital, Long Beach, CA, 1973.
[102] M.H. Bennett, J. Feldmeier, N. Hampson, R. Smee, C. Milross, The Cochrane Library, (2005).
[103] R.E. Marx, R.P. Johnson, S.N. Kline, Journal of the American Dental Association (1939), 111 (1985) 49-54.
[104] R.E. Marx, Journal of Oral and Maxillofacial Surgery, 41 (1983) 351-357.
[105] A. Muhonen, J. Muhonen, T. Lindholm, H. Minn, J. Klossner, J. Kulmala, R. Happonen, International journal of oral and maxillofacial surgery, 31 (2002) 519-524.
[106] N. Skeik, B.R. Porten, E. Isaacson, J. Seong, D.L. Klosterman, R.F. Garberich, J.Q. Alexander, A. Rizvi, J.M. Manunga, A. Cragg, Annals of vascular surgery, (2014).
[107] G. Granström, A. Tjellström, P.-I. Brånemark, Journal of Oral and Maxillofacial Surgery, 57 (1999) 493-499.
[108] A.R.M. Tahir, J. Westhuyzen, J. Dass, M.K. Collins, R. Webb, S. Hewitt, P. Fon, M. McKay, Asia-Pacific Journal of Clinical Oncology, 11 (2015) 68-77.
[109] M. Esposito, M.G. Grusovin, S. Patel, H.V. Worthington, P. Coulthard, The Cochrane Library, (2008).
[110] D. Rose, American family physician, 86 (2012) 888; author reply p. 888.
[111] T. Ueno, T. Omi, E. Uchida, H. Yokota, S. Kawana, Journal of Nippon Medical School, 81 (2014) 4-11.
[112] O. Shoshani, A. Shupak, A. Barak, Y. Ullman, Y. Ramon, E. Lindenbaum, Y. Peled, British Journal of Plastic Surgery, 51 (1998) 67-73.
[113] A.L. Brannen, J. Still, M. Haynes, H. Orlet, F. Rosenblum, E. Law, W.O. Thompson, Am Surg, 63 (1997) 205-208.
[114] A. Eskes, D. Ubbink, M. Lubbers, C. Lucas, H. Vermeulen, World J. Surg., 35 (2011) 535-542.
[115] J.A. Niezgoda, P. Cianci, B.W. Folden, R.L. Ortega, B.J. Slade, A.B. Storrow, Plastic and

reconstructive surgery, 99 (1997) 1620-1625.
[116] J. Wasiak, M. Bennett, J. Lehm, The Cochrane Library.
[117] C.K. Sen, S. Khanna, G. Gordillo, D. Bagchi, M. Bagchi, S. Roy, Annals of the New York Academy of Sciences, 957 (2002) 239-249.
[118] E. Berg, E. Barth, D. Clarke, L. Dooley, Investigative Surgery, 2 (1989) 409-421.
[119] A. Eskes, H. Vermeulen, C. Lucas, D.T. Ubbink, The Cochrane Library, (2013).
[120] R.P. Gruber, D.H. Heitkamp, L.J. Billy, J.J. Amato, Archives of Surgery, 101 (1970) 69-70.
[121] H.B. van der Worp, J. van Gijn, New England Journal of Medicine, 357 (2007) 572-579.
[122] D.E. Rusyniak, M.A. Kirk, J.D. May, L.W. Kao, E.J. Brizendine, J.L. Welch, W.H. Cordell, R.J. Alonso, Stroke, 34 (2003) 571-574.
[123] N. Nighoghossian, P. Trouillas, P. Adeleine, F. Salord, Stroke, 26 (1995) 1369-1372.
[124] K.H. Holbach, A. Caroli, H. Wassmann, J. Neurol., 217 (1977) 17-30.
[125] C.-H. Chen, S.-Y. Chen, V. Wang, C.-C. Chen, K.-C. Wang, C.-H. Chen, Y.-C. Liu, K.-C. Lu, P.-K. Yip, W.-Y. Ma, The Scientific World Journal, 2012 (2012).
[126] S. Efrati, G. Fishlev, Y. Bechor, O. Volkov, J. Bergan, K. Kliakhandler, I. Kamiager, N. Gal, M. Friedman, E. Ben-Jacob, PloS one, 8 (2013) e53716.
[127] M.H. Bennett, S. Weibel, J. Wasiak, A. Schnabel, C. French, P. Kranke, The Cochrane Library, (2014).
[128] N. Hatayama, M. Naito, S. Hirai, Y. Yoshida, T. Kojima, K. Seki, X.-K. Li, M. Itoh, Cell transplantation, 21 (2012) 609-615.
[129] J.E. Blatteau, J. Hugon, O. Castagna, C. Meckler, N. Vallee, Y. Jammes, M. Hugon, J. Risberg, C. Peny, PLoS One, 8 (2013) e67681.
[130] N. Reis, O. Schwartz, D. Militianu, Y. Ramon, D. Levin, D. Norman, Y. Melamed, A. Shupak, D. Goldsher, C. Zinman, Journal of Bone & Joint Surgery, British Volume, 85 (2003) 371-375.
[131] E.M. Camporesi, G. Vezzani, G. Bosco, D. Mangar, T.L. Bernasek, The Journal of Arthroplasty, 25 (2010) 118-123.
[132] G. Uzun, M. Mutluoğlu, Y. Özdemir, Arch Orthop Trauma Surg, 129 (2009) 1583-1584.
[133] L. Koren, E. Ginesin, Y. Melamed, D. Norman, D. Levin, E. Peled, Orthopedics, 38 (2015) e200-e205.
[134] B. Bernbeck, K.A. Krauth, A. Scherer, V. Engelbrecht, U. Göbel, Medical and Pediatric Oncology, 39 (2002) 47-48.
[135] A. Scherer, V. Engelbrecht, B. Bernbeck, P. May, R. Willers, U. Göbel, U. Mödder, RoFo: Fortschritte auf dem Gebiete der Rontgenstrahlen und der Nuklearmedizin, 172 (2000) 798-801.
[136] V. Richards, D. Pinto, P. Coombs, The American Journal of Surgery, 106 (1963) 114-127.
[137] A. Kumaria, C.M. Tolias, British Journal of Neurosurgery, 23 (2009) 576-584.
[138] H.K. Shin, F. Oka, J.H. Kim, D. Atochin, P.L. Huang, C. Ayata, The Journal of Neuroscience, 34 (2014) 15200-15207.
[139] Z. Qi, W. Liu, Y. Luo, X. Ji, K.J. Liu, Med Gas Res, 3 (2013) 2.
[140] A.B. Singhal, X. Wang, T. Sumii, T. Mori, E.H. Lo, J Cereb Blood Flow Metab, 22 (2002) 861-868.
[141] S. Liu, W. Liu, W. Ding, M. Miyake, G.A. Rosenberg, K.J. Liu, J Cereb Blood Flow Metab, 26 (2006) 1274-1284.
[142] H.K. Shin, A.K. Dunn, P.B. Jones, D.A. Boas, E.H. Lo, M.A. Moskowitz, C. Ayata, Brain, 130 (2007) 1631-1642.
[143] S. Magnoni, L. Ghisoni, M. Locatelli, M. Caimi, A. Colombo, V. Valeriani, N. Stocchetti, Journal of Neurosurgery, 98 (2003) 952-958.
[144] C.M. Tolias, M. Reinert, R. Seiler, C. Gilman, A. Scharf, M.R. Bullock, Journal of

Neurosurgery, 101 (2004) 435-444.
[145] S.B. Rockswold, G.L. Rockswold, D.A. Zaun, X. Zhang, C.E. Cerra, T.A. Bergman, J. Liu, Journal of Neurosurgery, 112 (2009) 1080-1094.
[146] S.B. Rockswold, G.L. Rockswold, D.A. Zaun, J. Liu, Journal of Neurosurgery, 118 (2013) 1317-1328.
[147] J. Weaver, K.J. Liu, Medical gas research, 5 (2015) 1-8.
[148] S. Efrati, S. Berman, G.B. Aharon, Y. Siman-Tov, Z. Averbukh, J. Weissgarten, Nephrology Dialysis Transplantation, 23 (2008) 2213-2222.
[149] M. Ahotupa, E. MÄNtylÄ, V. Peltola, A. Puntala, H. Toivonen, Acta Physiologica Scandinavica, 145 (1992) 151-157.
[150] Z. Tatarkova, I. Engler, A. Calkovska, D. Mokra, A. Drgova, S. Kuka, P. Racay, J. Lehotsky, D. Dobrota, P. Kaplan, General physiology and biophysics, 31 (2012) 179-184.
[151] Z. Tatarkova, I. Engler, A. Calkovska, D. Mokra, A. Drgova, P. Hodas, J. Lehotsky, D. Dobrota, P. Kaplan, Neurochemical research, 36 (2011) 1475-1481.
[152] D. Orbegozo Cortés, F. Puflea, K. Donadello, F.S. Taccone, L. Gottin, J. Creteur, J.-L. Vincent, D. De Backer, Microvascular Research, 98 (2015) 23-28.
[153] A. Kumaria, C. Tolias, British journal of neurosurgery, 22 (2008) 200-206.
[154] L.B. Goldstein, C.D. Bushnell, R.J. Adams, L.J. Appel, L.T. Braun, S. Chaturvedi, M.A. Creager, A. Culebras, R.H. Eckel, R.G. Hart, J.A. Hinchey, V.J. Howard, E.C. Jauch, S.R. Levine, J.F. Meschia, W.S. Moore, J.V. Nixon, T.A. Pearson, Stroke, 42 (2011) 517-584.
[155] J.G. Riess, M.P. Krafft, Artificial Cells, Blood Substitutes and Biotechnology, 25 (1997) 43-52.
[156] M. Pilarek, J. Glazyrina, P. Neubauer, Microb Cell Fact, 10 (2011) 50.
[157] A.T. King, B.J. Mulligan, K.C. Lowe, Nature Biotechnology, 7 (1989) 1037-1042.
[158] J.G. Riess, Artificial Cells, Blood Substitutes and Biotechnology, 33 (2005) 47-63.
[159] Q.A. Tawfic, R. Kausalya, Oman Medical Journal, 26 (2011) 4-9.
[160] M. Ragaller, T. Richter, Journal of Emergencies, Trauma and Shock, 3 (2010) 43-51.
[161] L.C. Clark, F. Gollan, Science, 152 (1966) 1755-1756.
[162] A. Sehgal, R. Guaran, INDIAN JOURNAL OF CHEST DISEASES AND ALLIED SCIENCES, 47 (2005) 187.
[163] K.C. Lowe, Journal of Materials Chemistry, 16 (2006) 4189-4196.
[164] T.H. Shaffer, M.R. Wolfson, J.S. Greenspan, R.E. Hoffman, S.L. Davis, L. Clark, Reproduction, fertility and development, 8 (1996) 409-416.
[165] J.G. Modell, M.K. Tham, J.H. Modell, H.W. Calderwood, B.C. Ruiz, Toxicology and applied pharmacology, 26 (1973) 86-92.
[166] C.J. Imber, S.D.S. Peter, I.L. de Cenarruzabeitia, D. Pigott, T. James, R. Taylor, J. Mcguire, D. Hughes, A. Butler, M. Rees, Transplantation, 73 (2002) 701-709.
[167] T.H. Shaffer, N. Tran, V.K. Bhutani, E.M. Sivieri, Pediatric research, 17 (1983) 680-684.
[168] T.M. Smith, D.M. Steinhorn, K. Thusu, B.P. Fuhrman, P. Dandona, Critical care medicine, 23 (1995) 1533-1539.
[169] D.M. Steinhorn, C.L. Leach, B.P. Fuhrman, B.A. Holm, Critical care medicine, 24 (1996) 1252-1256.
[170] Č.K.V.V.L. PEDIATRICKÉHO, Bratisl Lek Listy, 100 (1999) 481-485.
[171] D.M. Steinhorn, M.C. Papo, A.T. Rotta, A. Aljada, B.P. Fuhrman, P. Dandona, Journal of critical care, 14 (1999) 20-28.
[172] P. Bagnoli, S. Tredici, R. Seetharamaiah, D.O. Brant, L.A. Hewell, K. Johnson, J.L. Bull, M.L. Costantino, R.B. Hirschl, ASAIO Journal, 53 (2007) 549-555.
[173] K.M. Smith, J.D. Mrozek, S.C. Simonton, D.R. Bing, P.A. Meyers, J.E. Connett, M.C. Mammel, Critical Care Medicine, 25 (1997) 1888-1897.
[174] R.B. Hirschl, R. Tooley, A.C. Parent, K. Johnson, R.H. Bartlett, CHEST Journal, 108

(1995) 500-508.
[175] W.-Y. Lee, S.-C. Huang, K.-F. Hsu, C.-C. Tzeng, W.-L. Shen, Gynecologic oncology, 108 (2008) 377-384.
[176] W. Burkhardt, H. Proquitté, S. Krause, R.R. Wauer, M. Rüdiger, Biology of the Neonate, 82 (2001) 250-256.
[177] T. Shaffer, M. Wolfson, J. Greenspan, S. Rubenstein, R. Stern, Artificial Cells, Blood Substitutes and Biotechnology, 22 (1994) 315-326.
[178] C.L. Leach, J.S. Greenspan, S.D. Rubenstein, T.H. Shaffer, M.R. Wolfson, J.C. Jackson, R. DeLemos, B.P. Fuhrman, New England Journal of Medicine, 335 (1996) 761-767.
[179] R.M. Kacmarek, H.P. Wiedemann, P.T. Lavin, M.K. Wedel, A.S. Tütüncü, A.S. Slutsky, American journal of respiratory and critical care medicine, 173 (2006) 882-889.
[180] P.C. Rimensberger, Pediatric Critical Care Medicine, 9 (2008) 664-666.
[181] P.G. Gauger, T. Pranikoff, R.J. Schreiner, F.W. Moler, R.B. Hirschl, Critical care medicine, 24 (1996) 16-22.
[182] J.G. Riess, Chemical Reviews, 101 (2001) 2797-2920.
[183] E. Fiebig, Clinical orthopaedics and related research, 357 (1998) 6-18.
[184] H.J. Alter, H.G. Klein, blood, 112 (2008) 2617-2626.
[185] R.H. Walker, American journal of clinical pathology, 88 (1987) 374-378.
[186] J. Lavoie, Pediatric Anesthesia, 21 (2011) 14-24.
[187] K. Lowe, Blood reviews, 13 (1999) 171-184.
[188] B.D. Spiess, Journal of Applied Physiology, 106 (2009) 1444-1452.
[189] D.R. Spahn, Critical Care, 3 (1999) R93-R97.
[190] G.P. Biro, P. Blais, A.L. Rosen, Critical Reviews in Oncology/Hematology, 6 (1987) 311-374.
[191] T.H. Maugh, American Association for the Advancement of Science, 1979.
[192] G.M. Vercellotti, D.E. Hammerschmidt, P.R. Craddock, H.S. Jacob, Blood, 59 (1982) 1299-1304.
[193] W. Rudowski, Acta Medica Polona, 22 (1981) 161-180.
[194] S.F. Flaim, Artificial Cells, Blood Substitutes, and Biotechnology, 22 (1994) 1043-1054.
[195] J.E. Squires, Science, 295 (2002) 1002-1005.
[196] G. Biro, Transfusion medicine reviews, 7 (1993) 84-95.
[197] C.S. Cohn, M.M. Cushing, Critical care clinics, 25 (2009) 399-414.
[198] P.R. Steinmetz, C. Balko, R.P. Geyer, New England Journal of Medicine, 289 (1973) 1077-1082.
[199] L.C. Clark, F. Becattini, S. Kaplan, V. Obrock, D. Cohen, C. Becker, Science, 181 (1973) 680-682.
[200] K. Yokoyama, K. Yamanouchi, M. Watanabe, T. Matsumoto, R. Murashima, T. Daimoto, T. Hamano, H. Okamoto, T. Suyama, R. Watanabe, Federation proceedings, 1975, pp. 1478-1483.
[201] K.C. Lowe, Artificial Cells, Blood Substitutes and Biotechnology, 28 (2000) 25-38.
[202] S.A. Gould, A.L. Rosen, L.R. Sehgal, H.L. Sehgal, L.A. Langdale, L.M. Krause, C.L. Rice, W.H. Chamberlin, G.S. Moss, New England Journal of Medicine, 314 (1986) 1653-1656.
[203] D.J. Roberts, C.V. Prowse, Practical Transfusion Medicine, Fourth Edition, (2013) 399-409.
[204] E. Maevsky, G. Ivanitsky, L. Bogdanova, O. Axenova, N. Karmen, E. Zhiburt, R. Senina, S. Pushkin, I. Maslennikov, A. Orlov, Artificial Cells, Blood Substitutes and Biotechnology, 33 (2005) 37-46.
[205] M.P. Krafft, J.G. Riess, Journal of Polymer Science Part A: Polymer Chemistry, 45 (2007) 1185-1198.
[206] E. Niiler, Nature biotechnology, 20 (2002) 962-963.

[207] J.L. Johnson, M.C. Dolezal, A. Kerschen, T.O. Matsunaga, E.C. Unger, Artificial Cells, Blood Substitutes and Biotechnology, 37 (2009) 156-162.
[208] C. Stephan, C. Schlawne, S. Grass, I.N. Waack, K.B. Ferenz, M. Bachmann, S. Barnert, R. Schubert, M. Bastmeyer, H. de Groot, Journal of microencapsulation, 31 (2013) 284-292.
[209] R.E. Banks, B.E. Smart, J. Tatlow, Organofluorine chemistry: principles and commercial applications, Springer Science & Business Media, 2013.
[210] A. Yacoub, M.C. Hajec, R. Stanger, W. Wan, H. Young, B.E. Mathern, Journal of Neurotrauma, 31 (2014) 256-267.
[211] R. Bullock, DTIC Document, 2013.
[212] S.F. Flaim, D.R. Hazard, J. Hogan, R.M. Peters, Artificial Cells, Blood Substitutes and Biotechnology, 22 (1994) 1511-1515.
[213] C.I. Castro, J.C. Briceno, Artificial organs, 34 (2010) 622-634.
[214] T. Mitsuno, H. Ohyanagi, R. Naito, Annals of surgery, 195 (1982) 60.
[215] T. Kawamura, Y. Kuroda, Y. Suzuki, H. Fujiwara, Y. Fujino, K. Yamamoto, Y. Saitoh, Transplantation, 47 (1989) 776-778.
[216] S. Matsumoto, T.H. Rigley, S.A. Qualley, Y. Kuroda, J.A. Reems, R.B. Stevens, Cell transplantation, 11 (2002) 769-777.
[217] M.C. Gioviale, G. Damiano, V.D. Palumbo, M. Bellavia, F. Cacciabaudo, G. Cassata, R. Puleio, R. Altomare, M.A. Lo, The International journal of artificial organs, 34 (2011) 519-525.
[218] S. Atias, S.S. Mizrahi, R. Shaco-Levy, A. Yussim, The Israel Medical Association journal, 10 (2008) 273.
[219] Y. Tanioka, D.E. Sutherland, Y. Kuroda, T.R. Gilmore, T.C. Asaheim, J.W. Kronson, J.P. Leone, Surgery, 122 (1997) 435-442.
[220] T. Deai, Y. Tanioka, Y. Suzuki, Y. Kuroda, The Kobe journal of medical sciences, 45 (1999) 191-199.
[221] G. Zhang, S. Matsumoto, H. Newman, D.M. Strong, R.P. Robertson, J.-A. Reems, Cell and tissue banking, 7 (2006) 195-201.
[222] K. Papas, B. Hering, L. Gunther, M. Rappel, C. Colton, E. Avgoustiniatos, Transplantation proceedings, Elsevier, 2005, pp. 3501-3504.
[223] T. Kin, M. Mirbolooki, P. Salehi, M. Tsukada, D. O'Gorman, S. Imes, E.A. Ryan, A.M.J. Shapiro, J.R. Lakey, Transplantation, 82 (2006) 1286-1290.
[224] E. Maillard, M. Sanchez-Dominguez, C. Kleiss, A. Langlois, M.C. Sencier, C. Vodouhe, W. Beitigier, M.P. Krafft, M. Pinget, A. Belcourt, S. Sigrist, Transplantation Proceedings, 40 (2008) 372-374.
[225] S.A. Hosgood, M.L. Nicholson, Transplantation, 89 (2010) 1169-1175.
[226] E. Maillard, M. Juszczak, A. Langlois, C. Kleiss, M. Sencier, W. Bietiger, M. Sanchez-Dominguez, M. Krafft, P. Johnson, M. Pinget, Cell transplantation, 21 (2012) 657-669.
[227] J.G. Riess, Artificial Cells, Blood Substitutes and Biotechnology, 20 (1992) 183-202.
[228] H. Brandhorst, S. Asif, K. Andersson, B. Theisinger, H.H. Andersson, M. Felldin, A. Foss, K. Salmela, A. Tibell, G. Tufveson, Transplantation, 89 (2010) 155-160.
[229] S. Terai, T. Tsujimura, S. Li, Y. Hori, H. Toyama, M. Shinzeki, I. Matsumoto, Y. Kuroda, Y. Ku, Journal of Surgical Research, 162 (2010) 284-289.
[230] T. Marada, K. Zacharovova, F. Saudek, European Surgical Research, 44 (2010) 170-178.
[231] S.A. Hosgood, I.H. Mohamed, M.L. Nicholson, Medical Science and Technology, 17 (2010) BR27-BR33.
[232] B. Dirks, J. Krieglstein, H. Lind, H. Rieger, H. Schütz, Journal of pharmacological methods, 4 (1980) 95-108.
[233] H.D. Berkowitz, P. McCombs, S. Sheety, L.D. Miller, H. Sloviter, Journal of Surgical Research, 20 (1976) 595-600.
[234] O. Reznik, S. Bagnenko, I. Loginov, V. Iljina, A. Ananyev, Y. Moysyuk, Transplantation

proceedings, Elsevier, 2008, pp. 1027-1028.
[235] S. Asif, A. Sedigh, J. Nordström, H. Brandhorst, C. Jorns, T. Lorant, E. Larsson, P.U. Magnusson, G. Nowak, S. Theisinger, Journal of Surgical Research, 178 (2012) 959-967.
[236] K. Bando, S. Teramoto, M. Tago, S. Seno, T. Murakami, S. Nawa, Y. Senoo, The Journal of thoracic and cardiovascular surgery, 96 (1988) 930-938.
[237] J.N. Bhayana, Z.T. Tan, J. Bergsland, D. Balu, J.K. Singh, E.L. Hoover, The Annals of thoracic surgery, 63 (1997) 459-464.
[238] A. Bito, K. Inoue, M. Asano, S. Ando, T. Takaba, The Japanese Journal of Thoracic and Cardiovascular Surgery, 48 (2000) 280-290.
[239] M. Isaka, M. Imamura, I. Sakuma, N. Shiiya, S. Fukushima, K. Nakai, A. Kitabatake, K. Yasuda, ASAIO journal, 51 (2005) 434-439.
[240] L. Segel, J. Minten, F. Schweighardt, American Journal of Physiology-Heart and Circulatory Physiology, 263 (1992) H730-H739.
[241] S. WU, H.-l. ZHAO, Z.-g. HAN, Z. WANG, Journal of Shanxi Medical University, 5 (2008) 026.
[242] N. Kamada, R. Calne, D. Wight, J. Lines, Transplantation, 30 (1980) 43-48.
[243] H. Shiki, Y. Ku, Y. Kuroda, Y. Saito, Nihon Geka Gakkai Zasshi, 94 (1993) 1033-1042.
[244] E. Klar, T. Kraus, P. Reuter, A. Mehrabi, L.P. Fernandes, M. Angelescu, M.M. Gebhard, C. Herfarth, Transplantation Proceedings, 30 (1998) 3707-3710.
[245] T. Konno, A. Kakita, T. Taira, M. Minato, A. Tamaki, E. Sasaki, Y. Kasai, The Japanese journal of surgery, 11 (1981) 209-213.
[246] H. Bergert, K.-P. Knoch, R. Meisterfeld, M. Jäger, J. Ouwendijk, S. Kersting, H.D. Saeger, M. Solimena, Cell transplantation, 14 (2005) 441-448.
[247] D. Brandhorst, M. Iken, R.G. Bretzel, H. Brandhorst, Xenotransplantation, 13 (2006) 465-470.
[248] G.B. Richerson, P.A. Getting, Brain Research, 517 (1990) 7-18.
[249] D. Brandhorst, M. Iken, M.D. Brendel, R.G. Bretzel, H. Brandhorst, Transplantation Proceedings, 37 (2005) 229-230.
[250] D. Brandhorst, M. Iken, M. Brendel, R. Bretzel, H. Brandhorst, Transplantation proceedings, Elsevier, 2005, pp. 229-230.
[251] A. Schaschkow, C. Mura, W. Bietiger, C. Peronet, A. Langlois, F. Bodin, C. Dissaux, C. Bruant-Rodier, M. Pinget, N. Jeandidier, M.T. Juszczak, S. Sigrist, E. Maillard, Biomaterials, 52 (2015) 180-188.
[252] S. Matsumoto, Y. Kuroda, Transplantation, 74 (2002) 1804-1809.
[253] S. Matsumoto, Artificial cells, blood substitutes, and biotechnology, 33 (2005) 75-82.
[254] D.G. Maluf, V.R. Mas, K. Yanek, J.J. Stone, R. Weis, D. Massey, B. Spiess, M.P. Posner, R.A. Fisher, Transplantation Proceedings, 38 (2006) 1243-1246.
[255] T. Kurki, A. Harjula, L. Heikkilä, A. Lehtola, P. Hämmäinen, E. Taskinen, S. Mattila, The Journal of heart transplantation, 9 (1989) 424-428.
[256] J.E. HALL, I.C. EHRHART, W.F. HOFMAN, Critical Care Medicine, 13 (1985) 1015-1019.
[257] P. Hindryckx, L. Devisscher, D. Laukens, K. Venken, H. Peeters, M. De Vos, Laboratory Investigation, 91 (2011) 1266-1276.
[258] P. Degenhardt, M. Pelzer, B. Fischer, S. Kraft, N. Sarioglu, H. Mau, M. Rüdiger, European journal of pediatric surgery: official journal of Austrian Association of Pediatric Surgery...[et al]= Zeitschrift fur Kinderchirurgie, 19 (2009) 211-215.
[259] S.C. Davis, A.L. Cazzaniga, C. Ricotti, P. Zalesky, L.-C. Hsu, J. Creech, W.H. Eaglstein, P.M. Mertz, Archives of dermatology, 143 (2007) 1252-1256.
[260] A. Wijekoon, N. Fountas-Davis, N.D. Leipzig, Acta biomaterialia, 9 (2013) 5653-5664.
[261] R.L. Carrier, M. Rupnick, R. Langer, F.J. Schoen, L.E. Freed, G. Vunjak-Novakovic,

Tissue Engineering, 8 (2002) 175-188.
[262] M.H. Cho, S.S. Wang, Biotechnology letters, 10 (1988) 855-860.
[263] T.E. Douglas, M. Pilarek, I. Kalaszczyńska, I. Senderek, A. Skwarczyńska, V.M. Cuijpers, Z. Modrzejewska, M. Lewandowska-Szumieł, P. Dubruel, Materials Letters, 128 (2014) 79-84.
[264] H. Fujita, K. Shimizu, Y. Morioka, E. Nagamori, Journal of bioscience and bioengineering, 110 (2010) 359-362.
[265] H. Li, A. Wijekoon, N.D. Leipzig, Annals of biomedical engineering, 42 (2014) 1456-1469.
[266] S.F. Khattak, K.-s. Chin, S.R. Bhatia, S.C. Roberts, Biotechnology and bioengineering, 96 (2007) 156-166.
[267] M. Pilarek, I. Grabowska, I. Senderek, M. Wojasiński, J. Janicka, K. Janczyk-Ilach, T. Ciach, Bioprocess and biosystems engineering, 37 (2014) 1707-1715.
[268] F.S. Palumbo, M. Di Stefano, A.P. Piccionello, C. Fiorica, G. Pitarresi, I. Pibiri, S. Buscemi, G. Giammona, RSC Advances, 4 (2014) 22894-22901.
[269] A.D. Bollands, K.C. Lowe, Biotechnology letters, 11 (1989) 265-268.
[270] D.G. Seifu, T.T. Isimjan, K. Mequanint, Acta Biomaterialia, 7 (2011) 3670-3678.
[271] S. Dinkelmann, W. Röhlke, H. Meinert, H. Northoff, Artificial Cells, Blood Substitutes, and Biotechnology, 29 (2001) 57-70.
[272] G.A. Wilbanks, A.J. Apel, S.S. Jolly, R.G. Devenyi, D.S. Rootman, Cornea, 15 (1996) 329-334.
[273] K.C. Lowe, Journal of fluorine chemistry, 118 (2002) 19-26.
[274] B. Vallet, E. Futier, Current opinion in critical care, 16 (2010) 359-364.
[275] A. D'Alessandro, G. Liumbruno, G. Grazzini, L. Zolla, Blood Transfusion, 8 (2010) 82-88.
[276] R.H. Levin, P.D. Barrett, M.J. Cline, N.I. Berlin, E.J. Freireich, Archives of Internal Medicine, 114 (1964) 278-283.
[277] P.E. Marik, H.L. Corwin, Critical Care Medicine, 36 (2008) 2667-2674 2610.1097/CCM.2660b2013e3181844677.
[278] J. Meier, M.M. Mueller, P. Lauscher, W. Sireis, E. Seifried, K. Zacharowski, Transfusion Medicine and Hemotherapy, 39 (2012) 98-103.
[279] G. Liumbruno, F. Bennardello, A. Lattanzio, P. Piccoli, G. Rossetti, Blood Transfusion, 7 (2009) 49.
[280] K.L. Wilkinson, S.J. Brunskill, C. Doree, M. Trivella, R. Gill, M.F. Murphy, status and date: New, published in, (2014).
[281] D.H. Buchholz, The Journal of Pediatrics, 84 (1974) 1-15.
[282] G. Adair, Journal of Biological Chemistry, 63 (1925) 515-516.
[283] H.F. Bunn, W.T. Esham, R.W. Bull, The Journal of Experimental Medicine, 129 (1969) 909-924.
[284] J. O'hagan, Biochemical Journal, 74 (1960) 417.
[285] P. Cabrales, G. Sun, Y. Zhou, D.R. Harris, A.G. Tsai, M. Intaglietta, A.F. Palmer, Effects of the molecular mass of tense-state polymerized bovine hemoglobin on blood pressure and vasoconstriction, 2009.
[286] P. Cabrales, Journal of the American College of Surgeons, 210 (2010) 271-279.
[287] M. te Lintel Hekkert, G.P. Dubé, E. Regar, M. de Boer, P. Vranckx, W.J. van der Giessen, P.W. Serruys, D.J. Duncker, American Journal of Physiology-Heart and Circulatory Physiology, 298 (2010) H1103-H1113.
[288] D. Hathazi, A.C. Mot, A. Vaida, F. Scurtu, I. Lupan, E. Fischer-Fodor, G. Damian, D.M. Kurtz Jr, R. Silaghi-Dumitrescu, Biomacromolecules, 15 (2014) 1920-1927.
[289] H. Hosaka, R. Haruki, K. Yamada, C. Böttcher, T. Komatsu, PloS one, 9 (2014) e110541.
[290] Y. Sheng, Y. Yuan, C. Liu, X. Tao, X. Shan, F. Xu, Journal of Materials Science: Materials

in Medicine, 20 (2009) 1881-1891.
[291] J. Kakehata, T. Yamaguchi, H. Togashi, I. Sakuma, H. Otani, Y. Morimoto, M. Yoshioka, Journal of pharmacological sciences, 114 (2010) 189-197.
[292] J.D. McNeil, B. Propper, J. Walker, L. Holguin, L. Evans, K. Lee, P.T. Fox, J.E. Michalek, C.E. Baisden, The Journal of thoracic and cardiovascular surgery, 142 (2011) 411-417.
[293] A.T. Kawaguchi, M. Haida, M. Yamano, D. Fukumoto, Y. Ogata, H. Tsukada, Journal of Pharmacology and Experimental Therapeutics, 332 (2010) 429-436.
[294] W. Gao, B. Sha, W. Zou, X. Liang, X. Meng, H. Xu, J. Tang, D. Wu, L. Xu, H. Zhang, Biomaterials, 32 (2011) 9425-9433.
[295] A.T. Kawaguchi, Y. Okamoto, Y. Kise, S. Takekoshi, C. Murayama, H. Makuuchi, Artificial organs, 38 (2014) 641-649.
[296] J. Elmer, A.F. Palmer, P. Cabrales, Life Sciences, 91 (2012) 852-859.
[297] T.A. Silverman, R.B. Weiskopf, Transfusion, 49 (2009) 2495-2515.
[298] Z. Tao, P.P. Ghoroghchian, Trends in Biotechnology, 32 (2014) 466-473.
[299] M. Liu, L. Gan, L. Chen, D. Zhu, Z. Xu, Z. Hao, L. Chen, International Journal of Pharmaceutics, 427 (2012) 354-357.
[300] A.J. Waite, J.S. Bonner, R. Autenrieth, Environmental engineering science, 16 (1999) 187-199.
[301] Y. Sun, C. Tai, GEONANO ENVIRONMENTAL TECHNOLOGY INC (GEON-Non-standard), pp. 20.
[302] K. Ward, G. Huvard, E. Carpenter, G. Sandhu, R. Barbee, B. Spiess, UNIV VIRGINIA COMMONWEALTH (UVCU) WARD K (WARD-Individual) HUVARD G (HUVA-Individual) CARPENTER E (CARP-Individual) SANDHU G (SAND-Individual) BARBEE R (BARB-Individual) SPIESS B (SPIE-Individual), pp. 2024287-A2024281:.
[303] S. Koenigsberg, W.A. Farone, Google Patents, 1993.
[304] B.S. Harrison, D. Eberli, S.J. Lee, A. Atala, J.J. Yoo, Biomaterials, 28 (2007) 4628-4634.
[305] G. Camci-Unal, N. Alemdar, N. Annabi, A. Khademhosseini, Polymer international, 62 (2013) 843-848.
[306] M. Sepulveda, T. Dresselaers, P. Vangheluwe, W. Everaerts, U. Himmelreich, A. Mata, F. Wuytack, Contrast media & molecular imaging, 7 (2012) 426-434.
[307] I. Arany, J.K. Megyesi, H. Kaneto, S. Tanaka, R.L. Safirstein, Kidney international, 65 (2004) 1231-1239.
[308] S.-i. Kanno, A. Shouji, K. Asou, M. Ishikawa, Journal of pharmacological sciences, 92 (2003) 166-170.
[309] P.K. Chandra, C.L. Ross, L.C. Smith, S.S. Jeong, J. Kim, J.J. Yoo, B.S. Harrison, Wound Repair and Regeneration, (2015).
[310] T.L. Schenck, U. Hopfner, M.N. Chávez, H.-G. Machens, I. Somlai-Schweiger, R.E. Giunta, A.V. Bohne, J. Nickelsen, M.L. Allende, J.T. Egaña, Acta Biomaterialia, (2014).
[311] D. Scherson, L. Cali, S. Sarangapani, Meeting Abstracts, MA2014-02 (2014) 862.
[312] Accessed on Sep 14th, 2015.
[313] M.H. Bakri, H. Nagem, D.I. Sessler, R. Mahboobi, J. Dalton, O. Akça, E.E. Roselli, S.R. Insler, Anesthesia & Analgesia, 106 (2008) 1619-1626.
[314] I. Igwegbe, G. Onojobi, M.O. Fadojutimi-Akinsiku, A.M. Hirsh, N.J. Park, M. Yao, V.R. Driver, Advances in Skin & Wound Care, 28 (2015) 206-210.
[315] D. Stephanie Wu, D. Kemp.
[316] K.Y. Woo, P.M. Coutts, R.G. Sibbald, Advances in skin & wound care, 25 (2012) 543-547.
[317] M.H. Bakri, H. Nagem, S. Rajagopalan, R. Mahboobi, S. Insler, Anesthesiology, 107 (2007) A1666.
[318] A.K. Tracey, C.J. Alcott, J.A. Schleining, S. Safayi, P.C. Zaback, J.M. Hostetter, E.L.

Reinertson, The Canadian Veterinary Journal, 55 (2014) 1146-1152.
[319] K.F. Lairet, D. Baer, M.L. Leas, E.M. Renz, L.C. Cancio, Journal of Burn Care & Research, 35 (2014) 214-218.
[320] S. Zellner, R. Manabat, D.F. Roe, Journal of International Medical Research, 43 (2015) 93-103.
[321] N. Ivins, W. Simmonds, A. Turner, K. Harding, WOUNDS UK, 3 (2007) 77.
[322] D. Queen, P. Coutts, M. Fierheller, R.G. Sibbald, Advances in skin & wound care, 20 (2007) 200-207.
[323] C.J. Moffatt, J. Stanton, S. Murray, V. Doody, P.J. Davis, P.J. Franks, Wound Medicine, 6 (2014) 1-10.
[324] M. Ochoa, R. Rahimi, T.L. Huang, N. Alemdar, A. Khademhosseini, M.R. Dokmeci, B. Ziaie, Sensors and Actuators B: Chemical, 198 (2014) 472-478.
[325] J. Feldmeier, H. Hopf, R. Warriner III, C. Fife, L. Gesell, M. Bennett, (2005).
[326] C.H. Brimson, Y. Nigam, Journal of the European Academy of Dermatology and Venereology, 27 (2013) 411-418.
[327] C. Brimson, Y. Nigam, Journal of the European Academy of Dermatology and Venereology, 27 (2013) 411-418.
[328] Accessed on Sep 14th, 2015.
[329] Accessed on Sep 14th, 2015.
[330] Accessed on Sep 14th, 2015.
[331] V. Young, D. Roe, J. Ollerenshaw, WOUND REPAIR AND REGENERATION, WILEY-BLACKWELL 111 RIVER ST, HOBOKEN 07030-5774, NJ USA, 2015, pp. A46-A47.
[332] Y. Gross, H. Better, Google Patents, 2010.
[333] Accessed on Sep 14th, 2015.
[334] R. Magnus, Naunyn-Schmiedeberg's Archives of Pharmacology, 47 (1902) 200-208.
[335] J.H. Fischer, C. Funcke, G. Yotsumoto, S. Jeschkeit-Schubbert, F. Kuhn-Régnier, European journal of cardio-thoracic surgery, 25 (2004) 98-104.
[336] F. Kuhn-Régnier, W. Bloch, I. Tsimpoulis, M. Reismann, O. Dagktekin, S. Jeschkeit-Schubbert, C. Funcke, J.W. Fries, K. Addicks, E.R. de Vivie, Transplantation, 77 (2004) 28-35.
[337] F. Kuhn-Régnier, J.H. Fischer, S. Jeschkeit, R. Switkowski, R. Sobottke, E.R. de Vivie, European journal of cardio-thoracic surgery, 17 (2000) 71-76.
[338] B.D. Burns, J. Robson, G. Smith, Canadian journal of biochemistry and physiology, 36 (1958) 499-504.
[339] G. Yotsumoto, S. Jeschkeit-Schubbert, C. Funcke, F. Kuhn-Régnier, J.H. Fischer, Transplantation, 75 (2003) 750-756.
[340] T. Minor, P. Efferz, B. Lüer, Cryobiology, 65 (2012) 41-44.
[341] T. Minor, W. Isselhard, Transplantation, 61 (1996) 20-22.
[342] T. Minor, S. Saad, M. Nagelschmidt, M. Kötting, Z. Fu, A. Paul, W. Isselhard, Transplantation, 65 (1998) 1262-1264.
[343] T. Minor, J. Stegemann, A. Hirner, M. Koetting, Liver Transplantation, 15 (2009) 798-805.
[344] P.-W. So, B.J. Fuller, Cryobiology, 43 (2001) 238-247.
[345] D. Ridgway, D. Manas, J. Shaw, S. White, Clinical transplantation, 24 (2010) 1-19.
[346] W. Scott, T. O'Brien, J. Ferrer-Fabrega, E. Avgoustiniatos, B. Weegman, T. Anazawa, S. Matsumoto, V. Kirchner, M. Rizzari, M. Murtaugh, Transplantation proceedings, Elsevier, 2010, pp. 2016-2019.
[347] T. Minor, H. Klauke, W. Isselhard, Transplantation proceedings, Elsevier, 1997, pp. 2994-2996.
[348] J.H. Fischer, Organ Preservation and Reengineering, (2011) 105-126.
[349] F. Kuhn-Régnier, J.H. Fischer, S. Jeschkeit, Thorac Cardiovasc Surg, 46 Suppl 2 (1998)

308-312.
[350] W. Isselhard, M. Berger, H. Denecke, J. Witte, J.H. Fischer, H. Molzberger, C. Freiberg, D. Ammermann, M. Brunke, Pflügers Archiv, 337 (1972) 87-106.
[351] T. Minor, S. Akbar, R. Tolba, F. Dombrowski, Journal of Hepatology, 32 (2000) 105-111.
[352] M.S. Reddy, N. Carter, A. Cunningham, J. Shaw, D. Talbot, Transplant International, 27 (2014) 634-639.
[353] W.E. Scott Iii, T.D. O'Brien, J. Ferrer-Fabrega, E.S. Avgoustiniatos, B.P. Weegman, T. Anazawa, S. Matsumoto, V.A. Kirchner, M.D. Rizzari, M.P. Murtaugh, T.M. Suszynski, T. Aasheim, L.S. Kidder, B.E. Hammer, S.G. Stone, L.A. Tempelman, D.E.R. Sutherland, B.J. Hering, K.K. Papas, Transplantation Proceedings, 42 (2010) 2016-2019.
[354] W. Scott, B. Weegman, J. Ferrer-Fabrega, S. Stein, T. Anazawa, V. Kirchner, M. Rizzari, J. Stone, S. Matsumoto, B. Hammer, Transplantation proceedings, Elsevier, 2010, pp. 2011-2015.
[355] T.M. Suszynski, M.D. Rizzari, W.E. Scott, L.A. Tempelman, M.J. Taylor, K.K. Papas, Cryobiology, 64 (2012) 125-143.
[356] S.W. Ryter, D. Morse, A.M.K. Choi, American Journal of Respiratory Cell and Molecular Biology, 36 (2007) 175-182.
[357] J.A. Awad, A. Brassard, W.M. Caron, C. Cadrin, International surgery, 54 (1970) 276-282.
[358] N. Faithfull, J. Klein, H. Vanderzee, P. Salt, British journal of anaesthesia, 56 (1984) 867-872.
[359] J.A. Feshitan, N.D. Legband, M.A. Borden, B.S. Terry, Biomaterials, 35 (2014) 2600-2606.
[360] S. Chew, Y. Ip, Journal of fish biology, 84 (2014) 603-638.
[361] E. Kosenko, V. Felipo, C. Montoliu, S. Grisolía, Y. Kaminsky, Metab Brain Dis, 12 (1997) 69-82.
[362] C.L. Santos, L.D. Bobermin, D.G. Souza, B. Bellaver, G. Bellaver, B.A. Arús, D.O. Souza, C.-A. Gonçalves, A. Quincozes-Santos, Toxicology in Vitro, 29 (2015) 1350-1357.
[363] K. Rama Rao, A. Jayakumar, M. Norenberg, Metab Brain Dis, 29 (2014) 927-936.
[364] L.D. Bobermin, G. Hansel, E.B.S. Scherer, A.T.S. Wyse, D.O. Souza, A. Quincozes-Santos, C.-A. Gonçalves, Toxicology in Vitro, 29 (2015) 2022-2029.
[365] J.H. Seo, J.G. Fox, R.M. Peek Jr, S.J. Hagen, Gastroenterology, 141 (2011) 2064-2075.
[366] R. Satpute, V. Lomash, J. Hariharakrishnan, P. Rao, P. Singh, N. Gujar, R. Bhattacharya, Toxicology and Industrial Health, 30 (2014) 12-24.
[367] S. Levine, A. Saltzman, Renal failure, 23 (2001) 53-59.
[368] A. Hurria, A. Hurria, K. Brogan, K.S. Panageas, C. Pearce, L. Norton, A. Jakubowski, J. Howard, C. Hudis, Drugs & aging, 22 (2005) 785-791.
[369] J. Fang, M.H. Alderman, JAMA, 283 (2000) 2404-2410.
[370] D.S. Freedman, D.F. Williamson, E.W. Gunter, T. Byers, American Journal of Epidemiology, 141 (1995) 637-644.
[371] R.J. Johnson, D.-H. Kang, D. Feig, S. Kivlighn, J. Kanellis, S. Watanabe, K.R. Tuttle, B. Rodriguez-Iturbe, J. Herrera-Acosta, M. Mazzali, Hypertension, 41 (2003) 1183-1190.
[372] C. Bickel, H.J. Rupprecht, S. Blankenberg, G. Rippin, G. Hafner, A. Daunhauer, K.-P. Hofmann, J. Meyer, The American journal of cardiology, 89 (2002) 12-17.
[373] B.F. Culleton, M.G. Larson, W.B. Kannel, D. Levy, Annals of Internal Medicine, 131 (1999) 7-13.
[374] R.P. Obermayr, C. Temml, G. Gutjahr, M. Knechtelsdorfer, R. Oberbauer, R. Klauser-Braun, Journal of the American Society of Nephrology, 19 (2008) 2407-2413.
[375] N. Neirynck, R. Vanholder, E. Schepers, S. Eloot, A. Pletinck, G. Glorieux, International urology and nephrology, 45 (2013) 139-150.

[376] R. Vanholder, E. Schepers, A. Pletinck, E.V. Nagler, G. Glorieux, Journal of the American Society of Nephrology, (2014).
[377] K. Fischer, P. Hoffmann, S. Voelkl, N. Meidenbauer, J. Ammer, M. Edinger, E. Gottfried, S. Schwarz, G. Rothe, S. Hoves, K. Renner, B. Timischl, A. Mackensen, L. Kunz-Schughart, R. Andreesen, S.W. Krause, M. Kreutz, Blood, 109 (2007) 3812-3819.
[378] F. Meyer, J. Wardale, S. Best, R. Cameron, N. Rushton, R. Brooks, Journal of Orthopaedic Research, 30 (2012) 864-871.
[379] P.H. Sechzer, L.D. Egbert, H.W. Linde, D.Y. Cooper, R.D. Dripps, H.L. Price, Journal of Applied Physiology, 15 (1960) 454-458.
[380] P.S. Ge, B.A. Runyon, JAMA, 312 (2014) 643-644.
[381] J.O. Clemmesen, F.S. Larsen, J. Kondrup, B.A. Hansen, P. Ott, Hepatology, 29 (1999) 648-653.
[382] F. Nayve, Jr., M. Motoki, M. Matsumura, H. Kataoka, Cytotechnology, 6 (1991) 121-130.
[383] M. Imran, Y. Shah, S. Nundlall, N.B. Roberts, M. Howse, Clinical Biochemistry, 45 (2012) 363-365.
[384] I.D. Weiner, W.E. Mitch, J.M. Sands, Clinical Journal of the American Society of Nephrology, (2014).
[385] T. Addis, E. Barrett, L.J. Poo, D.W. Yuen, Journal of Clinical Investigation, 26 (1947) 869-874.
[386] T.M.S. Chang, S. Prakash, Molecular Medicine Today, 4 (1998) 221-227.
[387] T. Chang, Canadian journal of physiology and pharmacology, 47 (1969) 1043-1045.
[388] M.H. Alderman, H. Cohen, S. Madhavan, S. Kivlighn, Hypertension, 34 (1999) 144-150.
[389] J. Jerotskaja, F. Uhlin, I. Fridolin, K. Lauri, M. Luman, A. Fernström, Blood purification, 29 (2009) 69-74.
[390] B.H. Ali, M. Alza'abi, A. Ramkumar, I. Al-Lawati, M.I. Waly, S. Beegam, A. Nemmar, S. Brand, N. Schupp, Food and Chemical Toxicology, 65 (2014) 321-328.
[391] D. Fliser, E. Ritz, American Journal of Kidney Diseases, 37 (2001) 79-83.
[392] R.L. Mehta, J.A. Kellum, S.V. Shah, B.A. Molitoris, C. Ronco, D.G. Warnock, A. Levin, Critical care, 11 (2007) R31.
[393] M. Yu, Y.J. Kim, D.-H. Kang, Clinical Journal of the American Society of Nephrology, 6 (2011) 30-39.
[394] M. Yisireyili, H. Shimizu, S. Saito, A. Enomoto, F. Nishijima, T. Niwa, Life Sciences, 92 (2013) 1180-1185.
[395] S. Lekawanvijit, A.R. Kompa, M. Manabe, B.H. Wang, R.G. Langham, F. Nishijima, D.J. Kelly, H. Krum, PLoS One, 7 (2012) e41281.
[396] W.-J. Wang, M.-H. Cheng, M.-F. Sun, S.-F. Hsu, C.-S. Weng, The Journal of toxicological sciences, 39 (2014) 637-643.
[397] Y. Adelibieke, H. Shimizu, S. Saito, R. Mironova, T. Niwa, Circulation Journal, 77 (2013) 1326-1336.
[398] Y. Ishima, T. Narisoko, U. Kragh-Hansen, S. Kotani, M. Nakajima, M. Otagiri, T. Maruyama, Biochemical and Biophysical Research Communications, 465 (2015) 481-487.
[399] V.-C. Wu, G.-H. Young, P.-H. Huang, S.-C. Lo, K.-C. Wang, C.-Y. Sun, C.-J. Liang, T.-M. Huang, J.-H. Chen, F.-C. Chang, Angiogenesis, 16 (2013) 609-624.
[400] S. Hatakeyama, H. Yamamoto, A. Okamoto, K. Imanishi, N. Tokui, T. Okamoto, Y. Suzuki, N. Sugiyama, A. Imai, S. Kudo, International journal of nephrology, 2012 (2012).
[401] T. Niwa, H. Shimizu, Journal of Renal Nutrition, 22 (2012) 102-106.
[402] X. Tao, S. Thijssen, N. Levin, P. Kotanko, G. Handelman, Blood purification, 39 (2015) 323-330.
[403] J.A. Kraut, N.E. Madias, Nature Reviews Nephrology, 8 (2012) 589-601.

[404] H. Okada, S. Araga, T. Takeshima, K. Nakashima, Headache: The Journal of Head and Face Pain, 38 (1998) 39-42.
[405] J.A. Kraut, N.E. Madias, New England Journal of Medicine, 371 (2014).
[406] G. Arthurs, M. Sudhakar, Continuing Education in Anaesthesia, Critical Care & Pain, 5 (2005) 207-210.
[407] J. Crowley, M. Wubben, J.M.C. Martin, Google Patents, 2012.
[408] M. Bernal, J. Lopez-Real, Bioresource Technology, 43 (1993) 27-33.
[409] N. Booker, E. Cooney, A. Priestley, Water science and technology, 34 (1996) 17-24.
[410] F.R.P. Nayve Jr, M. Motoki, M. Matsumura, H. Kataoka, Cytotechnology, 6 (1991) 121-130.
[411] R.E. Sparks, N.S. Mason, P.M. Meier, M.H. Litt, O. Lindan, ASAIO Journal, 17 (1971) 229-238.
[412] C.J. Lee, S.T. Hsu, Journal of biomedical materials research, 24 (1990) 243-258.
[413] S. Prakash, T. Chang, Nature medicine, 2 (1996) 883-887.
[414] H.D. Humes, W.H. Fissell, W.F. Weitzel, D.A. Buffington, A.J. Westover, S.M. MacKay, J.M. Gutierrez, American Journal of Kidney Diseases, 39 (2002) 1078-1087.
[415] R. Karaman, International Journal of Clinical Toxicology, 2 (2015) 37-41.
[416] T. Nakamura, E. Sato, N. Fujiwara, Y. Kawagoe, T. Suzuki, Y. Ueda, S.-i. Yamagishi, Metabolism, 60 (2011) 260-264.
[417] C. Barisione, G. Ghigliotti, M. Canepa, M. Balbi, C. Brunelli, P. Ameri, Current drug targets, 16 (2015) 366-372.
[418] N. Alwall, L. Norviit, A. Martin Steins, The Lancet, 251 (1948) 60-62.
[419] G.E. Schreiner, A.M.A. Archives of Internal Medicine, 102 (1958) 896-913.
[420] J.P. Merrill, S. Smith, E.J. Callahan, G.W. Thorn, Journal of Clinical Investigation, 29 (1950) 425-438.
[421] C.W. Gottschalk, S.K. Fellner, American Journal of Nephrology, 17 (1997) 289-298.
[422] A. Tütüncü, B. Lachmann, Perfluorocarbons as an alternative respiratory medium, Sepsis, Springer, 1994, pp. 549-563.
[423] Q.L. Loh, C. Choong, Tissue Engineering. Part B, Reviews, 19 (2013) 485-502.
[424] H. Pilch, K. Schlenger, E. Steiner, P. Brockerhoff, P. Knapstein, P. Vaupel, International Journal of Gynecological Cancer, 11 (2001) 137-142.
[425] S.M. Auerbach, K.A. Carrado, P.K. Dutta, Handbook of zeolite science and technology, CRC press, 2003.
[426] J.T. McCarthy, J.M. Steckelberg, Mayo Clinic Proceedings, 75 (2000) 1008-1014.
[427] M.L. Krieg, (2010).
[428] J. Wright, World Wide Wounds, (2001).
[429] T.C. Lee, P.F. Niederer, Basic Engineering for Medics and Biologists: An ESEM Primer, IOS Press, 2010.
[430] H. Jiankang, L. Dichen, L. Yaxiong, Y. Bo, L. Bingheng, L. Qin, Polymer, 48 (2007) 4578-4588.
[431] K.D. Vandegriff, Expert opinion on investigational drugs, 9 (2000) 1967-1984.
[432] N. Torio-Padron, J. Borges, A. Momeni, M.C. Mueller, F.T. Tegtmeier, G. Bjoern Stark, Minimally Invasive Therapy & Allied Technologies, 16 (2007) 155-162.
[433] O.I. Butt, R. Carruth, V.K. Kutala, P. Kuppusamy, N.I. Moldovan, Tissue engineering, 13 (2007) 2053-2061.
[434] P.S. Grim, L.J. Gottlieb, A. Boddie, E. Batson, JAMA, 263 (1990) 2216-2220.
[435] M. Ochoa, R. Rahimi, N. Alemdar, M.R. Dokmeci, A. Khademhosseini, B. Ziaie, Solid-State Sensors, Actuators and Microsystems (TRANSDUCERS & EUROSENSORS XXVII), 2013 Transducers & Eurosensors XXVII: The 17th International Conference on, 2013, pp. 2712-2715.

[436] L. Chevalier, C.D. McCann, International Journal of Environment and Waste Management, 2 (2008) 245-256.
[437] I. Gago, Google Patents, 1981.
[438] J. Wang, Y. Zhu, H.K. Bawa, G. Ng, Y. Wu, M. Libera, H.C. van der Mei, H.J. Busscher, X. Yu, ACS Applied Materials & Interfaces, 3 (2010) 67-73.
[439] J. Wu, W.L. Nyborg, Advanced drug delivery reviews, 60 (2008) 1103-1116.
[440] S. van Stroe-Biezen, F. Everaerts, L. Janssen, R. Tacken, Analytica chimica acta, 273 (1993) 553-560.
[441] S.K. Jonas, P.A. Riley, R.L. Willson, Biochem. J, 264 (1989) 651-655.
[442] M. Husmann, S. Schenderlein, M. Lück, H. Lindner, P. Kleinebudde, International journal of pharmaceutics, 242 (2002) 277-280.
[443] S. Johnson, V. Nguyen, D. Coder, Assessment of Cell Viability, Current Protocols in Cytometry, John Wiley & Sons, Inc., 2001.
[444] C.M. Robinson, R. Neary, A. Levendale, C.J. Watson, J.A. Baugh, Respiratory Research, 13 (2012) 74-74.
[445] B. Burke, A. Giannoudis, K.P. Corke, D. Gill, M. Wells, L. Ziegler-Heitbrock, C.E. Lewis, The American journal of pathology, 163 (2003) 1233-1243.
[446] C. Jamart, N. Benoit, J.-M. Raymackers, H. Kim, C. Kim, M. Francaux, European Journal of Applied Physiology, 112 (2012) 3173-3177.
[447] C. Robinson, R. Neary, A. Levendale, C. Watson, J. Baugh, Respiratory Research, 13 (2012) 74.
[448] S. Heiligenstein, M. Cucchiarini, M.W. Laschke, R.M. Bohle, D. Kohn, M.D. Menger, H. Madry, The Journal of Gene Medicine, 13 (2011) 230-242.
[449] R.D. Guzy, B. Hoyos, E. Robin, H. Chen, L. Liu, K.D. Mansfield, M.C. Simon, U. Hammerling, P.T. Schumacker, Cell Metabolism, 1 (2005) 401-408.
[450] J. Gleadle, P. Ratcliffe, Hypoxia, eLS, John Wiley & Sons, Ltd, 2001.
[451] J.L. Badger, M.L. Byrne, F.S. Veraitch, C. Mason, I.B. Wall, M.A. Caldwell, Regenerative Medicine, 7 (2012) 675-683.
[452] J.G. Pastorino, J.W. Snyder, A. Serroni, J.B. Hoek, J.L. Farber, Journal of Biological Chemistry, 268 (1993) 13791-13798.
[453] J. Allen, C. Winterford, R.A. Axelsen, G.C. GobÉ, Renal Failure, 14 (1992) 453-460.
[454] H.H. Schmidt, R. Stocker, C. Vollbracht, G. Paulsen, D. Riley, A. Daiber, A. Cuadrado, Antioxidants & redox signaling, (2015).
[455] Matés, gt, J.M, Toxicology, 153 (2000) 83-104.
[456] S.M. White, C.R. Pittman, R. Hingorani, R. Arora, T.V. Esipova, S.A. Vinogradov, C.C. Hughes, B. Choi, S.C. George, Tissue Engineering Part A, 20 (2014) 2316-2328.
[457] Z. Lu, W. Zhang, S. Jiang, J. Zou, Y. Li, Fertility and Sterility, 101 (2014) 568-576.
[458] L. Leroux, B. Descamps, N.F. Tojais, B. Séguy, P. Oses, C. Moreau, D. Daret, Z. Ivanovic, J.-M. Boiron, J.-M.D. Lamazière, P. Dufourcq, T. Couffinhal, C. Duplàa, Molecular Therapy, 18 (2010) 1545-1552.
[459] E. Nezu, Y. Ohashi, S. Kinoshita, R. Manabe, Japanese journal of ophthalmology, 36 (1991) 401-406.
[460] I. Kozlova, Y. Khalid, G.M. Roomans, Liver transplantation, 9 (2003) 268-278.
[461] F.O. Belzer, J.H. Southard, Transplantation, 45 (1988) 673-676.
[462] M. Southard, James H, M. Belzer, Folkert O, Annual review of medicine, 46 (1995) 235-247.
[463] G. Opelz, B. Döhler, Transplantation, 83 (2007) 247-253.
[464] M. Ikeda, T. Bando, T. Yamada, M. Sato, T. Menjyu, A. Aoyama, T. Sato, F. Chen, M. Sonobe, M. Omasa, H. Date, Surg Today, 45 (2015) 439-443.
[465] M.A. Roman, S. Nair, S. Tsui, J. Dunning, J.S. Parmar, Transplantation, 96 (2013) 509-

518.
[466] S.M. Minasian, M.M. Galagudza, Y.V. Dmitriev, A.A. Karpov, T.D. Vlasov, Interactive CardioVascular and Thoracic Surgery, 20 (2015) 510-519.
[467] Y. Takada, K. Boudjema, D. Jaeck, M. Bel-Haouari, M. Doghmi, M.-P. Chenard, P. Wolf, J. Cinqualbre, Transplantation, 59 (1995) 10-16.
[468] P. Schnuelle, M. Wehling, F. van der Woude, B. Yard, Cold preservation injury in organ transplantation: beneficial effects of dopamine and carbon monoxide releasing, 22 (2008) 45.
[469] J.M. Goujon, A. Vandewalle, H. Baumert, M. Carretier, T. Hauet, Kidney international, 58 (2000) 838-850.
[470] J.G. Baust, J.M. Baust, Advances in biopreservation, CRC Press, 2006.
[471] S.D. St Peter, C.J. Imber, P.J. Friend, The Lancet, 359 (2002) 604-613.
[472] L. Bunegin, J.F. Gelineau, Biomedical Instrumentation & Technology, 38 (2004) 155-164.
[473] T. Marada, K. Zacharovova, F. Saudek, European surgical research. Europaische chirurgische Forschung. Recherches chirurgicales europeennes, 44 (2009) 170-178.
[474] K. Takigami, S. Sasaki, N. Shiiya, M. Kawasaki, E. Takeuchi, K. Yasuda, The Annals of Thoracic Surgery, 66 (1998) 362-366.
[475] L. Brasile, P. DelVecchio, U. Rudofsky, C. Haisch, J. Clarke, Artificial Cells, Blood Substitutes and Biotechnology, 22 (1994) 1469-1475.
[476] L. Brasile, P. DelVecchio, K. Amyot, C. Haisch, J. Clarke, Artificial Cells, Blood Substitutes and Biotechnology, 22 (1994) 1463-1468.
[477] C. Wilson, M. Gok, B. Shenton, S. Balupuri, A. Gupta, J. Asher, D. Talbot, Annals of Transplantation, 9 (2004) 31-32.
[478] S. Matsumoto, S.A. Qualley, S. Goel, D.K. Hagman, I.R. Sweet, V. Poitout, D.M. Strong, R.P. Robertson, J.A. Reems, Transplantation, 74 (2002) 1414-1419.
[479] C.W. White, D. Hasanally, P. Mundt, Y. Li, B. Xiang, J. Klein, A. Müller, E. Ambrose, A. Ravandi, R.C. Arora, T.W. Lee, L.V. Hryshko, S. Large, G. Tian, D.H. Freed, The Journal of Heart and Lung Transplantation, 34 (2015) 113-121.
[480] B.J. Fuller, C.Y. Lee, Cryobiology, 54 (2007) 129-145.
[481] R. Thuillier, G. Allain, O. Celhay, W. Hebrard, B. Barrou, L. Badet, H. Leuvenink, T. Hauet, Journal of Surgical Research, 184 (2013) 1174-1181.
[482] T. Wille, H. de Groot, U. Rauen, Journal of Vascular Surgery, 47 (2008) 422-431.
[483] R.J. Korthuis, J.K. Smith, D.L. Carden, American Journal of Physiology-Heart and Circulatory Physiology, 256 (1989) H315-H319.
[484] U. Rauen, B. Polzar, H. Stephan, H.G. Mannherz, H. De Groot, The FASEB Journal, 13 (1999) 155-168.
[485] D. Hanh, B. Rajbhandari, A. Annachhatre, Environmental technology, 26 (2005) 581-590.
[486] L. Góth, Z. Tóth, I. Tarnai, M. Bérces, P. Török, W.N. Bigler, Clinical chemistry, 51 (2005) 2401-2404.
[487] N. Ma, J.J. Chalmers, J.G. Auniņš, W. Zhou, L. Xie, Biotechnology progress, 20 (2004) 1183-1191.
[488] H. Hiemstra, L. Dijkhuizen, W. Harder, European journal of applied microbiology and biotechnology, 18 (1983) 189-196.
[489] Q. Xiang, J. Yu, P.K. Wong, Journal of Colloid and Interface Science, 357 (2011) 163-167.
[490] Fields-Mprime Industrial Problem Solving Workshop, (2014).
[491] V. Verde, V. Fogliano, A. Ritieni, G. Maiani, F. Morisco, N. Caporaso, Free Radical Research, 36 (2002) 869-873.
[492] S.D. Çekiç, A.N. Avan, S. Uzunboy, R. Apak, Analytica Chimica Acta, 865 (2015) 60-

70.
[493] L.I. Brueggemann, B.K. Mani, J. Haick, K.L. Byron, Journal of Visualized Experiments : JoVE, (2012) 4263.
[494] L. Brasile, B.M. Stubenitsky, M.H. Booster, C. Haisch, G. Kootstra, American Journal of Transplantation, 3 (2003) 674-679.
[495] X. Tillou, R. Thuret, A. Doerfler, Progrès en urologie, 24 (2014) S51-S55.
[496] H.U. Simon, A. Haj-Yehia, F. Levi-Schaffer, Apoptosis, 5 (2000) 415-418.
[497] C. Fleury, B. Mignotte, J.-L. Vayssière, Biochimie, 84 (2002) 131-141.
[498] A. Boveris, B. Chance, Biochem. J, 134 (1973) 707-716.
[499] M. Quintana, T. Kahan, P. Hjemdahl, American Journal of Cardiovascular Drugs, 4 (2004) 159-167.
[500] J. Wang, Y. Zhu, H.K. Bawa, G. Ng, Y. Wu, M. Libera, H. van der Mei, H. Busscher, X. Yu, ACS applied materials & interfaces, 3 (2010) 67-73.
[501] E. Maillard, M.T. Juszczak, A. Clark, S.J. Hughes, D.R.W. Gray, P.R.V. Johnson, Biomaterials, 32 (2011) 9282-9289.
[502] D. Maluf, V. Mas, K. Yanek, J. Stone, R. Weis, D. Massey, B. Spiess, M. Posner, R. Fisher, Transplantation proceedings, Elsevier, 2006, pp. 1243-1246.
[503] G. Chen, A.F. Palmer, Biotechnology and Bioengineering, 105 (2010) 534-542.
[504] G. Kroemer, L. Galluzzi, C. Brenner, Mitochondrial Membrane Permeabilization in Cell Death, 2007.
[505] E.J. Griffiths, Cardiovascular research, 46 (2000) 24-27.
[506] N. Sasaki, H. Horinouchi, A. Ushiyama, H. Minamitani, The Keio journal of medicine, 61 (2012) 57-65.
[507] R. Motterlini, H. Kerger, C.J. Green, R.M. Winslow, M. Intaglietta, American Journal of Physiology-Heart and Circulatory Physiology, 275 (1998) H776-H782.
[508] S.M. Schwartz, E.P. Benditt, The American journal of pathology, 66 (1972) 241.
[509] G. Olivetti, M. Melissari, G. Marchetti, P. Anversa, Circulation research, 51 (1982) 19-26.
[510] M.A. Howard, R. Asmis, K.K. Evans, T.A. Mustoe, Wound Repair and Regeneration, 21 (2013) 503-511.
[511] J.D. WHITNEY, AACN Advanced Critical Care, 1 (1990) 578-584.
[512] K. Jönsson, T.K. Hunt, S.J. Mathes, Annals of surgery, 208 (1988) 783.
[513] D.G. Scarpelli, R.A. Knouff, C.A. Angerer, Experimental Biology and Medicine, 84 (1953) 94-96.
[514] H. Hopf, T.K. Hunt, J.M. West, et al., Archives of Surgery, 132 (1997) 997-1004.
[515] D.B. Allen, J.J. Maguire, M. Mahdavian, C. Wicke, L. Marcocci, H. Scheuenstuhl, M. Chang, A.X. Le, H.W. Hopf, T.K. Hunt, Archives of Surgery, 132 (1997) 991-996.
[516] S.J. KLEBANOFF, Annals of Internal Medicine, 93 (1980) 480-489.
[517] S.A. Eming, T. Krieg, J.M. Davidson, Journal of Investigative Dermatology, 127 (2007) 514-525.
[518] S. Baranoski, Nursing2014, 38 (2008) 14-15.
[519] J.L. Jensen, J. Seeley, B. Gillin, Advances in Skin & Wound Care, 11 (1998) 1-4.
[520] R. Jayakumar, M. Prabaharan, P.T. Sudheesh Kumar, S.V. Nair, H. Tamura, Biotechnology Advances, 29 (2011) 322-337.
[521] P.H. Corkhill, C.J. Hamilton, B.J. Tighe, Biomaterials, 10 (1989) 3-10.
[522] O. Wichterle, D. Lim, (1960).
[523] P.H. Corkhill, A.M. Jolly, C.O. Ng, B.J. Tighe, Polymer, 28 (1987) 1758-1766.
[524] D. Knighton, I. Silver, T. Hunt, Surgery, 90 (1981) 262-270.
[525] T.K. Hunt, Journal of Trauma and Acute Care Surgery, 30 (1990) 122-128.
[526] T. Hunt, Surg Gynecol Obstet, 135 (1972) 561-567.

[527] M. Al-Abbasi, J. Tarlton, Spine Journal Meeting Abstracts, (2011).
[528] J.F. Lo, M. Brennan, Z. Merchant, L. Chen, S. Guo, D.T. Eddington, L.A. DiPietro, Wound Repair and Regeneration, 21 (2013) 226-234.
[529] D. Hohn, R. MacKay, B. Halliday, T. Hunt, Surgical forum, 1976, pp. 18.
[530] C.L. Hess, M.A. Howard, C.E. Attinger, Annals of plastic surgery, 51 (2003) 210-218.
[531] M. Jones, J.G. Ganopolsky, A. Labbé, M. Gilardino, C. Wahl, C. Martoni, S. Prakash, International wound journal, 9 (2012) 330-343.
[532] V. Agarwal, S. Aroor, N. Gupta, A. Gupta, N. Agarwal, N. Kaur, Indian Journal of Surgery, (2015) 1-4.
[533] N. Atrux-Tallau, T. Le, A. Denis, K. Padois, H. Zahouani, M. Haftek, F. Falson, F. Pirot, Skin pharmacology and physiology, 22 (2009) 210-217.
[534] S.L. Percival, S. McCarty, J.A. Hunt, E.J. Woods, Wound Repair and Regeneration, 22 (2014) 174-186.
[535] Y. Abramov, B. Golden, M. Sullivan, S.M. Botros, J.J.R. Miller, A. Alshahrour, R.P. Goldberg, P.K. Sand, Wound repair and regeneration, 15 (2007) 80-86.
[536] S.A. Eming, T. Krieg, J.M. Davidson, J Invest Dermatol, 127 (0000) 514-525.
[537] D.R. Knighton, V.D. Fiegel, T. Halverson, S. Schneider, T. Brown, C.L. Wells, Archives of Surgery, 125 (1990) 97-100.
[538] R.N. Pittman, (2011).
[539] G.M. Gordillo, C.K. Sen, The American Journal of Surgery, 186 (2003) 259-263.
[540] A.Y. Sheikh, J.J. Gibson, M.D. Rollins, H.W. Hopf, Z. Hussain, T.K. Hunt, Archives of Surgery, 135 (2000) 1293-1297.
[541] G.M. Gordillo, C.K. Sen, The international journal of lower extremity wounds, 8 (2009) 10.1177/1534734609335149.
[542] K. Jonsson, J.A. Jensen, W. Goodson 3rd, H. Scheuenstuhl, J. West, H.W. Hopf, T.K. Hunt, Annals of surgery, 214 (1991) 605.
[543] W. Bullough, M. Johnson, (1951).
[544] S. Dan Dimitrijevich, S. Paranjape, J.R. Wilson, R.W. Gracy, J.G. Mills, Wound Repair and Regeneration, 7 (1999) 53-64.
[545] M.A. Karasek, The Journal of Investigative Dermatology, 47 (1966) 533-540.
[546] P.G. Banks, C.H. Ho, The Journal of Spinal Cord Medicine, 31 (2008) 297-301.
[547] F. Hirsh, S.J. Berlin, A. Holtz, Advances in skin & wound care, 22 (2009) 20-24.
[548] H.K. Said, J. Hijjawi, N. Roy, J. Mogford, T. Mustoe, Archives of Surgery, 140 (2005) 998-1004.
[549] S. Chien, Wound repair and regeneration, 15 (2007) 928-935.
[550] P. Niethammer, C. Grabher, A.T. Look, T.J. Mitchison, Nature, 459 (2009) 996-999.
[551] L.M. Bang, C. Buntting, P. Molan, The Journal of Alternative & Complementary Medicine, 9 (2003) 267-273.
[552] O.M. Tepper, J.M. Capla, R.D. Galiano, D.J. Ceradini, M.J. Callaghan, M.E. Kleinman, G.C. Gurtner, Blood, 105 (2005) 1068-1077.
[553] K.S. Pinski, H.H. Roenigk, The Journal of Dermatologic Surgery and Oncology, 18 (1992) 179-186.
[554] T. Yamauchi, J. Kamon, H. Waki, Y. Terauchi, N. Kubota, K. Hara, Y. Mori, T. Ide, K. Murakami, N. Tsuboyama-Kasaoka, Nature medicine, 7 (2001) 941-946.
[555] T.T. Tran, C.R. Kahn, Nature Reviews Endocrinology, 6 (2010) 195-213.
[556] A. Casadei, R. Epis, L. Ferroni, I. Tocco, C. Gardin, E. Bressan, S. Sivolella, V. Vindigni, P. Pinton, G. Mucci, BioMed Research International, 2012 (2012).
[557] T.A. Moseley, M. Zhu, M.H. Hedrick, Plastic and Reconstructive Surgery, 118 (2006) 121S-128S.
[558] M. Cherubino, K.G. Marra, Regenerative Medicine, 4 (2008) 109-117.

[559] K. Yoshimura, K. Sato, N. Aoi, M. Kurita, T. Hirohi, K. Harii, Aesthetic Plast Surg, 32 (2008) 48-55.
[560] K. Yoshimura, K. Sato, N. Aoi, M. Kurita, K. Inoue, H. Suga, H. Eto, H. Kato, T. Hirohi, K. Harii, Dermatologic Surgery, 34 (2008) 1178-1185.
[561] B.L. Eppley, R.V. Snyders Jr, T. Winkelmann, J.J. Delfino, Journal of Oral and Maxillofacial Surgery, 50 (1992) 477-482.
[562] B.L. Eppley, R.A. Sidner, J.M. Platis, A.M. Sadove, Plastic and Reconstructive Surgery, 90 (1992) 1022-1030.
[563] U. Smith, The Anatomical Record, 169 (1971) 97-104.
[564] K.A. Carswell, M.-J. Lee, S.K. Fried, Methods Mol Biol, 806 (2012) 203-214.
[565] H. Suga, H. Eto, N. Aoi, H. Kato, J. Araki, K. Doi, T. Higashino, K. Yoshimura, Plastic and reconstructive surgery, 126 (2010) 1911-1923.
[566] Y. Xu, P. Malladi, M. Chiou, E. Bekerman, A.J. Giaccia, M.T. Longaker, Tissue engineering, 13 (2007) 2981-2993.
[567] J. Ye, International journal of obesity, 33 (2009) 54-66.
[568] J.H. Dolderer, K.M. Abberton, E.W. Thompson, J.L. Slavin, G.W. Stevens, A.J. Penington, W.A. Morrison, Tissue Engineering, 13 (2007) 673-681.
[569] X. Chen, A.S. Aledia, C.M. Ghajar, C.K. Griffith, A.J. Putnam, C.C. Hughes, S.C. George, Tissue Engineering Part A, 15 (2008) 1363-1371.
[570] N. Asakawa, T. Shimizu, Y. Tsuda, S. Sekiya, T. Sasagawa, M. Yamato, F. Fukai, T. Okano, Biomaterials, 31 (2010) 3903-3909.
[571] M.A. Brennan, J.-M. Davaine, P. Layrolle, Stem cell research & therapy, 4 (2013) 96.
[572] T.O. Pedersen, A.L. Blois, Z. Xing, Y. Xue, Y. Sun, A. Finne-Wistrand, L.A. Akslen, J.B. Lorens, K.N. Leknes, I. Fristad, Stem Cell Res Ther, 4 (2013) 52.
[573] S. Takeshita, L. Zheng, E. Brogi, M. Kearney, L. Pu, S. Bunting, N. Ferrara, J. Symes, J. Isner, Journal of Clinical Investigation, 93 (1994) 662.
[574] C.J. Frederickson, E. Kasarskis, D. Ringo, R. Frederickson, Journal of neuroscience methods, 20 (1987) 91-103.
[575] R.J. Hajjar, J.S. Hulot, Circulation Research, (2013).
[576] E.C. Perin, H.F.R. Dohmann, R. Borojevic, S.A. Silva, A.L.S. Sousa, C.T. Mesquita, M.I.D. Rossi, A.C. Carvalho, H.S. Dutra, H.J.F. Dohmann, G.V. Silva, L. Belém, R. Vivacqua, F.O.D. Rangel, R. Esporcatte, Y.J. Geng, W.K. Vaughn, J.A.R. Assad, E.T. Mesquita, J.T. Willerson, Circulation, 107 (2003) 2294-2302.
[577] H.C. Ott, T.S. Matthiesen, S.-K. Goh, L.D. Black, S.M. Kren, T.I. Netoff, D.A. Taylor, Nat Med, 14 (2008) 213-221.
[578] M. Lin, R. Liu, D. Gozal, W.B. Wead, M.W. Chapleau, R. Wurster, Z. Cheng, American Journal of Physiology - Heart and Circulatory Physiology, 293 (2007) H997-H1006.
[579] N. Tandon, C. Cannizzaro, P.-H.G. Chao, R. Maidhof, A. Marsano, H.T.H. Au, M. Radisic, G. Vunjak-Novakovic, Nat. Protocols, 4 (2009) 155-173.
[580] G. Turitto, J.M. Fontaine, S.N. Ursell, E.B. Caref, R. Henkin, N. El-Sherif, The American Journal of Cardiology, 61 (1988) 1272-1278.
[581] Y. Huang, J.C. Williams, S.M. Johnson, Lab on a Chip, 12 (2012) 2103-2117.
[582] J.A. Gaasch, P.R. Lockman, W.J. Geldenhuys, D.D. Allen, C.J. Van der Schyf, Neurochemical research, 32 (2007) 1196-1208.
[583] B. Halliwell, Journal of neurochemistry, 97 (2006) 1634-1658.
[584] C.W. Levenson, Physiology & behavior, 86 (2005) 399-406.
[585] S. Kern, H. Eichler, J. Stoeve, H. Klüter, K. Bieback, Stem cells, 24 (2006) 1294-1301.
[586] J. Justesen, K. Stenderup, E. Ebbesen, L. Mosekilde, T. Steiniche, M. Kassem, Biogerontology, 2 (2001) 165-171.
[587] M.F. Pittenger, A.M. Mackay, S.C. Beck, R.K. Jaiswal, R. Douglas, J.D. Mosca, M.A.

Moorman, D.W. Simonetti, S. Craig, D.R. Marshak, science, 284 (1999) 143-147.
[588] F.S. Loffredo, M.L. Steinhauser, J. Gannon, R.T. Lee, Cell stem cell, 8 (2011) 389-398.
[589] B.L. Krock, N. Skuli, M.C. Simon, Genes & Cancer, 2 (2011) 1117-1133.
[590] D. Liao, R. Johnson, Cancer Metastasis Rev, 26 (2007) 281-290.
[591] H.E. Abaci, R. Truitt, S. Tan, S. Gerecht, American Journal of Physiology-Cell Physiology, 301 (2011) C431-C440.
[592] T.K. Hunt, B. Zederfeldt, T.K. Goldstick, The American Journal of Surgery, 118 (1969) 521-525.

**Chapter 10**

**Submitted manuscript**

This chapter includes the manuscript submitted to Advanced Materials. This manuscript contains the key findings in this thesis.

DOI: 10.1002/(())

**Article type: Communication**

# Degradable synthetic micro-lungs for bloodless tissue viability

*Huaifa Zhang, Hani Shash, Yu Ling Zhang, Amal Al-Odaini, Daisuke Sato, Mirko S. Gilardino, Simon Tran, Jake E. Barralet**

H. Zhang, Y. L. Zhang, Dr. D. Sato, Prof. S. Tran, Prof. J. E. Barralet
Faculty of Dentistry, McGill University, Montreal, QC, H3A 0C7 Canada
E-mail: jake.barralet@mcgill.ca
H. Shash, Prof. M. S. Gilardino
Division of Plastic and Reconstructive Surgery, Department of Surgery, Faculty of Medicine, McGill University, Montreal, QC, H3G 1A4 Canada
A. AlOdaini
Division of Medical Oncology, Faculty of Medicine, McGill University, Montreal, QC, H3G 1A4 Canada
Prof. J. E. Barralet
Division of Orthopaedics, Department of Surgery, Faculty of Medicine, McGill University, Montreal, QC, H3G 1A4 Canada

Keywords: peroxide, oxygen delivery, tissue engineering, tissue preservation, microbead

Aside from some species of loriciferans [1], no animal is known to survive entirely in the absence of oxygen ($O_2$). Local loss of tissue oxygenation can occur by injury or disease of the blood vessels, for example following radiotherapy [2] or ischemic heart disease [3], following tissue or cell transplantation [4] or after cell, organ or tissue harvesting [5]. New blood vessels

can grow at a rate of around 150 μm per day [6] to alleviate small regions of ischemia, but avascular tissue volumes greater than ~0.17 mL become necrotic upon implantation indicating a maximal passive diffusion distance of up to ~2.8 mm is sufficient to maintain viability during revascularization [7, 8]. This discrepancy between revascularization rate and necrosis rate has been one of the fundamental impediments to creating large volumes of functional implantable engineered tissues despite numerous creative attempts to circumvent this problem. [9]

Prior strategies have included prevascularization, addition of angiogenesis inducing growth factors, layering of cell sheets, the use of arterial-venous grafts, perfusion of decellularized tissues, and the creation of perfusable synthetic channels using a variety of 3D printing, microfabrication and casting technologies. [10]

The inability of materials science to overcome this critical hurdle of maintaining oxygen delivery is a sad familiarity, with heart ischemia being the third most frequent cause of death, organ donor waiting times are static and 5% of donation candidates die annually [11], and the inability to transplant large tissue volumes that lack a vascular pedicle limits reconstructive surgery and organ/tissue transplantation.

Several synthetic biomaterials can release oxygen either by virtue of competitive gaseous solubility or binding (e.g. perfluorocarbons and crosslinked hemoglobin) or decomposition of inorganic compounds such as peroxides, perborates and perchlorates. [12, 13] The former group of materials was mainly developed as blood replacements and for liquid ventilation of the lungs. [14] The temporary loss of function of the heart and or lungs is successfully managed surgically by cardiopulmonary bypass and membrane oxygenators. [15] On a smaller scale, mechanical perfusion of oxygenated fluids is an approach to organ preservation, but is still mainly at an

experimental stage with cold storage, in order to slow metabolic rate and hence oxygen demand, being more usual. [16]

The oxygen delivery capability of thermodynamically unstable per-oxyanionic salts has been known for decades and was first used for artificial soil oxygenation. [17] They are also used in aquaculture for fish transportation and remediation of poor oxygen availability. [18] However, their efficacy of oxygen delivery to mammalian tissues and cells is limited.

The oxygen forming aqueous decomposition of calcium peroxide (CP) to calcium hydroxide proceeds via the formation of cytotoxic hydrogen peroxide ($H_2O_2$) and radical intermediates. [19, 20] To date, attempts to utilize this reaction in biological systems have been restricted to polymer embedded CP. [13, 21, 22] The polymer aims to retard water diffusion and hence control oxygen delivery and have had some limited success in prolonging cell survival in hypoxic culture conditions. [13, 22] Reduction of $H_2O_2$ levels has been addressed *in vivo* by using $MnCl_2$ and *in vitro* by using catalase catalysts. [23] While proof of concept was demonstrated, these approaches are non-ideal as $MnCl_2$ is itself toxic [24] and catalase, being a non-autologous protein, is not a favored approach for further clinical development.

To date there has only been one reported study on the implantation of peroxide containing materials namely a peroxidase free poly(lactic-co-glycolic acid) (PLGA)-sodium percarbonate film. [21] The intent was to aid partially ischemic skin flap survival. Sustained release was only achieved for 1 d, bubbles were formed and at 7 d the amount of necrosis was comparable between experimental and negative control groups.

This study then sought to develop the first implantable and degradable oxygen delivery system (ODS) that was able to achieve long-term sustenance of hypoxic cells and tissues *in vivo*. Key challenges overcome were to minimize $H_2O_2$ concentration locally, prevent reactive oxygen species damage, eliminate bubbling that could cause embolism, and maintain tolerable oxygen concentrations. In nature gaseous exchange structures (e.g. lungs, gills and leaves) have high surface areas not only to overcome diffusion kinetics but also to dissipate waste metabolites at sub-cytotoxic concentrations. For example fish gills have areas up to 1000 $cm^2$ [25] and have total ammonia excretion rates of ~ 2 mM $kg^{-1}$ $h^{-1}$ [26], yet acute ammonia toxicity levels for fish is only around 2 mM $L^{-1}$ [27]. All prior inorganic peroxide biomaterials systems were produced either in sheet or block form [13, 22] with areas in the range of only 0.2 $m^2$ $g^{-1}$ or less. By forming polymer embedded CP as porous microbeads (**Figure 1**a, Figure S1) that had a surface area of 6.3 $m^2$ $g^{-1}$ (Figure 1b) rather than monoliths we found that $H_2O_2$ concentrations were much lower after the initial aqueous reaction had occurred **(Figure 2**a). Moreover, the presence of hydrogel reduced the concentration of $H_2O_2$ in the storage media (Figure S2a) to below 1 ppm (Figure S2b). Radical concentrations around the material were not markedly different in the presence of hydrogel (Figure 2b, Figure S2c). Given their short lifetime [28], radical diffusion distances can be expected to be some ~nm therefore hydrogel encapsulation also minimized radical-cell membrane interactions. The decomposition of CP releases hydroxyl ions and can increase pH > 10 (Figure S2d, f). We established that in a buffered culture system and therefore likely also *in vivo*, the alkalinity was neutralized (Figure S2e), and calcite was formed which neutralized the system (Figure 1c). This simple microstructural change towards a more biomimetic form had a dramatic effect and cytotoxicity experiments confirmed a vast improvement in cell survival. The presence, of either $MnO_2$ or degradable $Fe_3O_4$, catalysts further greatly improved cell viability and, only the micro-lung system (MLS), i.e. microbeads with catalysts in hydrogel, effectively acted as micro-lungs and supported cell growth while

the other types of ODS nearly killed all the cells (Figure 2c). Cells cultured with the optimal oxygen-release material under anoxia maintained a cell growth rate similar to that cultured under normoxia (Figure 2c), suggesting that the oxygen-release material restored oxygen to a tolerable level for the cells.

Hypoxia is one of the major factors limiting tissue and organ preservation time. [29] Prolonging preservation under hypoxia by reduction of the metabolic rate is achieved by cooling (hypothermia) [30], but creates an additional issue namely reperfusion injury upon warming [31]. Warm perfusion avoids this but can result in shear damage to blood vessels and requires hardware to supply pressurized oxygenation fluids. [32] Preservation of a functioning vasculature is a fundamental impediment to any new approaches for normothermic tissue and organ preservation and tissue engineering [33].

Prior work on oxygen delivery has focussed solely on putting oxygen into tissue, presumably with the assumption that the tissues will consume it at a rate higher than or equal to the rate of supply. From 37 ˚C to 0 ˚C in air the oxygen content of saturated water increases from 200 µM to 457 µM. [34] In equilibrium with pure oxygen however, these values are five times higher, which is generally way beyond cytotoxic limits [27, 35]. One can appreciate then that delivery of pure oxygen in the absence of an oxygen sink can easily cause cell damage. A key discovery in our work was that the provision of an oxygen sink, namely flowing (200 mL $min^{-1}$) of $N_2$ gas through the culture system, appeared to provide more optimum oxygen ranges during culture. Experiments were performed attempting to preserve arteries with our degradable MLS. Anatomically these impermeable tissues transport highly oxygenated blood but little transluminal oxygenation occurs [36], and so MLS was placed inside, outside and completely surrounding the dissected arteries. Interestingly best survival was observed combining MLS

surrounding the tissue only with anoxic culture (**Figure 3**a, Figure S3). At 37 ˚C the mitochondrial membrane potential of the endothelial cells was maintained (Figure 3a) and the vessels retained 90% of their original KCl stimulated contraction force (Figure 3b) compared with the hypothermically stored control that had 5% membrane potential (Figure 3a), and 50% contraction force after 7 d (Figure 3b). The sample stored under normoxia, either with or without oxygen-release microbeads, displayed poor cell viability and lost mitochondrial membrane potential (Figure S3a, b). This approach then overcame a key obstacle in tissue and organ preservation and tissue engineering.

Externally, $H_2O_2$ is routinely used as an antibacterial [37] and we were keen to discover if the peroxide cytotoxicity we observed *in vitro* would be more potent an inhibitor of healing than oxygen deficiency. Using an ischemic wound healing model [38], we compared healing of 15 mm diameter full thickness wounds treated with alginate patches with and without the a disc form slab of PCL encapsulated $Fe_3O_4$ and CP. The control wounds became necrotic by day 7 (Figure 3c), possibly due to desiccation of the cartilage from lack of epithelial coverage, despite the use of an alginate hydrogel barrier, whereas the underlying tissue mainly survived with the oxygen delivery patch (ODP) and histologically granulation tissue formation (Figure S4) and reepithelisation occurred (Figure S4 arrow, Table S1).

One of the main obstacles for high density cell culture, approaching physiological tissue cell densities (~1-5×$10^8$ cells $mL^{-1}$) [39], is oxygen deficiency in the culture system [40]. Efforts have been made to increase cell density in bioreactors in the biopharmaceutical industry by oxygenating the culture medium by perfusion or gas sparging [41], but are limited [42]. We sought to use MLS to supply oxygen to Chinese Hamster Ovary (CHO) cells at a physiological density. Lactate dehydrogenase (LDH) release from dead cells was reduced twofold in the oxgyen

delivery scaffold (Figure 3d), indicating our oxygen-release system can alleviate oxygen shortage in high density cell culture. The cell viability in the experimental group was increased by 100% compared with the control group after 24 h (Figure S5),

Cell and tissue transplantation is frequently attempted clinically e.g. to restore hormonal function and cosmetic appearance [43, 44], but the lack of viability post implantation limits efficiency and in some cases raises doubt as to efficacy [44, 45]. We chose a hypoxia sensitive Madin-Darby canine kidney (MDCK) cell line [46] to test whether we could encapsulate such cells at a density of $1\times10^6$ cells $mL^{-1}$ in a 5 mm MLS sphere and then transplant them subcutaneously, since 3 mm adipose (a generally hypoxia resistant tissue) tissue transplants have been observed to become necrotic following transplantation [8].

The MLS maintained viability of transplanted MDCK cells and supported cell growth (**Figure 4**a, b) for four weeks. In addition, vascularization was promoted in MLS (Figure 4c, d). Although cell density was similar on the edge area of the implants either in the experimental or control group, MLS significantly increased cell density in the central area of the implant (Figure S6).

Current standard mammalian cell culture conditions developed some 60 years ago [47], i.e. serum and protein fortified media buffered with 5% $CO_2$, in equilibrium with air rather than haemoglobin, are often considered inadequate since they are usually 2D systems rather than 3D [48]. But more fundamentally incorrect than that is the issue that this 'standard culture condition' is hyperoxic compared with physiological conditions [49, 50]. What is often termed hypoxic culture (1-5% $O_2$) is often more close to physiological conditions [13, 49, 51]. Recently one report used an anoxic control [52] but prior work used inaccurately termed hypoxic controls.

Anoxic culture is more severe than subcutaneous implantation in hydrogel in terms of oxygen deprivation and appears that it can be used to replace animals during formulation optimisation. Finally to showcase how critical optimisation of the ODS microstructure is to getting this system to work efficiently, we attempted to maintain brain tissue viability in anoxia. The brain is extremely sensitive to foreign bodies and very few biomaterials are biocompatible with it. [53] The ability to maintain brain viability without a blood supply is currently not possible. Efforts have focused on perfused brain slice cultures and to date the limit for *in vitro* maintenance is 700 μm thick slices [54]. We used 2 mm thickness (Figure S7a) to evaluate whether it was technically possible to sustain brain tissue at normothermic conditions in oxygen-free buffered nitrogen. Impressively, 95% and 90% viability at 4 (Figure S7b) and 24 h (Figure 4e) respectively in comparison with complete cell death in controls (Figure S7b and Figure 4e) were obtained. It remains to be seen whether this degradable biomaterials system could be tolerated in the brain *in vivo,* but certainly this study for the first time highlights the importance of minimizing oxygen, $H_2O_2$ and radical accumulation and advances the field of synthetic materials for tissue oxygenation significantly and offers hope of new treatments strategies for conditions that currently end in severe reduction in quality of life, amputation and even death.

**Supporting Information**

Supporting Information is available from the Wiley Online Library or from the author.

**Acknowledgements**

BioPloymer for providing us with sodium alginate. Advanced Polymer Materials Inc. for providing us with PLGA. NSERC Strategic Grant, China Scholarship Council (CSC).

Received: ((will be filled in by the editorial staff))

Revised: ((will be filled in by the editorial staff))

Published online: ((will be filled in by the editorial staff))

[1] R. Danovaro, A. Dell'Anno, A. Pusceddu, C. Gambi, I. Heiner, R. M. Kristensen, *BMC Biol.* **2010**, *8*, 30.

[2] N. Imaizumi, Y. Monnier, M. Hegi, R.-O. Mirimanoff, C. Ruegg, *PLoS One* **2010**, *5*, e11084.

[3] K. A. Reimer, R. E. Ideker, *Hum. Pathol.* **1987**, *18*, 462.

[4] a) T. S. Leary, J. R. Klinck, G. Hayman, P. Friend, N. V. Jamieson, A. K. Gupta, *Anes.* **2002**, *57*, 1128; b) C. K. Colton, *Cell Transplant.* **1995**, *4*, 415; c) M. K. Smith, M. C. Peters, T. P. Richardson, J. C. Garbern, D. J. Mooney, *Tissue Eng.* **2004**, *10*, 63.

[5] S. Henry, E. Nachber, J. Tulipan, J. Stone, C. Bae, L. Reznik, T. Kato, B. Samstein, J. Emond, J. Guarrera, *Am. J. Transplant.* **2012**, *12*, 2477.

[6] a) P. J. Ferrone, J. J. Dutton, *Ophthalmology* **1992**, *99*, 376; b) C. L. Shields, J. A. Shields, R. C. Eagle, P. De Potter, *Am. J. Ophthalmol.* **1991**, *111*, 363.

[7] O. Gavrilova, B. Marcus-Samuels, D. Graham, J. K. Kim, G. I. Shulman, A. L. Castle, C. Vinson, M. Eckhaus, M. L. Reitman, *Am. J. Ophthalmol.* **2000**, *105*, 271.

[8] H. Eto, H. Kato, H. Suga, N. Aoi, K. Doi, S. Kuno, K. Yoshimura, *Plast. Reconstr. Surg.* **2012**, *129*, 1081.

[9] E. C. Novosel, C. Kleinhans, P. J. Kluger, *Adv. Drug Deliver. Rev.* **2011**, *63*, 300.

[10] a) A. G. Mikos, G. Sarakinos, M. D. Lyman, D. E. Ingber, J. P. Vacanti, R. Langer, *Biotechnol. Bioeng.* **1993**, *42*, 716; b) H.-L. M. Cheng, C. Wallis, Z. Shou, W. A. Farhat, *J.Magn. Reson. I.* **2007**, *25*, 137; c) L. Dew, S. MacNeil, C. K. Chong, *Regen.Med.* **2015**, *10*, 211; d) S. N. Nazhat, E. A. Abou Neel, A. Kidane, I. Ahmed, C. Hope, M. Kershaw, P. D. Lee,

E. Stride, N. Saffari, J. C. Knowles, *Biomacromolecules* **2007**, *8*, 543; e) J. Yang, W. Zhou, W. Zheng, Y. Ma, L. Lin, T. Tang, J. Liu, J. Yu, X. Zhou, J. Hu, *Cardiology* **2007**, *107*, 17; f) S. A. Hussaini, M. Ahmed, *J. Surg. Pakistan (Int.)* **2012**, *17*, 3; g) J. Haag, S. Baiguera, P. Jungebluth, D. Barale, C. Del Gaudio, F. Castiglione, A. Bianco, C. E. Comin, D. Ribatti, P. Macchiarini, *Biomaterials* **2012**, *33*, 780; h) H.-J. Sung, C. Meredith, C. Johnson, Z. S. Galis, *Biomaterials* **2004**, *25*, 5735; i) K. Matsuura, R. Utoh, K. Nagase, T. Okano, *J.Control. release* **2014**, *190*, 228.

[11] e-Statistics Report on Transplant, https://www.cihi.ca/en/types-of-care/specialized-services/organ-replacements/e-statistics-report-on-transplant-waiting-li-2, accessed: Octomber, **2015**.

[12] a) J. G. Riess, *Artif. cells Blood Substit. Biotechnol.* **2006**, *34*, 567; b) A. W. Sielenkamper, I. H. Chin-Yee, C. M. Martin, W. J. Sibbald, *Am. J. Respir. Crit. Care Med.* **1997**, *156*, 1066; c) M. Reuss (Reckitt Gmbh), *US5015408 A*,**1991**; d) C. B. Jackson, R. M. Bovard (Mine Safety Appliances Co), *US2558756 A*, **1951**.

[13] E. Pedraza, M. M. Coronel, C. A. Fraker, C. Ricordi, C. L. Stabler, *Proc. Natl. Acad. Sci. U. S. A.* **2012**, *109*, 4245.

[14] a) R. P. Geyer, *N. Engl. J. Med.* **1973**, *289*, 1077; b) T. Pranikoff, P. G. Gauger, R. B. Hirscl, *ASAIO J.* **1996**, *42*, 317.

[15] a) H. Huang, T. Yao, W. Wang, D. Zhu, W. Zhang, H. Chen, W. Fu, *Ann. Thorac. Surg.* **2003**, *76*, 136; b) N. Cavarocchi, J. Pluth, H. Schaff, T. Orszulak, H. Homburger, E. Solis, M. Kaye, M. Clancy, J. Kolff, G. Deeb, *J. Thorac. Cardiovas. Surg.* **1986**, *91*, 252; c) T. Fuehner, C. Kuehn, J. Hadem, O. Wiesner, J. Gottlieb, I. Tudorache, K. M. Olsson, M. Greer, W. Sommer, T. Welte, *Am. J. Respir. Crit. Care Med.* **2012**, *185*, 763.

[16] a) D. R. Monbaliu, C. Debbaut, W. J. Hillewaert, W. J. Laleman, M. Sainz-Barriga, J. Pirenne, P. Segers, *Int. J. Artif. Organs* **2012**, *35*, 119; b) J. Treckmann, C. Moers, J. M. Smits,

A. Gallinat, M. H. J. Maathuis, M. van Kasterop-Kutz, I. Jochmans, J. J. Homan van der Heide, J. P. Squifflet, E. van Heurn, *Transpl. Int.* **2011**, *24*, 548.

[17] a) D. P. Cassidy, R. L. Irvine, J. Hazard. Mater. **1999**, *69*, 25; b) T. Langan, J. Pendleton, E. Oplinger, *Agron. J.* **1986**, *78*, 769.

[18] W. Qinse, J. Jingnan, J. Zongyao, *J. Zhanjiang Ocean Univ.* **1997**, *1*, 002.

[19] A. C. Kulkarni, P. Kuppusamy, N. Parinandi, *Antioxid. Redox Signal.* **2007**, *9*, 1717.

[20] Y. Ma, B. T. Zhang, L. Zhao, G. Guo, J. M. Lin, *Luminescence* **2007**, *22*, 575.

[21] B. S. Harrison, D. Eberli, S. J. Lee, A. Atala, J. J. Yoo, *Biomaterials* **2007**, *28*, 4628.

[22] S. H. Oh, C. L. Ward, A. Atala, J. J. Yoo, B. S. Harrison, *Biomaterials* **2009**, *30*, 757.

[23] a) Z. Li, X. Guo, J. Guan, *Biomaterials* **2012**, *33*, 5914; b) P. K. Chandra, C. L. Ross, L. C. Smith, S. S. Jeong, J. Kim, J. J. Yoo, B. S. Harrison, *Wound Repair Regen.* **2015**.

[24] M. Sepulveda, T. Dresselaers, P. Vangheluwe, W. Everaerts, U. Himmelreich, A. Mata, F. Wuytack, *Contrast Media Mol. I.* **2012**, *7*, 426.

[25] a) B. Muir, *J. Fish. Board Can.* **1969**, 26, 165; b) I. E. Gray, *Biol. Bull.* **1954**, 219.

[26] C. B. Porter, M. D. Krom, M. G. Robbins, L. Brickell, A. Davidson, *Aquaculture* **1987**, *66*, 287.

[27] D. J. Randall, T. K. N. Tsui, Mar. *Pollut. Bull.* **2002**, *45*, 17.

[28] Q. Xiang, J. Yu, P. K. Wong, *J. Colloid Interface Sci.* **2011**, *357*, 163.

[29] T. M. Suszynski, M. D. Rizzari, W. E. Scott, L. A. Tempelman, M. J. Taylor, K. K. Papas, *Cryobiology* **2012**, *64*, 125.

[30] F. O. Belzer, J. H. Southard, *Transplantation* **1988**, *45*, 673.

[31] a) R. A. Gottlieb, K. Burleson, R. A. Kloner, B. Babior, *R. Engler, J. Clin. Invest.* **1994**, *94*, 1621; b) J. M. McCord, *N. Engl. J. Med* **1985**, *312*, 159.

[32] a) H. Xu, C. Y. Lee, M. G. Clemens, J. X. Zhang, *Transplantation* **2004**, *77*, 1676; b) A. Schlegel, P. Dutkowski, *Transpl. Int.* **2015**, *28*, 677.

[33] D. E. Pegg, *The principles of organ storage*, Springer, Heidelberg, BER, DE **2012**

[34] M. Geng, Z. Duan, Geochim. *Cosmochim. Ac*. **2010**, *74*, 5631.

[35] a) A. Mohyeldin, T. Garzón-Muvdi, A. Quiñones-Hinojosa, *Cell Stem Cell* **2010**, *7*, 150; a) B. Speers-Roesch, M. Mandic, D. J. Groom, J. G. Richards, *J. Exp. Mar. Biol. Ecol.* **2013**, *449*, 239.

[36] A. S. Popel, D. Goldman, A. Vadapalli, *Oxygen Transport to Tissue XXIV*, Springer, NJ, USA **2003**, 485.

[37] S. J. Klebanoff, *J. Bacteriol.* **1968**, *95*, 2131.

[38] M. Jones, J. G. Ganopolsky, A. Labbé, M. Gilardino, C. Wahl, C. Martoni, S. Prakash, *Int. Wound J.* **2012**, *9*, 330.

[39] R. L. Mauck, C. C. B. Wang, E. S. Oswald, G. A. Ateshian, C. T. Hung, *Osteoarthr. Cartilage* **2003**, *11*, 879.

[40] R. P. Baptista, D. A. Fluri, P. W. Zandstra, *Biotechnol. Bioeng.* **2013**, *110*, 648.

[41] Z. Chen, D. Lütkemeyer, K. Iding, J. Lehmann, *Biotechnol. Lett.* **2001**, *23*, 767.

[42] a) S. H. Cartmell, B. D. Porter, A. J. García, R. E. Guldberg, *Tissue Eng.* **2003**, *9*, 1197; b) R. S. Cherry, C. T. Hulle, *Biotechnol. Prog.* **1992**, *8*, 11.

[43] a) P. Maffi, G. Balzano, M. Ponzoni, R. Nano, V. Sordi, R. Melzi, A. Mercalli, M. Scavini, A. Esposito, J. *Peccatori, Diabetes* **2013**, *62*, 3523; b) B. J. Philips, K. G. Marra, J. P. Rubin, *Wound Repair Regen.* **2014**, *22*, 11.

[44] T. T. Tran, C. R. Kahn, *Nat. Rev. Endocrinol.* **2010**, *6*, 195.

[45] a) W. Arabi Eter, D. Bos, C. Frielink, O. Boerman, M. Brom, M. Gotthardt, *J. Nucl. Med.* **2015**, *56*, 591; b) Z.-l. Zhi, A. Kerby, A. King, P. Jones, J. Pickup, *Diabetologia* **2012**, *55*, 1081.

[46] R. W. Nash, B. S. McKay, J. M. Burke, *Inves. Ophthalmol. Vis. Sci.* **1994**, *35*, 2850.

[47] a) W. R. Earle, E. L. Schilling, T. H. Stark, N. P. Straus, M. F. Brown, E. Shelton, *J.*

*Nat. Cancer Inst.* **1943**, *4*, 51; b) J. Williamson, P. Cox, *J. Gen. Virol.* **1968**, *2*, 309.

[48] M. Yu, S. Huang, K. J. Yu, A. M. Clyne, *Int. J. Mol. Sci.* **2012**, *13*, 5554.

[49] N. R. Forsyth, A. Musio, P. Vezzoni, A. H. R. Simpson, B. S. Noble, J. McWhir, *Cloning Stem Cells* **2006**, *8*, 16.

[50] A. Carreau, B. E. Hafny-Rahbi, A. Matejuk, C. Grillon, C. Kieda, *J. Cell. Mol. Med.* **2011**, *15*, 1239.

[51] N. R. Forsyth, A. Kay, K. Hampson, A. Downing, R. Talbot, J. McWhir, Regen. Med. **2008**, *3*, 817.

[52] C. A. Cook, K. C. Hahn, J. B. Morrissette-McAlmon, W. L. Grayson, *Biomaterials* **2015**, *52*, 376.

[53] E. Fournier, C. Passirani, C. N. Montero-Menei, J. P. Benoit, *Biomaterials* **2003**, *24*, 3311.

[54] K. Rambani, J. Vukasinovic, A. Glezer, S. M. Potter, *J. Neurosci. Methods* **2009**, *180*, 243.

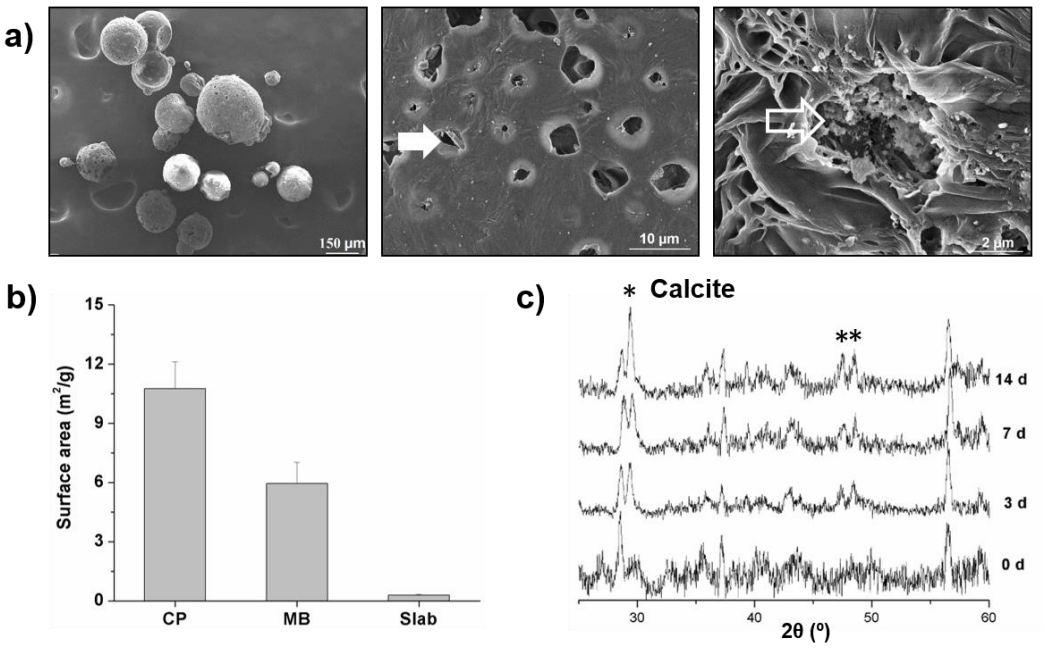


**Figure 1.** a) Scanning electron microscopy (SEM) images of oxygen-release microbeads. The microbeads had a diameter between 20-300 µm and appeared to be porous. $MnO_2$ (white arrow) and CP (empty arrow) located in the pores. b) Specific surface area of CP powders, microbeads (MB), and slabs. c) XRD patterns of the microbeads in cell culture media and 5% $CO_2$ incubator at 37 ˚C at different time points. Peaks representing $CaCO_3$ were observed after the decomposition of CP, and the signal intensity increased with time.

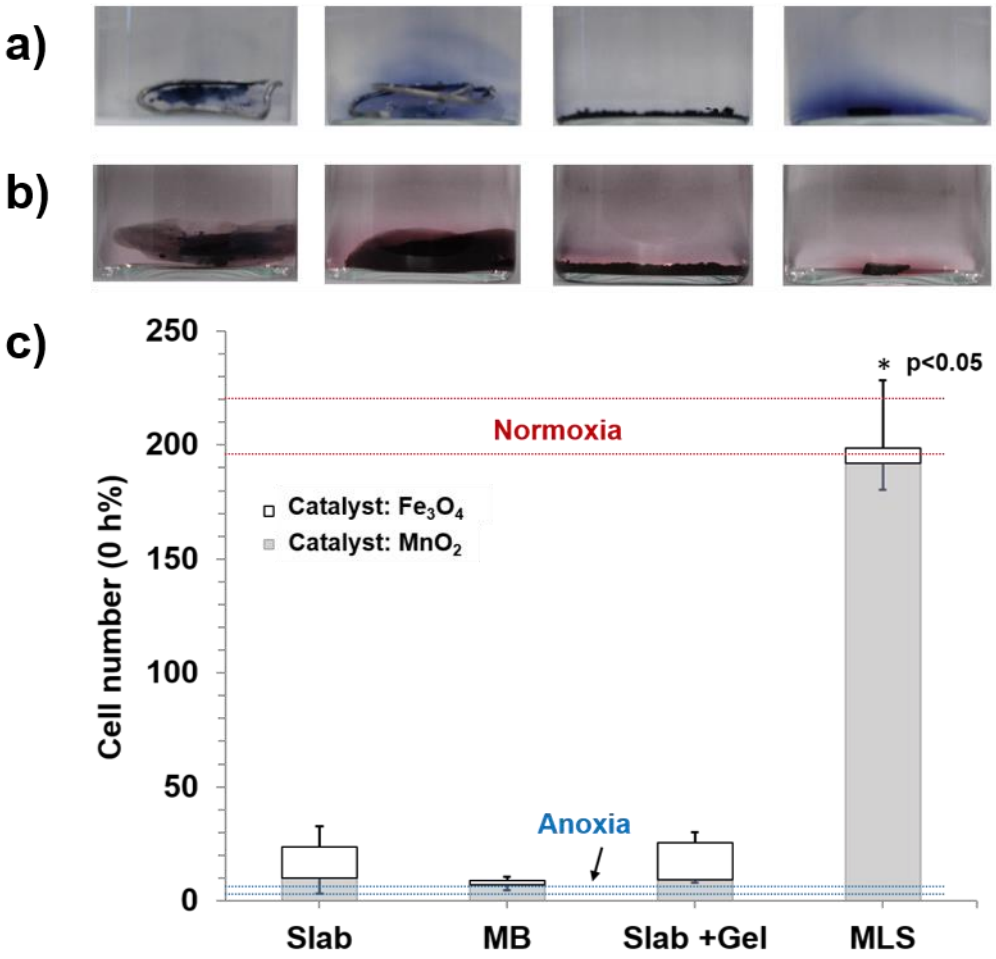


**Figure 2.** a) $H_2O_2$ release from (left to right) MLS, slab in hydrogel, microbeads (MB), and slab only after 24 h. The slab released more $H_2O_2$ compared with microbeads either with or without the hydrogel. b) Radical release from (left to right) MLS, slab in hydrogel, microbeads, and slab only after 24 h. Again, no obvious color changes were observed in the solution in the presence of hydrogel while the solution became pink without hydrogel. c) Cytotoxicity of slab, microbeads, slab in hydrogel (Slab +Gel), and MLS on MDCK cells under anoxia for 6 h using $Fe_3O_4$ or $MnO_2$ as the catalyst. The microbeads in hydrogel maintained a normal cell growth rate using either $Fe_3O_4$ or $MnO_2$ as the catalyst.

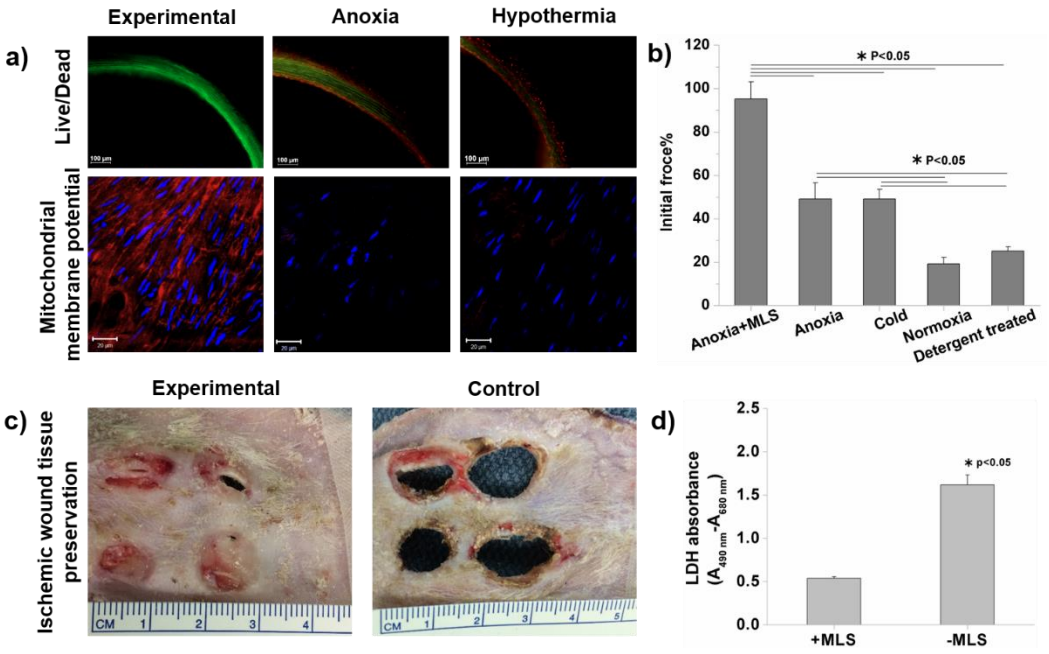


**Figure 3.** a) Fluorescent cross-sectional images of live/dead assay stained rat thoracic aorta and tetramethylrhodamine methyl ester (TMRM) stained mitochondrial membrane potential of endothelial of rat thoracic aorta after 7 d. Very few red stained nuclei from dead cells were observed in the experimental group. In contrast, a large number of dead cells were found in the samples stored under anoxia and hypothermia. The sample in the experimental group retained endothelial mitochondrial membrane potential while the samples in the other two groups lost the membrane potential. b) KCl induced contraction force of the aorta stored for 7 d. The sample in the experimental group retained the stimulated contraction force, but the other samples maintained < 50% of the stimulated contraction force. c) Ischemic wound tissue healing after 17 d. Ischemic wound tissue were necrotic in the control group but in comparison little tissue was lost with ODP. d) LDH release from CHO cells cultured at a physiological density ($2\times10^8$ cells $mL^{-1}$) after 24 h. MLS reduced LDH release from dead cells two-fold.

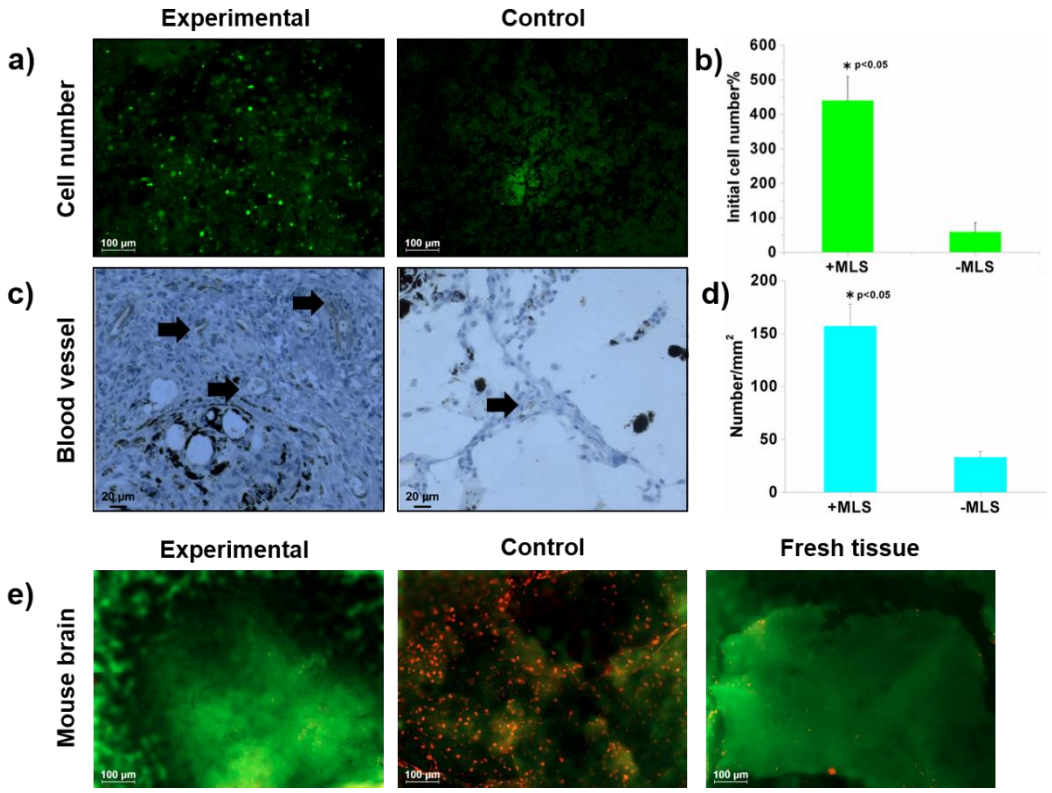


**Figure 4.** a, b) Fluorescent images of MDCK cells and quantified cell number change after being transplanted subcutaneously +/- MLS for four weeks. Cell quantification indicated proliferation had occurred with MLS but cell number had dereased without it. c, d) Blood vessel in the implants and quantified blood vessel density. Cells with MLS had a four-fold higher blood vessel denstiy than that in the control material. e) Fluorescent images of live/dead assay stained mouse brain tissue after 24 h. Very few dead cells were oberved in the experimental group and the fresh tissue, practically all cells were dead in the control.

**The table of contents**

**This work** presents a biodegradable micro-lung system, based on peroxides, for tissue engineering and wound healing. The micro-lung system has excellent biocompatibility and successfully maintains high cell viability in rodent blood vessels and preserves normal mitochondrial membrane potential of endothelial cells at physiological temperature. In contrast, blood vessels stored under hypothermia exhibit poor cell viability and lose mitochondrial membrane potential of endothelial cells after rewarming.

**Keywords:** peroxide, oxygen delivery, tissue engineering, tissue preservation, microbead

*Huaifa Zhang, Hani Shash, Yu Ling Zhang, Amal Al-Odaini, Daisuke Sato, Mirko S. Gilardino,*

*Simon Tran, Jake E. Barralet**

**Degradable synthetic micro-lungs for bloodless tissue viability**

ToC figure

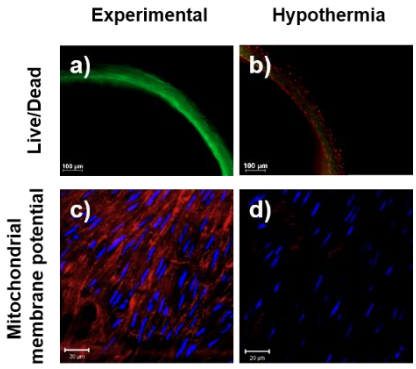

Supporting Information

**Degradable synthetic micro-lungs for bloodless tissue viability**

*Huaifa Zhang, Hani Shash, Yu Ling Zhang, Amal Al-Odaini, Daisuke Sato, Mirko S. Gilardino, Simon Tran, Jake E. Barralet**

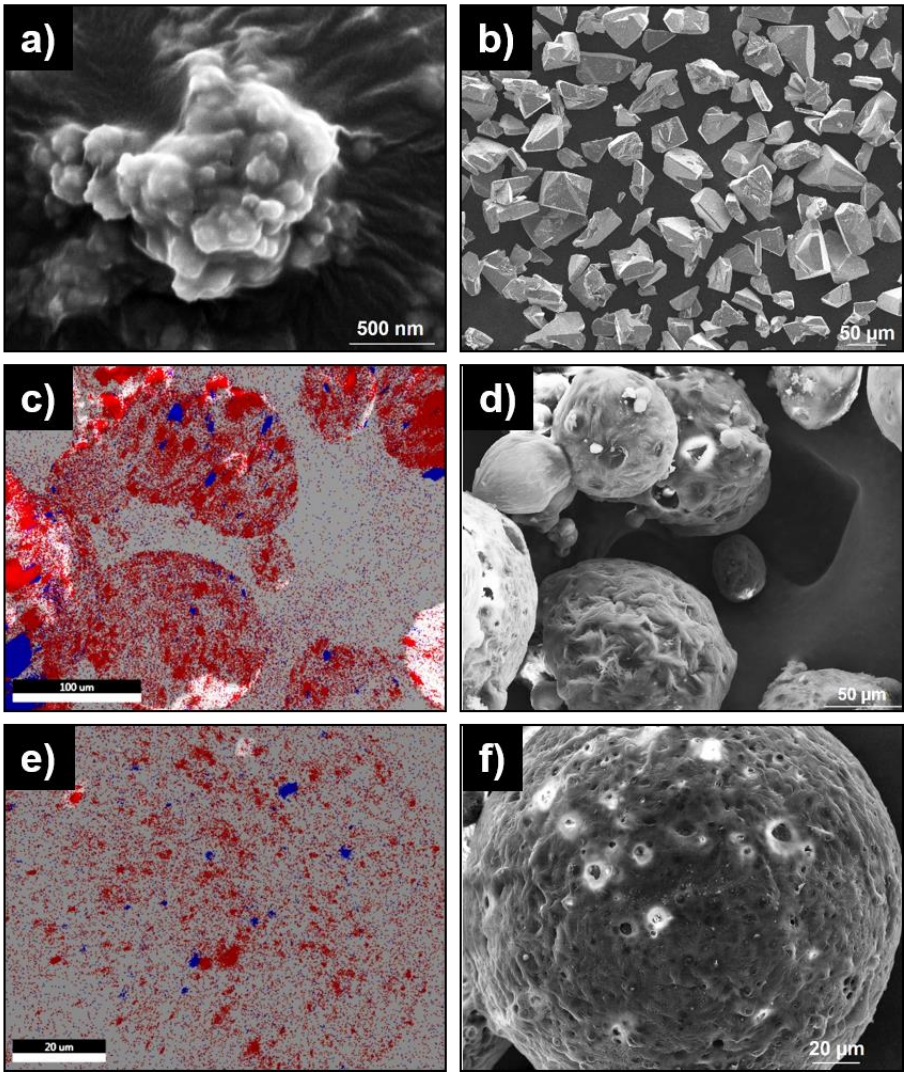


**Figure S1.** a) SEM image of CP powders. The CP powders were nano particles. b) SEM image of $MnO_2$. $MnO_2$ had a size between 10-80 µm. c) EDX mapping images of Ca (red) and Mn (green) elements on the surface of microbeads at a lower magnification. d) SEM image of the mapped microbeads at a lower magnification. e) EDX mapping images of Ca (red) and Mn (green) elements on the surface of microbead at a higher magnification. f) SEM image of the mapped microbead at a higher magnification.

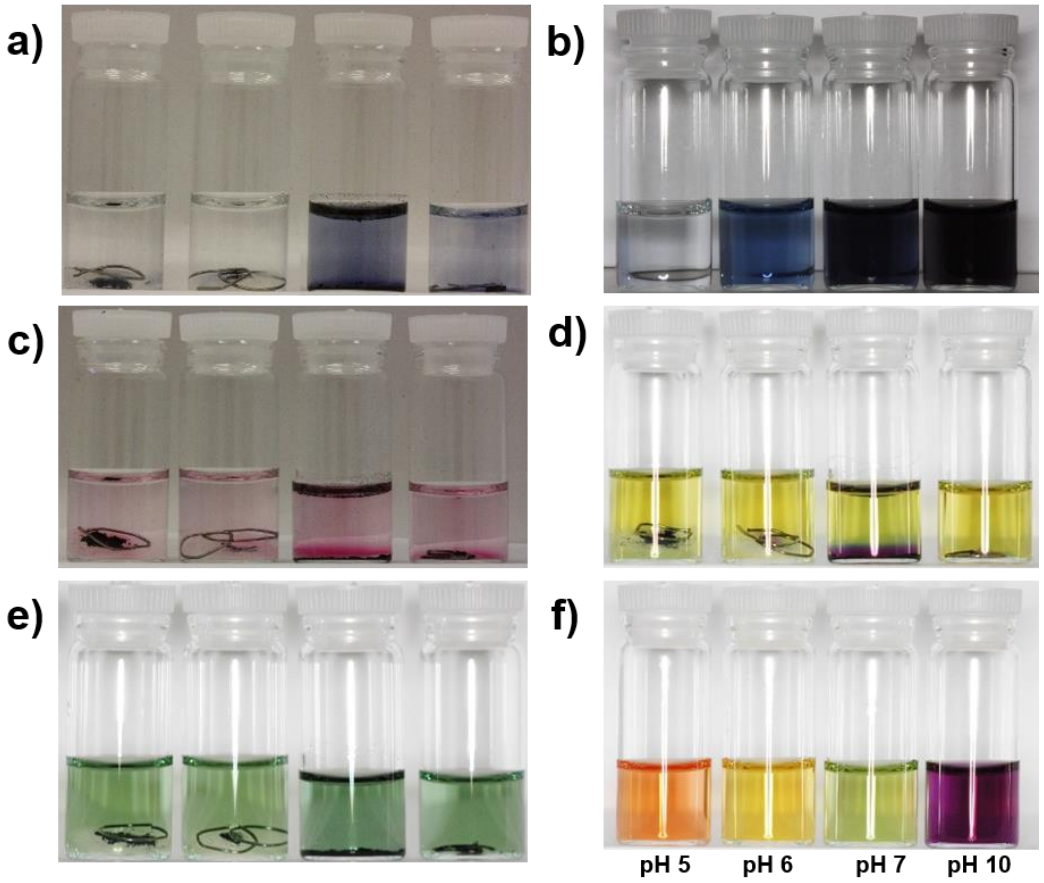


**Figure S2.** a) $H_2O_2$ release from (left to right) MLS, slab in hydrogel, microbeads, and slab after 10 min. No color change was observed in the presence of hydrogel for both microbeads and the slab, but the solution became blue in both cases without the hydrogel. b) Color changes corresponding to different concentrations of $H_2O_2$, left to right: 1, 10, 50 and 100 ppm. The color of the solution changed from light blue to dark blue as the concentration of $H_2O_2$ increased. c) Radical release from (left to right) MLS, slab in hydrogel, microbeads, and slab after 10 min. In the presence of hydrogel, red color was observed only inside the hydrogel for the both kinds of material, whereas in the absence of hydrogel the solution became red near the material. d) pH changes in water caused by (left to right) MLS, slab in hydrogel, microbeads and slab after 10 min. pH changes were observed in water and microbeads resulted in the largest pH change. e) pH changes in phenol red-free medium caused by (left to right) MLS, slab in hydrogel, MB and slab after 10 min. No color change was observed in culture medium. f) Color changes corresponding to various pH. The color of the solution changed from pink to dark red as the pH increased from 5 to 10.

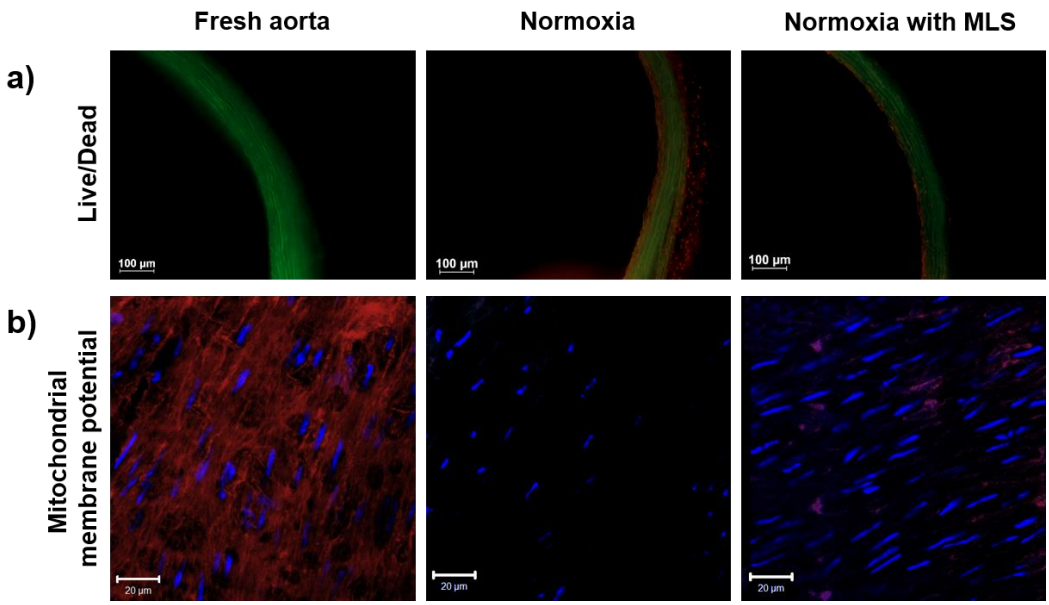


**Figure S3.** a) Fluorescent cross-sectional images of live/dead assay stained rat thoracic aorta after 7 d. Very few dead cells were found in the fresh aorta, but many red nuclei from dead cells were observed in the other two samples. b) Fluorescent images of tetramethylrhodamine methyl ester (TMRM) stained mitochondrial membrane potential of endothelial cells in rat thoracic aorta after 7 d. The mitochondrial of endothelial cells in fresh aorta had a high membrane potential, nevertheless, the mitochondrial of endothelial cells lost membrane potential in the other two samples.

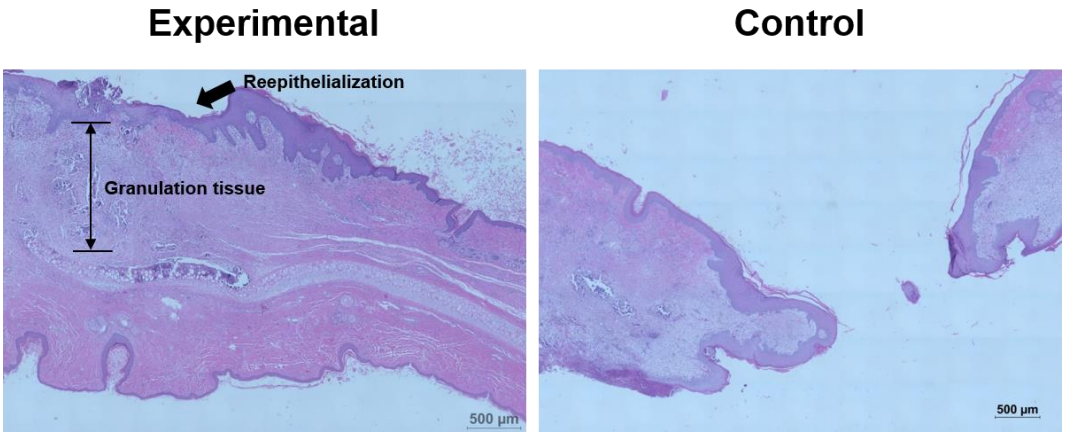


**Figure S4.** Hematoxylin and eosin (H&E) staining images of ischemia rabbit ear wounds with oxygen-release material after 17 d. Reepithelialization was observed in the experimental group (dark arrow) and granulation tissue was also formed as indicated in the figure. Tissue breakage was observed in the control sample.

**Table S1.** Histopathological scores of the wounds treated with oxygen-release patches. (Tissue was lost due to necrosis in the control group)

| | Score (0-3) [a] (n=8) |
|---|---|
| Granulation tissue amount | 2±0.75 |
| Granulation tissue fibroblast maturation | 1.88±0.35 |
| Collagen deposition | 1.63±0.74 |
| Neovascularization | 1.63±0.52 |
| Reepithelialization | 2.38±0.74 |

[a] 3 high, 0 absent.

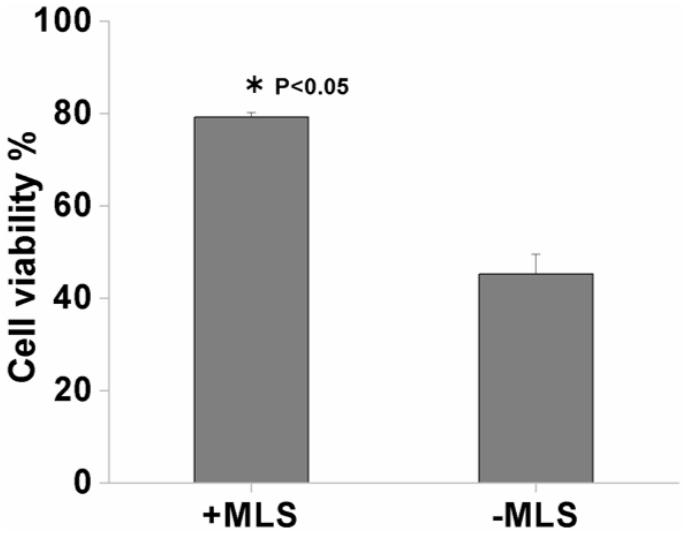


**Figure S5.** CHO cell viability after being cultured for 24 h at a density of $2\times10^8$ cells $mL^{-1}$. In the presence of MLS, the viability of CHO cells was one-fold higher than cells in the control group.

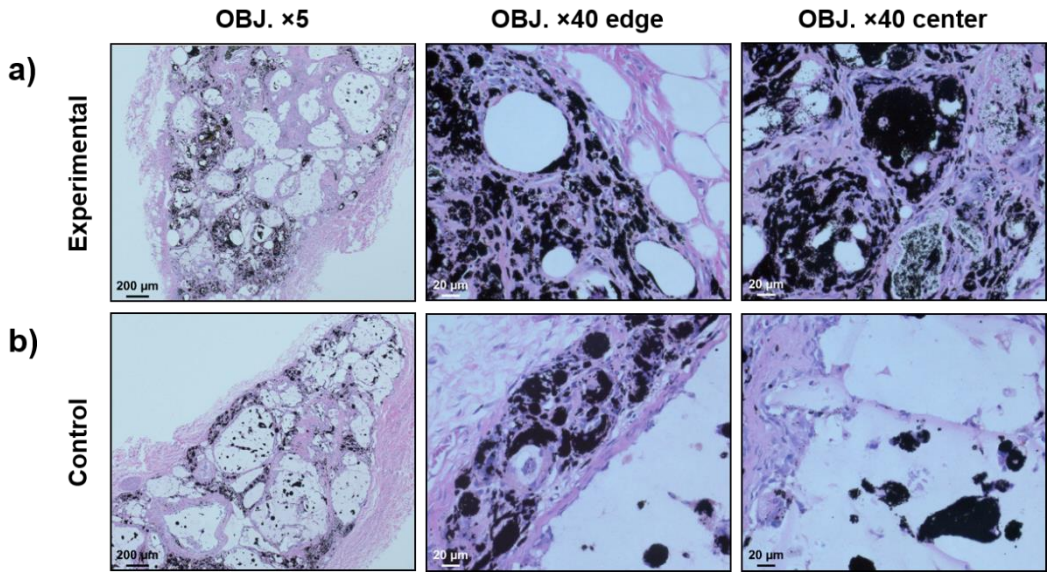


**Figure S6.** H&E staining images of the transplants containing MDCK cells after four weeks. The cell density around the material in the central area of the implant was much higher in MLS compared with the control group.

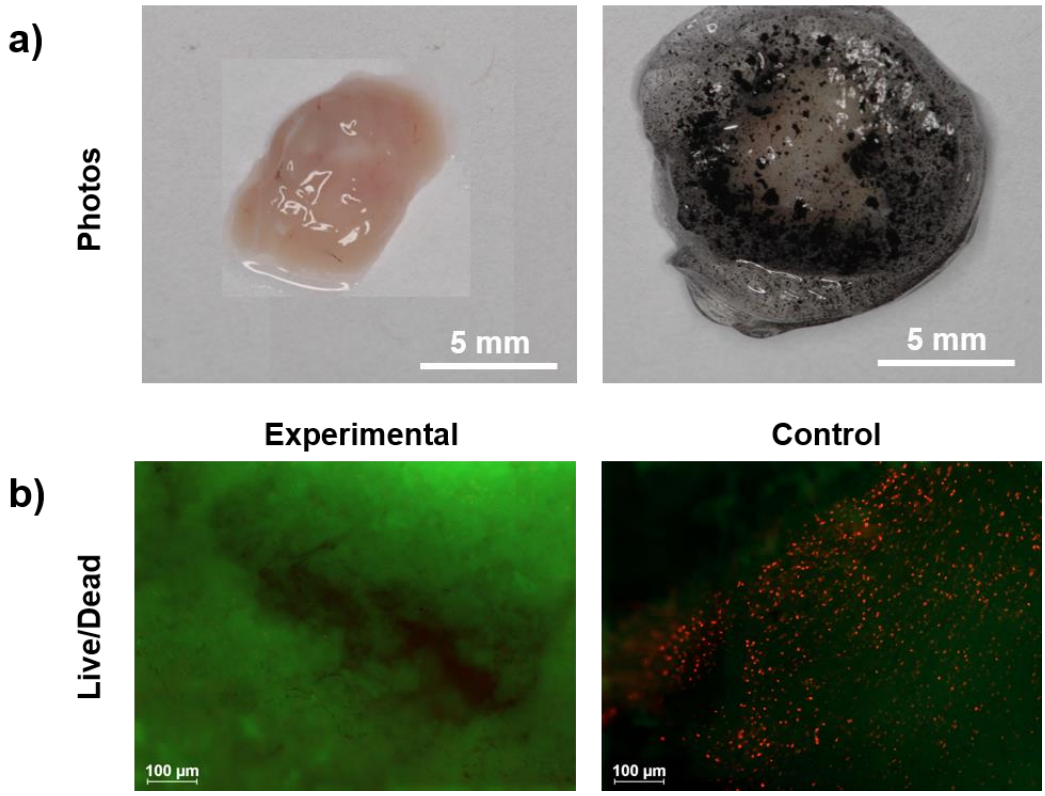


**Figure S7.** a) Photo of the mouse brain slice. The brain slice had a thickness of 2 mm and was encapsulated by MLS. b) Fluorescent images of live/dead assay stained brain slices stored for 3 h. Very few red nuclei from dead cells were observed in the experimental group, whereas a large number of dead cells were found in the control group.

*Preparation of oxygen-release microbeads:* Oxygen-release microbeads composed of calcium peroxide (CP), iron oxide ($Fe_3O_4$) or manganese dioxide ($MnO_2$), and poly(lactide-co-glycolide) (PLGA) were prepared using a phase separation method [1] in the absence of $H_2O$. CP powders (Aldrich, USA) and $Fe_3O_4$ (Fisher Scientific, Canada) or $MnO_2$ (Fisher Scientific, Canada) were first suspended in PLGA (50/50, Mw 28,000, Advanced Polymer Materials Inc, Canada) solution in chloroform (Fisher Scientific, Canada) with a weight ratio of 1/10/10 (CP/$Fe_3O_4$ or $MnO_2$/PLGA), then the suspension was added into glycerol (Fisher Scientific, Canada) containing 1 wt% polyvinyl alcohol (Mw 28,000-98,000, Aldrich, USA) (PVA) and stirred for

10 min at room temperature. When the beads dried in a fume hood, the microspheres were collected by centrifuging the suspension at 4000 rpm, which was then washed with alcohol three times and dried at room temperature.

*Preparation of oxygen-release slabs:* For the preparation of oxygen-release slabs, CP, $Fe_3O_4$ or $MnO_2$, and polycaprolactone (PCL, Mw 70,000-90,000, Sigma, USA) was mixed in chloroform with a weight ratio of 1/10/10 (CP/$Fe_3O_4$ (or $MnO_2$)/PCL). Then the mixtures were transferred into a round aluminum foil model with a diameter of 2 cm and dried in a fume hood at room temperature.

*Cell culture with oxygen-release materials:* Madin-Darby canine kidney (MDCK) cells were used to evaluate the cytotoxicity and the ability of the oxygen-release materials to support cell growth under anoxia. MDCK cells were seeded in 6-well plate wells, which had been separated through cutting, with a density of $1.0\times10^4$ cells per well and left to attach to the wells overnight. For anoxic culture, the oxygen-release material was added into the plate wells and culture medium replaced by the one that had been pre-degased in $N_2/CO_2$ (10% $CO_2$) for 20 h. The process was carried out in the biological sage cabinet by putting the individual wells into a 50 mL jar which had been flushed by $N_2/CO_2$ (10% $CO_2$) beforehand and sealed with a rubber stopper. The jar was flushed by a balloon filled with $N_2/CO_2$ in the cabinet during the operation. Cells were cultured under anoxia by putting the jars in a desiccator with grounded joint at 37 ˚C. The desiccator was constantly flushed by $N_2/CO_2$ (5% $CO_2$) at a flow rate of 200 mL $min^{-1}$ and the culture time was up to 6 h. Dulbecco's Modified Eagle Medium (DMEM) supplemented with 10% FBS and 1% penicillin-streptomycin was used. Normoxia culture was carried out in normal cell incubator with 20% $O_2$ and 5% $CO_2$ at 37 ˚C. Different kinds of

oxygen-release materials, including slab, microbeads, slab in hydrogel and microbeads in hydrogel, i.e. micro-lung system (MLS), containing either $MnO_2$ or $Fe_3O_4$ catalysts were used. To encapsulate the slab with hydrogel, 350 µL 1% sodium alginate (FMC BioPloymer, USA) solution was added onto a piece of filter paper that had been moistened with 0.1 M $CaCl_2$; then a piece of slab was put on the alginate solution; afterwards, another 350 µL of alginate solution was added on top of the slab; finally, 100 µL of 0.1 M $CaCl_2$ was used to crosslink the alginate to encapsulate the slab. Microbeads were encapsulated in the alginate hydrogel in a similar way.

*Preservation of blood vessels:* Thoracic aortas from rats (5-8 months old) were collected immediately after the euthanization of animals used in other non-pharmaceutical medical studies and kept in phosphate buffer solution (PBS) on ice for a maximum of 3 h. Following dissection of connection tissues, the aortas were cut into 5 mm in length and preserved under one of following conditions, anoxia (95% nitrogen ($N_2$), 5% carbon dioxide ($CO_2$), 37 ˚C), hypothermia (20% $O_2$, 4 ˚C) and normoxia (20% $O_2$, 5% $CO_2$, 37 ˚C). Oxygen-release microspheres were mixed with 1 wt/vol% sodium alginate solution and sterilized by ultraviolet (UV) light for 20 min; next 350 µL of the mixture was added onto a piece of filter paper that had been moistened with 0.1 M $CaCl_2$, using a 24-well plate well as the module; then a piece of aorta in the length of 5 mm filled with the bead-alginate mixture was put on the mixture; afterwards, another 350 µL of the mixture was added on top of the aorta; finally, 100 µL of 0.1 M $CaCl_2$ was added into the plate to to encapsulate the aorta in MLS by crosslinking the alginate. The aortas were cultured in Dulbecco's Modified Eagle Medium (DMEM) supplemented with 10% FBS and 1% Penicillin/Streptomycin solution (P/S). Aorta tissue encapsulated by oxygen-release scaffolds was cultured under anoxia and normoxia, respectively. Anoxic culture was carried out by putting the samples in a sealed jar (that had been flushed with 95% $N_2$ and 5% $CO_2$) in a desiccator which was constantly flushed with $N_2$.

Aortas preserved at 4 ˚C in Hanks' balanced salt solution (HBSS) with 10 mM glucose were taken as the positive control [2]. Aorta segments alone were also preserved under anoxia and normoxia in culture medium, respectively, to serve as negative controls. The culture medium was changed every 3 d. Anoxic environment was created by flushing the jar with balloons filled with $N_2$ during the change of culture medium.

*Wound healing:* The oxygen delivery patch (ODP) consisted of CP, $Fe_3O_4$, PCL, and an alginate hydrogel. CP, $Fe_3O_4$, and PCL were first mixed in chloroform with a weight ratio of 1/10/10, next the mixtures were transferred into a 3.5×3.5 cm foil mold. After that, chloroform was removed by evaporation to get a piece of CP-$Fe_3O_4$-PCL plate weighing around 600 mg, which was encapsulated by 6 mL 3 wt/vol% alginate hydrogel cross-linked by 1 M $CaCl_2$ subsequently, following the method mentioned before. Control patches were prepared using a similar method without oxygen-release plates. All the patches were sterilized by UV for 20 min before being used. New Zealand male white rabbits (3-3.5 kg) from Charles River were used in this study. All procedures were performed in accordance with the animal care and use committee. Each animal was anesthetized by intramuscular injection of 10 mg $kg^{-1}$ of xylazine and 1 mg $kg^{-1}$ of acepromazine followed by intramuscular injection of 35 mg $kg^{-1}$ of ketamine. Isoflurane mask was also used for anesthesia induction. A severe full thickness ischemic wound model (Ø 15 mm ) was created on the convex side to examine the effect of oxygen-release patch on tissue preservation and wound healing. Two ears on each rabbit were treated with ODP and hydrogel patch only, respectively. 3M™ Tegaderm™ transparent film dressings were used to fix the ODP onto the wounds and keep moisture of the wounds at the same time. The rabbits received 0.05 mg $kg^{-1}$ buprenorphine 30 min prior to the end of surgery and then a post-operative injection of buprenorphine every 8 to 12 h was administered (0.02-0.05 mg $kg^{-1}$), for a minimum of 72 h. The patches were changed every 3 d.

*MDCK transplantation:* Athymic "nude" male rats (Crl: NIH-Foxn1) used for subcutaneous implantation were 6- to 7-week old and 200-220 g in weight, and supplied by Charles River Laboratories. All experiments followed Canadian Institutional Animal Care Guidelines and were approved by the Animal Care Committee at McGill University. For subcutaneous implantation, MDCK cells were labeled with carboxyfluorescein succinimidyl ester (CFSE, Abcam, Canada) and encapsulated in hydrogel with and without oxygen-release material before surgery and kept on ice. For cell encapsulation, $1\times10^6$ cells $mL^{-1}$ MDCK cells were mixed with 1 wt/vol% alginate solution with CP-$Fe_3O_4$-PLGA microbeads, then the mixtures were extruded into 0.1 M $CaCl_2$ solution to form MLS beads of 5 mm in diameter. Cells were also encapsulated in 1 wt/vol% alginate hydrogel with $Fe_3O_4$-PLGA microbeads as the control. Before the surgery, the rats were anesthetized using isoflurane. Two places on the dorsal surface were shaved. A 4 cm skin incision was made and one pocket was created on each side of the incision to yield a total of 2 pockets, where the experimental sample (right side) and control sample (left side) were implanted. A post-operative injection of carprofen was performed every 24 h for 72 h. Implants were taken out after 4 weeks.

*Physiological density Chinese Hamster Ovary (CHO) cell culture:* CHO cells were encapsulated in alginate hydrogel and MLS at a density of $2\times10^8$ cell $mL^{-1}$. Briefly, CHO cells were mixed with 0.5 wt/vol% sodium alginate solution with or without oxygen-release microbeads at a concentration of $2\times10^8$ cell $mL^{-1}$; then 15 µL of the mixtures were dropped into 0.1 M $CaCl_2$ solution to form beads. The hydrogel beads containing CHO cells were cultured under normoxia for 24 h.

*Preservation of mouse heart and brain slices:* Mouse brains were obtained from freshly dead mice and kept on ice. The brain slices were cut by hand across the brain and were about 2 mm in thickness. The brain slices were encapsulated with 0.6 mL MLS containing 10 mg $mL^{-1}$ oxygen-release microbeads by crosslinking. Then the brain slices were cultured under anoxia for up to 24 h.

*Characterization:* The morphology of the microbeads, CP and $MnO_2$ was examined with a field emission scanning electron microscope (FE-SEM, FEI Inspect F-50, USA). The distribution of CP and $MnO_2$ on the surface of the microbeads was mapped through the energy dispersive X-ray spectroscopy (EDX). X-ray diffraction (XRD) of the samples in cell culture media and 5% $CO_2$ incubator was recorded with an X-ray diffractometer (D8 Discover, Bruker, USA). Moreover, the specific surface area of the microbeads was also examined (Micromeritics TriStar 3000, USA). A potassium iodide (Fisher Scientific, Canada) and starch solution (Fisher Scientific, Canada) was used to detect $H_2O_2$ in the system and the solution becomes blue in the presence of $H_2O_2$. N,N-dimethyl-p-phenylenediamine (DMPD, Sigma, USA) was employed to detect the radicals released from the materials. [3] The microbeads with and without alginate hydrogel were put into 2.5 mg $mL^{-1}$ DMPD solution and the released radicals turned the solution red. The changes of pH in both water and colorless culture medium was detected by a pH indicator (Riedel-deHaen (pH 4-10), Aldrich, USA)). The color changes were recorded with a camera (D70S, Nikon, Japan). The number of MDCK cells before and after anoxic culture with various matierals was counted with a hemacytometer [4]. Firstly the culture medium was removed and cells were washed with PBS three times. Then the cells were detached by 0.25% Trypsin-EDTA, which would be counteracted with culture medium containing 10% FBS. Afterwards the cells were collected by centrifugation for 5 min at 1200 rpm/min. Next the supernatant was discarded and cells were re-suspended in PBS and stained

with trypan blue. Finally cell number was assessed with a hemocytometer. The results were expressed as the percentage of cell number at 0 h. Three replicates were done for each sample and the results expressed as an average ± standard deviation. Cell viability in stored rat thoracic aorta, after being rewarmed at 37 ˚C in HBSS with 10 mM glucose for 150 min, was examine using a live/dead assay and observed under a fluorescent microscope (Imager.M2, Zeiss, Germany). Ethidium bromide-1 (Life technologies, USA) was used to stain the nuclei of dead cells and Calcein AM (Life technologies, USA) stain live cells in the tissue. The mitochondrial membrane potential of endothelial cells in stored rat aorta was further examined using the tetramethylrhodamine methyl ester (TMRM, Setareh Biotech, USA) staining [2]. The samples were rewarmed at 37 ˚C in HBSS with 10 mM glucose for 150 min and then stained with TMRM (500 nmol $L^{-1}$) for 30 minutes in HBSS with 10 mM glucose. Afterwards the stained samples were kept in 250 nmol $L^{-1}$ TMRM for maintenance. The stained aortas were placed into incubation chambers with a cover glass bottom with the endothelial side being downside. Fluorescence of the mitochondria of the endothelial cells was inspected using an inverted confocal microscope (LSM 510, Zeiss), under the condition of 116 µm pinhole, at λexc. = 543 nm, λem. = 585 nm. [2] Smooth muscle contraction force, stimulated by 120 mM KCl, was measured with a Mach-1$^{TM}$ mechanical testing system fitted with a 150 g load cell. The rat aortas were cut into 5-mm ring segments. Each ring segment was suspended in a tissue bath containing 300 mL of Krebs Henseleit (KH) solution (122 mM NaCl, 4.7 mM KCl, 1.2 mM $MgCl_2$, 15.4 mM $NaHCO_3$, 1.2 mM $KH_2PO_4$ and 5.5 mM glucose) and mounted between 2 stainless steel wire hooks. One hook was fixed to the bottom of the bath and the other hook was connected to the force transducer. The KH buffer was gassed continuously with 95% $O_2$ and 5% $CO_2$ at 37 ˚C and changed every 20 min. The baseline tension of all vessel rings was adjusted to around 1.0 g. After 60 min of equilibration, KH solution supplemented with 120 mM KCl was used to stimulate the contraction of the aorta tissue rings. Contraction force of

the aorta tissue rings was recorded by a tensiometer. [5] The stimulated contraction force of all the samples was expressed as the percentage of the stimulated force of fresh samples. Four replicates were performed for each sample. The results were expressed as an average ± standard deviation. The healing process of ischemic rabbit ear wounds was observed and recorded with a camera. For histology examination, the ear tissue was fixed in 4% paraformaldehyde in PBS and then embedded in paraffin. Hematoxylin and eosin (H&E) staining was performed. The stained slides were observed under a microscope (Imager.M2, Zeiss, Germany). Eight replicates were done for each sample. CHO cell viability in the beads were assessed using the trypan blue exclusion method [6] and LDH assay (Life technologies, USA). Three replicates were done for each sample and the results expressed as an average ± standard deviation. MDCK cell viability in the implants was examined under a fluorescence microscope (Imager.M2, Zeiss, Germany). To examine cell growth after transplantation, implants were retrieved and cells in the alginate hydrogel were released by dissolving the hydrogel with 100 µL 55 mM potassium citrate and 90 mM NaCl (pH 7.4) solution for 20 min at room temperature. The cells were stained with trypan blue and counted using a hemocytometer under a microscope to assess their population. [6] For histological characterization, the implants were fixed in 4% paraformaldehyde in PBS overnight and embedded in paraffin. H&E staining was performed to examine the structure and cell density of the implants. Blood vessels in the implants were stained using immunohistochemistry and the density of blood vessels was quantified by counting the number of blood vessels. Blood vessel density was expressed as the number of blood vessels per $mm^2$, five random fields under the microscope were counted for each sample. Three replicates were done for each sample and the results expressed as an average ± standard deviation. The viability of cells in preserved brain slices was examined using fluorescent live/dead staining and examined under a fluorescence microscope

(Imager.M2, Zeiss, Germany). Three replicates were done for each sample. Student's t-test was used to determine the statistical significance between samples in all the experiments.

[1] M. Husmann, S. Schenderlein, M. Lück, H. Lindner, P. Kleinebudde, *Int. J. Pharm.* **2002**, *242*, 277.
[2] T. Wille, H. de Groot, U. Rauen, *J. Vasc. Surg.* **2008**, *47*, 422.
[3] a) V. Verde, V. Fogliano, A. Ritieni, G. Maiani, F. Morisco, N. Caporaso, *Free Radical Res.* **2002**, *36*, 869; b) S. D. Çekiç, A. N. Avan, S. Uzunboy, *R. Apak, Ana. Chim. Acta* **2015**, *865*, 60.
[4] S. Johnson, V. Nguyen, D. Coder, *Current Protocols in Cytometry*, John Wiley & Sons, Inc., NJ, USA **2001**.
[5] L. I. Brueggemann, B. K. Mani, J. Haick, K. L. Byron, *J. Vis. Exp.* **2012**, *4263*.
[6] S. Heiligenstein, M. Cucchiarini, M. W. Laschke, R. M. Bohle, D. Kohn, M. D. Menger, H. Madry, *J. Gene Med.* **2011**, *13*, 230.